Understanding the link between Transglutaminase and the induction of Fibrosis in Cystic Fibrosis (CF)

Samuel Kabo Nyabam

Doctor of Philosophy

ASTON UNIVERSITY

August, 2014

Aston University

Understanding the link between TG2 and the induction of Fibrosis in Cystic Fibrosis

A thesis submitted by Samuel Kabo Nyabam

For the degree of Doctor of Philosophy, 2014

The emerging role of the multifunctional enzyme, Transglutaminase 2 (TG2) in Cystic Fibrosis (CF) has been linked to its increased expression and intracellular transamidating activity. However, a full understanding of the molecular mechanisms involved still remains unclear despite numerous studies that have attempted to delineate this process. These mechanisms include the NFκB and TGFβ1 pathway amongst others. This study reveals for the first time that the development of fibrosis in CF is due to a TG2-driven epithelial to mesenchymal transition (EMT) via a mechanism involving the activation of the pro-fibrotic cytokine TGFβ1. Using a human ΔF508/W1282X CFTR CF mutant bronchial cell (IB3-1), its CFTR corrected "add-back" cell (C38) as well as a primary human bronchial epithelial cell (HBEC), elevated TG2 levels in the CFTR mutant IB3 cell were shown to activate latent TGFβ1 leading to increased levels found in the culture medium. This activation process was blocked by the presence of cell-permeable and impermeable TG2 inhibitors while inhibition of TGFβ1 receptors blocked TG2 expression. This demonstrates the direct link between TG2 and TGFβ1 in CF. The presence of active cell surface TG2 correlated with an increase in the expression of EMT markers, associated with the CF mutant cells, which could be blocked by the presence of TG2 inhibitors. This was mimicked using the "add-back" C38 cell and the primary human bronchial epithelial cell, HBEC, where an increase in TG2 expression and activity in the presence of TGFβ1 concurred with a change in cell morphology and an elevation in EMT marker expression. Conversely, a knockdown of TG2 in the CF mutant IB3 cells illustrated that an inhibition of TG2 blocks the increase in EMT marker expression as well as causing an increase in TEER measurement. This together with an increase in the migration profile of the CF mutant IB3 cell against the "add-back" C38 cell suggests that TG2 drives a mesenchymal phenotype in CF. The involvement of TG2 activated TGFβ1 in CF was further demonstrated with an elevation/inhibition of p-SMAD 2 and 3 activation in the presence of TGFβ1/TG2 cell-permeable/impermeable inhibitors respectively. The use of a comparative airway cell model where bronchial epithelial cells were cultured at the air liquid interface (ALI) confirmed the observations in submerged culture depicting the robustness of the model and reiterated the importance of TG2 in CF. Using a CFTR corrector combined with TG2 inhibitors, this study showed that the correction and stabilisation of the ΔF508 CFTR mutation in the mutant cell forged an increase in matured CFTR copies trafficking to the apical surface by circumventing proteosomal degradation. Thus the results presented here suggests that TG2 expression is elevated in the CFTR mutant bronchial cell via a TGFβ1 driven positive feedback cycle whereby activation of latent TGFβ1 by TG2 leads in turn to an elevation in its own expression by TGFβ1. This vicious cycle then drives EMT in CF ultimately leading to lung remodelling and fibrosis. Importantly, TG2 inhibition blocks TGFβ1 activation leading to an inhibition of EMT and further blocks the emerging fibrosis, thus stabilizing and supporting the maturation, trafficking and conductance of CFTR channels at the apical surface.

Keywords: Transglutaminase 2, Cystic Fibrosis, TGFβ1, CFTR, TG2 inhibitors

Dedication

To my beloved family and most especially to my adorable wife, Dinci. Thank you all for believing in me

Acknowledgement

I will like to use this opportunity to thank God, who has blessed me with the gift of life and given me the strength through this project. He has been my refuge and strength and a pillar of support. I eternally remain grateful.

To my principal supervisor, Prof Martin Griffin, I am grateful for giving me the opportunity to work in his lab. He remained supportive and kept me on course during the project. I have enjoyed his invaluable advise, direction and patience during my course of research in his lab and the writing up process. To him, I am obliged and indebted. I will like to thank Dr Lindsay Marshall for her support with the ALI work and advice through the project. Also, I would like to thank Dr Zhuo Wang for her passionate and meticulous tutelage in the lab. She remained resolute and committed to my success. Thank you. I thank Dr Russell Collighan for his support during my PCR work. Thanks to Aston University for providing the scholarship/ funding for this project.

To my parents, I will like to thank them for their prayers, patience, advice, guidance and time during my course of study. You watched me grow and believed in my dream. All this wouldn't have been possible without you. Thank you. To my siblings, in-laws, nephews and niece, this is for your unflinching support, thank you. To my friends, for all the joy, pain, laughter, successes and failures, thank you for sharing this dream and shaping our future.

Table of contents

Table of Figures

List of Tables

Abbreviations

AEM……Airway epithelial medium

ALI……..Air Liquid interface

AMP……Adenosine monophosphate

ASL…….Air surface liquid

ATP…….Adenosine triphosphate

BALF……..Bronchoalveolar lavage fluid

BCD……Biotin cadaverine

cAMP…….Cyclic adenosine monophosphate

CE……..Cornified envelope

CF……..Cystic Fibrosis

CFTR…….Cystic fibrosis transmembrane conductance regulator

DAPI……..4',6-diamidino-2-phenylindole

db-cAMP…Dibutyryl cyclic adenosine monophosphate

DMSO……Dimethyl sulfoxide

ECM……...Extracellular matrix

EDTA…….Ethylenediaminetetraacetic acid

EMT……...Epithelial to mesenchymal transition

ENaC…….Epithelial sodium channels

ER……..Endoplasmic reticulum

FITC……...Fluorescein isothiocyanate

FXIII……Plasma transglutaminase

GTP……Guanosine-5'- triphosphate

HBEC…….Human bronchial epithelial cells

HBEC-T….TG2-transduced human bronchial epithelial cells

IL…….Interleukin

IPF……..Idiopathic pulmonary fibrosis

ITS……. Recombinant human insulin, transferrin, and sodium selenite

IκB…….Inhibitor of kappa B

LAP…….Latency associated peptide

LLC…….Large latent complex

LTβP……...Large latent TGFβ binding protein

MMP……Matrix metalloproteinase

mRNA……..Messenger ribonucleic acid

MSD…….Membrane spanning domain

NBD…….Nuclear spanning domain

NFκB……Nuclear factor kappa of activated B cells

OD……Optical density

OPD…….*o*-Phenylenediamine

PAGE……Polyacrylamide gel electrophoresis

PBS……. .Phosphate buffered saline

PMSF……Phenylmethanesulfonylfluoride

PTC……. .Premature termination codon

RGD……. Arg-Gly-Asp

RNA……...Ribonucleic acid

rTGFβ1……..Recombinant Transforming growth factor β1 protein

SDS……Sodium dodecyl sulfate

shRNA……Short hairpin ribonucleic acid

siRNA…….Small interfering ribonucleic acid

SMAD…….Subclass of mothers against decapentaplegic

TEER……..Trans-epithelial electrical resistance

TEMED……N,N,N´,N´-tetramethylethylenediamine

TG2…….Transglutaminase 2

TGase…….Transglutaminases

TGFβ1…….Transforming growth factor β1

TNF-α……..Tumor necrosis factor α

WB……Western blotting

WT……Wild type

α-SMA…….Alpha smooth muscle actin

ΔF508……..Deletion of phenylalanine at position 508 of the *CFTR* gene

1.1 INTRODUCTION

Transglutaminases, (EC 2.3.2.13: TGases), are a group of enzymes that are structurally related and responsible for the post-translational modification of proteins (Iismaa *et al.*, 2009). These enzymes are implicated in the crosslinking of proteins involving an acyl transfer reaction between the γ-carboxamide chain of glutamine and the ε-amino chain of lysine or any primary amino group of a polyamine serving as the acyl acceptor and if the primary amine is that from a peptide bound lysine, N^{ε} (γ-glutamyl) lysine bonds are formed (Greenberg *et al.*, 1991, Folk and Finlayson, 1977, Griffin *et al.*, 2002). The reaction is Ca^{2+} dependent as the binding of Ca^{2+} -reconfigures TGases from a quiescent, closed conformation into an open conformation, which exposes the active catalytic site to its substrates (Bergamini, 1988, Bergamini and Signorini, 1993, Tanfani *et al.,* 1993). Paradoxically one particular TGase, tissue transglutaminase (TG2) is also involved in Ca^{2+} independent reactions, where the structure is maintained in a closed conformation by GTP/GDP, blocking its crosslinking activity but acting as a high molecular weight GTP binding protein and GTPase (Lee *et al.*, 1993). In the case of TG2, its transamidating activity is synonymous with the prevailing environment since low levels of Ca^{2+} intracellularly maintains its GTPase functions whereas extracellularly as Ca^{2+} levels increase, extracellular TG2 and Factor XIII assume either a transamidation or a cell adhesion related function (Belkin, 2011, Komaromi *et al.*, 2011, Wang *et al.*, 2010).

Cystic Fibrosis (CF) is an autosomal recessive inherited disease which is characterized by abnormal chloride secretion due to a defect in the gene encoding the chloride channel, the Cystic Fibrosis Transmembrane Regulator Conductance (CFTR) gene (Riordan *et al.*, 1989). There are over 1900 mutations recognised with defects varying from an absolute loss of the synthesis of the channel, defective processing, defective regulation of the channels to partial processing and production defects (Vankeerberghen *et al.*, 2002, Bobadilla *et al.*, 2002). Mutations associated with defective processing have been linked to the deletion of phenylalanine at position 508 (ΔF508), which has been discovered to be the most predominant mutation in the world accounting for more than 70% of mutations (Dalemans *et al.*, 1991, Lukacs *et al.,* 1993). However, studies have shown variations in the phenotypic expression of heterozygous and homozygous mutations of ΔF508 (Shoshani *et al.*, 1992, 1993)(Anon., 1993).

Recent studies have centred on TG2 due to its pleiotropic and ubiquitous nature and the role it plays in the pathogenesis of certain diseases with underlying fibrosis, where via its crosslinking activity, it can directly increase the deposition of matrix proteins like collagen and fibronectin making them resistant to proteolysis (Verderio *et al.,*2004, Verderio *et al*., 2005; Collighan and Griffin, 2009). Under pathological conditions when intracellular Ca^{2+} is raised, TG2 can also activate NF_KB by a non-canonical pathway (Mirza *et al*., 1997, Kim *et al*., 2006). In addition, activation of latent TGFβ1 has been linked to TG2 and in turn to the progression of fibrosis which is associated with the activation of the latent cytokine in the extracellular matrix (ECM) (Sheppard, 2006b, Johnson *et al*., 2007, Nunes *et al*., 1997). Along with some other TGases, TG2 exhibits diverse roles in the pathology of neurodegenerative diseases (Kim *et al*., 1999), inflammatory diseases, cardiac and kidney disease and neoplasms, either directly by covalently crosslinking proteins or indirectly by activation of pro-inflammatory cytokines eg TGFβ1.

Consequently, this study will attempt to understand the link between TG2 and cystic fibrosis (CF). It correlates the induction of the fibrotic cascade involving the dysfunctional changes caused by the mutated CFTR chloride channel which causes loss of epithelial cell integrity to the expression and activity of TG2 and its partner proteins ultimately leading to the proposal of a mechanism by which TG2 is involved in the EMT process.

1.2 TRANSGLUTAMINASES (TGases)

1.2.1 Functional domains of TGases

Currently, 9 mammalian TGases have been characterised as shown in table 1. All the enzymes have 4 domains: an amino N-β sandwich terminal, a Tryptophan-Cysteine-Histidine-Aspartate catalytic centre and two carboxylic acid C-β barrel domains (Iismaa *et al*., 2009).

Table 1.1: Different Transglutaminases and their function (adapted from Griffin *et al*., 2002)

Transglutaminases	Synonyms	Function
Transglutaminase 1	Keratinocyte TGase, TG1	Differentiation of keratinocytes
Transglutaminase 2	Tissue TGase, TG2	Cell differentiation, cell adhesion, cell death
Transglutaminase 3	Epidermal TGase, TG3	Cell envelope formation
Transglutaminase 4	Prostate TGase, TG4	Spermatogenesis
Transglutaminase 5	TGase X	Epidermal differentiation
Transglutaminase 6	TGase Y	-
Transglutaminase 7	Tgase Z	-
Plasma Transglutaminase	FX IIIa	Wound healing and blood clotting
Protein 4.2	Erythrocyte Protein Band 4.2	Inactive TGase (loss of Cysteine at catalytic site)

A1 **A2**

B

Figure 1.1: Ribbon diagrams of TG structure and linear domain configuration. A1. Ribbon diagram of GTP bound, closed inactive conformation showing amino, **N** (blue), and carboxylic, **C** (yellow and red), domains (arrow indicates GTP binding site). **A2** Ribbon diagram of TG2 inhibitor bound open conformation. **B** showing the 4 domains of the protein (βS, core and barrel 1&2) with the exons encoding the different domains indicated underneath. The active site (green), shown to carry the catalytic triad; Cysteine (Cys), Histidine (His) and Aspartate (Asp) with a conserved Tryptophan (Trp), that stabilizes the transition state. FXIII and TG1 have 15 exons and 14 introns with exon 1 and 2 been non-coding and amino terminal pro-peptide respectively while TG2-7 and Erythrocyte Protein 4.2 have 13 exons and 12 introns with exon 10 and 11 separated by one intron. Dotted lines represent the exons encoding the different structural domains of protein (Iismaa *et al*., 2009).

The thrombin activated form of plasma transglutaminase, Factor XIII (Factor XIIIa) and TG1 have in addition to the thirteen exons and twelve introns present in the other TGases, two exons; a non coding exon one and exon two that codes for the transitional N- terminal pro-peptide which is cleaved on activation of the TGases. As indicated from Figure 1.1 above, TGases 2-7 and Band 4.2 protein do not have the intron present between exon 10 and eleven as found in Factor XIIIa and TG1.The presence of the catalytic triad, Cysteine, Histidine and Aspartate represent the core of the catalytic activity of the enzyme, however, the presence of tryptophan helps to stabilise the transition state (Iismaa, 2003).

Although, the activity at the catalytic core revolves around the four domains on the catalytic core, studies have shown that this is the region conserved within different TGases (FXIIIa, TG1 &2) with minor differences in TG3 (Kim, 2001). For TG2, the four domains span amino acids 1-687, with the domains having amino acids from 1-139 (1^{st}), 140-454 (2^{nd}) (Small *et al.*1999), 479-585 (3^{rd}) and 586-687(4^{th}) respectively (Casadio *et al.*, 1999). Using TG2 constructs generated with a domain deleting approach, Iismaa *et al.,* (1997), showed that domains one and two were essential for the transamidating activity of TGases, the initial 47 residues of domain two are responsible for the GTPase and ATPase activity and domain four aids in maintaining the integrity of the active GTPase conformation *(*Monsonego *et al., 1*998*).*

Domain one has been shown to contain 7 of the 10 short β-structures, having β_1 as the isolated strand, tightly packed anti-parallel $\beta_{2\text{-}6}$ strand interacting with a β-sandwich motif and leaving at the lower β-sandwich end, a short β_7 strand that interacts with the β_1 strand (Griffin *et al*., 2002). Domain two contains peptide chains running along its surface, upwards and downwards, β-strands $\beta_{8 \text{ and } 9}$ contain the amino acid residues Ser^{171} and Lys^{173} which embeds the GTPase activity. Domain two also has an additional β-strand $\beta_{10\text{-}13}$ as well as four α-helices, with three of these arranged triangularly in the direction of the active site, Cys^{277}, His^{335} and Asp^{358} and the last α-helix sheltering the amino acids (Ser^{449}, Glu^{451} and Glu^{452}) involved in Ca^{2+} binding (Griffin *et al*., 2002). The residues in the active site harbouring amino acids 454-478, importantly are functionally involved in the TGase activity of the enzyme as they essentially remain exposed to substrates, however, this active site residue has different functions in other TGases (TG1, TG3 and FXIII). The double barrel C-domains three and four have β-anti-parallel strands with domain three having six β-barrels and one β-barrel turn and domain four having seven anti-parallel β-strands that have been shown to control both GTPase and ATPase activity (Lai *et al*., 1996).

1.2.2 Mechanism of activity of TGases

Transglutaminases have been shown to be involved in the post-translational modification of proteins either by covalently crosslinking them via a transamidation reaction or by their esterification and/or hydrolysis. The crosslinking reaction involves the formation of an acyl enzyme intermediate, glutamyl thioester, which is a product of the interaction between the active site cysteine (Cys^{277} for TG2) with an acyl acceptor protein containing glutamine and release of ammonia as a by product.

Figure 1.2: Schematic representation of TGase catalysed reaction. Calcium stabilised Transglutaminase 2 (TG2; green circle) is involved in the catalysis of glutamine side chain of a protein using its active thiol group (SH), which forms an intermediate thiolester (middle figure). This subsequently reacts either with a primary amine substrate ($R\text{-}NH_2$) to transfer the acyl side chain (transamidation) to form a simple amine isopeptidyl adduct or a ε-(γ-glutamyl lysine) protein (transamidated protein) or unfavourably with water where it undergoes a deamidation/hydrolysis reaction where the glutamine is converted to a glutamic acid (adapted from Pinkas *et al.,* 2007)

Although, the conformation of TGases is conserved amongst them, two different conformations, open and close conformation, which delineates the functional roles for some of the family members (Collighan and Griffin, 2009). The intracellular milieu supports a low Ca^{2+} concentration (100-200nM) and high GTP (50-300μM) which studies have shown supports a compact TG2 conformation of which the core catalytic site is not exposed and the enzyme is normally inactive (Greenberg *et al*., 1991). The conformational change observed with TG2 as shown by Pinkas *et al*. (2007), indicates that, although intracellularly TG2 exists in a GTP bound form, when secreted to the extracellular environment (Gaudry *et al.*, 1999b) through an unknown mechanism,

because of the increase in calcium, the enzyme changes its conformation and assumes an open conformation that exposes the active catalytic core to its substrates. In addition to TG2's intracellular and GTPase activity (Mian *et al.*, 1995), it may also have protein disulfide isomerase activity (Hasegawa *et al.*, 2003).

1.2.3 Different Types of TGases

Currently, there are 9 different types of TGases that have been characterised: TG1-7, Factor XIIIa and the inactive TGase, protein band 4.2. As earlier mentioned, all the TGases share a similar homology in terms of conformation and domains which is conserved from species to species with slight variations in functionality of enzyme, even band 4.2 found in red blood cells has 37-51% homology with other TGases (Candi *et al.,* 1998; Casadio *et al.,* 1999; Noguochi *et al.,* 2001; Ilsmaa *et al.,* 2009). Whilst, the catalytic site of TG have the Cys-His-Asp triad which requires Ca^{2+} ions for enzymatic activity, band 4.2 has an Ala-His-Arg triad which accounts for its loss of activity due to an exchange of alanine for cysteine (Carsadio *et al*., 1999; Korsgren *et al*., 1990). Greenberg *et al*. (1991) described the structural homology existing between TGase active sites and the calcium binding site, hypothesising that different substrates would aid in identifying different TGases.

1.2.3.1 Factor XIII (Plasma Transglutaminase)

The tetramer exists either as an intracellular cytoplasmic or extracellular plasma Factor XIII zymogen, with two subunits; A_2B_2 subunits, however the B_2 subunit does not exist for cellular Factor XIII. Plasma FXIII has an A_2 subunit, which is an 83kDa active transglutaminase subunit coded for by the FXIIIA gene on chromosome 6p 24-25 and the B_2 80kDa regulatory subunit coded for by the FXIIIB gene on 1q 31-32.1, which is the carrier of the A_2 subunit (Iismaa *et al*., 2009). The activation of the zymogen associated with blood coagulation is orchestrated by thrombin, which converts FXIII to its active form. In the presence of calcium and fibronectin, FXIII activity forms ε-(γ-glutamyl) lysine bonds between fibronectin monomers ultimately leading to the formation of stabilised clots (Ichinose and Davie, 1988). Furthermore, the central role FXIII plays in wound healing involves platelet activation and laying down of granulation tissues which marks the beginning of tissue adhesion (Griffin *et al*., 2002).

Studies have shown that, in patients with fibrosing alveolitis and wheezy bronchitis, activated FXIIIa is present in bronchoalveolar lavage liquid (BALF). This has been linked to increased capillary permeability, favouring increased plasma leakage. These conditions have been associated with chronic inflammation where FXIII A_2 is up regulated four to five times and alveolar macrophages have been put forward as a possible source of the enzyme *(*Katona *et al.,* 2005*)*.

1.2.3.2 Transglutaminase 1 (Keratinocyte transglutaminase)

Transglutaminase 1,TG1, is a membrane bound and soluble transglutaminase which is involved in the terminal differentiation of the cornified envelope (CE) in keratinocytes (Sturniolo *et al*., 2005). Like FXIII, TG1 exists as a zymogen, (106 kDa) and subsequently becomes activated during terminal differentiation of keratinocytes to form the CE (Iismaa *et al*., 2009). The cleaved membrane bound form of TG1 is embedded in the plasma membrane by myristic and/or palmitic fatty acid side chains (Eckert, 1989). In this form, it is found distributed between proliferating and differentiating cells. The active form of the enzyme is a complex of 67/33/10kDa, which has been associated with the activity of TG1 (Hiiragi *et al*., 1999). The expression of TG1 has also been found in cell-cell adheren junctions in lung, liver and kidney epithelial cells where it has been shown to co localize with E-Cadherin and zonula occludens, which are markers of cell-cell adheren junctions (Hiiragi *et al*., 1999).

Using immunohistochemistry, IHC, Martinet *et al.* (2003) showed that all cell types found in normal airway epithelium expressed TG1 except basal cells, which are regulated by extrinsic and intrinsic factors like growth factors, hormones and extracellular mediators (Eckert, 1989, Martinet, 2003). In TGase 1 null mice, it was observed that the anomalous skin function phenotype caused by the distortion of the keratinization process showed the importance of TG1 in epidermal development and the non compensatory role of TG2 and TG3 as mice died due to dehydration (Martinet, 2003). In concert, Eckert *et al.* (1989) suggested that TG1 levels increase as cells differentiate from the basal layer. High extracellular calcium has been shown to be important for the activation of TG1 as concentrations less than 1.2mM supported proliferation and concentrations above that initiated the formation of stratified layers and expression of differentiation markers (Eckert, 1989). As the level of calcium influx into the cell increases, it orchestrates the terminal crosslinking of involucrin by TG1, which is a soluble constituent of CE. The disruption of this process leads to the

introduction of an abnormality which may be linked to the cause of epithelial related diseases like cancers, hyper proliferative diseases and viral infections (Eckert, 1989).

1.2.3.3 Transglutaminase 3

Transglutaminase 3, TG3, exists as a zymogen, which undergoes proteolytic activation into its active complex of 50/27 kDa transglutaminase. Its 77kDa inactive form undergoes cathepsin L mediated activation to form the active form found expressed in the inner root sheath (IRS) of the hair canal (Shah *et al*.1999) and the distal end of the outer root sheath (Thibaut *et al*., 2008, Iismaa *et al*., 2009). TG3 has been shown to be responsible for the crosslinking of trichohyalin and keratin intermediate filaments, which are the proteins that make up the structure of the hair follicle, giving the hair tensile strength and shape (Lee *et al*., 1996).

Studies have been performed to determine the activity of TG3 and using monodansylcadaverine incorporation, activity was found to be confined to the IRS and hair shaft (Thibaut *et al*., 2008). The role of TG3 was however concluded to be embedded in the hair shaft where it is responsible for scaffolding which serves a protective function.

1.2.3.4 Transglutaminase 4

Transglutaminase 4, prostate transglutaminase, TG4, is a 77kDa protein, which has 684 amino acids. TG4 enzyme expression has been limited to the prostate where it is stimulated by androgens (Dubbink *et al*., 1996). Not until recently, expression was limited to rodents where it has been shown that the enzyme is implicated in the female reproductive tract as a copulatory plug after intercourse and as a protective regulator of the immune system preventing against the destruction of sperms as antigens in the female reproductive system (Cho *et al*., 2010). The dorsal prostate protein, DP1, which makes up 25% of the dorsal rat prostate and coagulating gland, has 53% similarity to human TGase. Dot blots for DP-1 have been used to show that the expression is limited to the rat prostate (Dubbink *et al*., 1998). However, Northern blot analysis of different human tissues did not reveal TG4 expression (Dubbink *et al*., 1996).

Although, there has not been a link to TG4 activity in human semen (Lilja and Laurell, 1985), TG4 has been implicated to be active in seminal plasma (Porta *et al*., 1986). For

example castrated infertile male guinea pig with extended seminal liquefaction as shown by immunohistochemical staining (Seitz *et al*., 1990) and masked antigenicity of sperms in the female reproductive system thus modifying its maturation process (Cho *et al*., 2010).

1.2.3.5 Transglutaminase 5

Analogous to TG1 and TG3, TG5, is an 81kDa protein, which stands as the most recently discovered and uncharacterised TGase. Activation of TG5 has been associated with terminal differentiation of the cornified cell envelope (CE) and hair follicle (Candi *et al.*, 2001). In keratinocytes, TG5 has been found to be deposited in the cytosol and localized perinuclearly (Candi *et al*., 2001). In relation to Epithelial - Mesenchymal Transition (EMT), TG5 has been found to co-localise with the vimentin intracellular filament network in fibroblasts where vimentin serves as an acyl donor substrate (Candi *et al*., 2001, Iismaa *et al*., 2009).

1.2.3.6 Transglutaminase 2 (TG2)

Tissue transglutaminase, TG2, is a ubiquitous transglutaminase enzyme found distributed in various cells *in vivo* and *in vitro* where it has been shown to be involved in both calcium-dependent and independent activity (Greenberg *et al*., 1991). The enzyme was originally discovered in liver (and thus referred to as Liver transglutaminases) but its distribution in many other tissues has implicated its role in the pathogenesis of many diseases (Piacentini *et al.*, 1991, Mirza *et al*., 1997, Small *et al.*, 1999, Griffin *et al*., 1979). As an enzyme, TG2 has been suggested to play roles in cell differentiation, cell survival, acting via receptors in endocytosis, apoptosis and tumour metastasis (Fesus *et al.*, 1989, Aeschlimann *et al.*, 1993, Johnson *et al.*, 1994). However, extracellularly, TG2 has been shown to play a vital role in cell adhesion and maintenance of the extracellular matrix (Martinez *et al*., 1994).

Intracellularly, transglutaminases are normally inactive due to the low levels of Ca^{2+} and increased GTP binding which maintains the closed inactive conformation (Bergamini and Signorini, 1993, Bergamini, 1988, Tanfani *et al.*, 1993, Iismaa *et al*., 2009). However, following trafficking and secretion into the extracellular matrix by an undefined mechanism, TG2 assumes an open active conformation. Kawai *et al.* (2008) suggested cell damage as a method of TG2 externalisation in response to membrane

repair. Increased Ca^{2+} levels open up the compact state of TG2. This then exposes the catalytic site rendering it active and exposes it to protein substrates, which becomes modified. Wang *et al.* (2012) demonstrated using stably transfected Swiss 3T3 cells under the control of a tet-inducible promoter that syndecan shedding was involved in the rapid translocation of TG2 into the ECM. However, binding to fibronectin and subsequent oxidation of the active site thiol can render the catalytic transamidation site inactive. In this state, the enzyme acts as a cell adhesion protein via its binding to fibronectin, integrins β1, β3, β5 and the heparan sulphate receptor, syndecan 4 and the G-protein coupled cell adhesion receptor GPR56 (Iismaa *et al.*, 2009, Verderio *et al.*, 2003, Telci *et al*., 2008, Wang *et al.*, 2010). This adhesion property is independent of the transamidating property of TG2.

TG2 is essentially located intracellularly within the cytosol, plasma membrane or nucleus, although it is found extracellularly within the extracellular matrix. Studies have shown that TG2 possesses no ER/Golgi signalling tags which has been attributed to an unglycosylated enzyme even though it might have glycosylation sites (Folk and Finlayson, 1977).

Studies by Griffin *et al.* (1979), showed that pulmonary fibrosis induced in rats by paraquat treatment could be attributed to a protein found in the "nuclear/membrane pellet" which was suggested to be membrane bound transglutaminase. In parallel, TG2 has been implicated in scarring in liver, lungs and kidney, of which in the latter, TG2 has been extensively studied where it has been shown to be a major player in the pathogenesis of Chronic Kidney Disease (CKD). Here, TG2's externalisation and crosslinking of ECM matrix in the presence of high calcium concentration, prevents ECM degradation by matrix metalloproteinases (MMP) (Johnson *et al.*, 1999, Johnson *et al*., 2007). Paradoxically, intracellular TG2 activated by changes in intracellular milieu in traumatised cells leads to an increase in calcium concentration ultimately leading to rapid cell death as a means of averting cell necrosis and cell disruption (Verderio *et al*., 1998).

1.3 TRANSGLUTAMINASE 2 AND ASSOCIATED PATHOLOGIES

In a review of the involvement of TGases in chronic diseases, much attention has been focused on the role the enzyme plays in wound healing and inflammatory diseases such as fibrosis and autoimmune diseases, degenerative diseases and

neurodegenerative diseases e.g. Alzheimer's, Parkinson's, arthritis, atherosclerosis and neoplasms. A myriad of TGases function by reinstating the integrity of the tissue during wound healing. Notably, FXIIIa, which, by crosslinking fibronectin and activating platelets, orchestrates the wound healing process and lays down the tissues essential for repair. TG2 chiefly has been implicated in inflammatory conditions like fibrosis (liver, kidney and lung) and cirrhosis (liver) where the enzyme has been suggested to crosslink proteins in the matrix due to enhanced expression as a result of progressive deterioration from fibrogenesis to fibrosis (Richards *et al.*, 1991). This in turn might be linked to the concomitant dedifferentiation of precursor epithelial or other cells. Also cytokines, growth factors and chronic stress have been shown to regulate the expression of TG2 in inflammation (Iismaa *et al*., 2009, Johnson *et al*., 1999, Richards *et al.*, 1991). In the liver, TNF-α induces the activation of Inhibitor of κB kinase (IκK). This in turn phosphorylates IκB (IκBα and IκBβ), which unblocks sequestered NFκB and uncovers the nuclear localisation signal (NLS) of NFκB. This phosphorylation allows the dissociation and translocation of NFκB into the nucleus and the activation of various genes including TG2 which has a binding motif for NFκB on its promoter site (Kuncio *et al*., 1998). In addition, TGFβ1 is up regulated in inflammation where TG2 is thought to cross link the large latent TGFβ1 binding protein (LTBP1) to extracellular matrix proteins i.e. fibronectin and collagen leading to the subsequent activation of TGFβ1. This together with matrix crosslinking by the enzyme leads to increased deposition and stabilisation of matrix proteins (Verderio *et al*., 1999, Nunes *et al.*, 1997, Griffin *et al.,* 2002). TG2 expression is elevated in diseases such as arthritis and certain neurodegenerative diseases like Parkinson's and Alzheimer's disease, which are characterised by increased mineralization at diseased joints or deposition of insoluble protein plaques respectively (Johnson *et al.*, 1997a, Plenz *et al.*, 1996). Other diseases in which TG2 has been implicated include coeliac disease, type 1 diabetes and Sjögren's syndrome (Villalta *et al.*, 2002, Seissler *et al.*, 1999, Arentz-Hansen *et al*., 2000) and recently CF (Maiuri *et al.*, 2008).

1.4 CYSTIC FIBROSIS (CF)

CF is an autosomal recessive disease characterized by a defective chloride channel, which is coded by a 230kb gene found on chromosome 7. The *CFTR* gene encodes the 1480 amino acid polypeptide, the cystic fibrosis transmembrane conductance regulator (CFTR)(Rommens *et al.,* 1989; Riordan *et al*., 1989; Kerem *et al*., 1989). The channel functions as a cAMP regulated chloride channel found apically in many

epithelial cells including sweat glands, salivary glands, pancreas, vas deferens in males and airway epithelium. Anderson first made the description of the salty skin in children with CF in 1938 and this led to the first description of the disease as "Cystic Fibrosis" (Anderson, 1938). Studies thereafter showed that the disease was characterized by high salt content in sweat due to abnormal reabsorption of chloride ions (Di sant Agnese *et al.,* 1953). Notable symptoms of the disease include high salt content in sweat, nasal polyps, infertility in men and reduced fertility in women, liver disease, diabetes and chronic sinusitis (Bombieri *et al*., 2011, Mak *et al*., 2000, Zielenski, 2000).

The disease is rare affecting 70,000 worldwide with over 1900 mutations defined (Bobadilla, 2002, Sparbel and Tluczek, 2011) and defects vary from an absolute loss of synthesis of channel, defective processing, defective regulation of ion channels to partial processing, defective conductance, defective regulation of affiliated channels and production defects (Vankeerberghen *et al*., 2002). Typically, pancreatic insufficiency is associated with the first three classes of defects (section 1.4.1), which accounts for the highest incidence of CF defects. The other classes have a lower incidence of pancreatic insufficiency (Ratjen and Doring, 2003).

Bobadilla *et al.* (2002) studied the variation of CFTR mutation worldwide and concluded that there was a wide heterogeneity to *CFTR* gene mutations but the mutation at position 508 on the gene correlated with a high incidence of the disease. This mutation, ΔF508, accounts for 70% of the disease occurrence involves the deletion of 3 base pairs at position 508 coding for phenylalanine. It is associated with defective processing, defectively glycosylated CFTR is translated but loses its resistance to degradation proteases. Hence, it is ultimately tagged for ubiquination in the cytosol (Jilling and Kirk, 1997). However, there are other mutations, one is characterised by a substitution of G for A at position 3978 on the base pairs of exon 20 of *CFTR* causing tryptophan to become a stop codon at position 1282 (W1282X) (Shoshani *et al.,* 1992). Kerem *et al*. (1990) showed that patients homozygous for the W1282X mutation showed the same disease severity to that heterozygous for ΔF508 /W1282X. This phenotype, which occurs mainly as a heterozygote, ΔF508 /W1282X, was shown to be associated with increased CFTR degradation in the ER due to rapid misfolding of the ΔF508 protein and such that 99% of the channel is lost with very little getting apically expressed (Vankeerberghen *et al.,* 2002). Interestingly, studies have shown that the expression of CFTR is tissue specific for homozygous ΔF508 and expression of the ΔF508 mutation in respiratory tract and intestinal tissue was the same as that found in non-CF wild type cells (Kalin *et al*., 1999).

1.4.1 Classes of CFTR mutation

The mutational defect on the CFTR gene has been classified into 6 different classes according to the dysfunctional effect of the mutation on CFTR. They are:

- Class I: Defective protein synthesis
- Class II: Defective protein processing
- Class III: Defective protein regulation
- Class IV: Defective or altered protein conductance
- Class V: Reduced CFTR level
- Class VI: Reduce CFTR stability

1.4.1.1 Class I: Defective protein synthesis

Mutations of this type are characterized by premature termination codons (PTCs) due to frameshifts and nonsense codons. This introduces an interference ultimately leading to the formation of truncated proteins with diminished mRNA half-lives which impedes protein synthesis due to nonsense-mediated RNA decay (NMRD) (Frischmeyer and Dietz, 1999). One of the foremost-discovered mutations belonging to this class is the W1282X mutation which involves a change in the nucleotide G−A at position 3978, which introduces a tryptophan stop codon at position 1282 (Shoshani *et al.*, 1992). This imparts on the severity of the disease as mutations of this class produce deleterious phenotypes. The use of the aminoglycoside antibiotic, gentamicin has been shown to aid with the read-through of PTCs in CF cells with an expression of full length CFTR in patients administered intranasal gentamicin (Wilschanski *et al.*, 2003). Similarly, using the orally bioactive molecule, Ataluren (PTC124), studies have shown that in patients with at least one nonsense mutation, PTC124 alleviates electrophysiological aberrations associated with *CFTR* mutations (Kerem *et al.*, 2008, Wilschanski *et al.*, 2011).

1.4.1.2 Class II: Defective protein processing

Under normal physiological conditions, CFTR protein undergoes a series of post-translational modifications in the endoplasmic reticulum (ER) and the Golgi where the protein becomes glycosylated and is folded with the aid of chaperone proteins supporting its trafficking to the apical membrane. This process is impaired in class II mutations with processing defects. Hence CFTR proteins are susceptible to an abnormally high (>99%) early degradation by ER-associated protein degradation (ERAD) systems (Ward *et al.*, 1995). The ΔF508 mutation is the most common class II mutation, characterised by the deletion of phenylalanine on position 508 of the gene (Riordan *et al.*, 1989). However, aside from the premature degradation the protein undergoes by ERAD, the minute amount of protein that gets to the plasma membrane post-Golgi further undergoes exocytosis where abnormal recycling reduces the copies of the channel on the apical membrane (Sharma *et al*., 2004). Studies have shown that the ΔF508 mutation is found on the nuclear binding domain 1 (NBD-1) of the protein (Thomas *et al*., 1991). Recent studies have shown that in the presence of "CFTR correctors", conformational correction of membrane spanning domain 1(MSD-1) can impact on the stabilisation of the NBD-1 and allow the processing of CFTR in patients carrying the ΔF508 mutation (Ren *et al.*, 2013). Corrector compounds like VX-809, are currently under clinical trials as lead compounds to modify ΔF508 CFTR function. Clinical trials have attempted using combinatorial therapy of CFTR correctors and CFTR potentiators in ΔF508 mutation to alleviate the trafficking and conductance of chloride ions (Clancy *et al*., 2012, Rowe and Verkman, 2013). Similarly, the histone deacetylase inhibitor, sodium 4-phenyl butyrate, 4-PBA, has been found to increase CFTR trafficking by up regulating chaperone proteins like heat shock protein, Hsp70, involved in folding the N-terminal NBD-1 of CFTR (Choo-Kang and Zeitlin, 2001).

1.4.1.3 Class III: Defective protein regulation

This class of mutations is characterised by a default either in phosphorylation or dephosphorylation of CFTR, hence the channel loses the ability to be regulated by cAMP. The gating route, which requires ATP to regulate the opening and closing of the gate is faulty thus CFTR trafficked to the plasma membrane is impaired. Examples of this class include G551D and Y569D. The G551D mutation is linked with severe phenotype depicted by severe pulmonary dysfunction and pancreatic insufficiency (Cutting *et al*., 1990). Also the G551D mutated CFTR channel has little or no ATP-

dependent gating traits (Bompadre *et al*., 2007). However, certain compounds known as “CFTR potentiators” have been shown to enhance the gating properties of class III mutations (Pasyk *et al*., 2009, Yu *et al*., 2012, Accurso *et al*., 2010).

1.4.1.4 Class IV: Defective or altered protein conductance

This class of CFTR mutations are synonymous to class III however the rate of chloride efflux is distorted. Examples of mutations in this group include R117H and D1152H. R117H mutations possess intragenic mutations where its disease causing ability lies within the poly-T tract region of the gene. This dictates the severity of the phenotype, with 5T poly-T tract characterized by elevated sweat chloride and increased male infertility risk whilst 7T poly-T patients have the contrary. In addition, studies have shown that R117H mutation are diagnosed late compared to ΔF508 mutations (Anon.,(1993).

Figure 1.3: The classification of CFTR mutations. The 6 different classes of mutation in CFTR ranging from class I (synthesis), class II (processional), class III (regulation), class IV (defective conductance), class V (reduced CFTR levels) to class VI (reduced CFTR stability). The different mutations ultimately lead to the production of defective, inactive, normal or reduced copies of CFTR at the apical surface. Each classification overtly determines the number of CFTR copies on the apical membrane of the cell, hence differences in their phenotypic expressions (Adapted Rowe and Verkman (2013)

1.4.1.5 Class V: Reduced CFTR level

Class IV mutation account for <1% of CFTR mutations and are characterised by the aberration in normal protein transcription hence reduces the amount of channel present at the apical membrane (Proesmans *et al*., 2008). This consequently leads to the production of abnormal mRNA splicing including exon skipping or intron inclusions, which ultimately disrupts exon recognition. This leads to a dissimilarity in correctly and aberrant mRNA transcripts in different organs within a patient as well as amongst different patients (Ramalho *et al*., 2002). An example is the 3272-26 A-G mutation, a splicing mutation which has been demonstrated to show less severity of CF phenotype in terms of pancreatic sufficiency, airway disease and presence of *Pseudomonas aeruginosa* as compared to patients with the ΔF508 mutation (Amaral *et al*., 2001).

1.4.1.6 Class VI: Reduced CFTR stability

This is a new class characterised with a high turn over of CFTR at the apical surface. However due to a C-terminal truncation, the CFTR channels becomes highly unstable (Haardt *et al*., 1999). As a consequence of a frameshift or a nonsense codon, up to 100 base pairs could be truncated at the C-terminus. eg 4326delTC.

Table 1.2: CFTR classes and their mutational defects

	Class I	**Class II**	**Class III**	**Class IV**	**Class V**	**Class VI**
CFTR defect	Defective protein synthesis	Defective protein processing	Defective protein regulation	Defective or altered channel conductance	Reduced protein level	Reduced protein stability
Type of mutation	Nonsense; Frameshift	Missense; Deletion of amino acid	Missense; Change of amino acid	Missense; Change of amino acid	Missense; Splicing defect	Missense; Change of amino acid
Mutation example	W1282X	∆F508	G551D	R117H	3272-26A-G	4326delTC

1.4.2 The Chloride Channel: CFTR

The CFTR protein is an ATP Binding cassette (ABC) transporter which has a central hydrophilic regulatory domain (R), two nucleotide binding domains (NBD) and six membrane spanning helices /domains (MSD). The mRNA exits the nucleus where tRNA transcribes it on the endoplasmic reticulum (ER). A series of convoluted processes ensue and the protein is N-glycosylated. This leads to an increase the molecular weight from 130kDa to 150kDa and subsequently folded, which renders it resistant to protease degradation in the endoplasmic reticulum, thus transported to the Golgi apparatus. The folding process is overtly inefficient leading to the formation of misfolded protein in one half of wild type CFTR (Lukacs *et al*., 1994). The ER retains within it chaperones such as calnexin and calreticulin that regulate folding of CFTR and function in concert with ER proteins including Heat shock proteins, Hsp 70, to redirect misfolded proteins to be degraded. In addition, these chaperones coordinate the transfer of CFTR to the Golgi (Sun *et al*., 2008, Rosser *et al*., 2008). In the Golgi, further glycosylation occurs where the mannose core glycosylated form is converted to a matured protein with an oligosaccharide side chain attached to the fourth extracellular loop of the MSD-1 bearing the asparagine residue (Lukacs *et al*., 1994). The matured band C protein, 170kDa is then clathrin-transported in vesicles and apically expressed in the cell membrane as a chloride channel, which functionally undergoes endocytosis and recycles itself to the apical membrane (Jilling and Kirk, 1997). The protein has a half-life of 16h, where cAMP drives its recycling process until such time when the protein is tagged for proteosomal degradation (Lukacs *et al*., 1993).

Essentially, the folding process within the ER is not robust and about 75% of wild type CFTR is degraded and ~ 25% of the protease resistant translational product gets to the Golgi (Varga *et al*., 2004). This infers that a significant amount of the protein is not folded properly and ultimately, gets degraded as it is tagged for the ubiquitin pathway (Vankeerberghen *et al*., 2002).

Figure 1.4: **The CFTR channel structure.** The cartoon shows the 3 domains of mature CFTR: Regulatory domain, R, Nucleotide binding domains 1 and 2, NBD1&2 and membrane spanning domains,1 and 2 MSD1&2. The two-glycosylation sites on the fourth extracellular loop are indicated. Phosphorylation of the R domain induces the hydrolysis of ATP on NBD1, which in turn causes the partial opening of the MSD1 and this then allows the flow of anions in the direction of the electrochemical current. As more ATP is hydrolysed on NBD2, MSD2 is open and now the channel is fully open. As the R domain becomes dephosphorylated by phosphatases, the channel closes (Vankeerberghen *et al*., 2002).

1.4.2.1 Mechanism of action

The CFTR channel has been described as a chloride channel with regulatory functions on other channels. Studies have reported that CFTR regulates the epithelial sodium channel (ENaC) by negatively regulating its function via down regulating its production (Stutts, 1997; Mall *et al*, 1996). On the contrary, Reddy *et al.,* (1999) showed that CFTR is essential for the activation of ENaC and a mutation of the CFTR channel would lead to loss of activity of the ENaC.

The CFTR channel functions with the R domain, being phosphorylated by activated protein kinase A (PKA), which is dependent on cAMP (Winter and Welsh, 1997, Hegedus *et al.*, 2009). The response would be NBD1 binding and hydrolysis of adenosine triphosphate (ATP). This causes the channel to open through the pore in the MSD1 as against the gradient and allows anions to flow through it (Vergani *et al*., 2005). The continuous phosphorylation of the R domain causes the second NBD2 to bind and further hydrolysing ATP and this further opens the pore of MSD2, which stabilises the open state. At a point when the R domain becomes dephosphorylated as

a consequence of protein phosphatases, PP2A or PP2C, it inhibits the ability of the NBDs to bind ATP, the channel closes (Travis *et a*l., 1997, Luo *et al*., 1998).

1.4.3 CFTR mutational phenotype

In CF, the CFTR channel which carries the mutation loses its ability to escape the Endoplasmic Reticulum Quality Control (ERQC) system because of it being enormously misfolded and becomes susceptible to degradation and it is rapidly cleared with a significant reduction in the amount of the channel been trafficked to the apical membrane (Grove *et al*., 2009, Jacquot *et al.*, 2008). Ribeiro *et al.* (2005) showed that CFTR hyper-inflammatory phenotype favours an increase in secretion of cytokines and a consequent up regulation in the level of ER calcium, Ca^{2+}, stores. This enhances interleukin-8, IL-8, production beyond basal levels and thus increases inflammation. However, because of the variation in tissue expression of mutant ΔF508 CFTR (Kalin *et al*., 1999) and possibly other mutations of the channel, the phenotypic expression differs between patients with mutations having pronounced defective expression of the mutant channel than the other i.e. in patients with the R117H allele, where the mutation is a missense mutation, sufferers are affected with high incidence of pancreatic insufficiency compared to ΔF508 with a contrary phenotype (Anon,1993).The ΔF508 mutation has been seemly linked with an upsurge of sodium, sodium ion absorption with a consequent reduction in airway surface liquid volume (ASL), which creates a viscid mucus on the surface of the airway epithelium (Konstan *et al*., 1994). The viscid mucus truncates defensin, which protects the airway against bacterial attack leading to a myriad of infections found in CF patients (Ratjen and Doring, 2003). The disease has been characterised with high salt content in sweat, other pathogenic symptoms include meconium ileus, pancreatic insufficiency, chronic cough, recurrent lower tract infections, mucoid sputum, biliary cirrhosis, nasal polyps, azoospermia, infertility and other rare symptoms (Davis and di Sant'Agnese, 1984). In concert, studies have shown that patients with class I-III mutations suffer a spontaneous deterioration of lung function with minimal survival rates (de Gracia *et al*., 2005). This is due to a near loss or complete loss of CFTR function (<3% of functional CFTR) in these patients (Welsh and Smith, 1993). Kerem *et al.* (1989) also showed that these mutations were associated with a rapid increase in pancreatic insufficiency. Also it was observed that male patients carrying the R117H-7T/ΔF508 mutations were infertile due to the absence of vas deferens, however, they may show normal lung function but present with disease phenotype consistent with CF patients (Colin *et al*., 1996, Castellani *et al.*, 1999). Dumar *et al.,* (1990) further showed that the loss of vas deferens, congenital

bilateral absence of vas deferens (CBAVD) was associated with 9/17 infertile CF men, which were associated with meconium ileus, a condition characterised by an obstruction of the intestine. This was related to patients with pancreatic insufficiency across class I to class III mutations (Feingold and Guilloud-Bataille, 1999, Hamosh *et al*., 1992). Studies have pointed out the variations in CF phenotype amongst patients is largely influenced by environmental and genetic modifiers (Ferec and Cutting, 2012, Drumm *et al.*, 2005). Consequently, studies have linked the occurrence of certain diseases to mutations of CF and termed them collectively as "CF-related diseases", CF-RD (Bombieri *et al*., 2011). Some examples of CF-RD are idiopathic chronic pancreatitis and disseminated bronchiectasis. In all, these findings continue to improve on the therapy regimen for CF patients and provide insights into potential targets for patients based on their mutations.

1.5 TG2 and Fibrosis in the lungs

The multiplicity of functions of TG2 surrounds its ubiquitous nature and its involvement in the pathology of various diseases. Its role in tissue damage and cell stress has been elaborated in various studies where an increase in its transamidation activity has been observed (Upchurch *et al.*, 1991, Johnson *et al.*, 1999). Wound healing is made up of 5 basic phases; haemostasis, inflammation, proliferation, remodelling and scar formation and scar maturation phases (Enoch and Leaper, 2008). From the inflammatory to the remodelling phase, high levels of cytokines and growth factors are secreted which include VEGF, IL-1, TGFβ and TNFα. The proliferative phase includes fibroblast migration with TGFβ implicated, formation of the extracellular matrix with the deposition of collagens and fibronectin, formation of granulation tissue and reepithelialisation. With scar formation, the wound begins to contract and collagen turnover ensues via metalloproteinases, which are tightly controlled to prevent untoward distortion of the healing process. Remodelling further inactivates metalloproteinases, reduces macrophages and fibroblasts whilst allowing scars to mature. In chronic wounds, various proteases and inflammatory cytokines remain elevated and this forges the development of fibrotic tissues.

Increased expression of TG2 in wound healing is important as it regulates the inflammatory responses and modulates ECM deposition and remodelling (Shah *et al*., 1999). Its complex interaction with fibronectin (FN), which is important in cell adhesion and migration, requires an intact N-terminal FN binding site (Gaudry *et al.*, 1999a). In

concert, using Swiss 3T3 fibroblast cells under the Tet-regulated system, studies have linked an increase in fibronectin fibrils with an increase in TG2 expression in TG2-induced cells compared to control and have suggested the crosslinking activity of TG2 to be important in the stabilisation of the matrix (Verderio *et al.*, 1998). However, it was concluded in these studies that TG2 activity was independent of cell motility. Albeit, in a related study, cell surface TG2 was implicated in migration as TG2 targeting monoclonal antibody was shown to block the migration of 3T3 Swiss fibroblasts (Balklava *et al*., 2002). In this study 3T3 Swiss fibroblasts were transfected with catalytically active and inactive (Cys277Ser mutant) under the tet-inducible system, which showed increased activity in homogenates and cell surface as well as comparable activity to wild type protein. Increased TG2 activity sustained an elevation in TG2 externalisation. These results demonstrated that on fibronectin, migration was decreased in both active and inactive TG2 mutants transfected into fibroblasts suggesting that TG2 acts independently of its transamidating activity during migration. Interestingly, in all, TG2 was demonstrated to be important in wound healing as the TG2 deficient mouse ($Tgm2^{-/-}$) was shown to have delayed wound healing and delayed fibrosis compared to wild type (C57BL/6) after 21 days of administering bleomycin (2.5 U/kg) (Olsen *et al.*, 2011). At the epicentre of TG2's involvement with fibrosis is the study made by Griffin *et al*. (1978) showing that when rats were treated with bleomycin, TG2 expression and activity was elevated and this was illustrated to be associated with an increase in fibronectin deposition as well as the mesenchymal collagen synthesizing fibroblasts. Similarly, Mirza *et al*. (1997) showed in rats treated with carbon tetrachloride (CCl_4) that TG2 expression and activity increase in liver corresponding with the development of hepatic fibrosis. This was in concert with studies in renal fibrosis in rats having undergone subtotal nephrectomy and where extracellular TG2 levels were shown to be elevated and active within the ECM (Johnson *et al.*, 1997b).

Nunes *et al.* (1997) demonstrated the link between TG2 and TGFβ1 where latent TGFβ binding protein 1 (LTBP1) was shown to be a substrate of TG2, hence TG2 was suggested to be involved in the storage and activation of latent TGFβ1 in the ECM. Olsen *et al*., (2011) showed that TGFβ1 treatment of Human Lung Fibroblasts (HLF) caused an increase in extracellular TG2 expression and activity, which was commensurate to the progression of Idiopathic pulmonary fibrosis (IPF). These results were in agreement with that of Shweke *et al.* (2008) where TG2 knockout mice showed amelioration of collagen deposition, renal inflammation and myofibroblast infiltration corresponding to a reduction in TGFβ1 secretion. Also, the up-regulation of TG2 in 3T3 Swiss fibroblasts regulated by the tet inducible system was shown to significantly elevate the secretion of TGFβ1 and as well as deposition of collagen I, III, IV and

fibronectin in the ECM (Telci *et al*., 2009). Together, all these findings support the role TG2 plays in wound healing, migration, and activation of TGFβ1, which ultimately fosters the progression of fibrosis.

1.6 TGFβ1: A pleiotropic cytokine activated by TG2 in Fibrosis

1.6.1 Activation of TGFβ1 and induction of TG2 expression

TGFβ1, a pleiotropic cytokine, has been shown to be involved in fibrosis in various pulmonary diseases like asthma (Hackett *et al.*, 2009), IPF (Kasai *et al*., 2005), acute lung injury (Pittet *et al.*, 2001) and CF (Eickmeier *et al*., 2013, Drumm *et al.*, 2005). It is secreted as part of an inactive complex of latent TGFβ bound non-covalently to its propeptide, latency associated protein (LAP) forming the small latent complex (SLC). In turn, the SLC is bound covalently to a large TGFβ binding protein (LTBP) to form the large latent complex (LLC) (Munger *et al.*, 1997). Its activity has been linked to its activation from its inactive latency complex (LLC), where LTBP-1 is cross linked to the ECM by TG2 (Nunes *et al.*, 1997) and LAP bound to TGFβ dissociates from the LLC due to temperature and pH changes and becomes proteolytically activated to release the active TGFβ. Thus the presence of LAP inhibits the activation of TGFβ. Free active TGFβ can then bind to serine-threonine TGFβ receptors, Type RI and RII (Massaous and Hata, 1997). The phosphorylation and activation of RI recruits RII which activates the receptor where a complex is formed which binds to certain transcriptional factors intracellularly for signal transduction, either through the SMAD or non-SMAD pathway (Heldin *et al.*, 1997). TG2 has been shown to be involved in the activation of TGFβ1 by crosslinking the LLC via LTBP-1 to the extracellular matrix and releasing the small latency complex comprising the inactive TGFβ bound to latency associated peptide (LAP) (Nunes *et al*., 1997, Telci *et al.*, 2009). This has been suggested as the rate-limiting step in the activation of TGFβ1.

Figure 1.5: Activation of TGFβ1 by TG2. The latent TGFβ complex is secreted from the cell where TG2 activity crosslinks LTBP-1 to the matrix, releasing SLC with TGFβ and LAP. TGFβ is activated proteolytically dissociating LAP, with TGFβ binding to the receptor, RII, which recruits RI and the complex is phosphorylated hence activating intracellular SMADs 2 and 3 which are phosphorylated subsequently and form a complex with SMAD-4. This complex is translocated into the nucleus. The complex is then responsible for the activation of target genes which may include TG2 [Adapted from Bartram,(2004)]

Studies have also shown a marked up regulation of TG2 mRNA and activity levels in normal human epidermal keratinocytes (NHEK) treated with TGFβ1 within 4h of treatment (George *et al.*, 1990). Ritter and Davies (1998) subsequently showed that the increase in TG2 expressional levels could be attributed to a the presence of a composite TGFβ1 or bone morphogenetic protein-4, TGFβ1/BMP-4 response element, 868 base pairs from the transcription start site on the TG2 promoter. However, other studies have correlated the activation of TGFβ1 to the presence of αVβ6 and αVβ1 integrins and to a lesser extent αVβ5, where the avidity of the integrin for TGFβ1 via the RGD binding site on LAP induces an activation of TGFβ1 in a paracrine manner (Ritter and Davies, 1998, Sheppard, 2005, Munger *et al*., 1998). This has led to the suggestion that TGFβ1 activation by αVβ6 requires cell-to-cell contact, as activation does not release active TGFβ1. Similarly, αVβ8 integrin was shown to activate TGFβ1 by promoting the degradation of LAP on presenting latent complexes to metalloproteinases i.e. MMP-14 thus releasing the active TGFβ1 (Mu *et al*., 2002). In all, TG2 has been demonstrated to be involved in binding tightly fibronectin and other matrix proteins, thus aiding the incorporation of LTBP-1 into the matrix and increasing cell to cell contact which ultimately activates TGFβ1 (Verderio *et al*., 1999). In concert,

αVβ6 integrin has been shown to require fibronectin for the activation of latent TGFβ1 (Fontana *et al*., 2005). Also, studies have suggested other cytoplasmic proteins might be involved in αVβ6 dependent TGFβ1 activation as mutational deletion of β6 subunit blocks the ability of αVβ6 to activate TGFβ1 but not its adhesion to LAP (Sheppard, 2005). This suggests that TG2 and αVβ6 integrin might be working simultaneously in the activation of TGFβ1.

In a myriad of fibrotic conditions, TG2 and TGFβ1 have been illustrated to be elevated corresponding to the progression of the disease process. Various pathways have been postulated with these conditions. Notably is the NFκB pathway (Telci *et al*., 2009, Venkatakrishnan *et al.*, 2000, Vij *et al*., 2009, Luciani *et al*., 2009a) and more recently the Epithelial to Mesenchymal pathway (EMT) (Heldin *et al.*, 2012, Kasai *et al*., 2005, Olsen *et al.*, 2011, Miettinen *et al.*, 1994).

1.6.2 TG2 and NFκB

In CF, studies have attempted to show the involvement of the NFκB inflammatory pathway in the initiation of inflammation and progression of fibrosis. A mutational destabilisation of the internal cellular milieu in CF has been shown to account for an elevated level of calcium in the cell, which together with ERAD stress supports the activation of NFκB.

Pahl *et al.* (1996) proposed that for homozygous ΔF508, the mutation was associated with an increase in calcium levels and reactive oxygen species (ROS) and subsequent activation of NFκB. However, in a related study the mutant, G551D, with defective regulation, showed CFTR getting past the ER without being degraded and trafficking to the apical membrane with complete loss of CFTR protein function, but did not stimulate NFκB (Comer *et al*., 2009, Fulmer *et al*., 1995). Hudson (2004) also proposed that the ΔF508 mutation induces an imbalance in the physiological levels of anions of which glutathione, which protects against oxidants in the lungs is significantly reduced and this leads to a consequent increase in Ca^{2+} release from intracellular stores. Vij *et al*. (2009), described CFTR as a negative regulator of the NFκB mediated innate response with a decrease in IL-8 expression in wild type cells and a reversal in overexpressed CFBE41o^{-} cells. Studies have also shown that high levels of ROS were associated with increases in TG2 activity (Luciani *et al.,* 2009). Consequently, because TG2 activity (transamidating) is associated with high calcium levels, it could be inferred that as a consequence, TG2 activity could be linked to a high levels of calcium within the cell

due to the high levels of ROS in cell. However, the effects of intracellular Ca^{2+} depends on the levels of GTP in the cells as GTP alters the binding of TG2 to Ca^{2+} thus impeding the activation of the enzyme intracellularly (Bergamini, 1988). Studies have shown in IB3 cells, a CF cell with an heterozygous mutation, ΔF508 /W1282X and C38 cell, the corrected "add-back" CFTR cell line with a truncated but functional CFTR, that basal calcium levels were shown to be higher in IB3 cells and attributed to cell stress (Weber *et al*., 2001, Tabary *et al.*, 2006). As a result, using immunofluorescence, basal NFκB activation was illustrated as seen with the translocation of p65, NFκB homodimer into the nucleus in IB3 cells but minimal p65 was found in C38 (DiMango *et al*., 1998). Luciani *et al.,* (2009) suggested that SUMOylation, which is a process whereby proteins are modified post-translationally at their C-terminal and which alters binding and transport, accounts for the non-ubiquitination of TG2 for degradation thus prolonging its half-life. As a consequence, activated TG2 has been suggested to activate NFκB through a constitutive polymerisation of IκB-α, releasing NFκB for translocation into the nucleus where it acts as a transcriptional activator which then induces the transcription of TG2, CFTR (Trezise and Buchwald, 1991) and inflammatory cytokines, IL-8 (Bonfield *et al*., 1999), IL-1β, TNF-α and IL-6 (Osika *et al*., 1999). These cytokines orchestrate infiltration, serving as chemoattractants of polymorphonuclear cells (PMN), neutrophils into the lungs. The untoward effect is the production of elastase which damages lung tissue and truncates the mechanisms involved in the ingestion of bacteria thus allowing bacteria to thrive (Chmiel and Davis, 2003). This ultimately favours chronic inflammation.

1.6.3 TG2 and Epithelial to Mesenchymal transition (EMT)

The foremost role of EMT is in organogenesis where it coordinates cellular development via its ability to stimulate mesoderm synthesis from the epithelium during gastrulation and heart development (Hay, 1995, Boyer *et al.*, 1999). However in effect, EMT is a phenomenon where epithelial cells transcend into mesenchymal cells with a change in phenotype thus acquiring a motile myofibroblast-like morphology and loss of the characteristic cobblestone like structure and cell polarity (Miettinen *et al.*, 1994). This is accompanied by the acquisition of EMT markers, N-cadherin, fibronectin, α-smooth muscle actin, α-SMA and loss of the tight junction marker, E-cadherin (Lee *et al*., 2006, Willis and Borok, 2007).

Tight junctional proteins have been shown to provide a sealing on the lateral side of the cell where they function to impede paracellular diffusion providing a distinction between

apical and basolateral surfaces with proteins including occludin and zonula occludens (Tsukita *et al.*, 2001). Par proteins (3 and 6) are involved in maintaining the polarity complex on the apical surface of the cell as well as junction integrity (Assemat *et al.*, 2008).

The development of EMT is associated with elevated levels of cytokines which have been shown to elicit a proteolytic breakdown of the basal epithelial membrane thus supporting the invasive nature of the process (Kalluri and Neilson, 2003). TGFβ1, EGF, IGF-2 and other cytokines have been shown to be involved in promoting this process. TGFβ1 via SMAD-dependent or SMAD-independent pathways i.e. MAP kinase pathway enhances this process, causing an elevation in the expression and stabilisation of matrix proteins as well as TG2.

Figure 1.6: Schematic illustration of the process of EMT. An initial loss of tight junctional /adhesion markers (left of image) is followed by the loss of cell polarity and actin skeleton reorganisation leading to cell migration and basal cell membrane degradation. This is commensurate with loss of epithelial markers; E-cadherin, claudins and occludins and an increase in the EMT markers N-cadherin, fibronectin, collagen I/II and vimentin (from left to right of image). The cells lose their pseudostratified structure, with simultaneous loss of apical cilia and assume a fibroblast-like structure with migratory character (Adapted from Aroeira *et al*., 2007).

Studies have shown that TG2 is involved in mediating EMT in tumour epithelial cells (Kumar *et al.,* 2010). The induction of EMT was shown to progress with an increase in the expression of transcriptional repressors like *Snail, Slug, Twist and Zeb*, where the expression of vital proteins like *Par, Crumbs* and *Scribble*, involved in maintaining

apicobasal polarity and junctional integrity, are disrupted by the expression of these transcription repressors (Thiery, 2002).

The increased development of myofibroblasts cells, intermediate specialised fibroblast cells with both fibroblast and smooth muscle cell characteristics, serves as a hallmark of EMT as these cells have been shown to express α-smooth muscle actin (α-SMA), a marker of smooth muscle thickening and are stimulated to differentiate by TGFβ1 (Kasai *et al.*, 2005, Willis and Borok, 2007).

Studies have shown that when human lung fibroblast cells, expressing low levels of TG2, were transduced with viral TG2 plasmid and treated with 5ng/ml of TGFβ1, TG2 protein expression was significantly elevated (Olsen *et al.*, 2011, Kelley *et al.*, 1991). Likewise, when primary Human Bronchial Epithelial cells (HBEC) were treated with 5ng/ml of TGFβ1, an increase in N-cadherin, vimentin, α-SMA, p-SMAD2 and MMP-2 was observed with a reciprocal decrease in E-cadherin expression (Camara and Jarai, 2010). With these findings, it can be postulated that elevated levels of TG2 might be involved in driving EMT progression via TGFβ1 in epithelial cells.

1.6.3.1 SMAD dependent EMT

The intricate processes involved in the activation of TGFβ1 are followed by a sequential course of events required for its intracellular signalling. SMADs, which are a subclass of a closely related gene, *mothers against decephapentaplegic* (MAD) found in Drosophila. They were discovered in nematodes and have been shown to be an important transcriptional regulator involved downstream in the control of intracellular signalling for TGFβ in the cell (Kretzschmar and Massague, 1998, Massague, 1996). SMADs are subdivided into 3 classes based on structural and functional characteristics and includes; receptor/regulator SMADs, R-SMADs (SMAD 1,2,3,5 and 8), collaborating SMAD, Co-SMAD (SMAD 4) and Inhibitory SMADs (SMAD 6 and 7). R-SMADs are direct substrates for TGFβ with SMADs 1, 5 and 8 being BMP receptor substrates and SMADs 2 and 3 in addition to being substrates for TGFβ are substrates of activins (Graff *et al.*, 1996). Hence, R-SMADs have been demonstrated to translocate into the nucleus where they are involved in transcriptional activation of genes (Hoodless *et al.*, 1996). In concert, R-SMADs require co-SMAD 4, which constantly undergoes nucleocytoplasmic shuttling for signalling functions (Zhang *et al.*, 1996). Conversely, inhibitory SMADs, 6 and 7 act by blocking the binding of activated R-SMADs to SMAD 4 (Hata *et al.*, 1998).

In the resting cell, basal R-SMADs are located in the cytoplasm however, on phosphorylation which occurs within 15 min of TGFβ binding to its receptors and lasts for hours, they undergo nucleocytoplasmic shuttling where co-SMAD 4 binds to the c-terminus of R-SMADs to form complexes involved in activating target genes until their dephosphorylation occurs which causes R-SMADs to return to the cytoplasm (Massague *et al*., 2005, Chacko *et al*., 2004, Xu *et al*., 2009).

With regards to EMT, elevation of R-SMADs 2 and 3 together with co-SMAD 4 has been shown in murine mammary epithelial cells, NMuMG, treated with TGFβ to correspond to EMT and TGFβ inhibition has been shown to reverse the process (Piek *et al*., 1999). Interestingly, it was shown that while SMAD 3 expression was elevated in the presence of TGFβ, which causes renal tubular cells to undergo EMT, loss of SMAD 2 reciprocally promoted EMT in keratinocytes (Sato *et al*., 2003). Research has shown that 3 transcriptional families transitionally regulate induction of EMT by SMADs namely; *Snail, Zeb* and Helix-loop-helix family (Xu *et al*., 2009).

1.6.3.1.1 Snail

The *snail* transcriptional group function as transcriptional repressors, where their activity has been shown to be mediated by 3 distinct members, *snail1, snail2* (slug) and *snail 3* (Xu *et al*., 2009). Expression of *snail* 1 and 2 has been associated with TGFβ induced EMT (Barrallo-Gimeno and Nieto, 2005, Zavadil and Bottinger, 2005). SMADs 2 and 3 have been shown to be involved in mediating *snail* expression on binding to the promoter sites after TGFβ activation (Cho *et al.*, 2007, Hoot *et al.*, 2008). Thus an induction of EMT correlates with an increase in expression of EMT markers, N-cadherin, fibronectin, vitronectin and collagen V as well as with the repression of E-cadherin, junctional proteins and the cell polarity protein, *Crumb 3* expression (Ikenouchi *et al*., 2003, Wang *et al.*, 2007, Moreno-Bueno *et al*., 2006, Cano *et al*., 2000).

1.6.3.1.2 Zeb

This group of transcriptional repressors are made up of 2 members; *Zeb* 1 and *Zeb* 2 which have been shown to have SMAD interaction domains. TGFβ induced EMT increases *Zeb* expression via SMAD-3, where repression of proteins involved in maintaining epithelial cell integrity have been observed (Postigo *et al.*, 2003). Again,

Comijn *et al.* (2001) linked *Zeb 1* induction to the decreased expression of E-cadherin ultimately supporting cell invasiveness.

1.6.3.1.3 Helix-loop-helix

Amongst the members of the helix-loop-helix transcriptional repressors, *Twist 1* and *2* as well as E12 and E47 are the most well known. The down regulation of E-cadherin, occludin and claudin has been linked to the up regulation of *Twist* 1 and 2 which studies have shown to always heterodimerise with E12 and E47proteins and EMT markers, N-cadherin and vimentin (Yang *et al.*, 2004, Comijn *et al.*, 2001)

1.6.3.2 SMAD independent EMT

The induction of non-SMAD pathway signalling occurs via TGFβ RII or RI through adaptor proteins like TNF-receptor associated factor, TRAF-6, *Par-6* and PI3K and this occurs independently of SMAD signalling, thus blockage of TGFβ receptors abrogate signalling through this pathway (Xu *et al.*, 2009). Research has shown that the non-SMAD pathways are linked to TGFβ-induced EMT as they have been shown to regulate cellular processes involved in EMT like actin organisation, cell migration, growth and invasion (Derynck and Zhang, 2003). Together with the SMAD dependent pathway, non-SMAD pathways are involved in EMT progression as inhibition of this pathway abolishes EMT. Three downstream pathways have been classified namely; Erk MAP Kinase, Rho GTPase and PI3 Kinase/Akt pathway.

1.6.3.2.1 Mitogen activated protein kinase (MAPK) pathway

The MAPK pathway have been shown to be activated via tyrosine kinase receptors on binding of growth factors, which studies have linked to elevated pathway activity compared to MAPK activation by TGFβ (Derynck and Zhang, 2003). R-SMADs signalling is likewise blocked by the Erk-MAPK pathway by phosphorylation of the linker regions thus impeding their transcriptional activity (Xu *et al.*, 2009). Studies have shown using rat intestinal epithelial cells that a synergy between Ras-Erk-MAPK

pathway and TGFβ is driving EMT as E-cadherin expression was inhibited (Uttamsingh *et al*., 2008). Similarly, an up regulation and stabilisation of *Snail 1* was linked to an activation of the Ras-Erk-MAPK pathway, which was similar to a TGFβ induced elevation of N-cadherin and matrix MMP in pig thyroid epithelial cells (Grande *et al.*, 2002, Marchetti *et al.*, 2008).

1.6.3.2.2 Rho-GTPases

In accord with EMT progression, an elevation of Rho-GTPases has been linked to the increase in expression of its effector kinase, ROCK, leading to increased cell migration and development of stress fibres (Pellegrin and Mellor, 2007). The complex formed by TGFβ RI / *Par 6* which allows the phosphorylation of *Par 6* by TGFβ RII recruiting *Smurf-1*, an E3 ubiquitin ligase, which activates the ubiquitination of Rho-A, leading to the degradation of tight junction proteins (Ozdamar *et al*., 2005).

1.6.3.2.3 PI3 Kinase/Akt pathway

Unlike the marginal effect of TGFβ observed on tyrosine kinase receptors in stimulating the activation of MAPK pathway, TGFβ rapidly activates PI3 kinase activity, which regulates cell survival and cell migration (Yi *et al.*, 2005). Cho *et al.,* (2007) showed in primary lens epithelial cells that activation of R-SMADs 2 and 3 by TGFβ leads to the down-stream activation of *Snail* and this was linked to the activation of Akt signalling in these cells (Cho *et al*., 2007). Also, blocking of the PI3 kinase /Akt pathway reverses SMAD 2 phosphorylation in NMuMG mammary gland epithelial cells induced by TGFβ1 (Bakin *et al*., 2000). This implies a possible interaction between the SMAD and PI3 kinase/Akt pathway.

In all, these studies have been able to link TGFβ activation and signalling via its receptors to the phosphorylation of SMADs and activation of non SMADs pathways in epithelial cells ultimately leading to the progression of EMT. However, recent studies have linked the elevation of TG2 in mammary epithelial cell lines to the activation of TGFβ, which in turn down regulates E-cadherin expression and up regulates fibronectin, N-cadherin and transcriptional repressors, *Snail 1, Zeb 1, Zeb 2* and *Twist 1* (Kumar *et al.*, 2010). In a related study using ovarian cancer cells, elevation of TG2 by TGFβ caused an activation of the canonical SMAD pathway inducing EMT by the formation of spheroids and cell metastasis (Cao *et al*., 2012). Also in the study by

Tovar-Vidales *et al*., (2011) using non-transformed primary human tubercular meshwork cells treated with TGFβ, results showed an elevation of TG2 protein and activity corresponding to the phosphorylation of SMAD-3 (Tovar-Vidales *et al*., 2011). This all supports the hypothesis that TG2 is involved in driving EMT in epithelial cells.

1.7 Culturing of airway epithelial cells in air liquid interface (ALI)

Traditionally, submerged cultures have been long established for culturing cells of all types. The *in vitro* technique is quite robust and allows for easy manipulations of cells to obtain reproducible results. In submerged cultures, cells are grown on plastic plates, which allows the dispersed and isolated cells to adhere and proliferate under appropriate conditions (Yankaskas *et al.*, 1985). Typically, epithelial cells *in vivo* assume a pseudo-stratified columnar structure comprising of basal cells, secretory (mucus, goblet or serous) cells and apical ciliated cells, which make up about 50% of the cell population (BeruBe *et al.*, 2009). Studies have shown that epithelial cells in submerged culture grown in monolayers were flattened, with significant loss of cilia, which is a characteristic of epithelial cells *in vivo* and low electrical currents (de Jong *et al.*, 1994, Yamaya *et al.*, 1992). Paradoxically, cells cultured and induced to differentiate at Air Liquid Interface (ALI) using appropriate medium and growth conditions, which include substrate, simulated *in vivo* epithelial ultrastructure and this has been shown to be reproducible (Lee *et al*., 1996). At ALI, epithelial cells are grown on a membrane with high pore density and porosity which allows for the exchange of nutrients from the lower basolateral compartment with medium to the apical surface of the cells (Gruenert *et al.*, 1995).

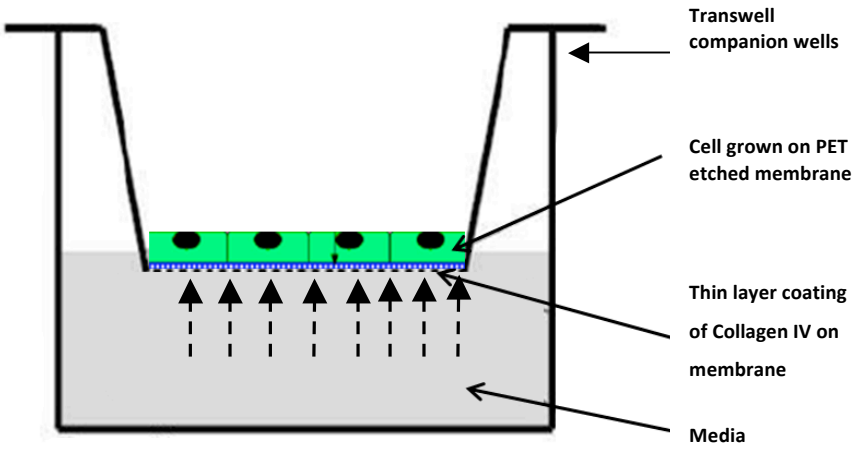

Figure 1.7: Schematic illustration of the ALI cell culture system. Transwell® inserts are placed into companion plates; the inserts have PET etched membrane with an area of 0.33cm^2 and a pore size of 0.4µm. The membrane has 100% porosity, which allows for the exchange of nutrients from medium and biologic waste from cells. Insert membranes are coated with collagen IV before cells are allowed to attach, after which the medium on the apical cell surface is removed and cells are presented in an air liquid interface.

Studies have shown that the three basic requirements for cells to undergo differentiation at ALI is the presence of retinoic acid (Ann *et al*., 1988, Chopra *et al.*, 1989) collagen gel and ALI (Wu *et al.*, 1990). Yamaya *et al.* (1992) suggested that at a plating density of 3 x 10^{5}cells/cm^2, differentiated cultures could be maintained at ALI for one month. It has also been shown from studies (Yankaskas *et al.*, 1985, Wu *et al.*, 1985, Gruenert *et al.*, 1995) that culturing of airway epithelial cells on collagen substratum increases ciliogenesis and hence mucus production which, *in vivo* serves as an artificial sieve that traps and prevents inhaled particles from getting to the epithelium .The growth of the cells on suitable substratum like collagen IV has been proven to support the activation of cell surface receptors and allows the cells to attach so as to form cuboidal epithelium by providing the suitable extracellular matrix (Robinson and Wu, 1993). In concert, this model favours higher aeration of cells which enhances differentiation (Johnson *et al.*, 1993).

1.8 Overall Aims

This project is chiefly aimed at finding the relationship between the expression and activation of TG2 and the development and progression of fibrosis in CF. The objectives include examining the link between TG2 activity and TGFβ1 activation and the effect on epithelial cell migration as well as regulation of EMT. In addition, by using TG2 knockdown cells, observe the effect of reduced TG2 expression on EMT progression. Conversely, using TG2 transduced cells to observe the effect of TG2 elevation on EMT progression. Finally, using CFTR correctors and TG2 inhibitors, to correct the maturation of CFTR protein and improve its trafficking to the apical surface where chloride could be evaluated.

Chapter 2

Materials and Methods

2.0 Materials and Methods:

2.1 Materials

2.1.1 Antibodies:

ANTIBODY	COMPANY	ISOTYPE	APPLICATION
Transglutaminase 2 (CUB7402 + TG100)(MA5-12989)	THERMO SCIENTIFIC	Mouse	ICC, WB
Transglutaminase 2(SAB4200072)	SIGMA ALDRICH	Rabbit	WB, ICC, C0-IP
Transglutaminase 1(B.C.1)	ABCAM,UK	Mouse	WB
E-Cadherin (H-108)	SANTA CRUZ,UK	Rabbit	WB, ICC
N-Cadherin (13A9)	SANTA CRUZ,UK	Mouse	WB, ICC
α-SMA (B4)	SANTA CRUZ,UK	Mouse	ICC
CFTR (A3)	SANTA CRUZ,UK	Mouse	WB, ICC
Na^+- K^+ ATPase (H3)	SANTA CRUZ,UK	Mouse	WB
Slug (H-140)	SANTA CRUZ,UK	Rabbit	WB
GAPDH (H-12)	SANTA CRUZ,UK	Mouse	WB
αv-Integrin (H-2)	SANTA CRUZ,UK	Mouse	WB, CO-IP
B-6 (H-110)	SANTA CRUZ,UK	Rabbit	WB, CO-IP
B-1	SANTA CRUZ,UK	Mouse	WB
B-3 (SAP)	SANTA CRUZ,UK	Mouse	WB
Twist (H-81)	SANTA CRUZ,UK	Rabbit	WB
Snail-1 (G-7)	SANTA CRUZ,UK	Rabbit	WB
fibronectin (F3648)	SIGMA ALDRICH,UK	Rabbit	WB, ICC
Cytokeratin 8 (M20)	ABCAM, UK	Mouse	WB
TGFβ-1 RI (R-20)	SANTA CRUZ,UK	Rabbit	WB
TGFβ-1 RII (C-16)	SANTA CRUZ,UK	Rabbit	WB
SMAD 2	SANTA CRUZ,UK	Mouse	WB
P-SMAD 2	SANTA CRUZ,UK	Rabbit	WB
SMAD 3	SANTA CRUZ,UK	Mouse	WB
P-SMAD 3	SANTA CRUZ,UK	Rabbit	WB
TGFβ1 Pan specific (AB-100NA)	R&D SYSTEMS	Rabbit	WB
Secondary antibodies			
FITC	DAKO, DENMARK	Mouse	ICC
TRITC	DAKO, DENMARK	Rabbit	ICC
Swine anti-rabbit HRP conjugated	DAKO, DENMARK	Rabbit	ICC
Goat anti-mouse HRP conjugated	DAKO, DENMARK	Mouse	ICC
ICC-immunocytochemistry **WB**- Western blotting **CO-IP**-Co-Immunoprecipitation			

2.1.2 Chemicals:

All lab reagents were purchased from **PAA Laboratories**, Yeovil, Somerset, UK unless otherwise specified.

Promocell® (Heidelberg, Germany)

Airway Epithelial Cell Media, AEM, (C-21260) with supplement mix: Insulin,hEGF-5, Hydrocortisone, Epinephrine, Triiodothyronine, Transferrin, Retinoic acid and Bovine pituitary extract BPE.

Sigma Aldrich, (UK)

- Insulin, Transferrin, Sodium Selenite (Sermet-Gaudelus et al.) medium, 10X
- Diethyl pyrocarbonate (DEPC) (159220)
- SIGMAFAST® OPD tablets (P9187)
- Cycloheximide (C7698)
- Valinomycin (V0627)
- Fibronectin (F0895)
- N-(Ethoxycarbonylmethyl)-6-Methoxyquinolium Bromide (MQAE) (46123)
- Forskolin (F6886)
- Dimethyl Sulfoxide (DMSO) (D2438)
- Cystamine (30050-25)
- Protein G Sepharose beads (P3296)
- Monodansylcadaverine (30402)
- Ponceau S stain (P7170)**:** 0.1%(w/v) Ponceau S and 5%(w/v) acetic acid ready to use.

Melford (UK)

- Acrylamide (29:1) (A2455)

Selleckchem (UK)

- VX-809 (S1565)
- VX-770 (S1144)

Tocris Bioscience (UK)

- Dibutyryl cyclic AMP (1141)

Life Technologies Ltd (UK)

- Lipofectamine® 2000
- TRIzol ® (15596-026)

Qiagen (UK)

- Sensiscript® Reverse Transcriptase, Qiagen
- Qiagen Quantitect® SYBR® Green PCR kit
- RT^2 First strand Kit

Pierce (UK)

- Sulfo-NHS-LC-Biotin

Zedira (Germany)

- N-(Biotinyl) Cadaverine
- Z-DON-Val-Pro-Leu-OMe (Z-DON)

Roche (UK)

- 2,3-bis-(2-methoxy-4-nitro-5-sulfophenyl)-2H-tetrazolium-5-carboxanilide (XTT)

Vector Laboratories (UK)

- Vectashield hard set mounting medium with DAPI (4',6-diamidino-2-phenylindole)

Aston University (Prof Martin Griffin's Lab)

- R281: (N-benzyloxycarbonyl(CBZ)-L-phenylalanyl-6-dimethylsulfonium-5-oxo-L-norleucine) (Jones *et al*., 2006)
- R283: (1,3-dimethyl-2-[(oxopropyl)thio] imidazolium. (Jones *et al*., 2006)
- R294: cell impermeable TG2 inhibitor (Griffin *et al*., 2008)
- 1-133: Peptido-mimetic cell impermeable TG2 inhibitor
- 1-155: Peptido-mimetic cell-permeable TG2 inhibitor

4x Tris-Cl/SDS, pH 6.8 (0.5M):

To make 100ml of solution, 6.05g of Tris base was dissolved in 40ml of distilled water with pH adjusted to 6.8. 0.4g of SDS was added and placed on a stirrer to dissolve completely. Solution was then stored at 4^{o}C.

4x Tris-Cl/SDS, pH 8.8 (1.5M):

To make 500ml of solution, 91g of Tris base was dissolved in 300ml of distilled water with pH adjusted to 8.8. Solution was made up to 500mls with distilled water. 2g of SDS was added and placed on a stirrer to dissolve completely. Solution was then stored at 4^{o}C.

***10x Transfer buffer:**

Transfer buffer (10x)	(w/v)
Tris base	3.03
Glycine	14.42

- *Methanol added when buffer is ready to be used

10x TBS-Tween buffer:

TBS-Tween (10x), pH 7.4	To make up 1L
Tris base	121.14g
NaCl	90g
Tween-20	5mls

Stripping buffer:

Buffer	Amount required to make up
Tris-Cl (pH 6.8)	62.5mM
SDS	2%(w/v)
2-β-Mecaptoethanol	100mM*

* To add freshly before use

2.1.3 Equipment:

Leica Microsystem (Milton Keynes, UK)

- Leica TCS SP5 II Broadband Confocal Microscope

MWG (USA)

- Primus 96 thermal cycler

Stratagene (UK)

- MX-3000P® Real-Time PCR machine

Worldwide Precision (USA)

- EVOM Epithelial Voltohmmeter

Syngene (UK)

- GEL box (G:BOX F3)

2.2 Methods:

2.2.1 Cell culturing:

2.2.1.1 Cell lines

IB3-1 (mutant tracheal epithelial cell line with a heterozygote mutation, ΔF508/W1282X, leading to the loss of CFTR channel function and immortalized by SV-40 transfection), C38 ("add back" IB3-1 cell line which has a truncated CFTR channel with 119 residues missing but functional with elevated basal Cl^- ion efflux) and Human Bronchial Epithelial cell (HBEC) (isolated from surface epithelium of human bronchi) obtained as a gift from Dr Lindsay Marshall (Aston University, Birmingham, UK).

2.2.1.2 Culturing of cells in submerged medium

IB3-1 and C38 cells were cultured in airway epithelial medium, AEM, substituted with supplements; 5%(v/v) Foetal Calf Serum (FCS), 1% (v/v) Penicillin/Streptomycin and 1%(w/v) L-Glutamine (GE Healthcare). The cells were cultured in plastic flasks to attain a confluency of 70% to 90%.

2.2.1.2.1. To determine TGFβ1 levels in cells cultured in submerged conditions

5 x 10^5 C38 or HBEC cells were cultured in complete medium to attach and spread for 6h then medium was changed to serum-free medium supplemented with 1x ITS and rTGFβ1 (3ng/ml) alone or in combination with TG2 inhibitor for 48 h.

2.2.1.3. Passaging of cells (submerged medium)

The cells were rinsed with 1x PBS pH 7.4 and then treated with 0.25%(v/v) trypsin (GE Healthcare) in 2mM EDTA in 1x PBS at pH 7.4 kept at 37^{o}C for 3-5 min. Cells were collected in fresh medium with serum to neutralise the trypsin and centrifuged at 250g for 5 min. Subsequently, cells were re-suspended in fresh complete medium.

2.2.1.4 Culturing of cells at Air Liquid Interface (ALI)

In order to culture airway epithelial cells to assume a pseudo-stratified structure, Transwell® (Corning Lifesciences, Amsterdam) inserts with an area of 0.33cm^2 and 0.4µm pore size were inserted in Transwell® companion plates. 33µl of 100µg/ml solution of collagen IV in 3%(v/v) acetic acid was added to each insert membrane and allowed to attach for 45 min at room temperature. Medium was used to rinse inserts to neutralise the acidity of the solution. 3 x 10^4 cells in 300µl of airway epithelial medium, AEM, were added to each insert apically and 600µl of complete medium added basally to each well underneath each insert. The cells were cultured for 4 days after which medium was removed from inserts and the cells were exposed to air. Medium in basal companion Transwell® plates was replaced and cells were cultured for 14 days during which basal medium was changed on alternate days. Afterwards, the TEER was measured.

2.2.1.5 Trans-Epithelial Electrical Resistance (TEER) of airway epithelial cells cultured at ALI.

In order to ensure airway integrity, Trans-Epithelial Electrical Resistance, TEER, was measured. Using electrodes, 300µl medium was carefully added to each insert not to distort cells. The electrodes attached to the voltohmmeter were then inserted into each insert with the longer arm extending into the basal compartment and the shorter arm inserted apically above the cells (EVOM Epithelial voltohmmeter). Caution was taken not to disrupt cells. The measurement was done passing AC current through the cells consequently, taking the resistance (in ohms) as the current passes through. This was done in triplicate with electrodes dipped intermittently in 70%(v/v) Industrial Methylated Spirit (IMS) and air dried before each use to keep electrodes sterile. As resistance attains 300Ω, the apical medium was removed from the surface of cells in inserts and inserts placed into basal medium in Transwell® with cells cultured at 37^{o}C.

$$\text{TEER } (\Omega cm^2) = \text{Mean of resistance measured across each membrane } (\Omega) \times \text{Area of Membrane } (cm^2) - \text{Mean of resistance measured across empty control membrane } (\Omega cm^2)$$

2.2.2 Lysing of cells

2.2.2.1 Lysing of cells cultured in submerged medium

The cells were washed with ice-cold 1x PBS, pH 7.4 twice and lysis buffer (5mM DTT, 50mM Tris-Cl, 150mM NaCl, 1mM EGTA, 1mM PMSF, 1%(V/V) protein Inhibitor cocktail and 1mM Sodium orthovanadate) was added to cells and scrapped into pre-cooled eppendorf tubes. The cells were incubated for 30min and centrifuged at 300g for 5 min. Supernatant was collected into fresh tube and protein was quantified by the Lowry method. For cell and matrix proteins, cells were rinsed with 1x PBS, pH 7.4 twice, collected in 2mM EDTA in 1x PBS, pH 7.4 which were lysed on ice for 30 min prior to centrifugation at 300g for 5 min. To the matrix, 40µl of 2x Laemilli buffer was added and scrapped into pre-cooled eppendorf tubes, which were boiled for 5 min before loading on polyacrylamide gels.

2.2.2.2 Lysing of cells (ALI)

Using a scalpel, membrane inserts rinsed with 1x PBS, pH 7.4, were carefully cut to avoid distorting the attached cells. The membrane was placed in eppendorf tubes with lysis buffer on ice and vortex to aid in detaching the cells from membrane. The cells are incubated on ice for 30min and centrifuged at 300g for 6min. The supernatant was collected into fresh tubes on ice and the membrane viewed to ensure cells were detached.

2.2.3 Sodium Dodecyl Sulphate Polyacrylamide gel Electrophoresis (SDS-PAGE) of lysates of airway epithelial cells

Protein homogenates were added to either 2x laemmli (125mM Tris- Cl, pH 6.8, 20% (v/v) glycerol, 10% 2-β mercaptoethanol, 4%(w/v) SDS and 0.01% bromophenol blue) or 6x laemmli buffer (5.91 g Tris-HCl, 6 %(w/v) SDS, 48%(v/v) glycerol, 9 ml 14.7 M 2-Mercaptoethanol, and 30 mg bromophenol blue and distilled water to make up volume to 100ml) (Laemmli, 1970) (1:1) and mixed prior to boiling for 5min. SDS gels were made depending on the proteins to be separated.

For 15ml of resolving gel;

Resolving solutions (w/v)	**6%**	**8%**	**12%**
30% (w/v)	2.25	3	4.5
4x Tris-Cl/SDS, pH8.8	3.75	3.75	3.75
Distilled water	9	8.25	6.75
10% ammonium persulphate	0.05	0.05	0.05
TEMED	0.01	0.01	0.01
Total volume (ml)	15	15	15

5ml of stacking gel:

Stacking solutions (w/v)	(ml)
30% (w/v)	0.4875
4x Tris-Cl/SDS, pH6.8	1.25
Distilled water	3.21
10% ammonium persulphate	0.025
TEMED	0.005
Total volume (ml)	5

The gels were allowed to polymerise at room temperature for 45min to 60min. The wells on stacking gel were washed with 1x running buffer (10x running buffer; 25.01mM Tris base, 190mM glycine and 0.1%(w/v) SDS with pH adjusted to 8.3. The solution was made up to 1000ml) placed in glass-plate chamber. Excess amount of running buffer was added to fill the chamber and protein homogenates boiled for 5 min in 2x laemmli and vortex gently to mix protein and loaded on the gels. Electrophoresis was conducted at 90mA through the stacking gel. As the protein front approached the end of stacking gel, the voltage was increased to 120mA and further ran for 30min to 45 min.

2.2.4 Western Blotting to detect separated proteins from lysates of airway epithelial cells

Western blotting was carried out according to the method as described by Towbin *et al.* (1979). The separated protein on the gel were transferred to nitrocellulose membrane using pre-cooled 1x transfer buffer [25.01mM Tris-base and 192mM glycine, pH 8.3] made up with methanol and distilled water (1:7:2). Transfer was carried out at 200mA for 2 h. A sandwich was made of cushions, gel, nitrocellulose membrane, packaged in a fitted cassette, which was degassed to remove any interfering bubbles and the assembly placed in a transfer rack where current passes and transfers protein to the membrane. The transfer was carried out under low temperatures as ice packs were placed in adjacent transfer rack. After 2 h, the assembly was dismantled and membrane was assessed for transferred proteins by staining them with Ponceau S stain (add stain to membrane and stain for 5 min. To destain membrane, wash with 1x PBS, pH 7.4). The membrane was then blocked with blocking buffer [5%(w/v) skimmed milk in 1x TBS-Tween, pH 7.4] for an hour. Thereafter, membrane was blotted with primary antibody in blocking buffer and incubated overnight at 4^{o}C on a rocking stirrer. Subsequently, the membrane was washed in wash buffer (1x TBS-Tween, pH 7.4) four times and incubated with HRP-conjugated secondary antibody for 2 h at room temperature. After incubation, the membrane was washed four times with washing buffer every 15min. Membrane was gently rinsed in 1x PBS, pH 7.4 and luminescence determined using ECL® chemiluminescent reagents (1:1 dilution) and images captured using the G-box system (Syngene®).

2.2.5 Membrane stripping:

Membrane stripping was performed to free the membrane of bound primary and secondary antibodies and reassess membrane other proteins or evaluate the amount of protein loaded on the gel at the same time. The membranes were rinsed with 1x TBS-Tween, pH 7.4 and placed in stripping buffer. The buffer was then placed in a heating chamber at 50^{o}C for 20 min and intermittently mixed to aid stripping of the membrane. The membrane was carefully removed from buffer in a HEPA filtered hood into 1x TBS-Tween, pH 7.4 and placed on a rotatory shaker to wash. The stripping buffer was aseptically discarded. The membranes were washed for an hour with washing buffer and changed every 15 min. The membranes were blocked as described in the section above and assessed for proteins as described.

2.2.6 Determination of protein expressed in whole cell lysates of airway epithelial cells

To detect total protein expressed by cells, whole cell lysates (WCL) were obtained as described below. Cells were cultured to a confluency of between 70% to 90%. Cells were then washed with ice- cold 1x PBS, pH 7.4 twice. To lyse the cells, lysis buffer was added and cells were placed on ice for 5 min. Using a scraper, cells were gently detached, collected into eppendorf tubes and placed on ice for 30 min. Subsequently, cell lysates were centrifuged at 300g for 5 min. The protein supernatant was collected into fresh tubes. Quantification was done using the Lowry protein quantification method (Lowry *et al*., 1951).

2.2.7 TG2 Activity assay using the Biotin Cadaverine Incorporation assay

2.2.7.1 TG2 activity in whole cell lysates (WCL) of cells cultured in submerged conditions or at ALI:

Activity assays were carried out using biotin cadaverine incorporation into fibronectin (FN). 5 x10^5 cells were cultured in 6-well plates for 6 h to attach and medium was changed and replaced with fresh medium. For treated groups, medium was supplemented with inhibitors, antibodies or chemical compounds. Whole cell lysates were obtained as described in section 2.2.6. TG2 activity assay was carried out in 96-well plates, coated with 50µl of a 5µg/ml fibronectin solution overnight at 4^{o}C. 50µg of WCL were pre-incubated on FN coated plates in the presence of 10mM calcium, 1mM DTT, 0.1mM biotin cadaverine (BCD) and made up to a final volume of 100µl/well (96 well plate) using 50mM Tris-Cl, pH 7.4. The positive and negative control were with purified 50µg of guinea pig liver TG2 (gplTG2) with the substitution of calcium for 10 mM EDTA in the negative control. The samples were done in triplicates. The plate was incubated at 37^{o}C, 5% CO_2 for 2 h. Thereafter, 2mM EDTA in 1 x PBS, pH 7.4 was added to wells to stop the reaction and the wells washed three times with the same buffer. The wells were washed with 50mM Tris-Cl, pH 7.4 three times then blocked with blocking buffer, heat inactivated 3%(w/v) Bovine Serum Albumin, BSA, in 50mM Tris-Cl, pH 7.4 for 30 min at 37 ^{o}C. The wells were washed with blocking buffer and then incubated with 100µl of 1:1000 dilution of Extravidin® peroxidise conjugate for 1 h at 37^{o}C. The wells were washed again with 50mM Tris- Cl, pH 7.4 three times. 100µl of

SigmaFast® OPD tablets dissolved (1:1) in 20ml of distilled water was added to the plates and the reaction was stopped by adding 50µl of 3M HCl. Absorbance was detected at 490nm.

Similarly, 3 x 10^4 cells were cultured at ALI as described in section 2.2.1.4. The cells were carefully rinsed with 1x PBS, pH 7.4 twice and membrane was cut out carefully with a scalpel into eppendorf tubes as described in section 2.2.2.2. 50µg of protein was used for TG2 activity assay as described above.

2.2.7.2 Detection of cell surface TG2 activity in airway epithelial cells cultured in submerged conditions.

Using T25 flasks, cells were cultured overnight to attain confluency of between 80%-90%. The cells were rinsed with 1x PBS, pH 7.4 twice and detached using 0.5mM EDTA in 1x PBS, pH 7.4, incubated at 37^{o}C for 5 min. The cells were centrifuged for 5min at 300g and supernatant discarded. The pellets were re-suspended in AEM without serum. 2 x 10^4 cells were counted and re-suspended in 400µl of medium containing 0.1mM biotin cadaverine. The mixture was added to a 96-well plate coated with 50µl of 5µg/ml fibronectin and incubated at 37^{o}C for 2 h. To treated groups, inhibitors, antibodies or chemical compounds were added and incubated with cells prior to the addition of 0.1mM biotin cadaverine. The reaction was stopped by addition and further washing wells with 2mM EDTA in 1x PBS, pH 7.4. 100µl of 0.1%(w/v) sodium deoxycholate in 2mM EDTA in 1x PBS, pH 7.4 was added to each well and incubated on a slow shaker for 10 min at room temperature. On discarding the mixture from the wells, the well were washed thrice with 50mM Tris-Cl, pH 7.4 and blocked with heat inactivated 3% (w/v) Bovine Serum Albumin, BSA, in 50mM Tris-Cl, pH 7.4 at 37^{o}C for 30 min. The wells were washed and the immunoassay detecting the incorporation of biotin cadaverine by cell surface TG2 into fibronectin was determined using a 1:1000 dilution of Extravidin® peroxidase conjugate incubated at 37^{o}C for 1h. On washing the wells with 50mM Tris-Cl, pH 7.4, 100µl of OPD tablets (1:1) dissolved in 20mls of distilled water was added to wells and the reaction stopped using 50µl of HCl (3M) and the absorbance determined at 490nm.

2.2.7 Migration studies of iB3 and C38 cells using wound/scratch assay:

To evaluate the *in vitro* migratory profile of epithelial cells, 1 x 10^5 cells were sub cultured into 96 well plates and allowed to grow to confluence over 16 h in complete medium with supplements. Cells were cultured in AEM with supplement mix and 5% (v/v) FBS and 1X L-glutamine. After 4 h, medium was changed and replaced with medium without FBS but supplemented with 1x ITS (Insulin, Transferrin and Sodium Selenite). The cells were cultured overnight in serum free medium. Thereafter, using the wound maker® device or a 10µl pipette tip, a scratch was made across each well for each cell line. Each cell line was divided into two groups: treated and untreated groups and then after medium change cultured in 2% (v/v) serum supplemented AEM. The cells were incubated in an Innocyte FLR® incubator at 37^{o}C for 24 h over which images were taken every hour in both treated and untreated groups at 37^{o}C in humidified incubator with 5% CO_2. The percentage relative wound closure i.e relative comparison between total area of scratch between cell migration front and space uncovered between migration fronts on both sides of the scratch over time.

2.2.8 Biotinylation, as a measure of the presence of cell surface TG2.

The biotinylation assay was carried out to selectively label proteins on basal or apical surface of cells. IB3 and C38 cells were cultured in submerged culture to determine cell surface TG2. Briefly, 5 x 10^5 cells where cultured on 10cm plates to attain a confluency of between 80-90% cells. The cells were washed with ice cold 1 x PBS, pH 7.4 twice. Cells were incubated with 80mM EZ Sulfo –NHS-LC-biotin dissolved in 1 x PBS, pH 7.4 on ice for 20min. Excess biotin solution was removed and washed three times with 50mM Tris-Cl, pH 8.0 and lysed in 1%(w/v) SDS in 1 x PBS, pH7.4. Cells were scraped off plates. A 1:1000 dilution of benzonase was then added. Following the incubation on ice for 30 min, the lysates were warmed up briefly and centrifuged at 300g for 5 min at room temperature. Protein concentration was determined using the Lowry quantification method. Supernatants containing 0.5mg-1mg of protein were added to Neutravidin® agarose beads rinsed with 1 x PBS, pH 7.4 and left overnight on a shaker at 4^{o}C. The lysates were centrifuged at 1,000g for 1min at room temperature and supernatant discarded. The beads were washed thrice with 1x PBS, pH 7.4 discarding supernatant after each wash. 40µl of 2x Laemmli sample buffer was then added and boiled for 5 min. The beads were pelleted at 1000g for 1 min. Supernatant was used for SDS-PAGE and Western Blots as described in section in 2.2.3 and 2.2.4. GAPDH was used to check for cytoplasmic contamination.

2.2.9 Determination of total TGFβ1 levels secreted from airway epithelial cells using Human/Mouse TGFβ1 ELISA Ready-SET-Go! (2nd Generation)

2.5×10^5 cells were cultured in complete AEM on 6-well plates. After the cells had attached to the plates, the medium was taken off and replaced with AEM with 1x ITS (Insulin, Transferrin and Sodium Selenite). Each cell line was assayed in duplicate and in groups with cells pre-treated with inhibitors, antibodies or chemical agents prior to the collection of medium. Plates were incubated for 24 h. Media was then taken off and centrifuged down at 300g for 5 min. The supernatant was then taken off and assayed for TGFβ1.

The assay was undertaken in 96-well plates pre-coated overnight with capture antibody (Ab) (1:250 dilution of capture Ab in coating buffer (1x: made from 10x buffer diluted with water). The wells were coated with 100µl /well and incubated at 4^{o}C overnight. Wells were aspirated and washed 5x with wash buffer (1x PBS, pH 7.4 with 0.05%(v/v) Tween-20) allowing soaking for 1 min between washes. The plates were then blotted to remove excess buffer. 200µl of assay diluent (5x assay diluent was diluted to 1x diluent with distilled water) was then used to block the wells, which were incubated at room temperature for 1 h. The wells were aspirated and washed with wash buffer, 5x. To the test samples collected from the cells, TGFβ1 was activated using 20µl of 1M HCl per 100µl of sample and incubated at room temperature for 10 min. The samples were then neutralized with 1M NaOH. Standard samples were prepared from a standard solution of 8000pg/ml with serial dilutions made using 1x assay diluent ie 1000, 500, 250, 125, 62.5 and 0pg/ml. 100µl of standard sample and test sample were added to the appropriate wells in a Nunc Maxisorp® ELISA plate in triplicates. The plates were covered and incubated overnight at 4^{o}C. Plates were washed 5x with wash buffer. 100µl of detection Ab in 1x assay buffer (1:250 dilution) was added to the treated wells and incubated at room temperature for 1 h. A repeat wash with wash buffer (5x) was done. 100µl of Avidin-HRP in 1x assay diluent (1:250 dilution) was added to each well and incubated at room temperature for 30 min. Wells were aspirated and washed with washing buffer (7x). 100µl of substrate solution (1x 3,3',5,5'-Tetramethylbenzidine,TMB, solution) was added to each well and incubated for 15 min. After a colour change was observed within 15min, 50µl of stop solution (2N H_2SO_4) was added to each well and plate absorbance was read at 450nm.

2.2.10 Cell viability assay for airway epithelial cells

Using XTT assays, cell viability is determined with the change in the soluble yellow tetrazolium derivative of XTT to an insoluble orange formazan derivative by mitochondrial dehydrogenases. 7 X 10^4 cells were counted and sub-cultured into 96 well plates and allowed to attach to the plates in complete medium at 37^{o}C. To medium, 40µl of XTT reagent (1ml of XTT labelling reagent and 40µl of electron coupling reagent were added together and mixed to get a homogenous mixture) was added and allowed to incubate with cells for 4 h at 37^{0}C, 5% CO_2. The assay was carried out at every 4h for 24h then every 24 h for 48 h ie 0, 4,8,12,18,20,24 and 48h. The absorbance was measured at 490nm. Assays were carried out in triplicate.

2.2.11 siRNA gene silencing of TG2 in airway epithelial cells

5 x 10^5 cells were seeded into 6-well plates in 2300µl of complete AEM with L-glutamine, 5%(v/v) serum. The cells were incubated overnight for 18-24 h. Cells were divided into six groups; untreated, TG2 plasmids TG2 #1, TG2 #5, TG2 #6, TG2 #7 (sequence of each siRNA plasmid shown in table 2.1 below) and global negative control. Using 100µl of serum free medium, 10nM of each siRNA was added to serum free medium. This was gently mixed with 12 µl of Hiperfect® Transfection reagent. The mixture was allowed to stand for 5-10 min and reagent added in a drop-wise manner to 2300µl of medium with serum in each well labelled according to the plasmid used. The plates were gently swirled around and incubated for 24 h at 37^{0}C, 5% CO_2. The cells were washed with ice-cold 1x PBS, pH 7.4 twice and lysed with lysis buffer for SDS/PAGE and Western Blotting according to the protocols described in section 2.2.3 and 2.2.4 respectively.

Table 2.1: siRNA sequences for TG2:

siRNA	CAT NO	SEQUENCE	Base pairs
TG2 #1	SI00743715	CCGCGTCGTGACCAACTACAA	21
TG2 #5	SI03020927	TGGGCTGAAGATCAGCACTAA	21
TG2 #6	SI03055465	CACAAGGGCGAACCACCTGAA	21
TG2 #7	SI03101966	GACGATGGGTCTGTGCACAAA	21

2.2.12. RNA isolation from IB3 and C38 cells

5 x10^5 cells were cultured on 60mm petri dishes in submerged medium to a confluent count of 80-90%. RNA was extracted using the TRIzol® method. Briefly, using a cell scraper, 1ml of TRIzol® reagent was added to each plate and cells were scraped from the petri dishes into 1ml eppendoff tubes on ice. To all the tubes, 0.2ml of chloroform was added, vortex for 20 seconds and incubated at room temperature for 3 min. Subsequently, the tubes were centrifuged at 12,000g for 15 min at 4^{o}C. The supernatant from each tube was then transferred into fresh tubes and 500µl of Isopropyl alcohol was added to samples, which were incubated at room temperature for 15 min. The samples where centrifuged at 12,000g for 10 min at 4^{o}C. The supernatant was removed completely and 1ml of 75%(v/v) ethanol was added to each tube, vortex and centrifuged at 7,500g for 5 min at 4^{o}C. This was done twice. Thereafter the RNA pellets were allowed to dry and re-suspended in RNAse free water. The samples were placed on ice and subsequently quantified using the Nanodrop® spectrophotometer.

2.2.13 Reverse Transcription of RNA to cDNA

Using the Qiagen® RT^2 First Strand Kit, RNA fragments from cells were transcribed into cDNA. 5ng of RNA template from each cell line was added to the master mix of genomic elimination mixture (2µl of 5x gDNA elimination buffer) to get rid of any genomic contaminants. 10µl of RNAse free water was added and gently mixed prior to incubation at 42^{o}C for 5 min. The tube was chilled on ice for a min and for each reaction a reverse transcription (RT) cocktail was made containing 4µl of 5x RT buffer

mix, 1µl of a primer and external control mix, 2µl of a RT enzyme mix and RNAse free water to make up a total volume of 10µl per reaction. This was added to 10µl of the genomic DNA elimination mix and mixed gently pipetting up and down. The mixture was incubated for 15 min at 42^{o}C and heating the tube to 95^{o}C for 5 min stopped reaction. To each mix of 20µl, 91µl of RNAse free water was added and mixed. This mix containing the cDNA was then used for PCR.

2.2.14 PCR using Qiagen® Taq polymerase Core Kit

The PCR was performed to determine the amount of TG1, TG2 and FX III in IB3 and C38 cells cultured in submerged conditions. Using annealing temperatures derived from the primers for Transglutaminases (TG); TG1-2 & FX III, the PCR was performed using a master mix containing: 10x PCR buffer, 10mM dNTP mix, 0.3uM of forward and reverse primers for TG1-2 and FX III, Taq polymerase and distilled water to make up the volume to 50µl. To aliquots of this mix, approximately 1µg of the cDNA was added mixed and the tubes were placed in the block wells of a Thermal Lightcycler machine. According to the most appropriate temperatures, the PCR was run: Denaturation 1min at 94^{o}C, Annealing at 62^{o}C for TG1-2 and FXIII and Extension for 1min at 72 ^{o}C. This was run for 35 cycles. A final extension for 10min at 72 ^{o}C was finally carried out. cDNA amplicons were run on Agarose gels (2%w/v) and gel pictures taken on a UV transluminator. The primer sequences of the genes used are:

Table 2.2: Forward and reverse primer sequence for genes used:

Primers	Forward	Reverse
TG1	5'-accgtgtgaccatgccagtg-3'	5'-gctgctcccagtaacgtgagg-3'
TG2	5'-atgagaaataccgtgactgccttac-3'	5'-cagcttgcgtttctgcttgg-3'
FX III	5'-gaccaatgaagaagatgttccgt -3'	5'-gaaggtcgtctttgaatctgcac -3'
fibronectin	5-'ggatgacaaggaaagtgtcccta-3'	5'-ggtggaagagtttagcggggt-3'
E-cadherin	5'-cctgggactccacctacaga-3'	5'-tggattccagaaacggaggc-3'
N-cadherin	5'-aacagcaacgacgggttagt-3'	5'-cagacacggttgcagttgac-3'
Slug	5'-acgcctccaaaaagccaaac-3'	5'-acagtgatggggctgtatgc-3'
Twist	5'-agctgagcaagattcagaccctc-3'	5'-ccgtctgggaatcactgtc-3'
Zeb2	5'-caagcctctgtagatggtcc-3'	5'-atcgcgttcctccagttttct-3'
TGFβ1	5'-tgcggcagtggttgagccgt-3'	5'-acctcggcggccggtagtga-3'
GAPDH	5'-tgcaccaccaacttgcttagc-3'	5'-ggcatggactgtggtcatgag-3'

2.2.15 Real Time Polymerase Chain Reaction (RT-PCR) to determine relative gene expression of TG2 and EMT markers in airway epithelial cells

This was performed according to the conditions on the Stratagene® MX-3000P real-time PCR machine of which the annealing temperature was updated to accommodate the primers used for the RT-PCR. RT-PCR was carried out incorporating the labels and dyes in each well with the PCR master mix and primers for TG1-2. The Qiagen Quantitect® SYBR® Green PCR kit was used which contains a 2x Quantitect SYBR® Green PCR Master mix with 2.5mM $MgCl_2$, 0.3μM of forward and reverse primers for TG1-2 and RNAse free water. The optimum temperatures for amplifying cDNA in 40 cycles are; activation 95^{o}C for 15 min, denaturation 94^{o}C for 15 sec, annealing 62^{o}C for 30 sec and extension 72^{o}C for 30 sec. This was followed by a dissociation curve, which began with 60 sec incubation at 95^{o}C, 30 sec at 55^{o}C and a final temperature ramp to 95^{o}C when the results are collected. After the experiments, the results were collected and analysed for amplification and dissociation curves. The housekeeping gene was GAPDH and relative level of expression was determined in relation to GAPDH expression.

2.2.16 Cell localisation studies (Immuno-fluorescence staining)

2.2.16.1 Submerged culture:

5 x 10^5 cells were cultured on 60mm petri dishes. The cells were cultured to confluency of about 70-90%. The cells were washed three times with 1x PBS, pH 7.4 for 3 min each. 200µl of 3.7% (v/v) paraformaldehyde in 1 x PBS, pH 7.4 was added to each well for 20min at 37^{o}C. Cells were washed 3 times with 1x PBS, pH 7.4 for 3 min each. To each petri dish, 200µl of primary antibody (Ab) in complete medium was added and incubated for 1h at 37^{o}C. The cells were washed 3 times with 1x PBS, pH 7.4 with 3 min for each wash. Subsequently, the cells were incubated with 200µl/petri dish with Fluorescein isothiocyanate, FITC (green) or Tetramethylrhodamine, TRITC (red) conjugated secondary antibody at 37^{o}C for 1h. Wells were then washed 3 times with 1 x PBS, pH 7.4 with 3 min for each wash. A repeat was done with primary and secondary Ab for co-localisation studies. The petri dishes were dabbed to remove excess liquid and a drop of 4',6 –diamidino- 2-phenylindole (DAPI) in mounting solution was added and cover slips placed on them. The petri dishes were wrapped and stored at 4^{o}C prior to imaging. The petri dishes were viewed using the Leica® SP5 confocal microscope.

2.2.16.2 ALI culture

The cells at air liquid interface (ALI) were used for immunocytochemistry after 28 days. The membranes were carefully cut out of inserts and placed cell uppermost in 12-well plates using a scalpel. Using 200µl of 1x PBS, pH 7.4, cells were carefully rinsed twice. 150µl of 3.7% (v/v) paraformaldehyde in 1x PBS, pH 7.4 was added to each insert for 20min at 37^{o}C. Cells were washed 3 times with 1x PBS, pH 7.4 for 3 min each. To each insert, 150µl of primary antibody (Ab) in complete medium was added and incubated for 1h at 37^{o}C. The cells were washed 3 times with 1x PBS, pH 7.4 with 3 min for each wash. Subsequently, the cells were incubated with 200µl of Fluorescein isothiocyanate, FITC (green) or Tetramethylrhodamine, TRITC (red) conjugated secondary antibody at 37^{o}C for 1h. Wells were then washed 3 times with PBS, pH 7.4 with 3 min for each wash. Samples were dabbed to remove excess fluid. The membranes were transferred to slides and a drop of DAPI in mounting solution was added to each membrane and covered with a cover slip. The slides were stored at 4^{o}C. Slides were visualised under Leica® SP5 confocal microscope.

2.2.17 Membrane fractionation

2.2.17.1 Submerged culture

5 x 10^5 IB3 cells were sub cultured into 60mm petri dishes and allowed to attach for 4h. Medium was discarded and replaced with treated medium with VX-809 (Selleckchem®) (10μM), R283 (500μM), a combination of VX-809 and R283 and with DMSO as control. The cells were cultured for 72 h with medium changed every 24 h. Cells were washed with ice cold 1x PBS, p.H 7.4 twice and lysed using a homogenization buffer (75mM Tris-Cl, p.H 7.4, 200mM NaCl, 15mM NaF, 1.5mM Na_3VO_4, 7.5mM EGTA, 7.5 mM EDTA, 1.5% Triton X-100, 0.75%(v/v) Igepal CA-630, Protease inhibitor cocktail). Cells were scraped into pre-cooled eppendorff tubes and place on ice for 30 min. The lysates were centrifuged at 300g for 10 min and supernatant transferred into fresh tubes. Protein was quantified using Lowry method and 250μg of protein was transferred into fresh tubes and centrifuged at 17,500g for 15 min. The supernatant was transferred into another fresh tube and the pellets were washed with 1x PBS, p.H 7.4 twice. 35μl of 2x Laemmli buffer was added to pellet and boiled. Western blotting was carried using the pellets as described in section 2.2.4.

2.2.17.2 ALI culture

3 x 10^4 IB3 cells were sub cultured into 0.33μm transwell® insert membrane coated with collagen IV (100μg/ml). The cells were allowed to attach for 6 h. The medium was changed in Transwell® inserts as well as in the companion plates. 300μl of complete medium was inserted into the Transwell® inserts supplemented with VX-809 (10μM), R283 (500μM), a combination of VX- 809 and R283 and with DMSO as control (1:1000). The groups were cultured in duplicates. The basal medium was changed daily for the first 4 days i.e. time required to attain basal ALI status. The medium was subsequently removed from the inserts and cells were then subject to ALI. The cells were treated afterwards every 2 days for another 14 days. TEER was measured using the voltohmmeter across the PET-itched polyethylene membrane. On attaining a TEER value of ≥300Ωm^{-1}, the cells were then subject to Western blotting or immunocytochemistry as described above in section 2.2.4 and 2.2.16.2.

2.2.18 Chloride channel activity assay in IB3 cells cultured in submerged conditions.

To determine CFTR chloride channel activity in IB3 cells, the assay was carried out as described by West and Molloy (1996). Briefly, 1 x 10^5 IB3 cells were sub cultured into 100µl in 96-well plates and allowed to attach for 6 h. The medium was changed and replaced with medium supplemented with TG2 inhibitors with or without the CFTR corrector, VX-809 (10µM). The TG2 inhibitors used were R283 (500µM), cystamine (250 µM) or 1-33 (50 µM). DMSO (1:1000) was used as a vehicle control. In order to load the cells with a chloride sensitive indicator, 10 mM MQAE was added to 100µl/well according to the previously published method (West and Molloy, 1996) and cells were incubated at 37^{o}C for 16-18 h. The cells were washed with chloride buffer (126mM NaCl, 5mM KCl, 1.5mM $CaCl_2$, 1.0mM $MgCl_2$, 20mM HEPES, 0.1%(w/v) BSA and 0.1%(w/v) D-Glucose; pH 7.2) and chloride free buffer (126mM $NaNO_3$, 5mM KNO_3, 1.0mM Mg $(NO_3)_2$, 1.5mM $Ca(NO_3)_2$, 20mM HEPES, 0.1%(w/v) BSA and 0.1%(w/v) D-Glucose; pH 7.2) twice and incubated with either Foskolin (10 µM) or Dibutyryl Cyclic Adenosine Monophosphate (dbcAMP) (1mM). The fluorescence was measured in a SpectraMax® Multi-mode microplate reader (Molecular Devices) with excitation at 350nm and emission at 450nm wavelengths. The fluorescence was measured for 8 min with readings taken every 25 sec. After this, the assay buffer was replaced with fluorescence quenching buffer containing potassium thiocyanate and 10mM valinomycin and fluorescence was measured for another 8 min.

2.2.19 Lentiviral Transduction of TG2 plasmids into IB3, C38 and HBE cells

2.2.19.1 Culturing of packaging cells, HEK293FT

Packaging cells, HEK293FT cells were cultured in T150 flask to 80% confluency in DMEM medium supplemented with 1x L-glutamine, 10%(v/v) FBS, 1mM sodium pyruvate, 400µg/ml G418 (the antibiotic is omitted immediately after defrosting and prior to transfection) and 1x Non- essential amino acids (NEAA). The cells were then trypsinised and sub cultured into T75 flasks prior to transfection. The cells were allowed to attach and proliferate overnight. The medium was changed and cells were then transfected with viral packaging mix and plasmids of interest TG2 shRNA (to

knockdown TG2 expression) and TG2 wild type with the conserved mutation to prevent shRNA inhibition (to over express TG2), W241A mutant (where tryptophan was replaced with alanine), R580A (where arginine is replaced with alanine) and C277S (where cysteine is been replaced with serine at position 277 at the catalytic site).

2.2.19.2 Viral production of TG2 plasmids

To the HEK293FT cells in T75 flasks, a transfection mix of packaging plasmid, **pPAX**, viral envelop, **VSV-G** and DNA of interest where mixed in a 9µg**:** 4.5 µg**:** 6µg ratio with Lipofectamine® 2000. The mixture was allowed to stand for 20 min to form the complex, which was added to the packaging cells in a drop wise manner. The mixture on the cells was swirled around gently to obtain a homogenous mix. The cells were allowed to transfect for 72 h within which viral particle were released into the medium. After this incubation period, the infectious medium was carefully collected. The medium was centrifuged at 500g for 10min to remove cell debris and viral aggregates. The supernatant was discarded aseptically.

2.2.19.3 Lenti-X viral concentration

The clarified supernatant was transferred into fresh tubes and to three volumes of clarified supernatant, one volume of Lenti-X virus concentrator was added (3:1) and gently inverted to mix. The mixture was incubated for 3-4 h at 4^{o}C or overnight. Virus was pelleted at 1,500g for 45min at 4^{o}C. The supernatant was discarded carefully without disturbing the pellet. The viral pellet was re-suspended in DMEM medium carefully with 1/10th of the original volume used. Aliquots were made in 250µl -300µl and stored at -80^{o}C.

2.2.19.4 Lentiviral Titre value

Lentiviral titre was determined using the Lenti-X® Go-stix. Using 20µl of the concentrated viral mix, this was added to the Lenti-X® Go-stix kit and 4 drops of Lenti-X® concentrator buffer was added. This was allowed to stand for 15 min. The presence of two visible bands indicates viruses present in them as well as the intensity predict the density of the viral particles collected.

2.2.19.5. Viral transduction for airway epithelial cells cultured in submerged culture or at ALI

To transduce cells with viral particles, 5 x 10^5 cells were sub cultured onto 6-well plates in complete medium and cultured overnight for 16-18 h. Media was changed and replaced with fresh medium. An aliquot of viral particle for the TG2 mutant of interest was added to wells in a drop-wise manner and plates were gently swirled to mix the viral particle and medium gently. The cells were then incubated at 37^{o}C for 48 h with re-infection (addition of fresh aliquot of viral particle to wells) carried out every 24 h. The cells were viewed under the Leica® DMI 4000 inverted wide field fluorescence microscope for GFP green expression. The medium was aseptically discarded and cells were rinsed with 1x PBS, pH 7.4 twice and cells were lysed and SDS/PAGE and Western blotting carried out as described in section 2.2.3 and 2.2.4. Similarly, in ALI systems, cells were cultured as described in section 2.2.1.4 and 2.2.1.5. However, an aliquot of the viral particle for the TG2 mutant was added to inserts on the first day and re-infected on the second day during the initial 4 days prior to exposure of cells to air. The viral containing medium was discarded aseptically and cells were cultured at ALI with Western blotting carried out on lysates as described in section 2.2.4.

2.2.20 Co-immunoprecipitation of TG2 and αV/β6 integrin in submerged medium

Co-immunoprecipitation is a technique used to capture protein-protein interaction by indirectly using protein specific antibody to detect proteins that are bound to them. Briefly, 5x 10^5 IB3 and C38 cells were cultured in 60mm petri dish in full AEM for 48 h. Cells were then washed with 1X PBS, pH 7.4 twice. The cells were lysed using 50mls of lysis buffer; 0.25%(w/v) sodium deoxycholate, 150mM NaCl, 0.1mM PMSF, 1%(v/v) benzonase 1%(v/v) protein inhibitor cocktail and 500μM, R283 TG2 inhibitor in 50mM Tris-Cl, pH 7.4. The cells were then scraped into eppendorf tubes and allowed to stand on ice for 30min. The cells were centrifuged at 300g for 5min and supernatant was collected. Protein was quantified using the Lowry method. 200μg of IB3 and C38 protein were placed into tubes and made up with lysis buffer (20μl). Correspondingly, 50μl of beads: Protein A beads for Rabbit Ab and Protein G beads for Mouse Ab were pre-washed with 25μl of 1x PBS, pH 7.4 twice spinning at 1000g for 1 min and discarding supernatant. Finally, the beads were suspended in 25μl of 1x PBS, pH 7.4. To beads, all the cell lysates were added to corresponding beads with the initial protein

complex to be detected (Mouse or Rabbit); αV (Mouse), β6 (rabbit) and TG2 (Rabbit). This was left on shaker for 90min at 4^{o}C (pre-clearing). The mixture was spun down at 1000g for 1min and supernatant was collected into new tubes. 0.5µg of antibody (200µg/ml) was added to supernatants and placed on a shaker for 90min at 4^{o}C. Again, beads corresponding to the "pull-down" protein were washed as described above and the mixture of antibody and proteins were added to the beads and allowed to incubate on shaker for 2 h at 4^{o}C. This was spun at 1000g for 1 min and lysates were collected and 30µl of 2x sample buffer was added and heated for 3min prior to running a Western blot. Pull-down antibodies were used in detection. 8%(w/v) gels were made and SDS-PAGE/Western blotting was performed as described in section 2.2.3 and 2.2.4.

2.2.21 Statistical analysis

All statistical analysis was carried out using either the One-way or Two-way Anova method with data presented as mean and standard deviations. Analysis was performed with the Graph pad Prism® software.

Chapter 3

TG2 expression and activity in Cystic Fibrosis (CF) cells

3.1 Introduction:

The catalytic mechanism of TGases is common amongst all members and involves a transamidation reaction resulting in the formation of N^{ε}-(γ-glutamyl) lysine bonds between proteins leading to high molecular weight complexes, resistant to proteolytic degradation (Griffin *et al.*, 2002). As a consequence, this important effect of TGases on their substrate proteins can account for a number of human pathologies including various fibrotic and neurological diseases, illustrating the significance of this family of enzymes in disease progression.

Tissue transglutaminase (TG2) is the most ubiquitous member of this family of compounds and the most studied in the group. Studies have shown its involvement in the pathogenesis of many diseases with underlying fibrosis where a depletion of energy levels, destabilisation of calcium homeostasis and elevation of reactive oxygen species lead to TG2 activation (Grosso and Mouradian, 2012). The normal physiological level of calcium within the cell is about 100-200nM, at which, TG2 ceases to function either due to the presence of inhibitory levels of GTPase (50-300μM) or other regulatory processes. This suggests that the activation of intracellular TG2 requires an immense distortion of physiological conditions which in turn promotes the covalent Ca^{2+}-mediated crosslinking by TG2 of glutamine containing protein and peptide substrates to lysine containing peptides or to primary amines (Folk and Finlayson, 1977, Greenberg *et al.*, 1991, Griffin *et al.*, 2002, Siegel and Khosla, 2007). This reaction however occurs at the catalytic domain of the enzyme (Beninati and Piacentini, 2004). Hence, TG2 assumes an active, open (Ca^{2+}-bound) or an inactive closed (GTP bound) conformation, which regulates its activity intracellularly or extracellularly when secreted through an unknown mechanism. Studies have shown that this secretory pathway obviates the ER/Golgi pathway due to the lack of a signal sequence however its trafficking to the cell surface requires an intact N-terminal β-sandwich domain (Balklava *et al.*, 2002, Gaudry *et al.*, 1999a, Gaudry *et al.*, 1999b) and its interaction with the cell surface heparan sulphate proteoglycan syndecan-4 (Wang *et al.*, 2012).

As studies unfold about the importance of TG2 activity in inflammation, evolving studies have shown the TG2 gene to be activated by various factors. With the TG2 protein having a half-life of around 11 h, the sustainability of its activity would depend on either a constitutive or non-constitutive activation of its gene. Retinoid and steroid hormones have been shown to increase TG2 transcription (Verderio *et al.*, 1998, Melino *et al.*, 1988, Piacentini *et al.*, 1988). Various cytokines and inflammatory factors

like TGFβ1 via a TGFβ response element and TNF-α via IκB phosphorylation have been shown to increase TG2 gene expression by acting directly on the TG2 promoter site (Ritter and Davies, 1998, Kuncio *et al.*, 1998). This suggests that with an increase in co-factors that increase TG2 gene expression in pathological conditions, a consequential progression of inflammation followed by fibrosis might ensue in a number of diverse diseases where TG2 is implicated.

TG2 and TGFβ1 have been shown to interact in a vicious circular relationship in various fibrotic diseases and this association has been characterised by the elevation of both activities (Kojima *et al.*, 1993, Nunes *et al.*, 1997, Akimov and Belkin, 2001b, Telci *et al.,* 2009). In addition, this relationship promotes TG2 externalisation to the cell surface and deposition into the matrix via a cell heparan sulphate- dependent mechanism where active cell surface and matrix bound TG2 cause an increase in TGFβ1 activation via its crosslinking of the large latent TGFβ binding protein (Akimov and Belkin, 2001b, Verderio *et al*., 1999, Verderio *et al*., 1998). In CF, lung remodelling and fibrosis has been linked to an increase in TGFβ1 where elevation of TGFβ1 has been shown to down regulate the expression of the CFTR channel (Bremer *et al.,* 2008, Pruliere-Escabasse *et al*., 2005, Snodgrass *et al*., 2013). Studies by Olsen *et al.* (2011) have linked elevated TG2 expression in the lungs with an increase in fibrosis where elevation of TGFβ1 increases externalisation and activity of TG2 on the cell surface. It was further investigated and shown by Olsen *et al.* (2013) that TG2 activity was inhibited using electrophilic molecules that abrogate fibrosis in Idiopathic Pulmonary Fibrosis (IPF).

Recent studies have correlated the progression of fibrosis in CF with an increase in TG2 expression. Maiuri *et al*. (2008) and Luciani *et al.* (2009) showed that SUMOylated TG2 prevents enzyme degradation but elevates activity which in turn increases reactive oxygen species (ROS), down regulates PPAR-γ and activates the NFκB inflammatory pathway with sustained inflammation in the lungs. They further extended the work to show that a defect in cellular autophagy occurred due to an increase in sequestration of beclin 1 and its associate partner, phosphatidylinositol-3-Kinase (PI(3-)K), as a consequence of TG2 SUMOylation, thus sustaining the unremitting inflammation in CF.

3.2 Aims:

In this chapter, work will be undertaken to determine if in CF cell models;

- The elevation of TG2 protein levels can be correlated with an increase in TG2 activity.
- To determine the levels of TGFβ1 in CF cells. This will include the mutant CF cell line, IB3 and its corrected “add-back” cell, C38 as well as primary human bronchial epithelial cells, (HBEC) cultured in submerged conditions.
- Also, to evaluate the effect of TG2 cell-permeable and impermeable inhibitors on TG2 activity on whole cell lysates and on cell surface.
- In addition, to evaluate the effect of TG2 inhibition on TGFβ1 secretion and activity.

3.3 Methods:

3.3.1 RNA purified from IB3 and C38 cells cultured in submerged medium

To purify RNA from IB3 and C38 cells, 5 x10^5 cells were cultured in 10mm petri dishes to a confluency of 80-90%. RNA was extracted using the TRIzol® method as described in chapter 2.2.12. The RNA levels in samples were quantified using the Nanodrop® spectrophotometer.

3.3.2 IB3 and C38 RNA reverse transcribed to cDNA

Using the Qiagen® RT^2 First Strand Kit, RNA fragments from IB3 and C38 cells were transcribed into cDNA as described in chapter 2.2.13. cDNA obtained from the cells was then used for PCR.

3.3.3 TG1-4 and FX III gene expression determined using PCR

The PCR was performed using annealing temperatures derived from primers for Transglutaminases (TG); TG1-4 & Factor 13, FX III. The PCR was performed as described in chapter 2.2.14. PCR was run for 35 cycles and cDNA amplicons were separated on agarose gel (2%w/v) and gel pictures taken on a G:BOX UV transilluminator.

3.3.4 SDS-PAGE/Western Blotting to determine whole cell and cell surface protein expression of TG2

8%(w/v) polyacrylamide gels were made and protein samples (50µg of protein per lane) separated as described in chapter 2.2.3. Western blotting as described in chapter 2.2.4 using TG2 antibody was used to immunoblot membranes and bands detected using luminescence obtained using ECL reagent (1:1) and images captured using the G:Box (Syngene®).

3.3.5 Surface proteins biotinylation to determine cell surface TG2 in IB3 and C38 cells

The biotinylation assay was carried out on IB3 and C38 cells cultured in submerged culture to determine cell surface TG2 as described in chapter 2.2.8. Western blotting as described in chapter 2.2.4 was carried out using biotinylated protein samples.

3.3.6 TG2 activity determined on whole cell lysates and cell surface proteins using the Biotin Cadaverine incorporation assay

5 x10^5 IB3 and C38 cells were cultured in 6-well plates for 6 h to allow attachment and medium was changed and replaced for treated groups supplemented with TG2 cell-permeable inhibitor, R283 (500μM). Whole cell lysates from IB3 and C38 cells, were obtained as described in chapter 2.2.2.1 were used for TG2 activity assay as described in chapter 2.2.6.1. For cell surface TG2 activity, IB3 and C38 cells were treated with TG2 cell-permeable inhibitors; R283 (500μM) and Z-Don (50μM) and cell impermeable inhibitors; R292 (250μM) and R294 (250μM) in the presence of 0.1mM biotin cadaverine in fibronectin (5μg/ml) coated plates. Assays were carried out as described in chapter 2.2.6.2.

3.3.7 Determination of Total TGFβ1 Assay using Human/Mouse TGFβ1 ELISA Ready-SET-Go!® (2nd Generation)

2.5 x 10^5 IB3 and C38 cells were cultured in 400μl per well complete AEM in 12 well plates. The cells were cultured for 6 h to allow attachment in complete medium. The cells were then treated with TG2 inhibitors; R292 (500μM), R294 (500μM), R283 (500μM), (50μM) and Z-Don (100μM) in serum free medium supplemented with 1x ITS supplement and incubated for 24 h. The medium was collected and centrifuged at 300g for 5min to remove cell debris. The ELISA for TGFβ1 was performed as per the manufacturer's instructions (eBiosciences). All experiments were carried out in triplicate as described in chapter 2.2.9.

3.4 Results:

3.4.1 Differential TGases expression in CF cells

Previous studies have not elaborated on the differential gene expression of transglutaminases in the lung. Although a myriad of findings have been made on the gene expressional levels of TG1 and TG2 in the lungs. Studies have shown in human bronchial epithelial cells (HBEC), that mRNA levels of TG1 and TG2 are elevated by the presence of the pro-fibrotic cytokine, TGFβ1(Vollberg *et al*., 1992). Schittny *et al.,* (1997) described the presence of TG2 mRNA and protein in whole lung homogenates from Wistar rats obtained one day before term. Also Hiiralgi *et al.,* (1999) showed using mouse lungs, liver and kidney that TG1 was distributed in these tissues with the kidneys and liver expressing higher amount than the lungs. Here, an attempt is made to show the differential gene expression of TGases in CF cells using the CF cell line, IB3 and its "add-back" cell, C38 in submerged culture. Results show that TG1 and TG2 genes were expressed in IB3 and C38 cells compared to the control. No gene expression was observed for TG3 and FX III in either cell line (Figure 3.1A). Comparing TG1 and TG2 gene expression using RT-PCR (Figure 3.1B) showed that IB3 cells expressed higher gene levels of TG1 over C38 cells whilst for TG2, a similar increase in gene expression was observed between C38 cells and IB3 cells. IB3 and C38 cells expressed more TG2 than TG1 with IB3 cells significantly showing more TG2 expression. This result supports earlier studies of TGases gene expression in the lung and further suggests that an increase in TG1 and TG2 genes in CF cells occurs either in a reparative or pathological manner.

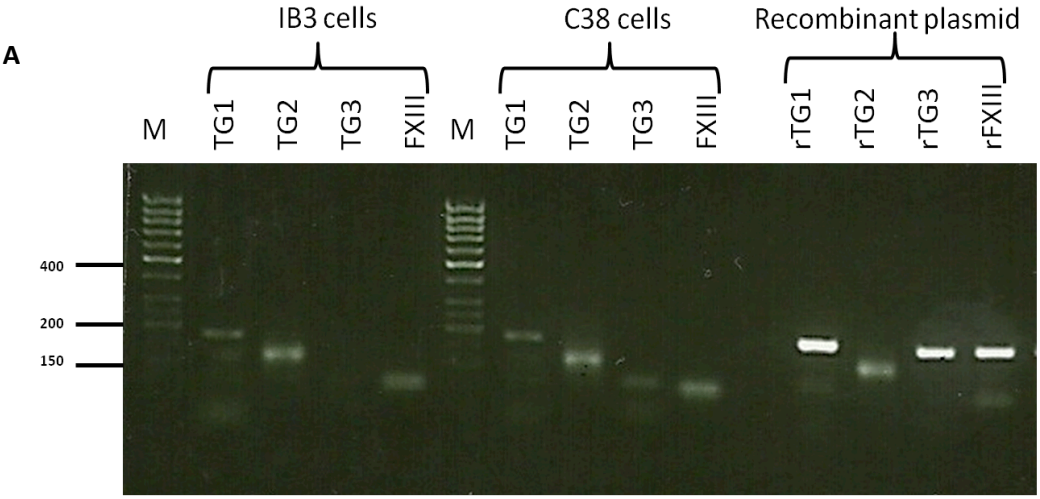

Figure 3.1A: TG gene expression in IB3 and C38 cells. cDNA products of IB3 and C38 cells were run on 2% agarose gel. Lanes are labelled with marker, M, TG1-3 and FXIII for IB3-1 and C38 cDNA. Recombinant TG1-3 and FXIII were used as positive controls (labelled recombinant plasmid). Gels were stained with ethidium bromide and images were taken using the G:Box. Experiments were carried out twice. Result shows gene expression of TG1 (172bp) and TG2 (167bp) in IB3 and C38 cells.

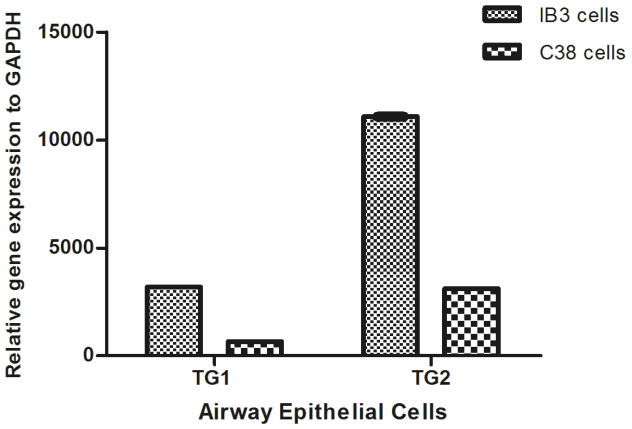

Figure 3.1B: Relative TG1 and TG2 expression in IB3 and C38 cells cultured in submerged culture. RNA was extracted from IB3 and C38 cells and RT-PCR was carried out with primers for TG1 and TG2. C_T values were analysed using $\Delta\Delta$Ct method using GAPDH as house keeping gene. Values indicate mean and standard deviation of two independent experiments carried out in triplicates. Results show high TG1 and TG2 expression in IB3 cells compared to C38 cells however the TG2 expression was shown to be higher than TG1 expression in both cell lines.

3.4.2: CF phenotype correlates with elevated TG2 protein expression levels

Elevated TG2 protein expression has been associated with the progression of various fibrotic conditions as mentioned in chapter 1. At the epicentre of the discussion in chapter 1, studies have linked high TG2 protein expression in CF with the sequestering of peroxisome proliferator activated receptor gamma (PPAR-γ) (Maiuri *et al.,* 2008), SUMOylation (Luciani *et al*., 2009b) and defective autophagy (Luciani *et al*., 2010b, Luciani *et al.*, 2012). To demonstrate the protein levels of TG2 expressed in CF, IB3, a CF cell line and the corrected "add-back" cell, C38 were used for this study. Results show elevated TG2 protein expression in whole cell lysates of IB3 cells compared to C38 cells. C38 cells showed a 5-fold decrease in TG2 expression compared to IB3 cells (Figure 3.2B). These observations concur with the results shown by Maiuri *et al*. (2008) where TG2 protein expression in IB3 cells was higher compared to protein expression in C38 cells.

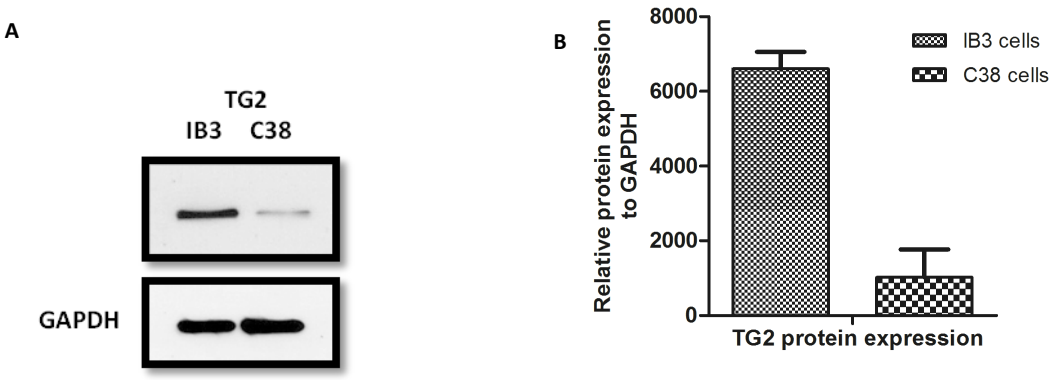

Figure 3.2A-B: TG2 expression in whole cell lysates of IB3 and C38 cells. IB3 and C38 cells were cultured in submerge culture for 48h. Cells were lysed and 50µg of protein was used for SDS/PAGE and Western blotting (WB) was carried out as described in methods. The WB represents a typical result of three independent repeats. Densitometry analysis shows the mean values and standard deviation of 3 experiments normalised to GAPDH expression and indicates that IB3 cells express higher TG2 protein compared to C38 cells. A 5-fold increase in TG2 expression was observed in IB3 cells compared to C38 cells.

Studies have implicated cell surface TG2 in fibronectin assembly where they crosslink these matrix proteins and form high molecular weight complexes (Jones *et al.*, 1997, Verderio *et al.*, 1998). Also Martinez *et al.* (1994) demonstrated using hepatocytes and endothelial cells that TG2 crosslinks fibronectin forming high molecular weight complexes. Here an attempt is made to evaluate cell surface TG2 protein expression in IB3 and C38 cells in submerged culture. The results observed in Figure 3.3A shows an elevation of TG2 cell surface protein expression in IB3 cells compared to C38 cells. TG2 expression in IB3 cells was >5 fold more than protein expression observed in C38 cells. This is in concert with what was observed in whole cell lysates in Figure 3.2. This suggests an involvement of cell surface TG2 in orchestrating the effect of TG2 in these cells.

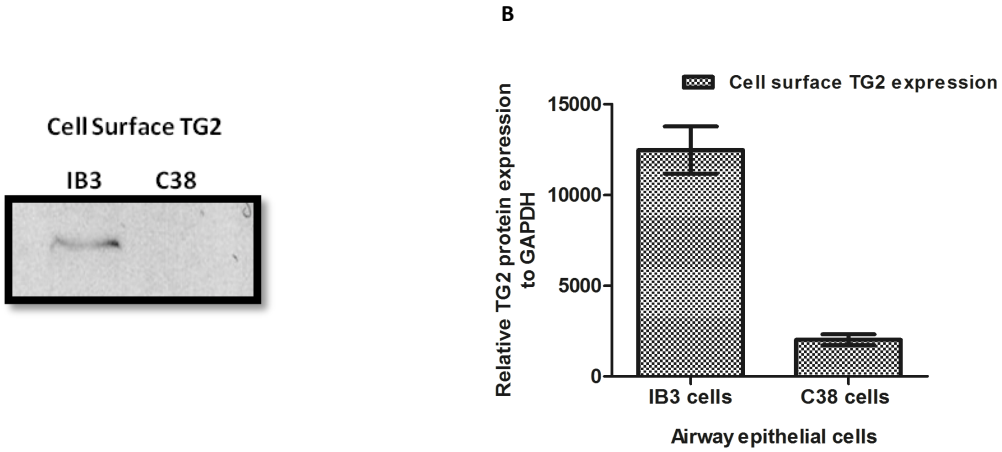

Figure 3.3A&B: TG2 expression on the surface of IB3 and C38 cells. IB3 and C38 cells were cultured in 60mm petri dishes and cell surface TG2 was captured using biotinylated Sulfo NHS biotin to label cell surface proteins as described in methods. 500µg of biotinylated proteins were loaded on 8% (w/v) gels for Western blotting as described in methods. GAPDH was used to check for cytosolic protein contamination. The image represents a typical result from three independent repeats. Densitometry analysis show high TG2 cell surface protein in the total biotylated protein of IB3 compared to C38 cells with a >5-fold decrease in TG2 cell surface expression was observed in C38 cells. Data represent mean values and standard deviation of 3 independent experiments normalised to total TG2 expressed.

Using normal primary human bronchial epithelial cells, HBEC, TG2 protein expression was compared with IB3 cells to demonstrate the pathological variation of TG2 protein, expressed in CF and non-CF cells, cultured in submerged medium. Cell culturing and Western blotting was carried out as described chapter 2.2.1.2 and 2.2.4. Results show HBEC protein blots from passage 2 cells. It was observed that HBEC cells express very low levels of TG2 compared to IB3 cells (Figure 3.4 A&B). Densitometry shows an increase in TG2 protein expression in IB3 cells compared to normal HBEC cells. Luciani *et al*. (2009, 2010) suggested TG2 SUMOylation to be responsible for the elevated TG2 observed in the disease linking that to ER stress and an increase in reactive oxygen species (ROS) levels, which results from the effect of the mutated CFTR channel. Although, the results showed here are preliminary, this is indicative of TG2s involvement in the disease.

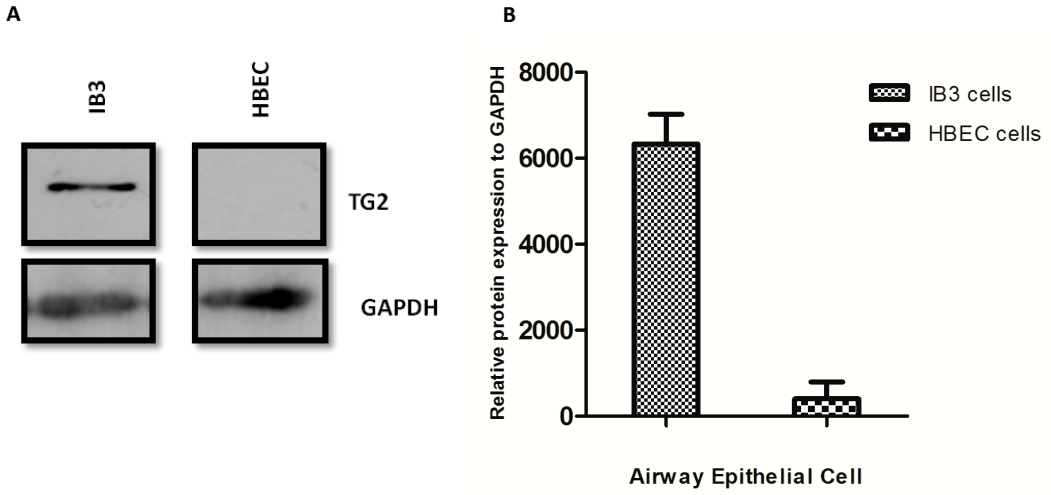

Figure 3.4A&B: TG2 expression in whole cell lysates of IB3 cells compared to primary human bronchial epithelial cell (HBEC) cells. IB3 and HBEC cells were cultured in 6-well plates for 48h prior to cell lysis and 50µg of protein used for Western blotting as previously described in chapter 2.2.4. GAPDH was used to normalise protein loading. **A:** The blot image is a characteristic result from two independent repeats. **B:** Densitometry represents the mean values and standard deviation of 2 independent experiments normalised to GAPDH intensity. Results suggest relatively high TG2 protein expression in IB3 cells compared to HBEC cells. This suggests there is more TG2 protein expressed in CF cells than normal cells.

3.4.3: Elevated TG2 activity concurs with increased TG2 protein expressed in CF cells

A number of airway diseases where TG2 has been implicated have demonstrated the activity of the TG2 in these diseases to be directly linked to the presence of the protein. Olsen *et al*. (2011) showed that an elevation of TG2 protein in IPF correlated with an increase in TG2 activity, which was further augmented in the presence of TGFβ1. As observed in CF IB3 cells, TG2 protein levels were shown to be markedly elevated. Here, using IB3 and C38 cells, TG2 activity is determined to observe the correlation between protein expression and activity. Whole cell lysates and intact cells (for cell surface activity) were obtained and an assay was carried out to determine TG2 activity as described in chapter 2.2.6.1 and 2.2.6.2. The results from Figure 3.5A&B show elevated TG2 activity in IB3 cells compared to C38 cells for both whole cell lysates and cell surface TG2. However, in the presence of R283, a cell-permeable TG2 inhibitor (Skill *et al*., 2004, Harrison *et al.*, 2007), a 2-fold inhibition in activity in IB3 and C38 cells was observed in whole cell lysates. This was however mirrored with cell surface TG2 activity showing a 2-fold increase in TG2 activity in IB3 cells compared to C38 cells. However in the presence of both TG2 cell-permeable (R283, Z-Don) and impermeable inhibitors (R292 and R294), a significant inhibition was observed in cell surface TG2 activity in IB3 cells but only marginally observed in C38 cells. Compared to the negative control where activity was abolished with 10mM EDTA (not shown), C38 cells showed no significant surface activity.

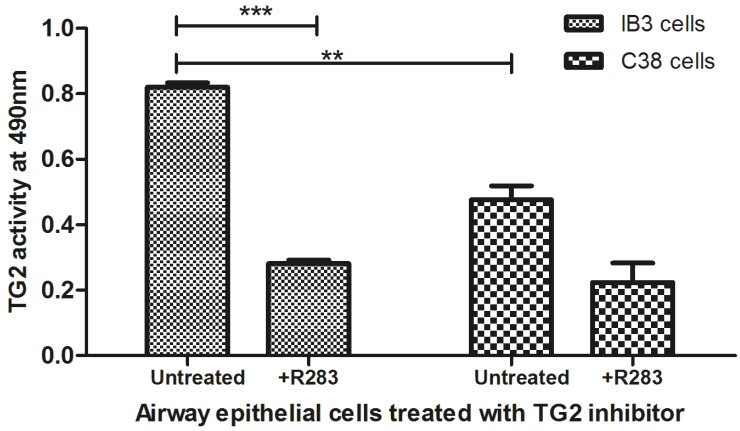

Figure 3.5A: TG2 activity in whole cell lysates of IB3 and C38 cells. IB3 and C38 cells were cultured under submerged conditions in 6 well plates for 48 h. Cell lysates were collected and incubated with TG2 cell-permeable inhibitor; R283 (500µm). Results show significantly higher expression of TG2 in untreated IB3 cells compared to untreated C38 cells. However, in the presence of R283, TG2 expression was significantly inhibited in both cell lines with a >2-fold inhibition in IB3 cells and an estimated 2-fold inhibition in C38 cells. The results represent means and standard deviation of three independent experiments carried out in triplicates. Two-way Anova with Bonferroni post-tests: **p<0.01, ***p<001.

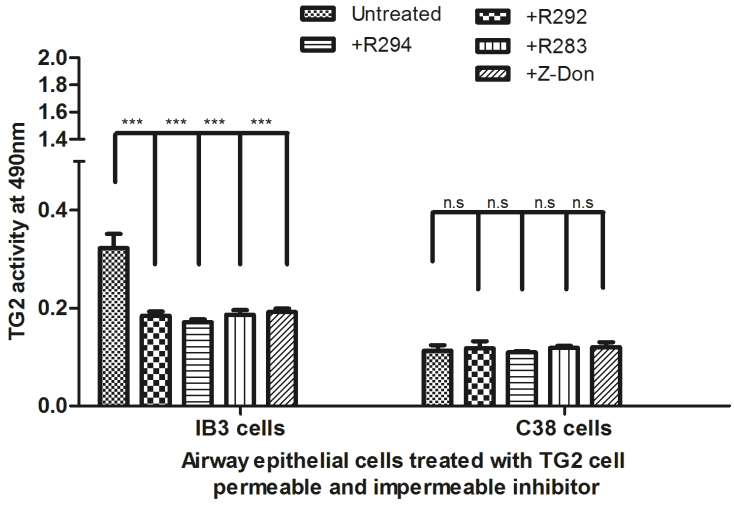

Figure 3.5B: TG2 cell surface activity in IB3 and C38 cells. IB3 and C38 cells cultured for 48 h and cells detached from matrix using 0.5mM EDTA in 1x PBS, pH 7.4. The cells were plated on fibronectin coated plates and incubated with TG2 inhibitors; impermeable {R292 (500µm), R294 (500µm)} and permeable {R283 (500µm) and Z-Don (50µm)}. Cell surface TG2 expression is higher in IB3 cells compared to C38 cells however, in the presence of both cell permeable and impermeable inhibitors, TG2 expression was inhibited 2-fold in IB3 cells. Results represents mean values and standard deviation of 3 independent experiments carried out in triplicates. One-way Anova with Dunnett's multiple comparison tests: ***p<0.0001, n.s p>0.05.

3.4.4: TG2 is involved in the activation of TGFβ1 in CF cells.

Previous studies have shown a link between TG2 activity and TGFβ1 activation in various cells. In bovine aortic endothelial cell (BAEC), an elevation of TG2 levels by retinoids correlated with an increase in activation of TGFβ1 from its latent form (Kojima *et al.*, 1993). In addition, an inhibition of TG2 activity via TG2 inhibitors or neutralising antibody abolished this process. Similarly, Nunes *et al.* (1997) demonstrated that both latent TGFβ1 binding protein (LTBP-1) and large latent complex are TG2 substrates, which are covalently cross-linked into the matrix serving as intermediates for the activation of TGFβ1. To show that TGFβ1 receptors play a role in TG2 activation of TGFβ1, the serine-threonine kinase receptors of TGFβ1, RI and RII protein expression was determined. Results in Figure 3.6A show expression of TGFβ RI and RII in IB3 and C38 cells with expression of TGFβ RI shown to be higher in both cells compared with RII. These results show that CF cells express TGFβ receptors and suggest the possible involvement of TGFβ1 in CF disease in these cells.

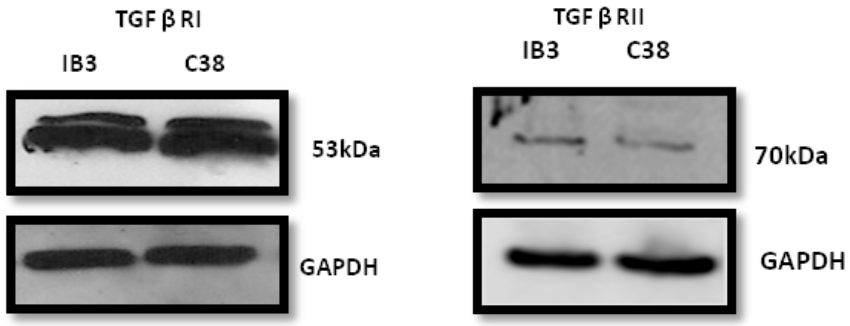

Figure 3.6A: TGFβ receptor 1 and 2 (RI and RII) expression in IB3 and C38 cells. Cells were cultured for 48h in complete medium before lysis and 50μg of protein used for Western blotting (WB). The WB images represent a characteristic result of 2 independent experiments. GAPDH was used to normalise protein loading. Results show expression of TGFβ RI and RII in both cell lines with relatively more TGFβ RI expressed in both IB3 and C38 cells.

To evaluate the level of TGFβ1 in the CF cells, TGFβ1 gene expression and levels were measured. To determine gene expressional levels, cDNA from IB3 and C38 cells were used with specific TGFβ1 primers as listed in table 2.2. The ΔΔCT method was used with GAPDH serving as housekeeping gene. Results shown in Figure 3.6B indicate that TGFβ1 gene expression is higher in IB3 cells compared with C38 cells. C38 cells showed similar expressional levels to negative control, which indicates marginal TGFβ1 gene expression in these cells. Further replicates will determine if the observations made are significant. Also secreted TGFβ1 levels were evaluated in serum free medium collected from IB3 and C38 cells cultured in submerged conditions. To quantify soluble TGFβ1, standard curves were first constructed using recombinant human TGFβ1 protein and TGFβ1 levels in cell culture samples were determined relative to the standard values.

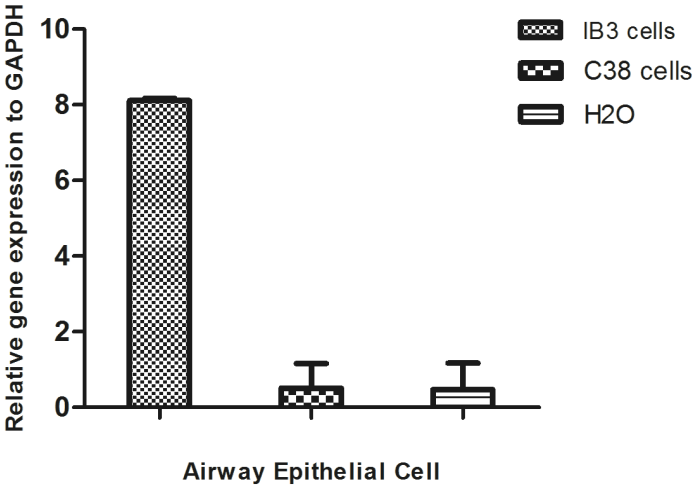

Figure 3.6B: TGFβ1 gene expression in IB3 and C38 cells. The cells were cultured for 48 h and RNA was extracted using the TRIzol method. cDNA was used for the RT-PCR. GAPDH was used as housekeeping gene and RNAse free water (H20) as negative control. Results show high TGFβ1 expression in IB3 cells and negligible expression in C38 cells. Results represent mean values and standard deviation of two independent experiments carried out in triplicates.

The results shown in section Figure 3.6B with TGFβ1 gene expression was confirmed when TGFβ1 levels were determined in serum free medium. The results (Figure 3.6C) show that minute TGFβ1 cytokine was secreted by C38 and HBEC. However, TGFβ1 levels found in the culture medium of IB3 cells was significantly elevated ($p<0.002$) as a 4-fold increase was observed compared to C38 cells. These observations correlate with TG2 gene and protein expression and could reflect a hypothetical link between the expression of TG2 and TGFβ1.

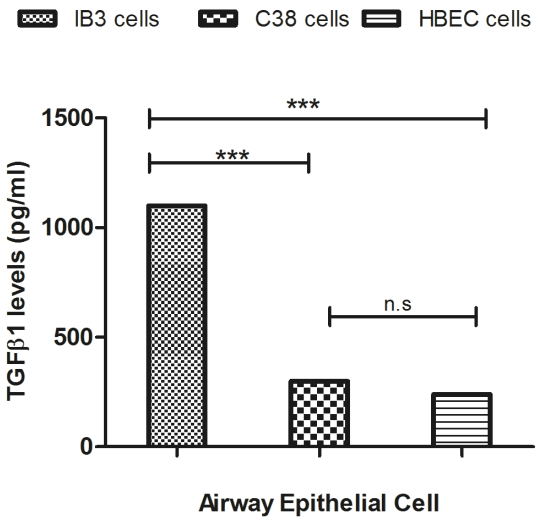

Figure 3.6C: TGFβ1 levels in IB3, C38 and HBEC cells. The cells were cultured in serum free medium for 24h before supernatants were collected and TGFβ1 levels measured by ELISA. AEM was used as the negative control (not shown). Results show a 4-fold increase in TGFβ1 levels secreted by IB3 cells compared to C38 or HBEC cells. HBEC and C38 cells secrete very low levels of TGFβ1. Results represent mean values and standard deviation of three independent experiments carried out in triplicates. One way Anova analysis with Bonferroni's Multiple comparison test; ***$p<0.002$.

Consequently, since this study hypothesises an activation of TGFβ1 from its latent forms by TG2, an inhibition of TG2 by TG2 inhibitors should consequentially block that activation thus impeding the release of TGFβ1 from its latent complex. Hence, IB3 and C38 cells were treated with cell permeable and impermeable TG2 inhibitors. Results show a significant decrease in TGFβ1 levels in IB3 cells in the presence of TG2 inhibitors. As shown in Figure 3.6D, a > 2-fold decrease in TGFβ1 levels was observed between IB3 and the control CF cell, C38 cells, which expresses marginal TGFβ1 gene expression and mirrors TGFβ1 levels in the presence of TG2 inhibitors which show similar low levels of TGFβ1. This result suggests that TG2 is involved in the activation

of TGFβ1 from its latent forms and proposes a direct link between TG2 and TGFβ1, where TG2 drives TGFβ1 activation.

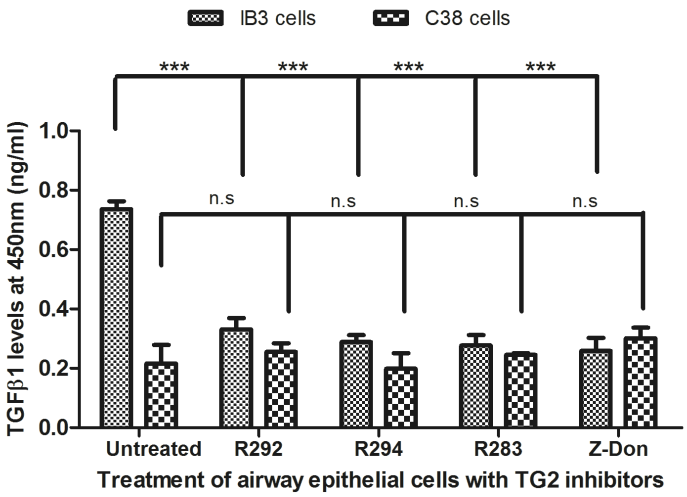

Figure 3.6D: TGFβ1 levels in IB3 and C38 cells incubated with TG2 cell-permeable and impermeable inhibitors. The cells were cultured in serum free medium for 24 h. Media was collected and TGFβ1 levels were determined. AEM medium was used as negative control (not shown). It was observed that for IB3 cells in the presence of TG2 cell permeable and impermeable inhibitors, soluble TGFβ1 was significantly inhibited. The inhibition observed to be >2-fold compared to untreated cells. C38 cells produced low levels of TGFβ1 and did not change in the presence of inhibitors. Results represent mean values and standard deviation of three independent experiments carried out in triplicates. One- way Anova with Dunnett's multiple comparison test: ***$p<0.0001$, n.s $p>0.05$.

3.5 Discussion:

The previously elucidated role for TG2 in CF was centred on increased protein expression and transamidation activity with recent studies attributing this to a faulty degradation mechanism involving TG2 SUMOylation and its ability to obviate the ubiquitin-proteosomal system (Luciani *et al.*, 2009b). The main mechanism of accomplishing this role relies on the transamidation activity of TG2. Here the results show that in CF cell lines, TG2 expression is driven by its intricate regulation by TGFβ1, the pro-fibrotic cytokine highly secreted and activated in CF. Although, studies have shown its relationship in other respiratory diseases, this is the first account of TG2 shown to be activating TGFβ1 in CF cells.

These studies have shown, using the CFTR mutant cell, IB3, that TG2 expression correlates with high TGFβ1 secreted from these cells (Figure 3.2 and 3.6D). Hence TG2 gene expression was shown to be elevated in contrast to its corrected cell, C38. Consequently, TG2 protein expression in IB3 cells was significantly increased which coincided with an elevated TG2 activity as measured by a TG2 incorporation assay in fibronectin (Figure 1.5A). Importantly, these results show that cell surface TG2 plays a vital role in orchestrating TG2 function in CF. Verderio *et al.,* (1999) and Akimov e*t al.,* (2001a) reported on the role of cell surface TG2 and the effect of activating TGFβ1 in relation to matrix growth. Elevated active cell surface TG2 is present in IB3 cells, which is inhibited by both cell-permeable (R283 and Z-Don) and cell impermeable TG2 inhibitors (R292 and R294) but is minimally expressed in C38 cells. These results show that the protein expression and activity of TG2 in whole cell lysates can be reversed significantly in the presence of inhibitors and demonstrates the importance of cell surface TG2 in the total TG2 activity of the cell. This also implies that TG2 is active in CF cells and suggests further that the activity observed in CF cells might be originating from the cell surface as calcium was augmented in whole cell lysates therefore a slightly elevated TG2 activity observed and the presence of cell-permeable inhibitors did not markedly change the inhibitory pattern observed on the cell surface. It therefore can be postulated in concert with literature that high TG2 protein in CF cells may account for elevated TG2 activity and cell surface TG2 activity might be responsible for the observed TG2 effects.

In retrospect, the overarching role of TGFβ1 has been elucidated in various pulmonary diseases including asthma (Hackett *et al*., 2009, Drumm *et al*., 2005), IPF (Olsen *et al.,* 2011) and CF (Arkwright *et al.*, 2000, Drumm *et al.*, 2005) and remains an important

physiological driver of fibrosis in the lungs. This study has shown elevated levels of TGFβ1 in IB3 cells but interestingly TG2 inhibitors abrogate TGFβ1 secretion (Figure 3.6D). Also, the inhibition was observed equally between all TG2 inhibitors, which suggest that cell surface TG2 might principally be involved in the secretion of TGFβ1 in CF. The study has showed that both IB3 and C38 cells bear TGFβ1 receptors RI and RII on their cell surface. This supports the hypothesis that TG2 is principally involved in the release of TGFβ1 from its latent complex and so might serve as a rate limiting step necessary in driving disease processes where TGFβ1 plays a major lead role. In comparison, the study observed that HBEC cells show minimal TGFβ1 levels that are similar to C38 cells. This suggests that in normal bronchial epithelial cells, although TGFβ1 plays a role as a proinflammatory cytokine in normal wound healing, an unremitting TG2 in CF maximises its inflammatory characteristics leading to a pro-fibrotic cascade. Also the marginal expression of TG2 in HBEC cells suggests that although TG2 might be present in normal lungs, its probable activity centres on TG2s pathological role, where it can drive or is driven to support the progression of airway diseases.

3.6 Conclusion

Although the findings are in their nascent stages, it can be hypothesised that since TG2 inhibitors reduce TGFβ1 levels, active TG2 in CF cells may be involved in the release and activation of TGFβ1 from its latent forms and might be involved in the pathology of CF.

Chapter 4

The Role of TGFβ1 in CF: An outlook on EMT and the effect of TG2 inhibition and knockdown on EMT in CF cells

4.1 Introduction:

A large number of studies have correlated the progression of pulmonary fibrosis with the pro-fibrotic cytokine, TGFβ1 (Bartram, 2004, Olsen *et al*., 2011, Frank *et al*., 2003, Sheppard, 2006b, Kwong *et al*., 2006). Evidence suggests that the increased growth and stabilisation of the matrix contributes significantly to the progression of fibrosis. However, Kaminski *et al.,* (2000) hypothesised in a comprehensive review of genes regulating pulmonary fibrosis, that aside from elevated TGFβ1 and its cohort of inducible genes, other regulatory factors contribute to the progression of fibrosis.

In CF, the insidious progression of fibrosis has been attributed to elevated levels of TGFβ1 (Snodgrass *et al*., 2013). Gene profiling has shown that amongst 10 important genetic modifiers of CF, the polymorphism carried on the TGFβ1 gene significantly accentuates pulmonary fibrosis in CF (Drumm *et al*., 2005). Arkwright *et al.,* (2000) observed that the polymorphism in TGFβ1 on codon 10 accounts for the chronic pernicious fibrosis in CF airways. Later, Hilliard *et al.,* (2007) observed in bronchoalveolar lavage (BALF) of children (< 17 yrs), a correlation between the elevated levels of TGFβ1 with the thickening of reticular basement membrane, primarily linked to airway remodelling in CF. This occurs due to the inhibition of matrix degradation by TGFβ1 thus decreasing metalloproteinases, collagenases and stromelysin production whilst the level of protease inhibitors like tissue inhibitor of metalloproteinases (TIMP) are elevated (Edwards *et al*., 1987). In contrast, TGFβ1 in normal lungs plays a vital role in regulating tissue remodelling in wound injury (Grande, 1997), maintaining lung homeostasis and cell proliferation/differentiation (Bartram, 2004).

In relation to TG2, studies have shown that the large latent TGFβ1 binding protein (LTBP-1) is a substrate of TG2 and demonstrated that TG2 mediated crosslinking is important in TGFβ1 dissociation from the TGFβ pro-peptide, latency activated peptide (LAP), in the activation of TGFβ1 (Nunes *et al*., 1997). TG2, in its role at the cell surface/matrix is involved in crosslinking LTBP-1 to the matrix and hence can release the small latency complex, which on exposure to pH changes, heat or proteolysis releases active TGFβ1. This culminates in the activation of TGFβ1 by TG2 and this complex interaction has been shown to account for the increased activation of TG2 by TGFβ1 via the TGFβ response element on the TG2 promoter site (Kojima *et al*., 1993,

Ritter and Davies, 1998, Telci *et al*., 2009). Thus it can be hypothesised that in the presence of exogenous TG2 or TGFβ1, an elevation of TGFβ1 or TG2 can be observed. Munger *et al.* (1999) and Mu *et al.* (2002) described the activation of TGFβ1 in epithelial cells to depend chiefly on the integrins, αV, where certain subsets, αVβ6 and αVβ8 could bind directly to the RGD motif of LAP and in some cases induce conformational changes which exposes latent TGFβ1 to membrane type-1 MMP cleavage thus activating TGFβ1. A large number of studies have attempted to show the role αVβ6 integrin plays in the activation of TGFβ1 by ultimately linking its association with LAP via binding to the recognition sequence, RGD and activating the cytokine. This was shown with co-cultures of bovine aortic endothelial cell (Cho *et al.*, 2007) or bovine aortic smooth muscle (BSM) which were β6 transfected expressing αVβ6 on the cell surface as well as Mink stably lung epithelial reporter cells transfected with the TGFβ responsive portion of the plasminogen activator inhibitor 1 promoter driving the expression of firefly luciferase (Abe *et al.*, 1994), where an elevation in luciferase activity was measured. However, this was abrogated in the presence of TGFβ or αVβ6 antibodies (Sheppard, 2005). Research has also shown that the β6 integrin subunit exists only as αVβ6 as deletion of the β6 domain abrogated TGFβ1 activity without impairing adhesion to LAP (Busk *et al.*, 1992, Sheppard, 2005). Although epithelial injury is associated with the increase of αVβ6 integrin, its paracrine effect depicts its peculiarity in activating TGFβ1 devoid of the release of the cytokine from its latent complexes (Breuss *et al.*, 1995). This was depicted by the loss of TGFβ1 activity in mink TGFβ reporter cells plated across a microporous plate with β6-transfected cells. The result observed was attributed to the loss of direct cell-cell contact (Henderson and Sheppard, 2013). Together, this suggests that although αVβ6 might be involved in the activation of TGFβ1, other proteins/mechanisms may be involved.

In fibrosis, the lung epithelial microenvironment has been shown to undergo extracellular reorganisation described as Epithelial to Mesenchymal Transition (EMT) chiefly orchestrated by TGFβ1 as part of its pro-fibrotic role (Kasai *et al*., 2005, Doerner and Zuraw, 2009). Here, TGFβ1 plays the central role of promoting fibrosis as a consequence of an exaggerated reparative cytokine, hence elevating fibroblast proliferation, increased synthesis of mesenchymal growth factors, suppression of matrix degradation, actin skeleton reorganisation, loss of cell polarity, down regulation of tight junction and adheren junction markers which ultimately leads to epithelial cell migration (Xu *et al*., 2009, Bartram, 2004, Leask and Abraham, 2004). This all culminates into changing the cell morphology and phenotype. Similarly, it has been

shown that TG2 promotes EMT in cancer with its elevation associated with increased cell invasiveness and cell survival (Kumar *et al.*, 2010). Although, this study showed that TGFβ1 induces EMT via TG2 (Ritter and Davies, 1998) it failed to show that TG2 orchestrated the progression of EMT via TGFβ1. However, Kasai *et al.* (2005) and Hackett *et al.* (2009) showed in their study of Idiopathic Pulmonary Fibrosis (IPF) and asthma that TGFβ1 induced EMT in these disease conditions via SMAD 2 and SMAD 3 phosphorylation. Similarly, Camara and Jarai, (2010) showed using human bronchial epithelial cells (HBEC), an elevation in p-SMAD 2 expression in the presence of TGFβ1 with cells losing cell-cell contact and assuming a morphology consistent with EMT. Interestingly, Munger *et al.* (1999) had described the importance of actin cytoskeleton in αVβ6 mediated activation of TGFβ1 where a blockade of actin polymerisation leads to the abrogation of TGFβ1 activation via αVβ6. This suggests that as EMT involves active matrix deposition and thickening with adjacent cell migration leading to actin reorganisation, a hypothesis that an inhibition of TG2 activity by TG2 inhibitors will block EMT with TGFβ1 activity abolished independent of αVβ6. Noteworthy of mentioning is the recent work by Niger *et al*. (2013) where human bone marrow derived mesenchymal stem cells (hbMSCs) were cultured on collagen II pre-incubated with TG2 or TGFβ1 or both for 48 h and SMAD dependent luciferase activity was measured. A 4-fold increase in SMAD dependent luciferase expression was observed in the presence of collagen II pre-incubated with TG2. This suggests that the link between TG2 and TGFβ1 is SMAD dependent. This report is in concert with that of Olsen *et al.,* (2011) who indicated that elevated TGFβ1 levels were associated with increased cell surface TG2 and that TG2 knockout mice showed a reduction of matrix protein production in the fibrotic lung. Also, TG2 was hypothesised as increasing TGFβ1 activation thus promoting EMT in the lungs as shown in TG2 knockout mice (Shweke *et al*., 2008).

CF is a disease associated with the loss of CFTR function due to diverse mutations of the gene. CFTR regulates epithelial channel activity maintaining the balance between airway surface liquid (ASL), cilia movement and ion transport. This ultimately controls broncho-alveolar integrity. TGFβ1 has been observed to be a negative regulator of CFTR (Snodgrass *et al.*, 2013, Pruliere-Escabasse et al., 2005). Vij *et al.* (2009) described CFTR as a negative regulator of the inflammatory pathway involving NFκB via its effect on NFκB translocation. Also CFTR regulates the expression of the epithelial sodium channel (ENaC) where CFTR down regulates ENaC expression to maintain ASL (Schwiebert *et al*., 1999, Reddy *et al*., 1999). This suggests that the

down regulation of CFTR is associated with an up regulation of inflammatory pathways mediators/cytokines as well as an increase in ENaC channel activity, viscidity of mucus and loss of ciliary currents.

In the previous chapter, it was observed that an elevation of TG2 and TGFβ1 in CF cells could culminate in supporting the inflammatory process in CF cells. TGFβ1 induced EMT has been linked to fibrosis in various diseases in the lungs. TG2 knockout in the mammary epithelial cell line, MCF-10A has been shown to inhibit TGFβ1 induced EMT (Kumar *et al.*, 2010). Hence, the hypothesis is that in CF, where cells are in a continuous state of stress with elevated levels of various cytokines, TG2 up regulation can promote EMT via TG2 dependent activation of TGFβ1.

4.2 Aims:

In this chapter, the aim is to show that in a CF bronchial epithelial cell, the progression of fibrosis is mediated through EMT, driven by TG2 via TGFβ1. Hence the objectives are to:

- Evaluate TG2 and EMT marker gene expression in CF and control cells in the presence of TG2 inhibitors and TGFβ1.

- To show that CF cells express more EMT markers compared to control and that in the presence of TG2 inhibitors this can be reversed.

- To attempt to up regulate TG2 expression in control cells using rTGFβ1 to measure TG2 and EMT expression and use TG2 inhibitors to reverse this process.

- To evaluate the involvement of αVβ6 subunit in EMT via a direct or indirect link with TG2.

- To observe the role that SMAD 2 and 3 play as downstream mediators of TGFβ1 in regulating EMT in relation to elevated TG2 levels.

4.3 Methods:

4.2.1 Detection of gene expression using Real Time (RT)-PCR

To determine gene expression of TG2, TGFβ1, EMT markers ie fibronectin and N-cadherin, transcriptional repressors ie *Slug*, *Twist* and *Zeb 2* and the adherens junction marker, E-cadherin, RT-PCR was used. 5 x 10^5 IB3 or C38 cells were cultured on 60mm plates for 48 h in complete medium. RNA was extracted using the TRIzol® method as described in chapter 2.2.12. cDNA was made as described in chapter 2.2.13 using 5ng of RNA per cell line. Gene expression was determined from cDNA using RT-PCR, performed as described in chapter 2.2.15. cDNA was amplified in 40 cycles. The housekeeping gene was GAPDH. Relative levels of expression of genes were determined by normalising mean expression to GAPDH. ΔΔCT method was used in determining gene expression relative to GAPDH.

4.2.2 Evaluation of TG2 and TGFβ1 inhibition on gene expression

To investigate the involvement of TG2 and TGFβ1 on the expression of EMT markers, transcriptional repressors and adherens junction marker, the TG2 cell-permeable inhibitor, R283 (500μM) or rTGFβ1 (3ng/ml) were incubated with IB3 or C38 cells respectively and gene expression determined using RT-PCR. 5 x 10^5 of IB3 and C38 cells were cultured in submerged culture for 48 h, within which cells were treated with R283 and rTGFβ1 respectively prior to RNA extraction and cDNA production as described in chapter 2.2.12 and 2.2.13. Subsequently, using TGFβ1 primers, RT-PCR was carried out as described in chapter 2.2.15.

4.2.3 Expression of EMT markers and/or transcriptional repressor in IB3 and C38 cells

To investigate the protein expression of EMT markers ie fibronectin and N-cadherin and transcriptional repressors ie *Slug,* Western blotting was used as well as immunofluorescent staining. 5 x10^5 cells of IB3 and C38 cells were cultured in 60mm petri dishes for 48 h in complete medium and protein was extracted using lysis buffer

after washing the cells with 1x PBS, pH 7.4 twice as described in chapter 2.2.2.1. Western blotting was carried out as described in chapter 2.2.4. The membrane was blotted with TG2 (MA5-12989) (1:1000) in 5%(w/v) skimmed milk in 1x TBS-Tween (1M), pH 7.4 as described in section 2.2.4.

4.2.4 Immunostaining of IB3, C38 and HBEC cells

5 x 10^5 of IB3 and C38 cells were sub-cultured on 60mm petri dishes. The cells were cultured to confluency of 70-80%. The cells were washed three times with 1x PBS, pH 7.4 for 3 min each. Immunostaining was carried out as described in chapter 2.2.16.1. Antibodies to TG2, fibronectin (F3648) or N-cadherin (13A9) (1:100) were used to blot cells.

4.2.5 Inhibition of TG2 expression in IB3 and C38 cells

The presence of TG2 both on the cell surface and intracellularly suggests that the observed effect of the enzyme might be due to its activity in either compartment. To determine this, cell-permeable TG2 inhibitors ie R283 (500μM), 1-155(200nM), Z-Don (50μM) and cell-impermeable TG2 inhibitors ie R292 (500μM), R294 (500μM) and 1-133 (100μM) were used. 5 x10^5 cells of IB3 and C38 cells were incubated with inhibitors for 48 h where after fresh medium was added together with aliquots of the inhibitor compounds every 24 h. To determine cellular and matrix protein expression, cells were collected using 2mM EDTA in 1x PBS, pH 7.4 and matrix collected into 2x Laemmli buffer and boiled to denature protein. For whole cell lysates, the cells were lysed as described in chapter 2.2.2.1. Western blotting was performed for cell lysates and matrix proteins as described in chapter 2.2.4 of methods. Antibodies to TG2, fibronectin, N-cadherin and *Slug* (1:1000) were used to blot membrane using GAPDH staining as loading control.

4.2.6 Migration assay of IB3 and C38 cells in submerged culture

1 x 10^5 of IB3 and C38 cells were cultured in complete medium for 16h at 37^{o}C. The migration assay was carried out in serum free medium supplemented with 1 x ITS and in the presence of TG2 cell-permeable inhibitor R283 (500μM). Migration assays were carried out as described in chapter 2.2.7.

4.2.7 Effect of TGFβ1 inhibition in IB3 cells using TGFβ1 neutralizing antibody on EMT markers

5 x 10^5 of IB3 cells was cultured in 6-well plates for 48 h at 37^oC. The cells were incubated with TGFβ neutralizing inhibitor, Nab, (20µg/ml). The cells were rinsed with 1x PBS, pH 7.4 twice and cells were lysed as described in chapter 2.2.2.1. Western blotting was carried out as described in chapter 2.2.4. Antibodies to TG2, fibronectin, N-cadherin and *Slug* were used at 1:1000 dilution.

4.2.8 Co-immunoprecipitation of TG2 and αV/ β6 integrins

To determine TG2 and αV/ β6 integrins protein interaction in IB3 and C38 cells, proteins were immunoprecipitated. 5x 10^5 of IB3 and C38 cells were cultured in 60mm petri dish in complete AEM for 48 h. IB3 cells were treated with TG2 cell-permeable inhibitor, R283 (500µM) and C38 cells were treated with rTGFβ1 (3ng/ml). Cells were then washed with 1X PBS, pH 7.4 twice. Co-immunoprecipitation assay was carried out as described in chapter 2.2.20. The lysates collected from the assay were used for SDS/PAGE and Western blotting as described in chapters' 2.2.3 and 2.2.4 respectively.

4.3 Results:

4.3.1: TG2 inhibitors reverse EMT gene expression in CF

4.3.1.1: Inhibition of TG2 gene expression in IB3 cells impedes fibronectin, N-cadherin, *Twist*, *Slug* and *Zeb2* expression.

Previous results from chapter 3 have shown high TG2 expression in IB3 cells compared to C38 cells. This was linked to the high TGFβ1 levels in this cell. This study further seeks to assess the correlation between elevated TGFβ1 expression and EMT in IB3 cells. Figure 4.1 shows that elevated TG2 gene expression in IB3 cells is commensurate with an increase in fibronectin, N-cadherin, *Twist* and *Slug* gene expression. However, in the presence of R283, there was < 2-fold inhibition of TG2 expression. N-cadherin expression was slightly inhibited in the presence of R283 but was significant ($p<0.001$) compared to untreated cells along with a 2-fold inhibition in fibronectin, *Twist* and *Slug* expression. The expression of *Zeb 2* remained unperturbed in the presence of R283. From these results, it can be suggested that an inhibition of TG2 gene expression correlates with the blockade of EMT marker expression. This however does not show whether the activity of TG2 is involved as TG2 binds to fibronectin independent of its transamidating activity. However, it suggests that in IB3 cells, the fibrotic process may involve a cascade of processes where TG2 plays a role.

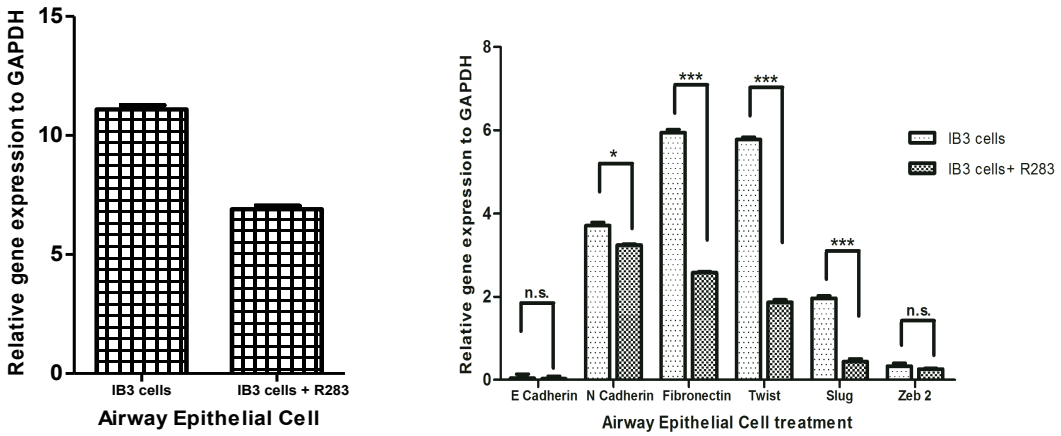

Figure 4.1: TG2 inhibition corresponds with a decrease in gene expression of EMT markers in IB3 cells. RT-PCR was performed using cDNA from IB3 cells to determine the gene expression of TG2 (left panel) and EMT markers, fibronectin, N-cadherin, *Twist*, *Slug* and *Zeb 2* (right panel) in the presence of R283 (500μM). Gene expression was determined using the ΔΔCT method with GAPDH used as house keeping gene to normalise gene expression. Results show an inhibition of TG2 gene expression in the presence of R283 compared to untreated IB3 cells, which corresponded to a decrease in fibronectin, *Twist and Slug* gene expression in these cells. N-cadherin expression was slightly reduced in the presence of the inhibitor however, E-cadherin and *Zeb 2* showed no change in gene expression in the presence of R283. Experiments were carried out in triplicates and results represent mean values and standard deviation of 3 independent experiments carried out in duplicates Two-way Anova analysis with Bonferronni's Posttests; *** $p<0.001$, n.s. $p>0.05$.

4.3.1.2: TGFβ1 promotes EMT progression via TG2 in C38 cells

Considering the effect of TGFβ1 on TG2, experiments were undertaken using the CF "corrected add-back" cell line, C38 in determining whether TGFβ1 can reversibly increase TG2 and markers of EMT expression. The results show low TG2 expression in C38 cells unlike IB3 with a corresponding marginal expression of fibronectin, *Twist*, *Slug* and *Zeb2* expression in C38 cells (Figure 4.2). Interestingly, N-cadherin expression was slightly elevated compared with other EMT markers and E-cadherin expression was shown to be significantly lower than the expression in IB3 cells. In the presence of rTGFβ1, a 6-fold increase in fibronectin expression as well as a 2-fold increase in N-cadherin expression was observed. Expression of *Twist* and *Zeb 2* remained unaltered. This concurs with the observation of Ritter and Davies (1998) who observed an up regulation of TG2 expression due to the TGFβ1 response element on the TG2 gene promoter site. Hence, it can be postulated that TGFβ1 serves as a mediator of EMT with TG2 positioned as the driver of the process, however, it cannot be ruled out that this relationship might be co-dependent.

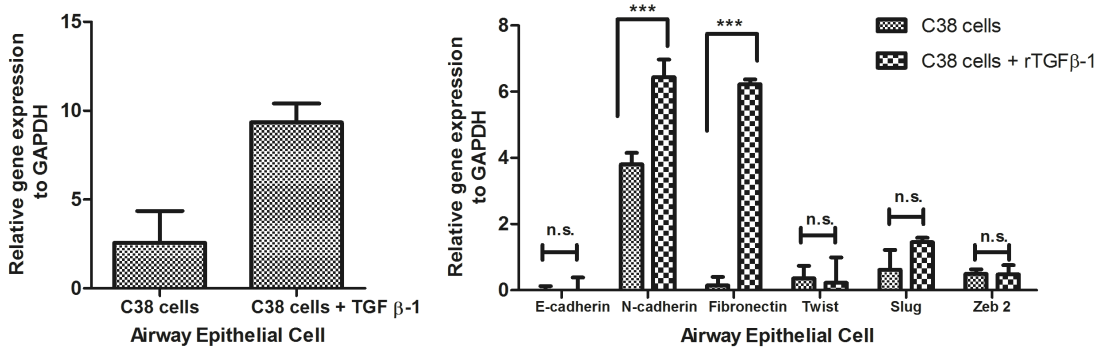

Figure 4.2: Elevated TG2 gene expression correlates with the increase in EMT markers expressed by C38 cells. cDNA from C38 was analysed for the effects of rTGFβ1 (3ng/ml) on the expression of TG2 and the EMT markers, fibronectin, N-cadherin, *Twist*, *Slug* and *Zeb 2.* Gene expression was determined using the ΔΔCT method. Results show a significant increase in TG2 gene expression in the presence of rTGFβ1 (left panel). In concert, an increase in N-cadherin and fibronectin expression was observed although there was only marginal gene expression of E-cadherin, *Twist, Slug* and *Zeb 2* gene (right panel). Data represents the mean and standard deviation of 3 independent experiments carried out in triplicates. Two-way Anova analysis with Bonferronni's Posttests;*** $p<0.001$, n.s. $p>0.05$.

4.3.2: IB3 cells express higher protein levels of fibronectin, N-cadherin and Slug than C38 cells

In order to verify the results obtained from gene expression studies, protein analysis was carried out on IB3 and C38 cells using Western blotting. IB3 and C38 cells were cultured in submerged medium as described in chapter 2.2.1.2. The results show elevated levels of fibronectin and N-cadherin in IB3 and C38 cells as shown by densitometry. Comparatively, in Figure 4.3A&B, a 2 and 7-fold increase in expression in fibronectin and N-cadherin respectively was observed in IB3 cells compared to C38 cells. However, the expression of *Slug* was different in both cells with IB3 cells showing slightly higher expression compared to C38 cells (Figure 4.3C). These results verify the hypothesis that elevated levels of TG2 correlate with the elevated levels of fibronectin, N-cadherin and *Slug* expression. Also, this concurs with previous results in section 4.1 with elevated gene expression of EMT markers as well as elevated expression of TG2 in CF cells compared to C38 cells.

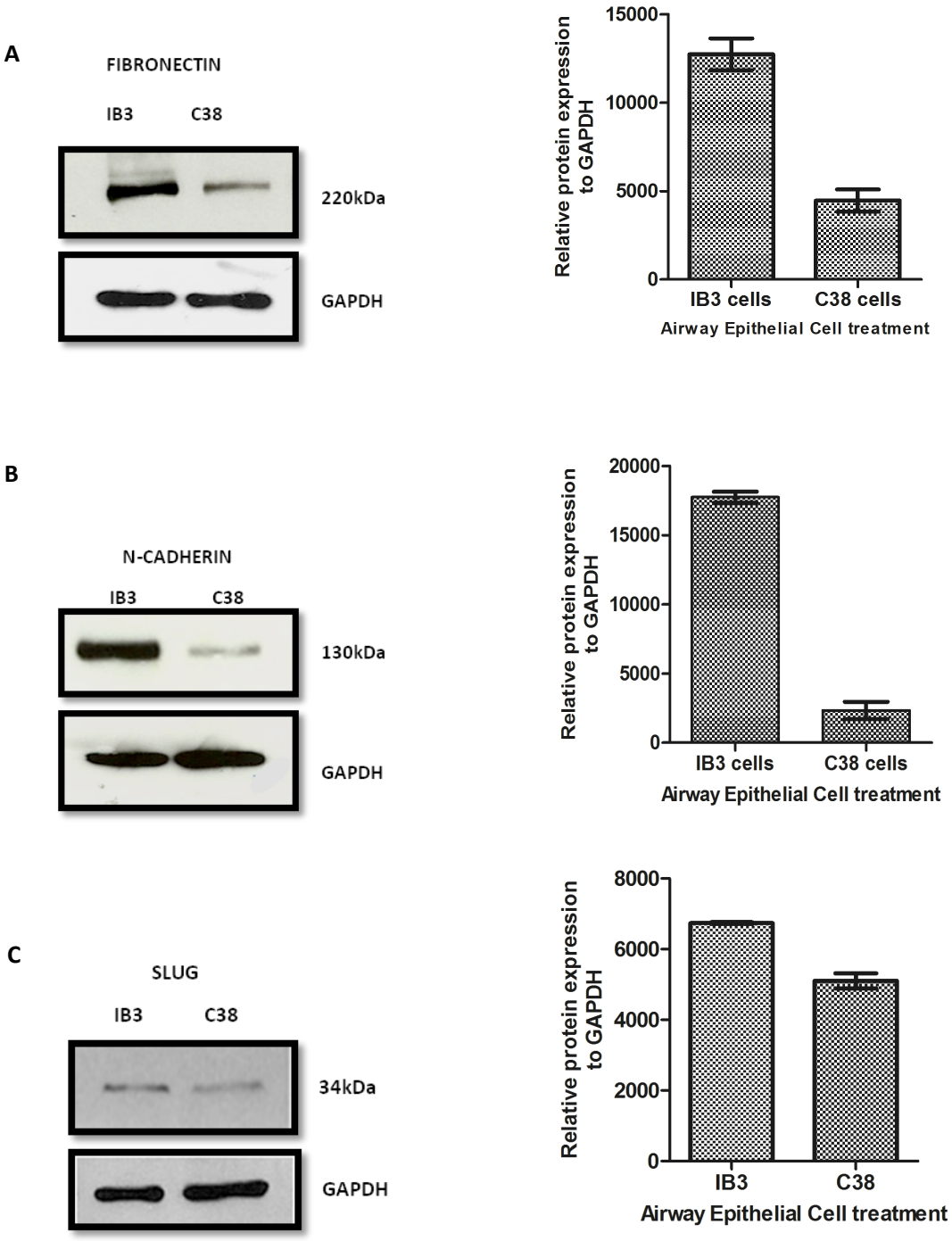

Figure 4.3 A,B&C: IB3 cells express higher protein levels of fibronectin, N-cadherin and *Slug* than C38 cells. Western blotting showing **A** fibronectin, **B**, N-cadherin, and **C,** *Slug* protein expression in IB3 and C38 cells. 50µg of protein was used loaded on 6% (w/v) and 8% (w/v) gels. GAPDH was used as loading control to normalise protein expression. Results show elevated TG2, fibronectin and *Slug* expression in IB3 cells compared to C38 cells. Densitometry results represent the mean and standard deviation of 3 independent experiments.

Similarly, using immunostaining, TG2, fibronectin and N-cadherin protein levels were determined in IB3 and C38 cells as well as the localisation of these proteins in the cells. Figure 4.4 shows that in IB3 cells, an increase in TG2 expression was followed with an up-regulated fibronectin and N-cadherin expression around the cell surface. Results further showed a network of fibronectin fibres, which together with elevated expression of N-cadherin demonstrates the disorientation of the cellular matrix of IB3 cells compared to C38 cells. Likewise, the level of TG2 expressed concurred with that of fibronectin and N-cadherin in IB3 cells, which was shown to co-localise around the cells. The expression in C38 cells appeared in a similar pattern around the cell surface but was lower than the expression observed in IB3 cells. This reflects the consistent results observed with an increase in TG2 gene expression corresponding to an increase in protein expression as shown with Western blots and immunocytochemistry.

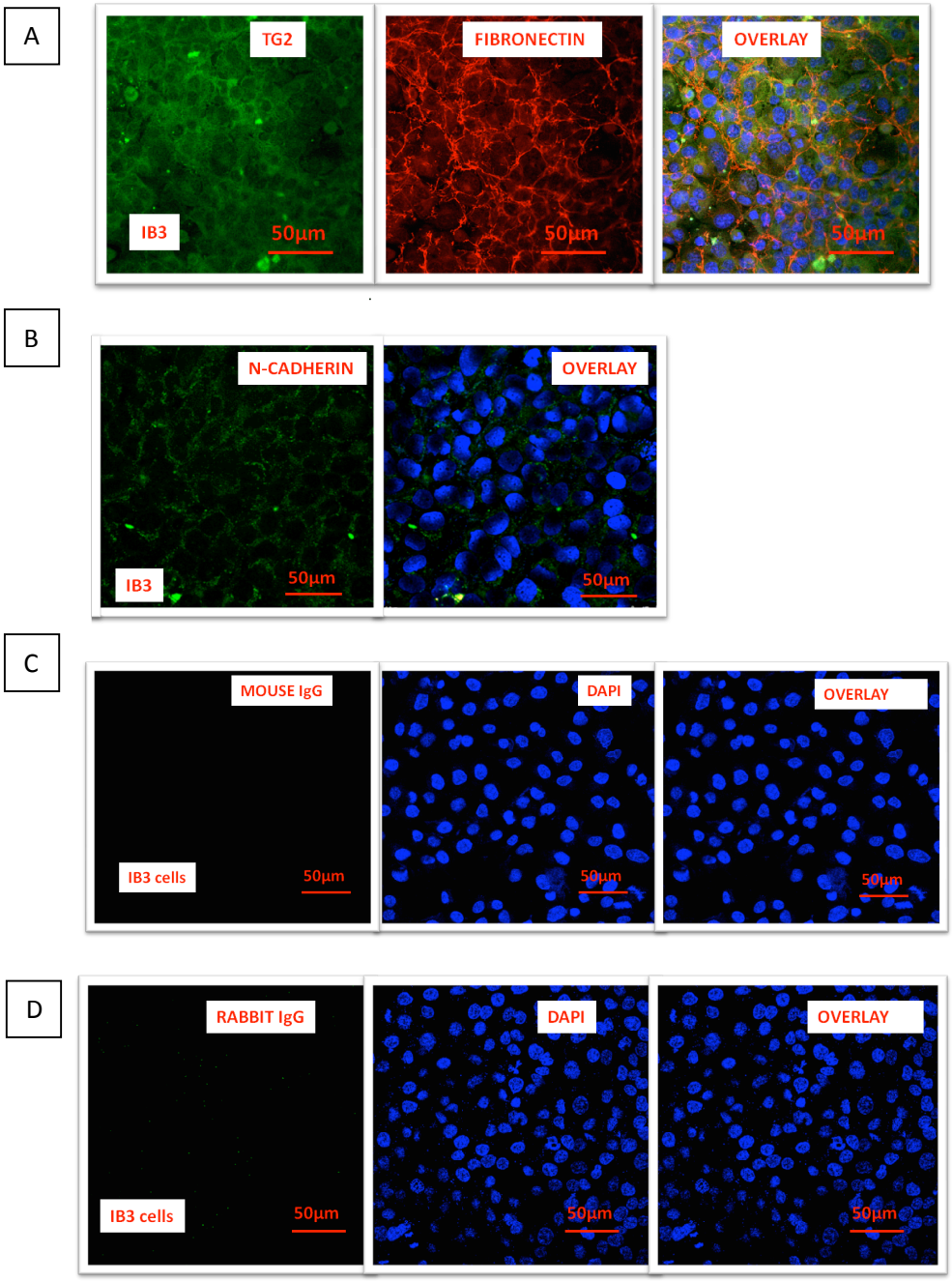

Figure 4.4A-D: IB3 cells express TG2, fibronectin and N-cadherin proteins when cultured in submerged conditions. Immunofluorescence staining of IB3 cells was carried out to detect TG2 (**A**), fibronectin (**A**) and N-cadherin (**B**) expression. TG2 [monoclonal (mouse) and polyclonal (rabbit)], fibronectin [polyclonal (rabbit)] and N-cadherin [monoclonal (mouse)] antibody (1:100) were used. Mouse IgG (**C**) and Rabbit IgG (**D**) were used as control in the cell. The cells were visualised using the Leica® SP5 confocal microscope. Results show high expression of TG2 and fibronectin co-localising with each other in IB3 cells (**A**), with N-cadherin expression shown to be high as well (**B**). Scale bar represents 50µm. Images are representative of 2 independent experiments.

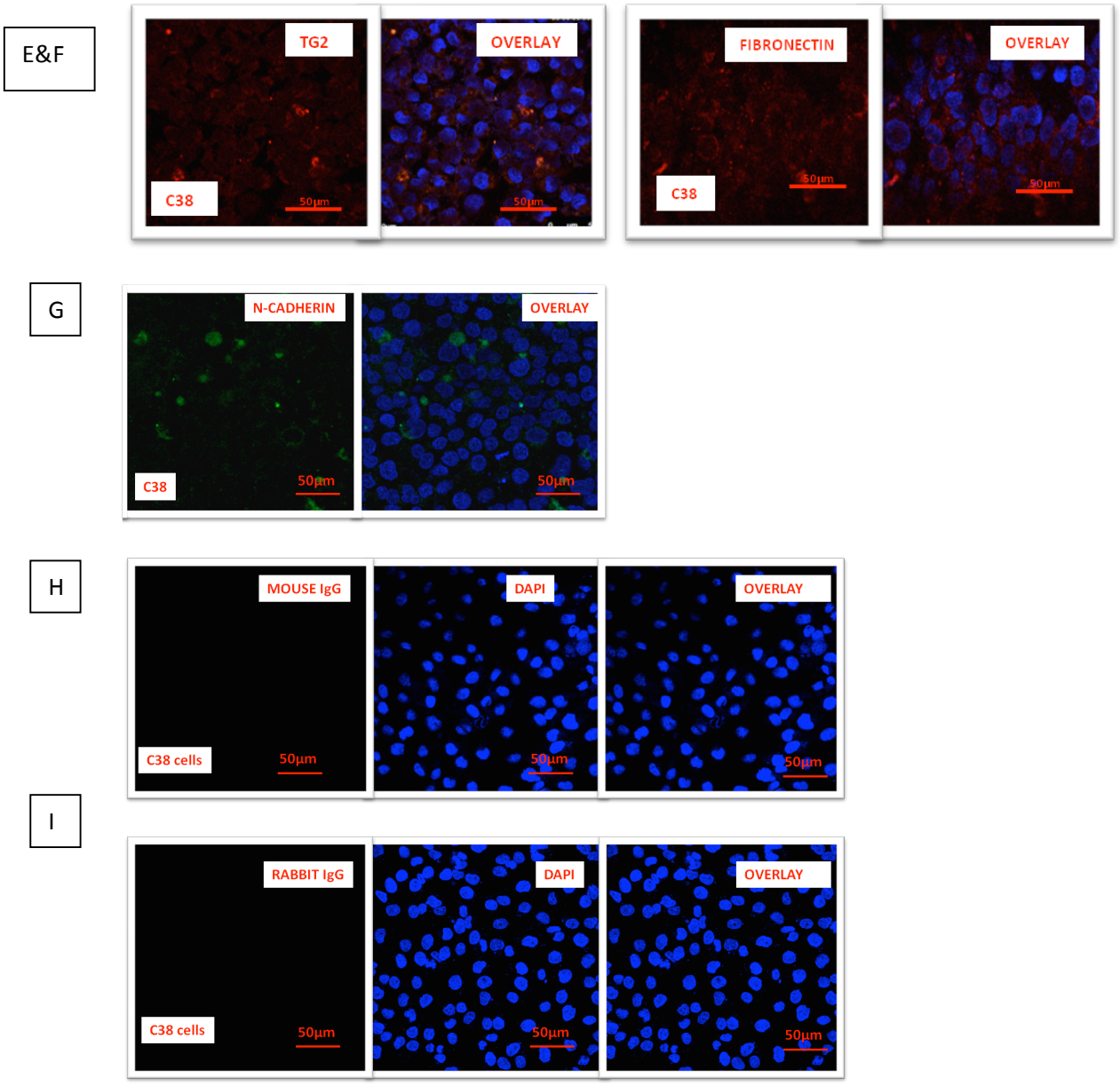

Figure 4.4E-I: C38 cells show marginal expression of TG2, fibronectin and N-cadherin proteins when cultured in submerged conditions. Immunofluorescence staining of C38 cells carried out to detect TG2 (**E**), fibronectin (**F**) and N-cadherin (**G**) expression. TG2 [monoclonal (mouse) and polyclonal (rabbit)], fibronectin [polyclonal (rabbit)] and N-cadherin [monoclonal (mouse)] antibody (1:100) were used. Mouse IgG (**H**) and Rabbit IgG (**I**) were used as controls. The cells were visualised the Leica® SP5 confocal microscope. Results show low expression of TG2, fibronectin and N-cadherin. Scale bar represents 50µm. Images are representative of 2 independent experiments.

4.3.3: Inhibition of TG2 protein expression reverses the development of EMT in CF.

4.3.3.1: Inhibition of cellular and matrix TG2 reduces the expression of EMT markers in IB3 cells.

To investigate the role played by intracellular and cell surface TG2 in promoting EMT, cellular and extracellular proteins were extracted from IB3 cells treated with TG2 cell-permeable and impermeable inhibitors and examined for fibronectin, N-cadherin, E-cadherin, *Slug* and TG2 expression using Western blotting. Results show that TG2 inhibition caused an elevation of cellular TG2 levels corresponding with low levels of E-cadherin (Figure 4.5A). This concurs with earlier results that showed low E-cadherin gene expression in wild type IB3 cells (Figure 4.1). In the presence of the cell-permeable TG2 inhibitor, Z-DON, a significant inhibition of TG2 expression (>4-fold: $p<0.001$) was observed compared to control. This was associated with a 2-fold increase in E-cadherin expression in the presence of Z-DON. Interestingly, it was observed that incubating the cells with a cell impermeable TG2 inhibitor, R294 significantly inhibited ($p<0.001$) the expression of TG2 as well as elevating the levels of E-cadherin expressed in this cell. Similar results were observed for fibronectin expression. Results show that elevated matrix fibronectin levels coincided with increased TG2 expression and TG2 inhibitors significantly ($p<0.001$) reversed fibronectin expression however, R294 was slightly less inhibitory compared to the others. Using new in-house synthesised peptido-mimetic TG2 specific inhibitors, attempts were made to distinguish whether the observed results were due to cell surface or intracellular TG2 activity. The TG2 inhibitors were; 1-133, which is cell impermeable and 1-155, a cell-permeable TG2 inhibitor. The observed results (Figure 4.5B) shows that in the presence of these inhibitors, TG2, fibronectin, N-cadherin and *Slug* expression were significantly reversed ($p<0.001$) with 1-133 showing enhanced inhibitory characteristic compared to 1-155 (Figure 4.5B). Overall, the findings suggest TG2 expression to be involved in EMT where increased TG2 externalisation accounts for high levels of active TG2, which increasingly binds to fibronectin and other matrix proteins and is accountable for the gradual establishment of EMT in CF.

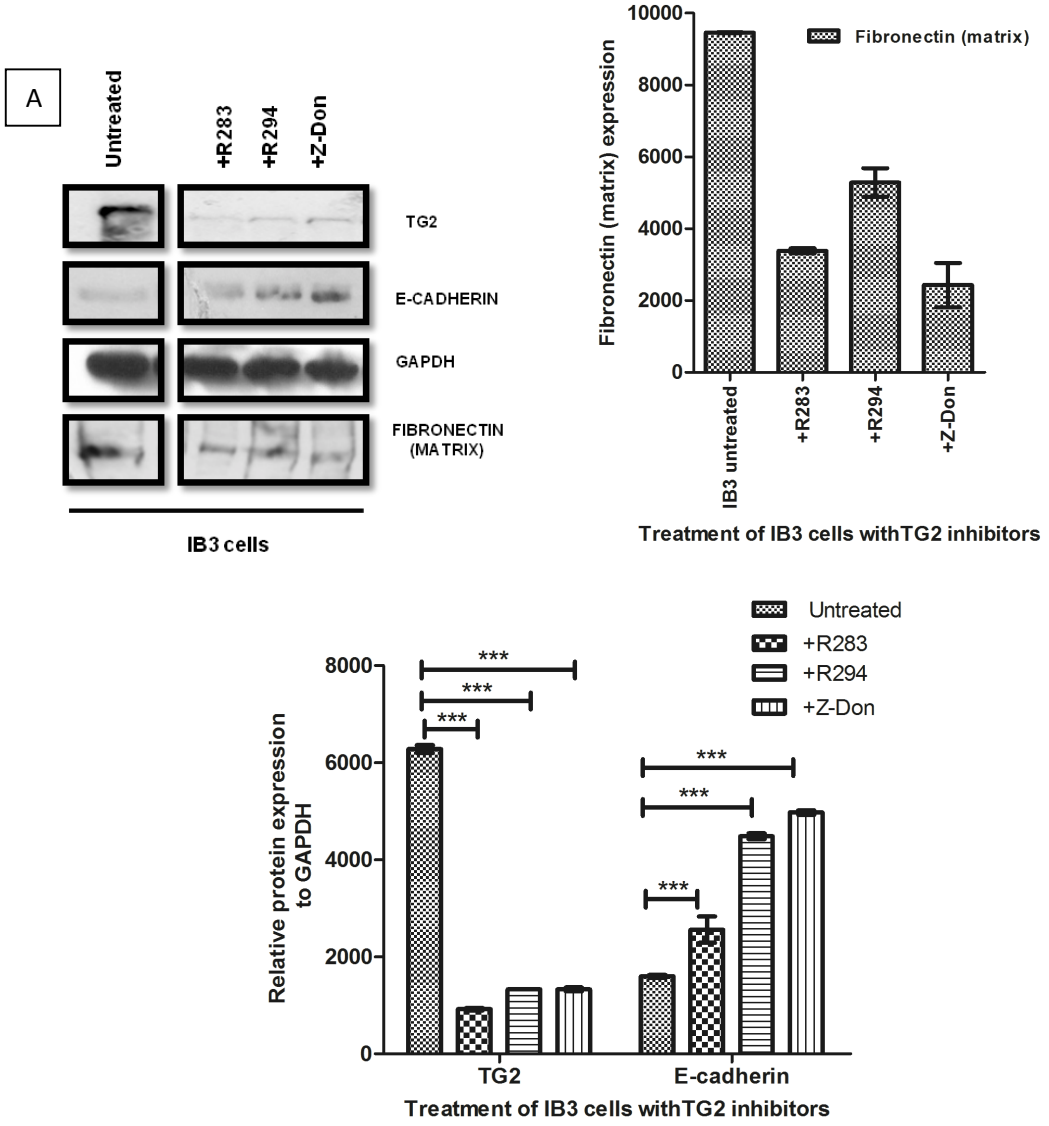

Figure 4.5A: Inhibition of cellular or matrix TG2 reduces EMT marker expression, but enhances matrix fibronectin deposition in IB3 cells. Western blotting showing cellular TG2 and E-cadherin expression (bottom panel) and matrix fibronectin expression (top panel) in IB3 cells incubated with cell-permeable TG2 inhibitors {Z-DON (100µm) and R283 (500µM)} and impermeable inhibitor, R294 (500µM). 50µg of protein was used for the Western blot assay. Monoclonal mouse anti-TG2 and anti-E-cadherin antibodies as well as polyclonal rabbit anti-fibronectin antibody (1:1000) were used to probe blots. Results show a significant inhibition of cellular TG2 and matrix fibronectin expression in IB3 cells in the presence of R283 and Z-Don as well as with the cell impermeable TG2 inhibitor, R294. However, E-cadherin expression was significantly increased in the presence of all TG2 inhibitors compared to untreated control. Western blotting is characteristic of 3 independent experiments with equal number of cells used at all times. Densitometry represents the mean values and standard deviation of 3 independent experiments adjusted relative to GAPDH staining intensity. One-way Anova analysis with Dunnett's Multiple comparison test; *** $p<0.0001$

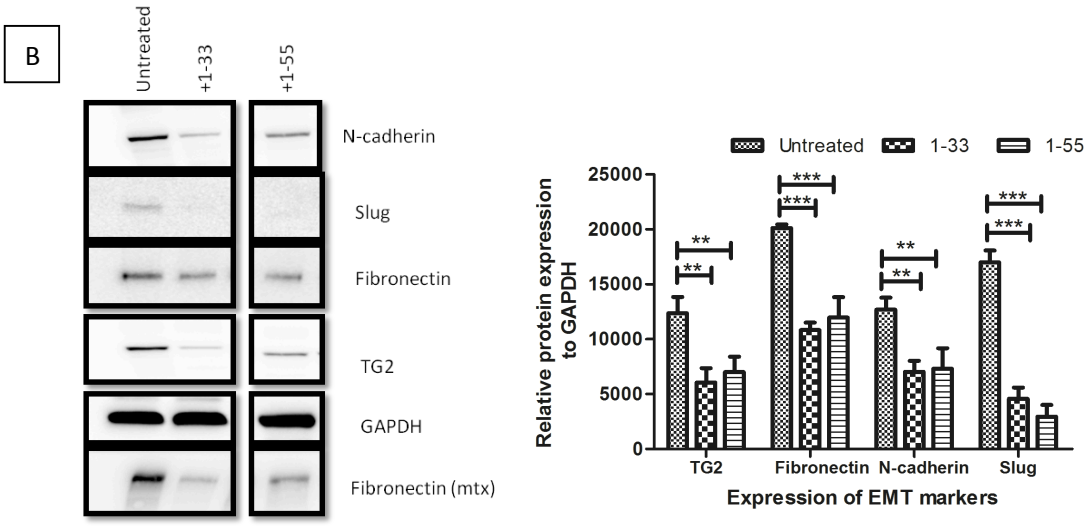

Figure 4.5B: Inhibition of cellular or matrix TG2 activity reduces EMT marker protein expression in IB3 cells. Western blotting showing cellular TG2, N-cadherin, *Slug* and fibronectin expression as well as matrix fibronectin expression in IB3 cells incubated with the peptido-mimetic cell-permeable TG2 inhibitor, 1-155 (200ng/ml) and the equivalent cell impermeable TG2 inhibitor, 1-133 (100μM). 50μg of protein was used for the Western blot assay. Monoclonal mouse anti-TG2, anti-*Slug* and anti-E-cadherin antibodies as well as polyclonal rabbit anti-fibronectin antibody (1:1000) were used to probe blots. Results show that both 1-155 and 1-133 inhibitors significantly block cellular N-cadherin, TG2, *Slug* and both cellular and matrix fibronectin expression compared to control. GAPDH was used as a loading control to normalise cellular protein expression. The blot image is representative of 3 independent experiments with equal number of cells used at all times. Densitometry represents the mean values and standard deviation of 3 independent experiments. One-way Anova analysis with Dunnett's multiple comparison tests; *** $p<0.0001$, **<p0.0029, .

4.3.3.2: Abrogation of TG2 expression impedes cell migration

TG2 has been termed a "cell adhesion" protein because of its involvement in wound healing and matrix deposition (Telci and Griffin, 2006). The key role of cell surface TG2 in cell migration has been linked to the binding of active TG2 to matrix fibronectin (TG2-FN) which depends somewhat on its transamidating activity (Verderio *et al.*, 1998). Here, the effect of active cell surface TG2 on the migration of CF cells is demonstrated. The migration assay was carried out as described in chapter 2.2.7.

Cell viability assays were used to show that IB3 cells proliferate faster than C38 cells with non-proliferative rates observed to be within 16h (Figure 4.6A). Migratory profiles of IB3 and C38 cells were therefore carried out within this time frame. The results here show that in IB3 and C38 cells, rapid wound closure was observed with IB3 cells

migrating at a faster rate compared to C38 cells (Figure 4.6B). The relative wound closure shows around a 13% increase in migratory rate between IB3 and C38 cells. In the presence of R283, migration was inhibited more in IB3 cells with around 10% decrease in migratory rates compared to C38 cells, which showed a lower migratory rate at approximately 3%. Together, it can be can be hypothesised that, in both IB3 and C38 cells, due to the levels of TG2, TGFβ1 and EMT markers expressed, the migratory profile of both cells reflects their phenotypic traits and shows the effect of TG2 on matrix organisation in CF cells.

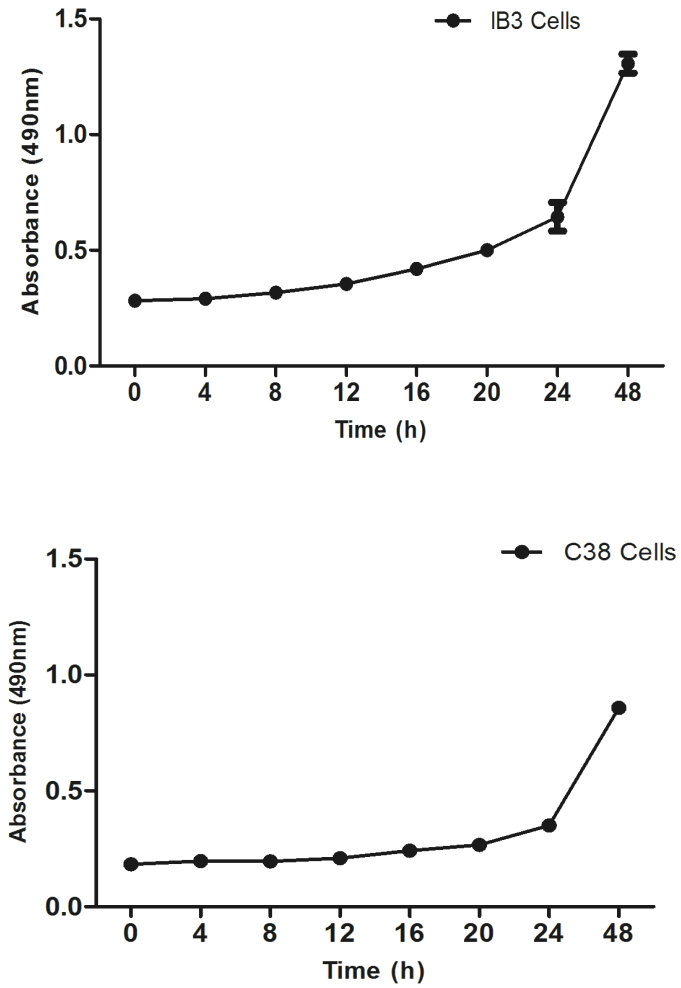

Figure 4.6A: IB3 cells have accelerated doubling times compared to C38 cells. IB3 and C38 cells were cultured in submerged medium and viable cell numbers quantified for up to 48 h using the XTT assay with reagents added and incubated for 4 h before absorbance was read at 490nm. Results represent mean values and standard deviation of 3 independent assays carried out in duplicates. Results show that in both IB3 and C38 cells, doubling of cell number was observed above 20 h and the absorbance values were consistently higher for IB3 cells compared to C38 cells suggesting greater proliferation of IB3 cells.

B

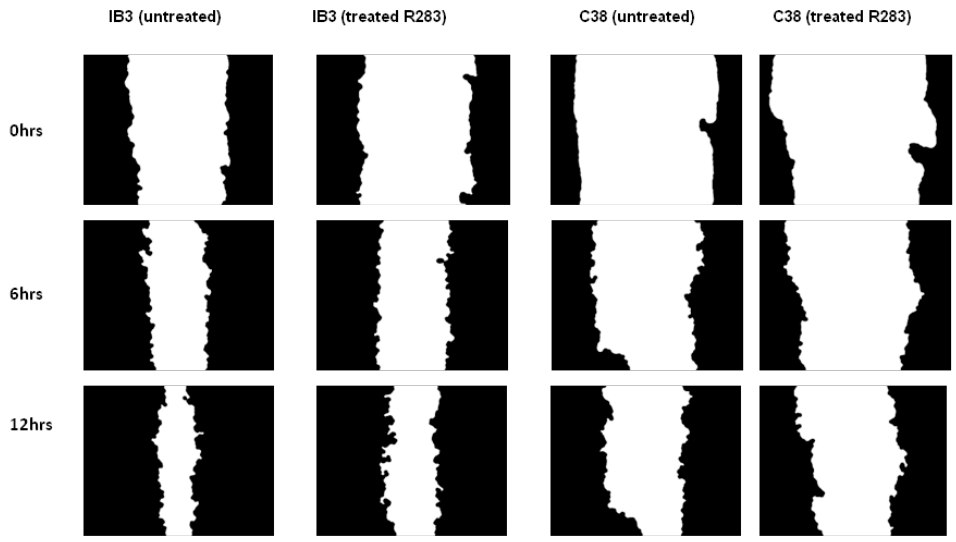
IB3 (untreated)
IB3 (treated R283)
C38 (untreated)
C38 (treated R283)
0hrs
6hrs
12hrs

C

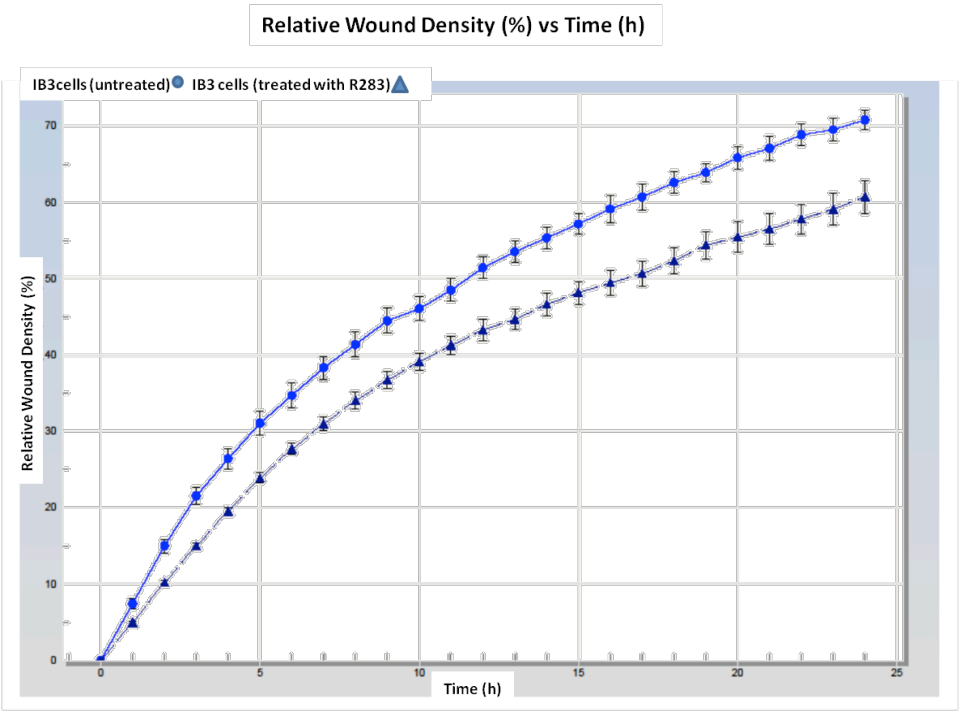
Relative Wound Density (%) vs Time (h)
IB3cells (untreated)
IB3 cells (treated with R283)
Relative Wound Density (%)
Time (h)
0
10
20
30
40
50
60
70
0
5
10
15
20
25

D

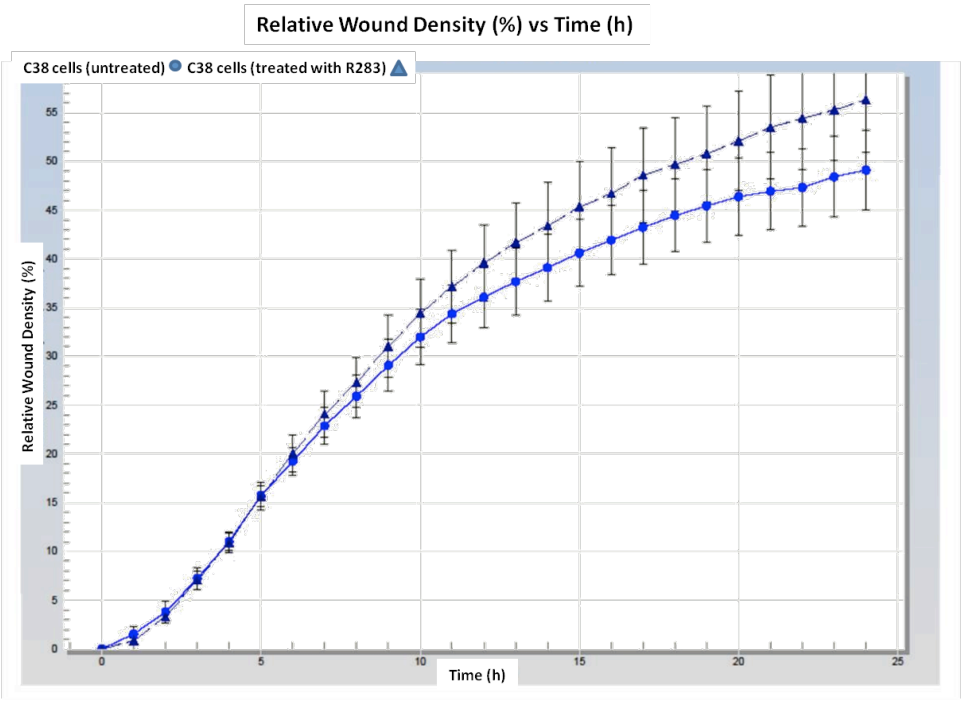

Figure 4.6 B,C&D: TG2 inhibitors impede migration rates of IB3 and C38 cells. Scratch assay was performed showing the migratory profile, of IB3, **C** and C38, **D,** cells cultured in submerged culture in the presence of the TG2 cell-permeable inhibitor, R283 (500μM). Migration was monitored for 16 h post wounding. Images (**B**) represent the plots of 2 independent experiments carried out in triplicates and graph shows mean values of wound closure in untreated and treated groups. The graph shows the % relative wound density (closure) against time. Results show that IB3 cells migrate faster than C38 cells with an inhibition in wound closure rate in the presence of R283 for both cell types

4.3.4: Induction of TG2 expression correlates with the elevation of EMT markers in CF

4.3.4.1: Reversal of TG2 expression restores epithelial phenotype in IB3 cells

In the presence of TGFβ1, airway epithelial cells lose their phenotypic traits and assume an undesirable morphology, which consequently leads to the loss of cell polarity and cell-cell adhesion (Xu *et al.*, 2009). In continuation of the previous work on the link between TG2 and EMT, this study is aimed at correlating the outcomes of TGFβ1 exposure on gene expression in C38 cells, to the effect of TGFβ1 on TG2, fibronectin and N-cadherin at protein levels. Phase-contrast images show that treating C38 cells with TGFβ1 changes the phenotype from a cobblestone like structure to a fibroblast-like morphology (Figure. 4.7A). Similarly, as cells were stained with TG2 and the myofibroblast marker, α-SMA, images illustrates that the change in cell morphology correlated with an increase in TG2 and α-SMA expression as shown in Figure. 4.7B. This ultimately verifies that an up regulation of TG2 expression in the presence of TGFβ1 drives EMT as an increase in α-SMA expression defines a transformation of epithelial cells to myofibroblasts, which supports the findings as shown by Zhang *et al*., (2009).

As C38 cells were treated with R283, a reversal of the EMT process was observed in Figure.4.8A. Using Western blotting, an increase in fibronectin expression was observed in the presence of rTGFβ1 in C38 cells, which was significantly inhibited ($p<0.001$) in the presence of R283 (Figure. 4.8B). TG2 expression was marginally inhibited which might be due to the overarching presence of active TGFβ1 on the cell surface thus causing the overproduction and then down regulation of TG2 which limits the amount present on the cell surface (Johnson *et al.,* 2007). Comparatively, using a cell-permeable inhibitor for TG2, 1-155 as opposed to the cell impermeable TG2 inhibitor, 1-133, results show that elevated TG2 expression was reduced in the presence of the former compared to the latter (Figure. 4.8C). 1-155 showed higher potency at blocking both cell surface and intracellular TG2 compared to 1-133, which is impermeable and blocked cell surface TG2 only. Differing IC_{50} of these inhibitors might be responsible for the inhibition shown. However, the results showed an enhanced inhibition of fibronectin and N-cadherin expression with 1-155 compared to 1-133. This suggests an involvement of cell surface TG2 in the EMT process.

A

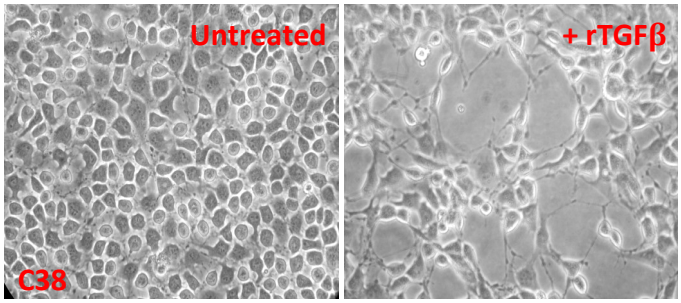

B

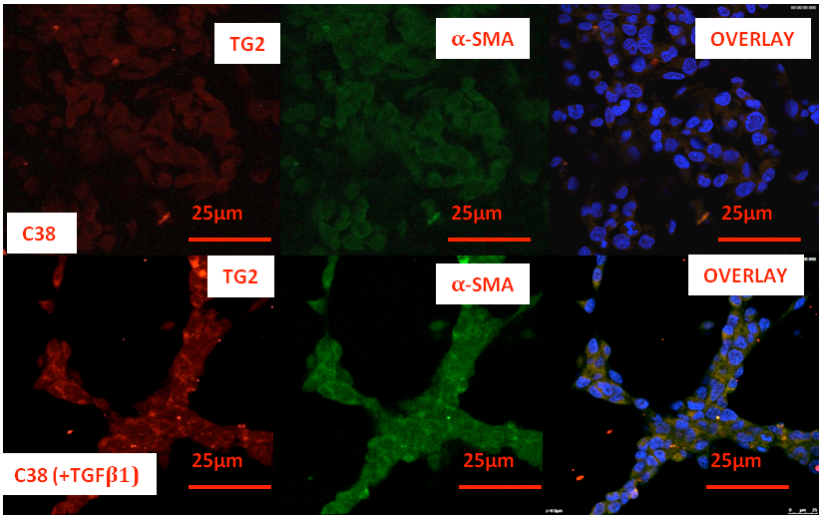

Figure 4.7A&B: Elevation of TG2 levels drives C38 cells into EMT. Phase contrast images, (**A**) and immunofluorescent staining, (**B**), of C38 cells treated with rTGFβ1 (3ng/ml) in serum free medium for 48h. Images were taken from a Nikkon camera mounted on a microscope. Results show a change in the cobblestone-like structure of the cells in the presence of rTGFβ1, with cells assuming a fibroblast-like morphology. C38 cells were then stained with polyclonal anti-TG2 (rabbit) or monoclonal anti-α-SMA (mouse) antibodies. Scale bar represents 25µm. Images were taken using the Leica® SP5 confocal microscope. Mouse and Rabbit IgG were used as control (data shown in figure 4.4F&I). Images are representative of 2 independent experiments. Images show an increase in TG2 staining in C38 cells in the presence of rTGFβ1 corresponding to an increase in α-SMA expression as the cells become fibroblast-like in morphology.

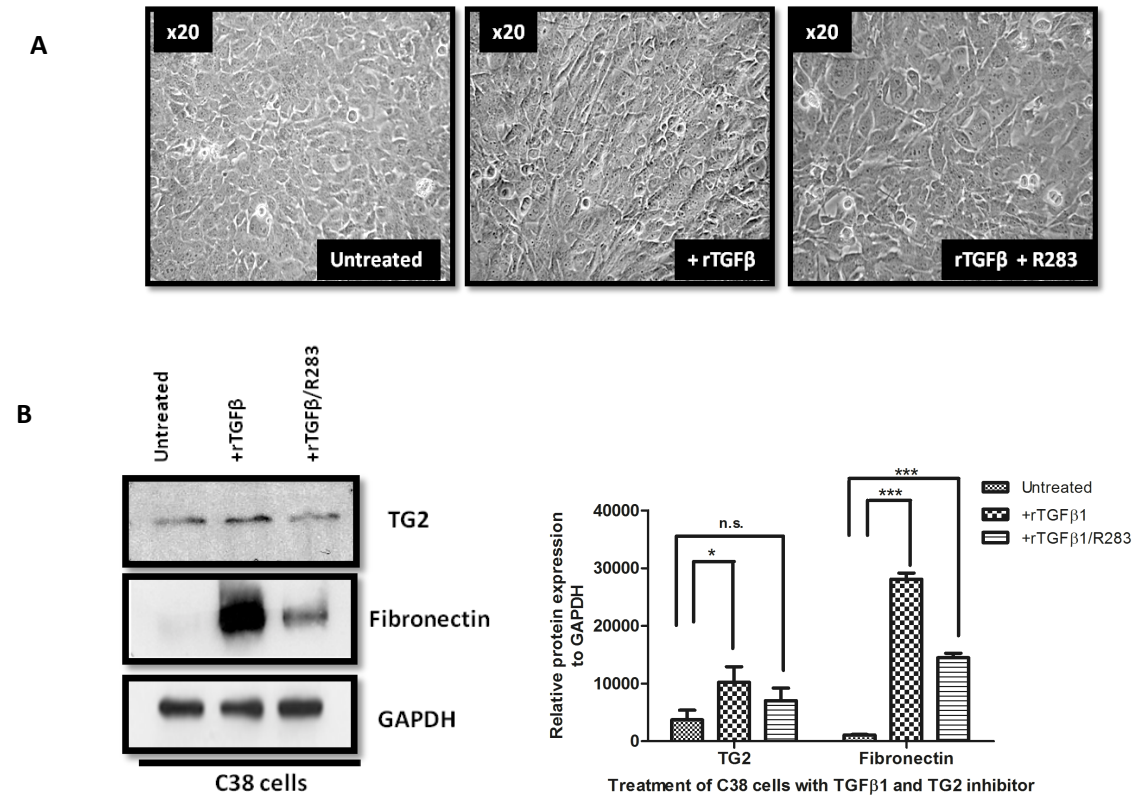

Figure 4.8A-C: TG2 induced EMT is reversed in the presence of TG2 inhibitors. Phase contrast images, **A** and Western blotting, **B&C** of C38 cells treated with cell-permeable, R283 (500μM) and 1-155 (200nM) and cell impermeable TG2 inhibitors, 1-133 (50μM) in submerged culture. The images were taken with a Zeiss camera (**A**) showing the change in C38 cell morphology in the presence of rTGFβ1 and this is inhibited in the presence of R283. 50μg of protein was used for the Western blot assay. Monoclonal mouse anti-TG2 and anti-N-cadherin antibodies as well as polyclonal rabbit anti-fibronectin antibody (1:1000) were used to probe blots. Results show a significant increase in TG2 and fibronectin expression in the presence of rTGFβ1 (**B**), which was inhibited in the presence of R283. Also in the presence of 1-133 and 1-155 (**C**), the rTGFβ1-dependent increase in expression of TG2, fibronectin and N-cadherin was inhibited. Western blotting images are representative of characteristic results of 3 independent experiments. Densitometry represents mean and standard deviation of 3 independent experiments. GAPDH was used a loading control to normalise protein expression. Magnification of images (x200). One-way Anova analysis with Dunnett's multiple test: *** $p<0.0001$,*$p<0.0323$, n.s. $p>0.05$.

Using the same hypothesis, human bronchial primary epithelial cells (HBEC) possessing similar phenotypic characteristics as *in vivo* bronchial cells were evaluated to determine the effect of rTGFβ1 on TG2, fibronectin, N-cadherin and E-cadherin expression. The aim was to illustrate that in normal physiological conditions, an up regulation of TG2 in bronchial epithelial cells can provoke the initiation of EMT. The results here show a change from the tight cobblestone-like structure to a distorted organisation of cells characterized by a loss in cell cohesiveness and with cells assuming a fibroblast –like morphology in the presence of TGFβ1 after 48 h (Figure. 4.9A). The presence of R283 impedes the process with HBEC regaining cell cohesion. Western blot analysis shows that at baseline, HBEC display a typical epithelial phenotype with diminished TG2, fibronectin and N-cadherin expression with high E-cadherin expression. A decrease in E-cadherin expression was observed in the presence of TGFβ1 in HBEC cells, which in turn increases TG2 and fibronectin expression whilst N-cadherin expression was marginal (Fig. 4.9B). In the presence of R283, TG2 expression was shown to decline to basal levels in untreated cells. The expression of fibronectin and N-cadherin was slightly changed in the presence of R283, with protein levels marginally elevated. In concert, E-cadherin was also shown to increase slightly compared to levels in the presence of TGFβ1. These results suggest that although TGFβ1 increases TG2 and EMT marker expression, the amelioration of EMT is a relatively gradual process, where TG2 inhibition restores epithelial integrity progressively.

A

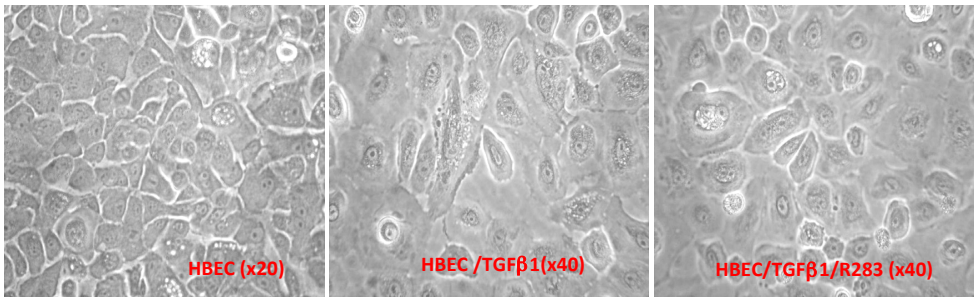

B

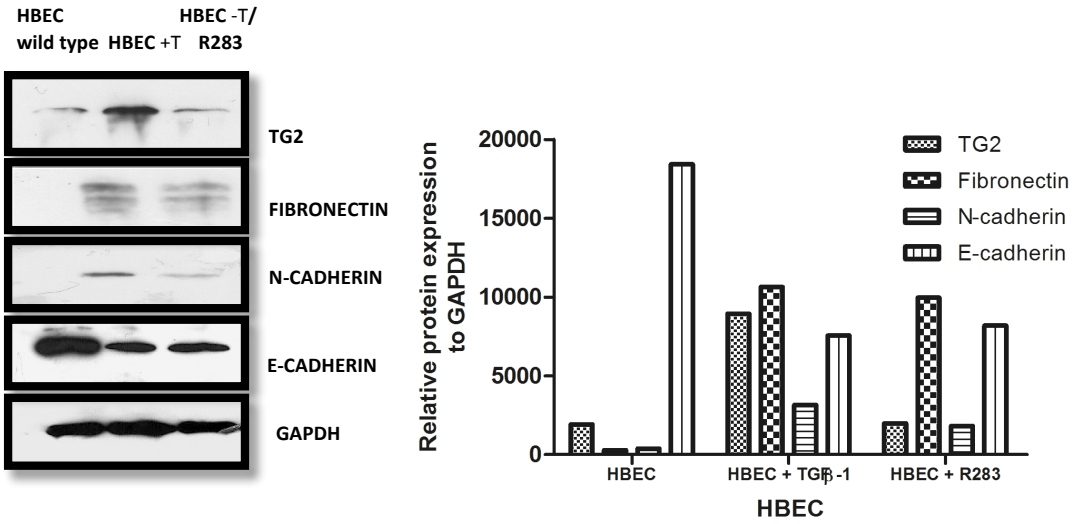

Figure 4.9A&B: Inhibition of TG2 in HBEC primary cells reduces the expression of EMT markers. Phase contrast images (**A**) and Western blot analysis (**B**) of TG2, fibronectin, N-cadherin and E-cadherin expression by HBEC cells treated with rTGFβ1 (3ng/ml) or R283 (500μM). Cells were imaged with a Zeiss camera. 50μg of protein was used for the Western blot assay. Monoclonal mouse anti-TG2, anti-N-cadherin and anti-E-cadherin antibodies as well as polyclonal rabbit anti-fibronectin antibody (1:1000) were used to probe blots. GAPDH was used as loading control to normalise protein levels. Results show an increase in TG2 level in HBEC cells in the presence of rTGFβ1, with increase in fibronectin and N-cadherin expression. However, E-cadherin expression is decreased. The presence of R283 inhibits the increase in EMT marker expression but does not increase E-cadherin. Magnification of images (x400).

4.3.4.2: Inhibition of TGFβ1 ameliorates EMT in CF

In the preceding chapter, results showed IB3 and C38 cells possessing TGFβ receptors, RI and RII. Studies have shown the importance of TGFβ receptors in the downstream signalling of TGFβ (Bartram, 2004). Within the ambits of this chapter, attempts have been made to observe the importance of the interaction of TGFβ1 with its receptors as well as how it relates to active cell surface TG2 in EMT in IB3 cells. Here result shows that in the presence of TGFβ neutralizing antibody (Nab), TG2, N-cadherin and fibronectin expression were significantly inhibited ($p<0.01$ or $p<0.001$) compared to untreated cells whilst E-cadherin was marginally up regulated (Figure 4.10). TG2, fibronectin and N-cadherin expression were inhibited about 4-fold compared to untreated control. The reduction in TG2 expression in the presence of Nab antibody shows a link between inhibition of TGFβ1/TGFβ receptors interaction and activation of TG2. It also shows the importance of TGFβ1 in promoting EMT expression as well as providing the link between TG2 and TGFβ1 activation.

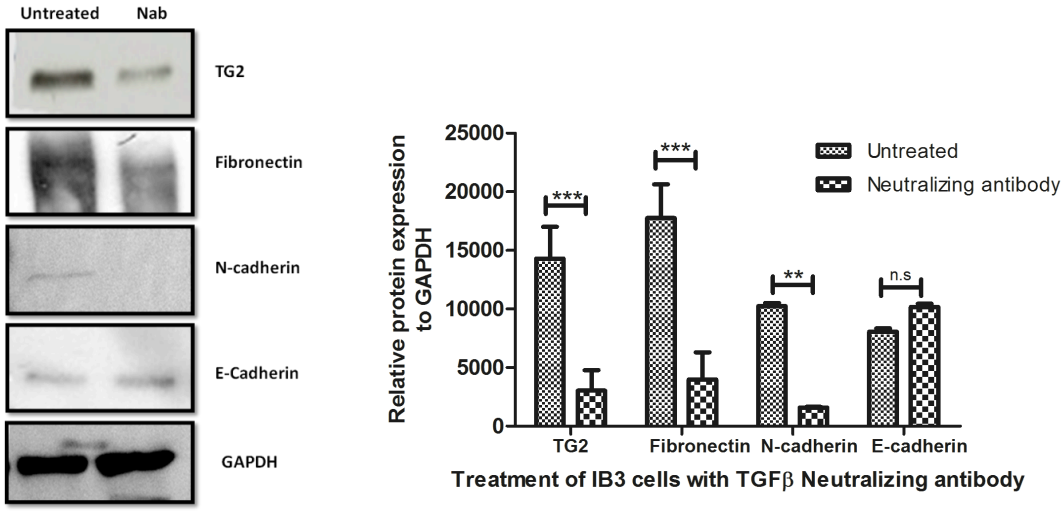

Figure 4.10: Blocking TGFβ1 impedes TG2, E-cadherin and EMT marker expression in submerged culture. IB3 cells were treated with the TGFβ neutralizing inhibitor (Nab) (20μg/ml) in submerged culture prior to analysis for TG2 and EMT markers using monoclonal mouse anti-TG2, anti-N-cadherin and anti-E-cadherin antibodies as well as polyclonal rabbit anti-fibronectin antibody (1:1000). 50μg of protein was used for the Western blot assay. GAPDH was used as loading control to normalize protein loading. Western blot image represents a characteristic result of 3 independent experiments. Densitometry represents mean and standard deviation of 3 independent experiments. Results show a decrease in TG2 expression corresponding to a significant decrease in fibronectin and N-cadherin expression compared to untreated control, however, E-cadherin expression was shown to be slightly elevated in the presence of the TGFβ neutralizing inhibitor (Nab). Two-way Anova analysis with Bonferroni's post-tests; *** $p<0.001$, ** $p<0.01$, n.s. $p>0.05$.

4.3.5: TG2 involvement in the activation of TGFβ1 by the integrin, αVβ6.

Studies have shown that αVβ6 activation of TGFβ1 occurs via the known RGD sequence present on the Latency Associated Protein (LAP), which is a propeptide directly bound by disulphide linkages to TGFβ1 (Munger *et al.*, 1999) . However, the Latency TGFβ binding protein 1, LTBP-1, was shown to be required for the activation of latent TGFβ1 by αVβ6 (Annes *et al.*, 2004). TG2 has also been associated with the activation of TGFβ1, with LTBP-1 and large latent complex shown to be substrates of TG2 where TG2 covalently crosslinks LTBP-1 to the matrix (Nunes *et al.*, 1997). When binding integrins to ligands via their RGD sites, studies have observed that only α8β1, αVβ1, αVβ3 and αVβ5 could bind to LAP coated dishes with avidity dependent on high concentrations of substrate (Sheppard, 2005). However, αVβ6 was shown to bind at low concentrations with high avidity. In line with this studies, it was hypothesised as shown below in Figure 4.11 that since TG2 binds to LTBP-1 and covalently crosslinks it to matrix and studies by Fontana *et al.* (2005) have shown that fibronectin is required for the activation of TGFβ1 by αVβ6, the activation of TGFβ1 would involve a TG2-αVβ6 interaction.

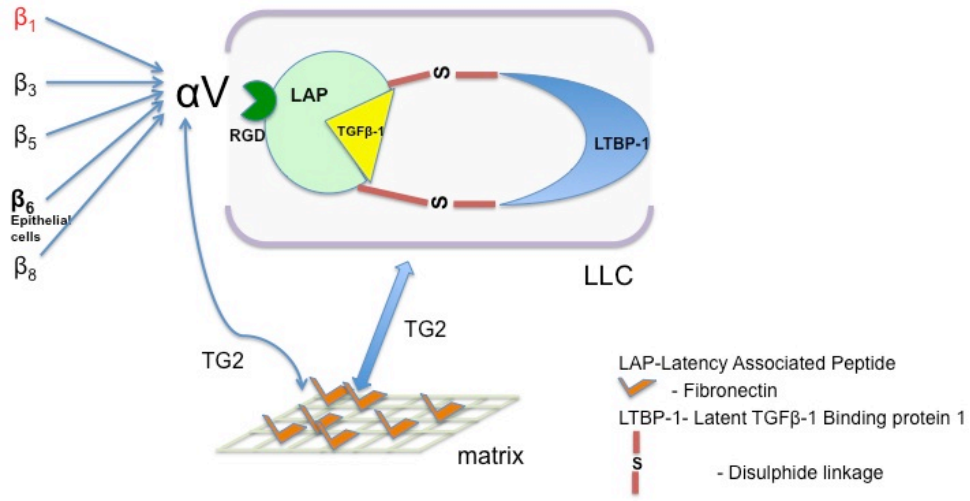

Figure 4.11: Schematic representation of a proposed mechanism of interaction between TG2, αV and β6 integrin in epithelial cells. This might be involved in the activation of TGFβ1. The interaction between TG2 and fibronectin aids in crosslinking LLC to the matrix and thus is involved in the activation of TGFβ1. However, αVβ6 also has been shown to activate TGFβ1. Hence a direct interaction between TG2 and αVβ6 might exist driving the activation of TGFβ1.

To investigate this correlation between TG2 and αVβ6, Western blotting analysis was carried out on IB3 and C38 cells cultured in submerged culture. Co-immunoprecipitation was carried out as described in chapter 2.2.20.

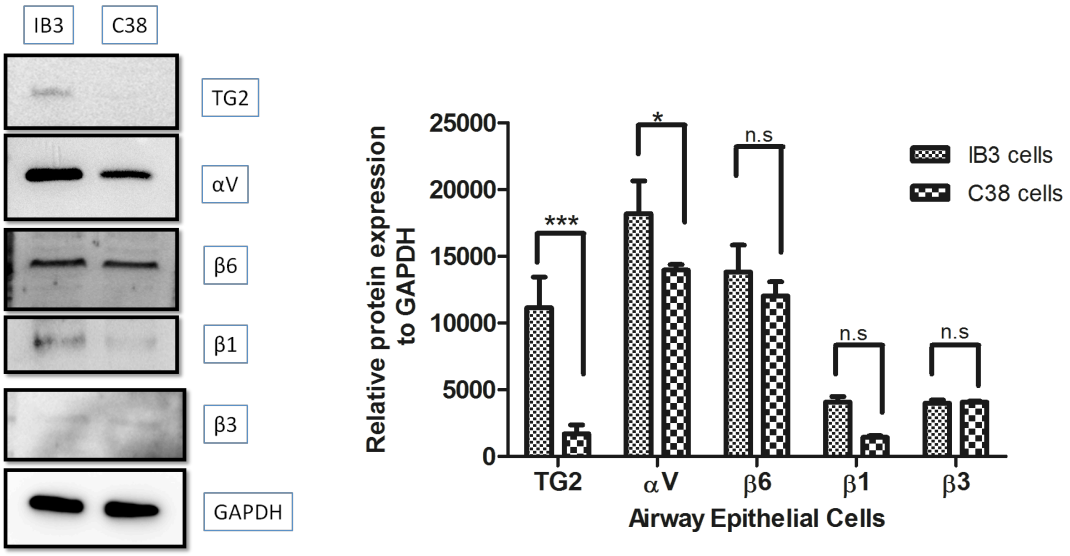

Figure 4.12: TG2 expressed in CF cells interacts with integrins. To determine TG2 interactions with integrins, Western blot analysis of TG2, αV, β6, β1 and β3 in IB3 and C38 cells was carried out. 50µg of protein was used for the Western blot assay. The membranes were blotted with antibodies for TG2, αV, β6, β1 and β3 (1:1000). GAPDH was used to normalise loaded protein. Results show increased TG2 expression in IB3 cells compared to C38 corresponding to elevated levels of αV protein. β6, β1 and β3 expression was shown to remain unchanged between cells. WB represents a characteristic result of 3 independent experiments. Results represent mean and standard deviation of 3 independent experiments. Two-way Anova analysis with Bonferroni post-tests; ***$p<0.001$, *$p<0.05$, n.s. $p>0.05$

The results have shown that αV protein expression corresponds with TG2 expression as IB3 cells were shown to express high levels of αV protein. β6, β1 and β3 expression was shown to remain unchanged between both cell lines. These data suggest that elevated levels of TG2 in IB3 cells which correlates with the activation of TGFβ1 might be related to the high levels of αV observed in these cells. Since LTBP-1 has been shown to interact with TG2 and its interaction involves crosslinking with fibronectin covalently, it suggests that TG2's involvement in the activation of TGFβ1 might be through αV interaction with LAP (Verderio *et al.*, 1999). To demonstrate the possible interaction between TG2, αV and β6 in IB3 and C38 cells, co-immunoprecipitation studies were carried out on these cells. Results show in Figure 4.13A1 that basal levels of TG2 immnoprecipitated αV or β6 in IB3 and C38 cells showed an elevated TG2-αV complex in IB3 cells compared with C38 cells and no change in expression of TG2 between cells in TG2 immunoprecipitated β6. These results were similar for TG2 expressions in both cells for αV but not β6. However, as TG2 expression was inhibited by R283 in IB3 cells and elevated by rTGFβ1 in C38 cells, TG2 immunoprecipitated αV showed an inhibition of TG2 levels in IB3 cells and an up regulation in C38 cells (Figure. 4.13A2). Interestingly, it was observed that with TG2 immunoprecipitated β6, TG2 expression were inhibited in IB3 cells and elevated in C38 cells. These results might have been due to the quiescent nature of αVβ6 in normal bronchial epithelial cells (where C38 cells are a model) where low levels are expressed however injury leads to a dramatic up regulation of the integrin (Breuss *et al.*, 1995, Breuss *et al.*, 1993). On evaluating αV immunoprecipitating β6, under control conditions, there was equal expression of αV in IB3 and C38 cells. This transformed when IB3 cells were treated with R283 and C38 cells with rTGFβ1, with an inhibition or elevation in αV levels in the cells respectively (Figure. 4.13B1&2).

This study shows an exaggerated response as TGFβ1 and consequently TG2 levels are up regulated. Conversely, results show no increase in basal expression of β6 in IB3 and C38 cells for β6 immunoprecipitating αV as well as β6 marginal inhibition in IB3 cells in the presence of R283 as oppose to C38 cells where rTGFβ1 failed to elevate β6 expression (Figure. 4.13C). This is in concert with results as shown in Figure 4.13 where basal levels of β6 were shown to remain unchanged in both cells. Together, these results demonstrate some interaction between TG2 and αV as well as β6 in the cells following TGFβ1 activation.

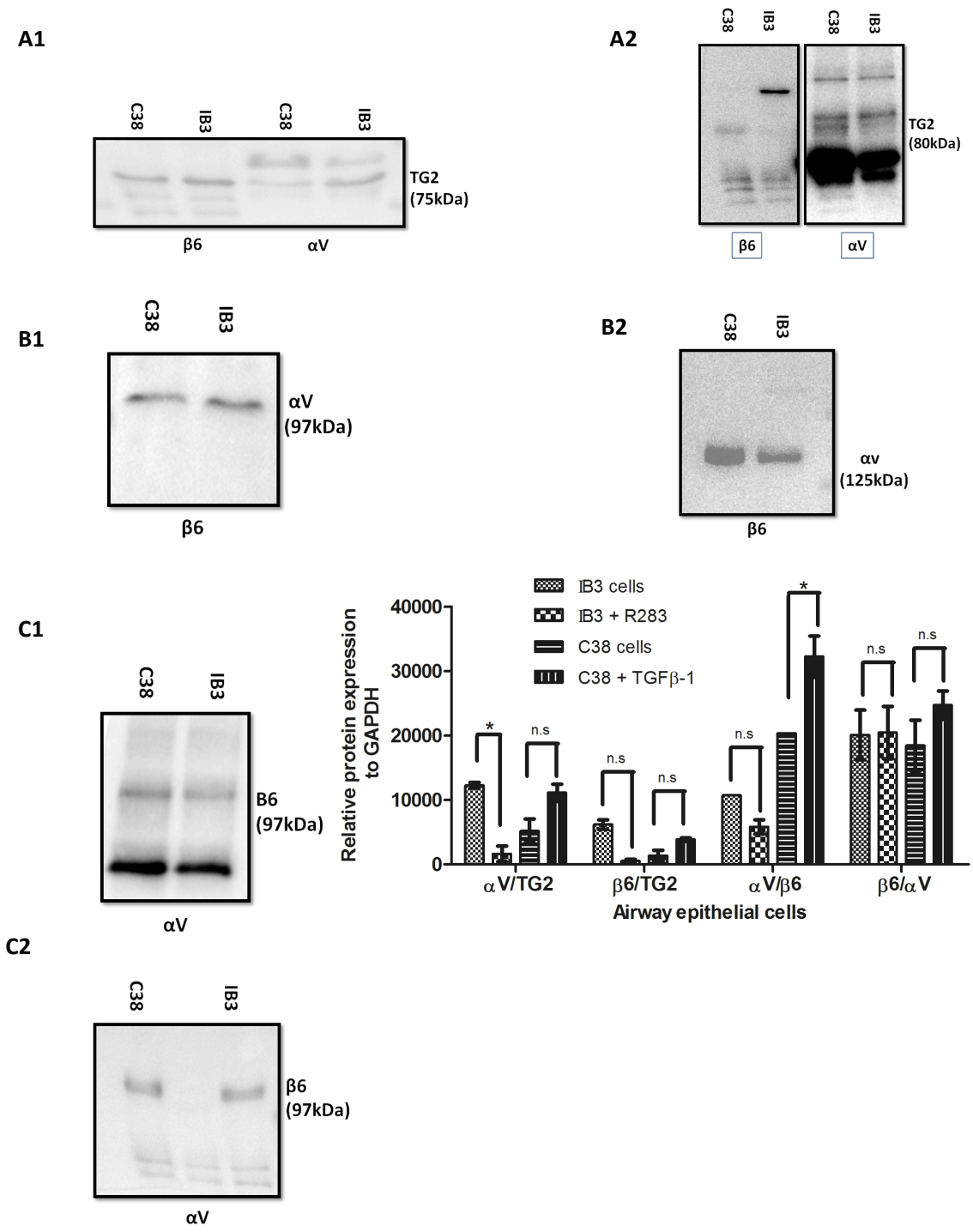

Figure 4.13A,B&C: TG2 interaction with integrins is blocked in the presence of TG2 inhibitors. Co-immunoprecipitation (Co-IP) analysis of TG2, **A** αV, **B** and β6, **C** expression in IB3 and C38 cells treated with the cell-permeable TG2 inhibitor, R283 (500μM) or rTGFβ1 (3ng/ml). 200μg of protein was loaded on 8%(w/v) gels for Western blot assay. Western blots images represent a characteristic result of 3 independent experiments. Densitometry represents mean and standard deviation of 3 independent experiments. Results show TG2 interacting with αV and β6 control at basal levels, **A1** as well as αV and β6 interaction with each other (**B1** and **C1)**. However, in the presence of R283 or rTGFβ1, IB3 and C38 cells decrease and increase TG2 and αV interaction respectively (**A2** and **B2)** with no change in β6 and αV interaction (**C2**). Two way Anova analysis with Bonferroni's post-tests; * $p<0.05$, n.s. $p>0.05$.

4.3.6: TG2-TGFβ1 induced EMT is SMAD dependent

Studies have correlated the induction of EMT in bronchial epithelial cells to elevated levels of TGFβ1 (Doerner and Zuraw, 2009, Kasai *et al.*, 2005). As TGFβ1 functions via different mechanistic pathways, its SMAD dependent pathway has been shown to be involved in the induction of EMT in airway pathologies (Hackett *et al*., 2009, Yanagisawa *et al*., 1998, Camara and Jarai, 2010). Here, it is hypothesised that as TG2 induces the activation of TGFβ1 and TGFβ1 functions via its receptors and down signalling partners, SMAD 2&3, blockade of TG2 activity with cell-permeable and cell impermeable TG2 inhibitors would show whether the progression of EMT driven by TG2 is SMAD dependent and illustrate the involvement of cell surface or intracellular TG2 in this process. Results show an elevation of phosphorylated-SMAD 2 and 3 expression (p-SMAD) commensurate with TG2 expression in untreated IB3 cells (Figure. 4.14A). However, expression of p-SMAD 2 was higher than p-SMAD 3. In the presence of 1-133, R283 and R294, expression of p-SMAD 2 was inhibited compared to untreated control. Similarly, p-SMAD 3 and TG2 expression were inhibited compared to untreated control. Total SMAD 2 and 3, T-SMADs, had equal protein expression in the presence of 1-133, R283 and R294. However, in C38 cells, an up regulation of TG2 was shown to correspond with an elevation of p-SMAD 2 and an elevation in p-SMAD 3 expression in the presence of rTGFβ1 (Fig. 4.14B). In the presence of 1-133, R283 and R294, p-SMAD 2 and 3 expression was observed be inhibited. In all cases, no basal p-SMAD expression was observed in untreated C38 cells. Comparing the results with that from IB3 cells, T-SMAD 2 and 3 levels remained unchanged in the presence of inhibitors in C38 cells. These results show no difference in inhibition of p-SMADs for cell impermeable inhibitors, 1-133 and R294 and R283. The non-differential inhibition of TG2 in the cell or on the cell surface by TG2 cell permeable or impermeable inhibitors suggests that cell surface TG2 might be involved in the SMAD related effect observed via its activation of TGFβ1 in CF cells.

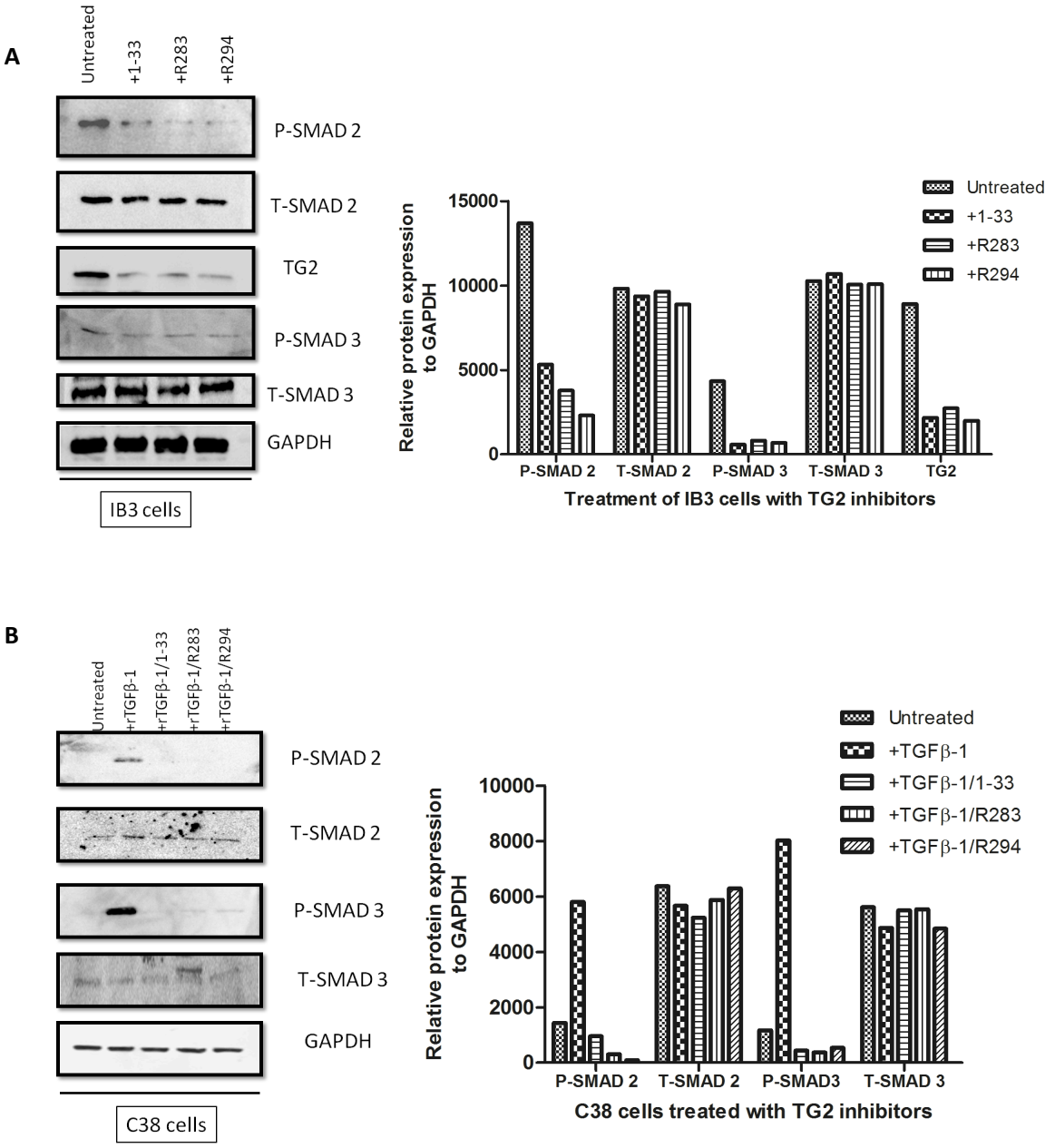

Figure 4.14A&B: SMAD 2 and 3 regulate TGFβ1 downstream signaling in CF cells. Western blot analysis to determine SMAD expression in IB3 and C38 cells treated with cell-permeable and impermeable TG2 inhibitors; 1-133 (100uM), R283 (500uM) and R294 (500uM). 50µg of protein was used for the Western blot assay. GAPDH was used to normalise protein loading for densitometry analysis. Both cell permeable and impermeable TG2 inhibitors inhibited P-SMAD 2 and 3 expressions in IB3 cells, without affecting T-SMAD levels.

4.4 Discussion:

The requisite for the progression of EMT in CF cells is the elevation of TG2, which increases the activation of TGFβ1 and through its downstream partner proteins, sustains the fibrotic process. Previously in chapter 3, results showed that raised levels of TG2 corresponded with elevated expression of TGFβ1. Here elevated levels of TG2 correlates with an increase in EMT markers whilst TG2 inhibitors impede the EMT process via the inhibition of active TGFβ1. This study also shows that inhibiting TGFβ1 activation blocks SMAD-dependent regulation of EMT.

This study has observed that high levels of TG2, corresponds with elevated expression of EMT markers in IB3 cells. It was shown that as gene expression of EMT markers was raised, the level of TGFβ1 was also elevated. This was inhibited in the presence of TG2 inhibitors. Preliminary results show that the comparative inhibition between TG2 cell-permeable and impermeable inhibitors suggest that active cell surface TG2 was more likely to be involved in regulating TG2 activity in IB3 cells. Pinkas *et al*., (2007) observed that the open conformation of TG2 corresponds with the inhibitor bound structure of the enzyme suggesting that the inhibitors would function only with an open active structure of TG2 unless mutated. Furthermore, Siegel *et al.,* (2008) showed that activation of extracellular TG2 depended on tissue injury which was hypothesised to be commensurate with increased matrix deposition and stabilisation leading to elevated levels of fibronectin and collagen 1 thus enhancing the fibrotic process. This can be suggested to correlate with the progression of certain diseases, in which TG2 is involved.

In a related study, using 3T3 Swiss fibroblast cells, it was demonstrated that in the presence of the TG2 monoclonal antibody, CUB7402, cell migration was reduced in a dose dependent manner (Balklava *et al*., 2002). Verderio *et al.(1998)* also observed that when cells were incubated with CUB7402, there was a reduction in cell attachment. In addition, Akimov and Belkin, (2001b) showed in a study of monocytes that elevated levels of cell surface TG2 and integrin-bound TG2 were observed during the conversion of monocytes to macrophages which aids in macrophage adhesion. This further characterises the role of TG2 as a migration and adhesion mediator for fibronectin. This agrees with the results obtained where IB3 cells were shown to migrate more rapidly than C38 cells, with reduced migration of cells observed in the

presence of R283 inhibitor supporting the hypothesis that active cell surface TG2 might be involved in cellular migration in IB3 cells.

Studies have shown that TGFβ1 plays a role in wound healing which involves expediting wound contraction, increasing matrix synthesis, repressing MMP production and elevating TG2 expression (Leask and Abraham, 2004, Ritter and Davies, 1998). Interestingly, this study observed that in the presence of TGFβ1 in C38 cells, TG2 protein levels were markedly increased and that this was analogous to elevated EMT marker expression. The elevation of TG2 was in line with a change in cell morphology and an elevation of the myofibroblast marker, α-SMA. Again, TG2 inhibitors reversed this process. Noteworthy, is the morphological change in C38 cells in the presence of TGFβ1, which was blocked by TG2 inhibitor, R283. This illustrated a conventional phenomenon characterised by epithelial cells undergoing EMT in the presence TGFβ1. Doerner and Zuraw (2009) and Hackett *et al.,* (2009) discovered in two separate studies that in the presence of TGFβ1, epithelial cells undergo morphological transformation where they lose their cell-cell contact and exhibit decreased expression of tight junction markers like E-cadherin and zonular occludin-1 and increase expression of myofibroblast markers like α-smooth muscle actin (α-SMA). This is concomitant with induction of the transcriptional marker, *Slug* and assumption of an EMT phenotype associated with an increase in fibronectin and collagen 1 deposition. Subsequently, when HBEC cells were treated with rTGFβ1 and R283, a loss of E-caherin was observed (Figure 4.9A&B). In order to show TGFβ1 activation was linked directly with TG2 expression, TG2, fibronectin and N-cadherin expression was inhibited with TGFβ neutralizing antibody (Nab). It was observed that TG2 levels were markedly decreased compared to untreated control cells. Also, fibronectin and N-cadherin expression were significantly inhibited. A commensurate elevation of E-cadherin expression in IB3 cells was observed, which was similar to the results using TG2 inhibitors (Figure 4.10). This suggests that as TGFβ1 is blocked from interacting with its receptors, this impedes the activation of TG2 gene expression by TGFβ on TG2 promoter site, which might lead to a decrease in gene and protein expression of TG2.

Lauzier *et al.,* (2012) demonstrated using fibroblast-like synoviocytes (FLSs) obtained from control rats (C-FLS) that the invadopodia formation of cells deposited on gelatin matrix induced by TG2 was significantly inhibited in the presence of Nab. This proposes together with the results from this study that activation of TGFβ1 depends on

TG2 and that EMT ensues as a downstream event mediated by TGFβ1. Consequently, observing the effect of TG2 inhibitors on matrix proteins with the TG2 inhibitor, R283, showed that TG2 inhibitors reduce TG2 expression in IB3 cells thus impeding migration of the cells. Additionally, the comparative inhibition of matrix fibronectin deposition by 1-133 and 1-155 in IB3 cells was shown to illustrate the role of cell surface TG2 in matrix deposition and EMT.

A myriad of studies have linked αVβ6 expression to the activation of TGFβ1 as well shown the involvement of this integrin in TGFβ1 induced EMT (Mamuya and Duncan, 2012, Katoh *et al*., 2013, Henderson and Sheppard, 2013). This study has highlighted possible interactions between TG2 and the αV subunit and suggested that this interaction might be involved in the activation of TGFβ1.The results showed an elevated αV protein expression in IB3 cells which was inhibited in the presence of TG2 inhibitor, R283. The protein-protein interaction as shown using co-IP suggests a direct inhibition of αV expression as a consequence of TG2 inhibition.

SMADs are downstream regulators of TGFβ1 signaling. The intricate cascades of interactions involved in the activation of SMADs are managed through TGFβ receptors, RI &RII. Previous results from chapter 3 have shown that the CF cell line IB3 express both RI and RII receptors and secrete high TGFβ1 levels compared to the corrected cell line, C38. These results show that IB3 cells express high levels of phosphorylated SMAD 2 and 3 compared to C38 cells. However, in the presence of TG2 inhibitors; 1-133, R283 and R294, p-SMAD 2&3 were inhibited. In C38 cells, treatment with rTGFβ1 increased p-SMAD 2 & 3 expression. However, this was inhibited in the presence of TG2 inhibitors. Notably, these results demonstrate that 1-133 and R294, which are cell impermeable inhibitors, show comparable inhibition to the cell-permeable inhibitor, R283. These suggest that cell surface TG2 might play a major role in the progression of EMT as inhibition of cell surface TG2 blocks the downstream signaling of TG2 via TGFβ1.

4.5 Conclusion

Although, the role shown by cellular TG2 remains resolute in the fibrotic process, the evidence presented in this chapter suggests that active extracellular TG2 might play a central role in the EMT process occurring in CF cells. The pathway for this occurrence seemingly might be through the activation of TGFβ1 and its downstream signalling pathways.

Chapter 5

The effect of TG2 knockdown/ overexpression on the development of EMT in CF cells

5.1 Introduction:

Generally, studies have linked the ubiquitous nature of TG2 to its involvement in various diseases where the transamidation reaction catalyzed by TG2 has been linked to its matrix deposition/pro-fibrotic function. The Ca^{2+} dependence of TG2 plays a vital role in determining its enzymatic activity and its ability to cross-link multiple substrates, leading to the progression of a number of different human diseases (Gundemir *et al.*, 2012, Smethurst and Griffin, 1996).

Once activated, TG2 plays an essential role in either a reparative or pathological manner in tissue injury by stabilising matrix fibronectin or collagen deposition thus enhancing cell migration and stimulating wound healing (Nicholas *et al.*, 2003, Telci and Griffin, 2006, Wang *et al.*, 2012). Studies have established the importance of extracellular TG2 in stabilising matrix proteins in differentiating cartilages (Aeschlimann *et al.*, 1995) and by using TG2 transfected cells, it has been shown that the role extracellular TG2 plays is important in increasing cell adhesiveness (Johnson *et al.*, 1994). Jones *et al.* (1997) demonstrated in the study using the human endothelial-like cell, ECV304, that cell spreading on fibronectin which normally depends on the crosslinking activity of TG2, could be impeded using the monoclonal mouse anti-TG2 antibody, CUB7402. Also, Heath *et al.,* (2002) revealed in a study on human osteoblasts cells that cell adhesion and spreading depended on a TG2-fibronectin heterocomplex. This was further confirmed by the study of Verderio *et al.* (2003) which showed that this interaction was resilient and withstands the effect of Arg-Gly-Asp (RGD) peptides thus maintaining cell adhesion. Taken together, this TG2 effect was attributed to extracellular TG2 interacting with the ECM protein, fibronectin and cell surface sulphates, which was independent of the formation of ε-(γ-glutamyl) lysine bonds.

Intracellularly, TG2 assumes a closed inactive GTP-bound conformation where activity is sequestered due to high levels of GTP and low levels of calcium in approximately a 150μM/100nM ratio (Smethurst and Griffin, 1996). This however, is reversed in diseased conditions where the cellular milieu is distorted and calcium levels can be elevated up to 100μM or above (Achyuthan and Greenberg, 1987). Here TG2 assumes an open conformation, exposing the active catalytic triad to substrates and crosslinks peptidyl glutamine residues acting as acyl donors to suitable primary amines, to form isopeptide bonds (Griffin *et al.*, 2002). Studies have shown that certain domains are involved in modulating TG2 activity as mutations of such domains interferes with the multi-functionality of the enzyme. The C227S mutant is a cysteine to serine mutation at

position 227, which leads to a loss in transamidating activity and defective GTP binding capacity (Liu *et al*., 2002). The W241A and R580A mutants are TG2 constructs where tryptophan and arginine respectively are mutated and replaced by alanine. The former mutant is devoid of transamidating activity with little effect on its GTP binding capacity whilst on the contrary the R580A mutant is devoid of GTP binding with complete transamidating activity (Ruan *et al*., 2008, Murthy *et al.*, 2002). These TG2 mutants have recently been used extensively to illustrate the importance of TG2 activity in diseases, hence proffering answers to whether TG2 is a "cause" or an "effect" in these diseases.

In concert with TG2 mutations, studies have employed the use of TG2 inhibitors to demonstrate the importance of TG2s active spatial conformation on its enzymatic activity as well as the elasticity of the enzyme to respond to extracellular and intracellular levels of GTP/GDP and calcium. Consequently, Pinkas *et al.* (2007) demonstrated that the inhibitor-bound TG2 complex assumed an open conformation comparable to that in the presence of calcium-activated TG2. This suggests a hypothesis that an active site directed TG2 inhibitor could mainly function when TG2 is in an open active TG2 state. However, the different classes of TG2 inhibitors further aids in determining the location of TG2 as the inhibitors juggle between intracellular and extracellular compartments of the cell. Such inhibitors include the cell-permeable ie Cystamine, R283, Z-Don and the peptidomimetic inhibitors EB1-155, EB1-133 and the competitive substrate ie Monodansylcadaverine (MDC) and cell impermeable peptidic inhibitors eg R292, R294 and R281 (Griffin *et al.,* 2008, Badarau *et al*., 2013, Telci *et al.*, 2009, Aeschlimann *et al*., 1995). Recent studies have shown an upward rise in the potential use of compounds with TG2 inhibitory activity as part of a treatment cocktail in cancer (Kumar *et al.*, 2010, Antonyak *et al.*, 2004, Jones *et al.*, 2006), coeliac disease (Maiuri *et al.*, 2005), neurodegenerative diseases (Junn *et al.*, 2003, Bailey and Johnson, 2006, Karpuj *et al*., 2002, Wakshlag *et al*., 2006), chronic kidney disease (Johnson *et al*., 2007, Johnson *et al*., 1999) and cystic fibrosis (Maiuri *et al*., 2008, Luciani *et al.*, 2010a).

The use of gene transduction has had broad applicability in research and gene therapy where genes of interest are efficiently transferred into target cells. For this purpose, development of viral and non-viral vectors have aimed at efficient transduction and the continual expression of the transduced gene whilst maintaining high levels of safety (Miyoshi *et al.*, 1998). Consequently, retroviruses were developed with wide use of onco-retroviruses ie Murine Leukaemia Virus (MLV) which was marred by the requisite for cells to be proliferating thus limiting their use. This lead to the development of the second generation vesicular stomatitis virus glycoprotein (VSV-G) pseudotyped Human

Immunodeficiency virus type-1 (HIV-1) based vector with high efficiency in transducing non-dividing cells *in-vitro* and *in-vivo* as well as a broad range of other tissues with high titres (Naldini *et al*., 1996). Interestingly, Lewis *at al.* (1992) had previously shown that HIV infection of non dividing cells produces more viral particles than infection with onco-retroviral MLV.

Also, eliminating the virulent genes in the viral genome further enhances the efficiency of the viral transduction. Furthermore, on developing a self-inactivating lentiviral (SIN) vector, Miyoshi *et al.* (1998) was able to replace the U3 region of the 5' long terminal repeat (LTR) with a CMV promoter, obviating the need for the trans-activator of transcription protein, tat, encoded for by the *tat* gene in HIV-1, thus transcription occurs independent of tat. This produces high expression levels as the deletion of 133 base pairs from the U3 of 3' LTR was transferred to the 5' LTR after reverse transcription yielding the SIN which gets integrated into the host cell inactivating transcription of LTR in proviruses. Thus, as the vector construct is transfected into the packaging HEK 293T cells together with VSV-G plasmid, transcription ensues at the U3/R border of the 5'LTR through to the R/U5 border of 3'LTR. On infection, the U3 regions of both LTRs are derived from the U3 region of the 3'LTR that serves as the template for reverse transcription to form double stranded DNA. Hence, both LTRs have a copy of the U3 region of the 3' LTR in the proviruses (Miyoshi *et al.*, 1998). This third generation SIN forms the basis for the FIGB plasmid used in this study as shown below.

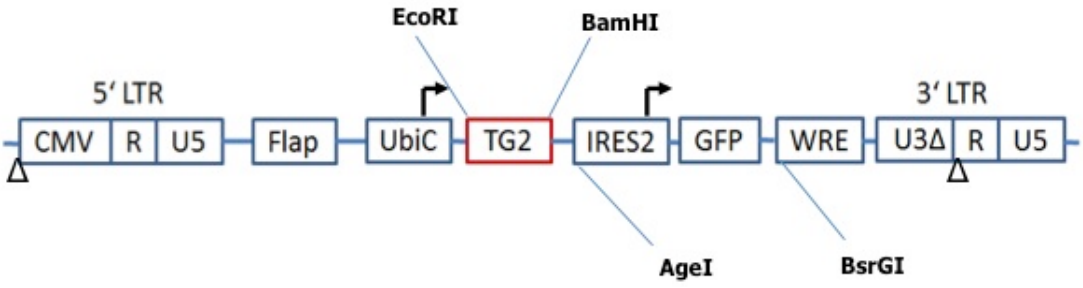

Figure 5.1: Structure of FIG B plasmid carrying the TG2 gene. The schematic shows the CMV promoter/enhancer replacing the tat promoter of the HIV-1 gene on the 5' LTR region with a flap region. The TG2 gene has an UBiC promoter, an ubiquitous promoter allowing TG2 to be expressed in various cells as well as the GFP region. The triangles represent U3 deleted regions. Viral transcription of TG2 begins from the 5'LTR to the 3'LTR with GFP gene expression as the hallmark of TG2 expression in the cell.

The plasmid utilises the CMV promoter/enhancer making the plasmid tat independent as well as the UbiC and IRES 2 promoter to increase the ubiquitous expression of TG2 gene in various tissues. Inclusion of GFP allows assessment of successful transduction via expression of the fluorescent green protein seen in cells under the microscope (Schorpp *et al.*, 1996). Since the toxicity of the first generation HIV-1 derived vectors depended on the tat and rev proteins as well as the accessory factors, *gag* and *pol* genes in *cis* acting sequences, replacement of tat with an active promoter in *trans* with *rev,* produces high titre vectors when HIV-1 derived vectors are transduced with packaging vectors with *gag* and *pol* (Berkowitz *et al*., 1995, Zufferey *et al*., 1998, Dull *et al.*, 1998). The Flap promotes nuclear importation of the viral genome and the woodchuck hepatitis posttranscriptional regulatory element (WRE) increases RNA processing and averts polyadenylation site read-through (Zufferey *et al*., 1999, Zennou *et al*., 2000).

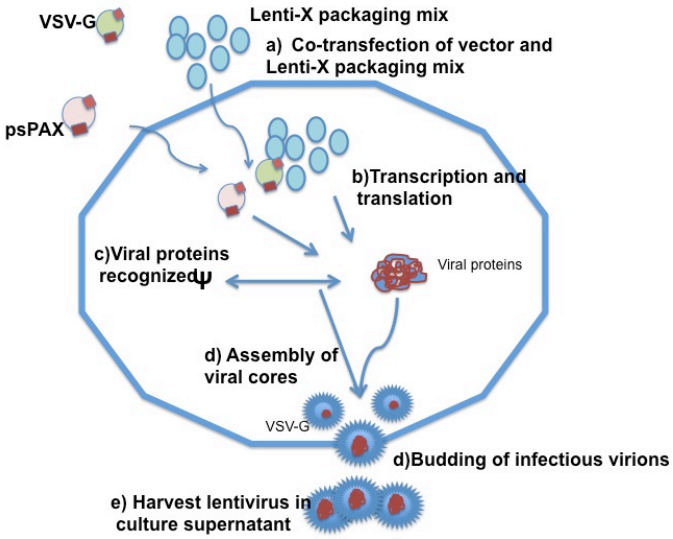

Figure 5.2: Schematic representation of lentiviral production of TG2 plasmids. TG2 mutants (TG2-WT, shRNA, W124A and R580A) were transfected into packaging HEK293T cells in submerged culture. The packaging mix in a ratio of pPAX, envelop plasmid, VSV-G and DNA of interest; TG2 WT, R580A, W241A, scramble and empty plasmid transfected into HEK293T cells, **a**. The plasmid is integrated, undergoes transcription to form viral particles, **b.** The packaging proteins recognise the packaging sequence on the viral RNA, **c**. The viral particles are assembled and transported to the cytoplasm, **d**. VSV-G envelopes the viral particles and this buds out of the cell, **e**. The medium is collected and viral particles are harvested on centrifuging.

Limited studies have been performed using TG2 shRNA knockdown in airway cells. Recently, Olsen *et al.,* (2011) showed in a study of Idiopathic Pulmonary Fibrosis (IPF) using human lung fibroblasts deficient in TG2 that further knockdown of TG2 prevented TGFβ1 mediated elevation of TG2 protein levels and a consequent impedance of fibroblast migration following a scratch assay. In the same study, extracellular TG2 protein and activity was increased in the presence of TGFβ1 as human lung fibroblasts were treated for 72h. This suggests the correlation between TG2 protein and activity levels and the effects of its knockdown on disease progression.

The work in this chapter is centered around transducing TG2 mutants into CF cells, IB3 and C38 and the human primary epithelial cell, HBEC and observing the effect of these mutations on the pattern of expression of EMT markers as well as on TG2 activity. The work will examine the effect of over-expressing and knocking down TG2, transiently or stably in the cells on EMT.

5.2 Aims:

In this chapter, TG2 functional mutants are used to determine TG2s involvement in normal and CF cells by:

- Transducing cells with Lenti-viral vectors containing wild type (WT) and TG2 mutants. The mutants to be used include the GTP binding mutant, R580A, and the transamidating deficient mutant, W241A. This is carried out employing IB3, C38 and HBEC.
- Determining TGFβ1 levels in the stably transduced TG2 shRNA IB3 cells.
- Investigating the effect of elevated TG2 levels in C38 and HBEC cells on EMT marker expression.

5.3 Methods:

5.3.1 siRNA Transfection of TG2 plasmids in IB3 cells

To investigate the effect of TG2 silencing on EMT marker expression in IB3 cells, Qiagen® TG2 siRNAs were employed; TGM2_1, TGM2_5, TGM2_6 and TGM2_7. 5 X 10^5 cells were seeded in complete medium overnight for 18-24 h. siRNA transfection was carried out as described in chapter 2.2.11. The cells were subsequently washed with 1x PBS, pH 7.4 twice and lysed as described in chapter 2.2.2.1 with SDS/PAGE and Western blotting carried out on lysates as described in chapter 2.2.3 and 2.2.4 respectively.

5.3.2 Western blotting of IB3, C38 and HBEC cells

Using lysates from IB3, C38 or HBEC, 50µg of protein was added to pre-cast 6%(w/v), 8%(w/v) or 12%(w/v) polyacrylamide gels and SDS/PAGE carried out as described in chapter 2.2.3. Western blotting was then performed for the detection of TG2, fibronectin, N-cadherin, *Slug*, E-cadherin and CFTR as described in chapter 2.2.4.

5.3.3 TG2 activity determined using the Biotin Cadaverine assay

TG2 activity was measured in lysates of IB3, C38 and HBEC cultured in full medium. The assay was carried out on 96-well plates coated with fibronectin (5µg/ml) suspended in 50mM Tris-Cl, pH 7.5. The assay was performed as described in chapter 2.2.6.1.

5.5.4 Lentiviral transduction of IB3, C38 and HBEC cells

To produce viral particles for the different plasmids, HEK293FT packaging cells were cultured as described in chapter 2.2.19.1. HEK293FT packaging cells were transfected with packaging plasmids in a packaging mix as described in chapter 2.2.19.2. The viral particles were harvested and concentrated as described in chapter 2.2.19.3 and viral

titre determined as described in chapter 2.2.19.4. To 700µl of complete medium on IB3, C38 or HBEC, aliquots of viral particles of interest were added and transduction was carried out as described in chapter 2.2.19.5. The cells were rinsed aseptically with 1 x PBS, pH 7.5 twice and cells were lysed and SDS-PAGE/Western blotting were carried out on lysates from the cells as described in chapter 2.2.3 and 2.2.4 respectively.

5.5.6 TGFβ1 activity assay in IB3 wild type and shRNA transduced cells

To determine TGFβ1 levels in IB3 wild type and transduced cells**,** $4x10^5$ of IB3 wild type or shRNA-transduced cells were cultured in 12 well plates in complete medium for 6 h to allow cell attachment. The cells were then cultured overnight for 18-24 h in 1x ITS supplement without serum. Medium was collected and centrifuged and the TGFβ1 assay carried out as described in chapter 2.2.9.

5.4 Results:

5.4.1: TG2 knockdown abrogates Epithelial to Mesenchymal (EMT) progression in CF cells.

5.4.1.1: N-cadherin expression is transiently abolished in the presence of siRNAs.

A myriad of TG2 studies have demonstrated the effect of TG2 inhibition or knockdown on disease progression. Recent studies by Nadalutti *et al*. (2011) showed that using TG2 siRNA, transient TG2-induced cell adhesion was impeded and apoptosis was induced, however, this was partially reversed in the presence of exogenous TG2. Previous results in chapter 4 have shown that in the presence of TG2 cell-permeable and impermeable inhibitors, EMT markers expression was significantly repressed. Here, first using siRNA, TG2 expression is reduced in order to observe changes in cell phenotype, which would affirm whether the observations on its effect on EMT, are directly related to TG2 expression. Using 4 different TG2 siRNA plasmids, TG2 siRNA silencing in IB3 cells was carried out as described in chapter 2.2.11. From the results as shown in Figure 5.3, it was observed that TG2 siRNA #6 significantly ($p<0.0001$) silenced TG2 expression (≥2-fold) compared to untreated groups. TG2 siRNAs #1,5 and 7 slightly inhibited TG2 expression. Similarly, it was observed that the silencing of TG2 was commensurate to the inhibition observed in N-cadherin expression with siRNA #6. Hence, it could be suggested as previous results have shown in chapters 3 and 4 that inhibition of TG2 expression concurs with the silencing of TG2 protein leading to loss of N-cadherin expression.

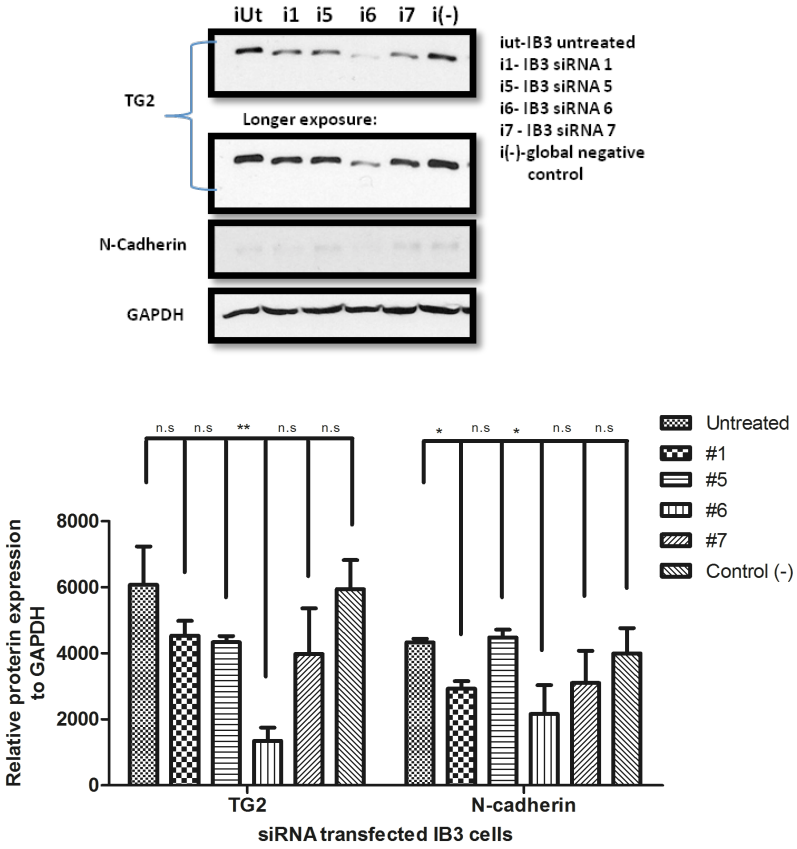

Figure 5.3: N-cadherin expression is reduced in the presence of TG2 siRNA. Left panel images showing representative Western blot of IB3 cell expression of TG2 and N-cadherin after transfection with TG2 siRNA plasmids #1,5,6,and 7. Iut indicates untreated cells and (-) indicates global negative control. 50µg of protein was used for the Western blot assay. Monoclonal mouse anti-TG2 and anti-N-cadherin antibodies (1:1000) were used to probe blots. The images represents a characteristic blot from 3 independent experiments with equal number of cells used at all times. GAPDH was used to normalise protein loading. Densitometry represents the mean value and standard deviation of 3 independents experiments. Results show a significant inhibition of TG2 expression in the presence of siRNA #6 and reduced N-cadherin expression in the presence of TG2 siRNA #1 and #6. One-way Anova analysis with Dunnett's multiple test; **p<0.0125, **p<0.0572, n.s. p>0.05.

As observed with TG2 protein expression, Figure 5.4 shows an inhibition of TG2 activity with the knockdown of TG2 expression. This illustrates in concert with earlier results in chapter four that in the presence of TG2 siRNA #6, there was a 2-fold inhibition of TG2 enzymatic activity. However, TG2 siRNA#1 inhibited N-cadherin expression (Figure 5.3) as well as enzymatic activity with siRNA#5, 6 and 7 inhibiting TG2 activity as well (Figure 5.4). Interestingly, the inhibition of TG2 activity by TG2 specific siRNA silencing corresponds with inhibition of TG2 activity using TG2 inhibitors. Although, the mechanism may remain different with an introduction of a silencing strand of RNA into the host genome as supposed to the interference of the

transamidating activity at the catalytic triad site, together they show that the knockdown/inhibition of TG2 is responsible for the abrogation of N-cadherin expression and this phenomenon might be occurring due to TG2 transamidating activity.

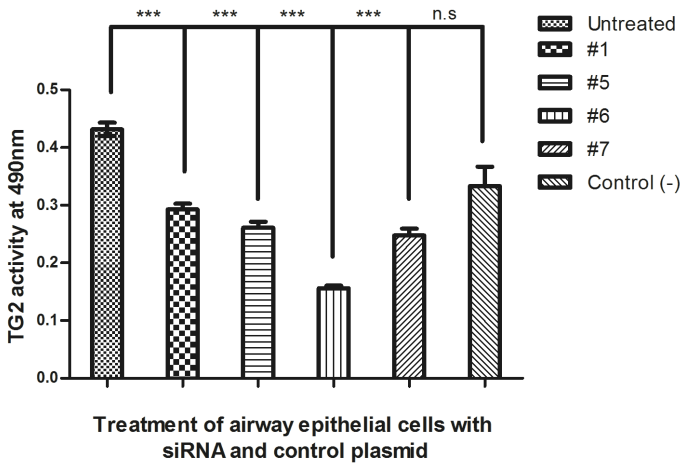

Figure 5.4: TG2 siRNA inhibits TG2 activity in IB3 cells. TG2 activity assay in IB3 cells transfected with TG2 siRNA #1,5,6 and 7 was assayed using the Biotin Cadaverine assay. Global control plasmid was used as negative control (-). Results represent mean and standard deviation of 3 independent experiments carried out in triplicates. Results show a significant inhibition of TG2 activity in IB3 cells transfected with TG2 siRNA #1,5,6 and 7 compared to untreated control. One Anova analysis with Dunnetts's Multiple tests; ***p<0.0001.

5.4.1.2: Stable knockdown of TG2 mimics TG2 inhibition and abrogates EMT

Evidence as shown by Wang *et al*.(2013) indicates that stable knockdown of TG2 in HUVEC cells inhibits tubule formation and cell migration and this result was comparable to that shown with TG2 inhibition achieved via site directed irreversible TG2 inhibitors. This suggests that the results observed in Figure 3.5 & 4.5 with TG2 protein/activity inhibition using TG2 inhibitors can be confirmed using TG2 knockdown. Initially, using TG2 siRNAs was a pilot study to observe the effect of TG2 knockdown on EMT. With the results obtained, further attempts were made to knockdown TG2 using TG2 shRNA containing virions, transduced into IB3 cells to recreate this observed trait. The TG2 shRNA plasmid was purified and propagated using Maxipreps. The purified TG2 shRNA plasmids were then transfected into packaging cells using Lipofectamine® 2000 as previously described in chapter 2.2.19.5. The TG2 shRNA viral particles were subsequently transduced into IB3 cells. The cells were then carefully lysed and TG2, fibronectin, N-cadherin and *Slug* protein expression was determined

using Western blotting as described in chapter 2.2.2.1 and 2.2.4 respectively. TG2 activity was measured in whole cell lysates using fibronectin- coated plates, measuring the incorporation of biotin cadaverine into fibronectin. Results show in Figure 5.5A&B that knocking down TG2 protein expression with TG2-shRNA significantly inhibited TG2 expression in IB3 cells. Also, fibronectin, N-cadherin and *Slug* expression were significantly inhibited. The transduction of IB3 cells was shown not to affect the expression of TG2 and EMT markers as scrambled shRNA transduced IB3 cells showed no significant change in expression compared to IB3 wild type cells. Figure 5.5C demonstrates that a knockdown of TG2 protein expression significantly inhibits ($p<0.001$) TG2 activity >6-fold in IB3 shRNA transduced cells. These results verify the link between TG2 expression and activity and suggest a link between progression of EMT and inhibition of TG2 activity in IB3 cells.

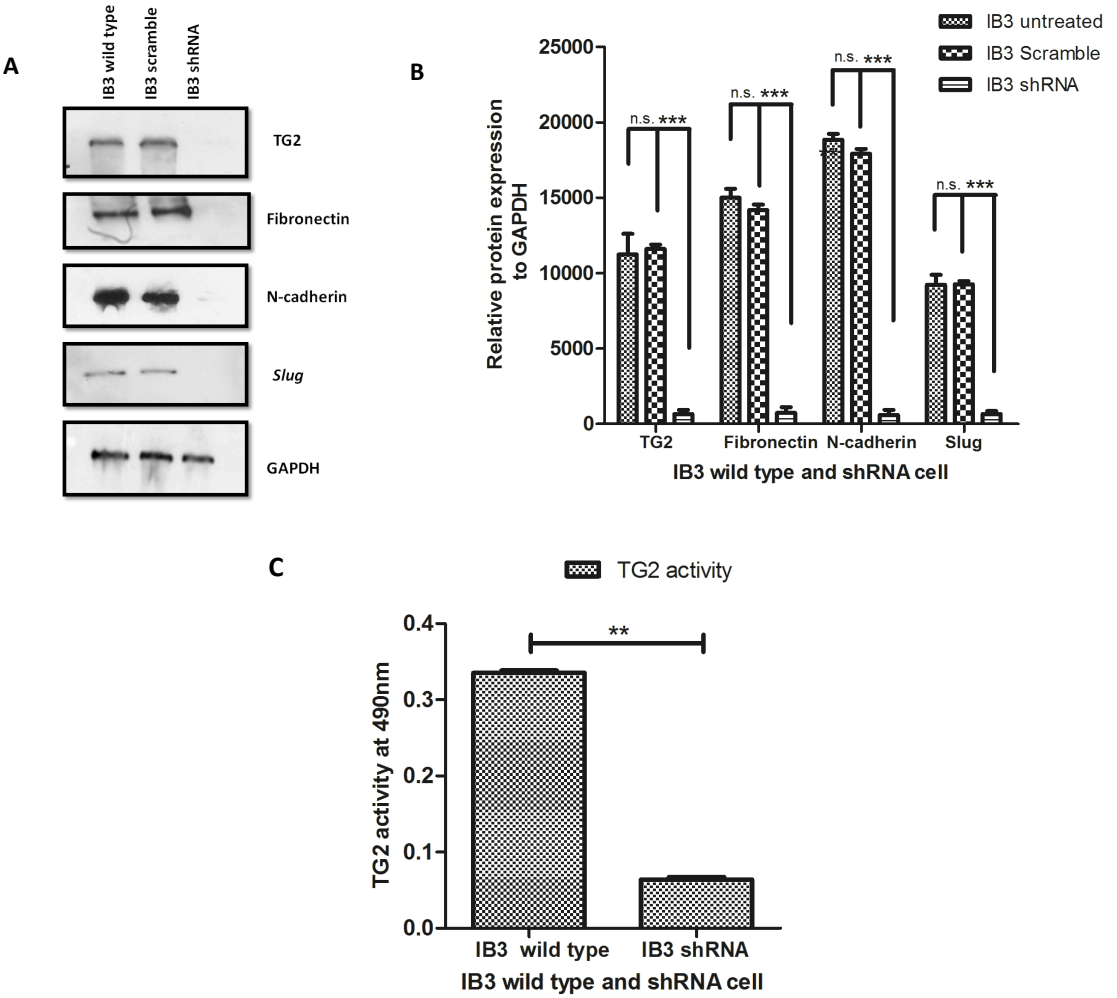

Figure 5.5A-C: TG2 knockdown impedes expression of EMT markers and inhibits TG2 activity. A. Western blot analysis of protein expression, **B**. Densitometry analysis and **C**, TG2 activity in lysates of IB3 cells using the biotin cadaverine assay. 50µg of protein was loaded on 6%(w/v), 8%(w/v) and 12%(w/v) gels for Western blot assay. IB3 cells in submerged culture were transduced TG2 shRNA or control scramble plasmid. Monoclonal mouse anti-TG2, anti-*Slug* and anti-N-cadherin antibodies as well as polyclonal rabbit anti-fibronectin antibody (1:1000) were used to probe blots. GAPDH was used to normalise protein loading. Blot image is characteristic of 3 independent experiments with equal number of cells used at all times. Densitometry represents mean values and standard deviation of 3 independent experiments. Results show that as TG2 protein is knocked down with shRNA, fibronectin, N-cadherin and *Slug* expression is significantly inhibited compared to control. Similarly, TG2 activity is significantly inhibited in the presence of TG2 shRNA. Two-way Anova analysis with Bonferroni post-tests; **p<0.001, n.s. p>0.05.

These results have shown that the knockdown of TG2 protein expression using shRNA provides a reduction of TG2 expression. Consequently, it also shows a consistent inhibition of fibronectin, N-cadherin and *Slug* protein expression corresponding to TG2

knockdown in IB3 cells. Comparatively, it can be deduced from these results that the observations from TG2 inhibition either via protein expression or activity reveals a role for TG2 in regulating the expression of EMT markers in IB3 cells.

Using medium collected from these cells, TGFβ1 levels were analysed as shown in Figure 5.6. The IB3 wild type and shRNA cells were cultured in serum free medium supplemented with 1 x ITS medium to avoid growth factors present in serum. The medium was analysed for TGFβ1 levels as described in chapter 2.2.9.

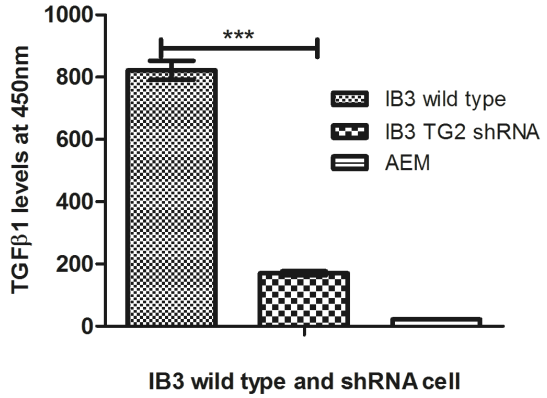

Figure 5.6: TG2 knockdown in IB3 cells transduced with TG2 shRNA decreases TGFβ1 levels. TGFβ1 levels in medium collected from IB3 cells transduced with TG2 shRNA cultured in submerged conditions in serum free medium (AEM). AEM used as negative control. Result represents mean values and standard deviation of 3 independent repeats using the same number of cells. Results show a significant decrease in TGFβ1 levels from IB3 cells transduced with TG2 shRNA compared to untreated cells (IB3 wild type). One-way Anova analysis of variance post-test; ***$p<0.0001$.

5.4.2: Mutation at the TG2 transamidation active site and the GTPase site unveils the function of TG2 in EMT.

5.4.2.1: TG2 transamidating activity plays an important function in EMT progression.

Studies have highlighted the importance of various TG2 functional mutants driving various disease processes ie cancer (Kumar *et al.,* 2012). Gundemir and Johnson, (2009) showed whilst examining the role of TG2 in cell death in HEK293A that the GTP binding deficient mutant, R580A facilitates the pro-death characteristic of TG2 as observed. Also, Wang *et al*. (2013) demonstrated using the transamidation deficient GTP binding mutant, W241A, that the transamidating activity of TG2 was vital for endothelial tubule formation as transduction of the mutant into TG2 knockdown HUVEC cells failed to restore tubule formation hence inhibiting angiogenesis in these cells. Here, an attempt was made using the CFTR "add-back" cell, C38, to observe whether transducing the TG2 mutants into these cells, can dissect out the role TG2 plays in the fibrotic process in CF disease.

Initially, C38 cells were transduced with wild type TG2 (TG2-WT) plasmid to observe the effects of TG2 overexpression in C38 cells. In addition by transducing the TG2 Cys277Ser and R580A TG2 mutants, the role of transamidation and GTP binding was assessed in the progression of this disease. Western blotting was carried out as earlier described in chapter 2.2.19.5 and 2.2.4 respectively.

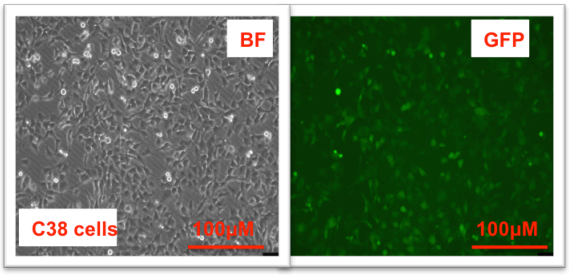

Figure 5.7: Phase contrast images of C38 cells transduced with TG2 WT plasmid. Images were taken using the Leica® Fluorescent microscope. The experiment was repeated 3 times. Scale bar present 100 µm. Transfection efficiency was shown by the presence of GFP-fluorescence in the cells and C38 cells transduced with TG2-WT plasmid (BF-Bright field, GFP-Green Fluorescent Protein).

This study has observed together with other studies the importance of TG2 mutants in analysing the role of TG2 in diseases. Here, this study has demonstrated that the mutation, W241A does not alter the EMT phenotype however, the R580A mutant, though devoid of GTP binding but with transamidating activity showed a change in phenotype as expected with an increase in TG2 protein expression. This suggests that the TG2 GTP binding activity is not essential but its crosslinking activity is required for EMT progression. Furthermore, it shows that overexpression of TG2 supports EMT progression as transduction of TG2-WT increased TG2 and EMT marker expression in C38 cells.

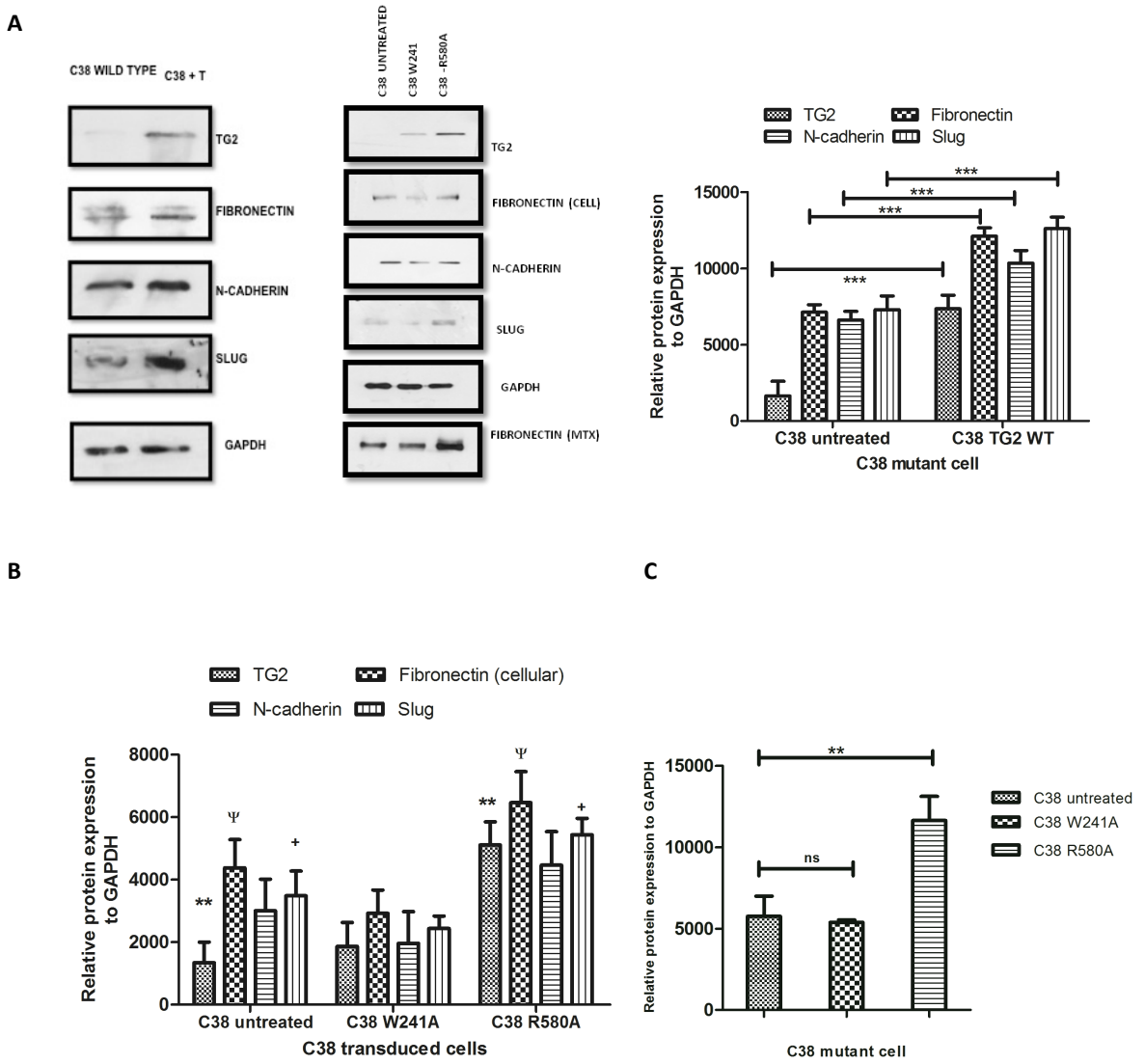

Figure 5.8A,B&C: **TG2 conformation determines phenotype in transduced C38 cells.** Using Lentiviral transduction, C38 cells were infected with viral particles carrying TG2-WT, W241A and R580 mutants. For W241A and R580 transfected cells, both cells and matrix were collected. 50µg of protein was used for the Western blot assay. Monoclonal mouse anti-TG2, anti-*Slug* and anti-N-cadherin antibodies as well as polyclonal rabbit anti-fibronectin antibody (1:1000) were used to probe blots. GAPDH was used to normalise protein loading. **A.** Results show elevated TG2 expression in C38 cells in the presence of TG2-WT plasmid, which corresponds with an elevation in fibronectin, N-cadherin and *Slug* expression**.** Similarly, in the presence of R580 transduced cells, cellular and matrix, EMT markers were shown to be elevated as TG2 expression increased however, W241A transduced cells did not show any change in the levels of expression both in the cells or matrix. Images represent characteristic blots from 3 independent experiments with equal number of cells used at all times**.** Densitometry represents mean values and standard deviation of 3 independent experiments One-way Anova analysis with Dunnett's multiple comparison test; **p<0.0014, Ψ =*p<0.0080, n.s p>0.05, **B**, and One-way Anova analysis with Dunnett's multiple comparison test; **p<0.0023, n.s p>0.05, **C**.

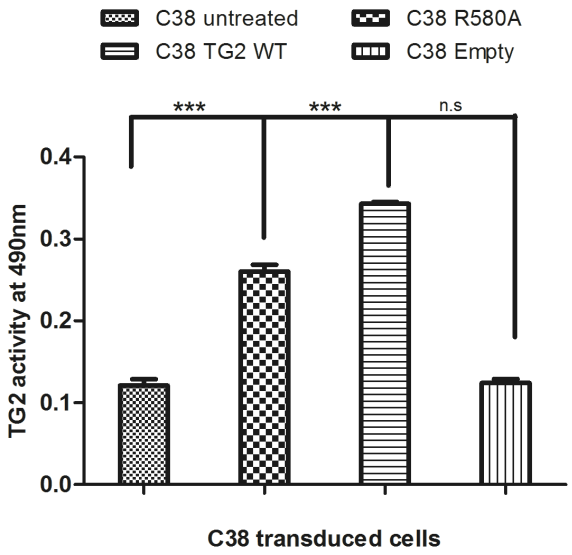

Figure 5.9: Transduction of wild type or R580A mutant increases TG2 activity in C38 cells. TG2 activity assay in C38 cells transduced with wild type TG2 (TG2-WT), mutant TG2 (R580A) and empty vector using the Biotin cadaverine assay using whole cell lysates. 50µg of protein was used for the Western blot assay. Results represent mean and standard deviation of 3 independent experiments. Results indicate that transduction of C38 cells with wild type TG2 significantly increases TG2 activity as well as with R580A mutant. However, TG2 activity in R580A transduced cells was slightly less than in C38 cells with TG2-WT mutants. One-way Anova analysis with Dunnett's Multiple comparison test; ***$p<0.0001$, n.s $p>0.05$.

This study shows that the elevation in transamidation activity corresponds with TG2 protein levels in these cells (Figure 5.8). Its also confirms that the R580A mutant possess transamidation activity (Figure 5.9) which accounts for certain TG2 traits ie cellular pro-death function (Gundemir and Johnson, 2009) and EMT as observed in this study.

5.4.2.2: Up-regulation of EMT expression in HBEC negatively regulates the CFTR channel.

Previous studies shown in chapters three and four, have demonstrated that in the CF cell line, IB3 , TG2 protein and activity levels are elevated together with EMT markers. It also demonstrated that in CF "add-back" cell, C38, the occurrence of EMT could be augumented by an elevation of TG2 in the cell. Noteworthy of mentioning is that these cells are transformed cells which for *in vitro* purposes aid in understanding the underlying mechanism involved in diseases. However, although their cell proliferative

characters have been exploited in research, their loss of certain differentiation functions neccesitates the need to obtain primary cell lines with epithelial origin (Gruenert *et al.*, 1995). Hence, primary human bronchial epithelial cells were used in demonstrating the phenotypic traits associated with the normal, non-CF bronchial cells, thus providing relevant evidence likened to *in vivo* conditions.

HBEC were employed to validate earlier results with IB3 and C38 cells thus showing the reproducibility of the results in *in vitro* cell culture conditions. HBEC were transduced with TG2-WT plasmid to investigate whether an elevation of TG2 in these cells corresponds with an increase in EMT markers expressions. Consequently, in order to show the effect of elevated TG2 on the expression of the epithelial adhesion maker, E-cadherin and the CFTR chloride channel, protein expression was determined for these two proteins.

HBEC in submerged culture were transduced for 48 h with TG2-WT particles with re-infection carried out once every 24 h. The cells were subsequently rinsed carefully with 1x PBS, pH 7.4 and Western blotting carried out as described in chapter 2.2.4 to determine TG2, fibronectin, N-cadherin, *Slug*, E-cadherin and CFTR expression.

A

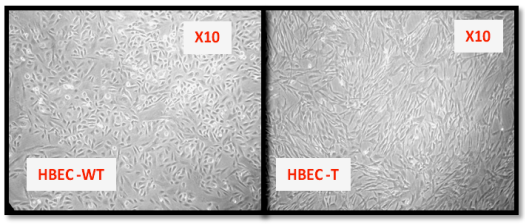

B

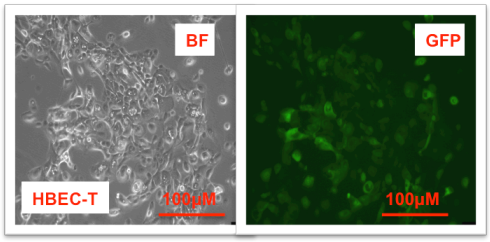

Figure 5.10A&B: Transducing TG2 to elevate TG2 levels induces a change in cell morphology in HBEC. A. Phase contrast images of HBEC wild type, HBEC-WT and cells transduced with TG2-WT plasmid, HBEC-T, showing a change in cell morphology from cobblestone-shaped to a spindle fibroblast-like morphology with higher TG2 levels after transduction with TG2-WT plasmid**. B** shows images of HBEC-T cells with GFP indicating transduction efficiency. Images were taken under the electron microscope and Leica® Fluorescence microscope respectively. Magnification of images (x100). Images are characteristic of 2 independent repeats.

C1

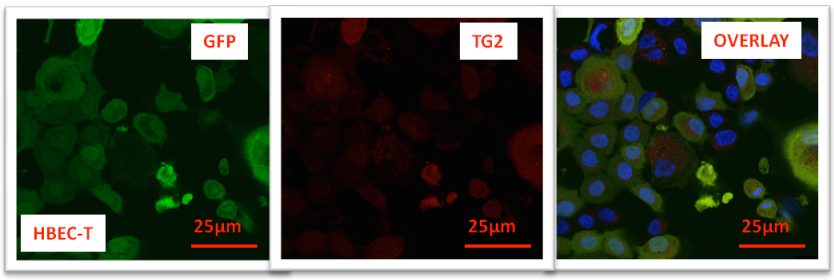

C2

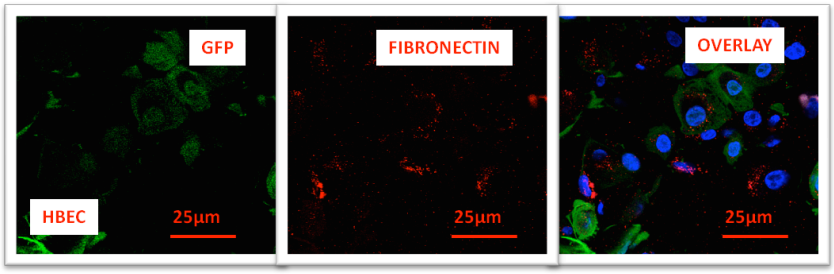

Figure 5.10C1-2: TG2 and fibronectin co-localise in HBEC-T cells. Cellular localisation analysis of TG2 and fibronectin expression in HBEC transduced with TG2 viral particles, HBEC-T in submerged culture. The cells were stained for polyclonal anti-TG2 (1:100), **C1** and polyclonal anti-fibronectin (1:100), **C2** in submerged culture. Scale bar represents 25µm. GFP indicates successful transduction of TG2-WT. Images were taken using a Leica® Fluorescence microscope. Results show an increase in TG2 and fibronectin expression following transduction with TG2-WT viral particles. An elevation of TG2 and fibronectin expression corresponds to the increase in GFP expression (Figure 5.10B) showing that only the transduced cells express the high levels of the proteins. The increase in deposition of fibronectin fibrils, **C2,** around the cell suggests an increase in matrix deposition around these cells.

The change in morphology of HBEC-T cells suggests that TG2 possibly plays a role in inducing cell matrix reorganization leading to EMT. As observed previously in chapter 3, elevated levels of TG2 in IB3 cells is associated with an increase in matrix protein expression notably fibronectin. Hence, the implication is that TG2 expression leads to an elevation of EMT marker expression and a change in the matrix deposition. Consequently, in the HBEC-T cell, elevation in TG2, which was shown by the co-localisation of fluorescent GFP and TG2 protein (Figure 5.10) accounts for the increase in fibronectin expression and deposition. Thus Figure 5.10C shows the matrix proteins that might be involved in EMT and the effect of matrix reorganisation after elevation of TG2 expression takes place. Further experiments need to be performed with HBEC transduced with empty vector as control to verify the results.

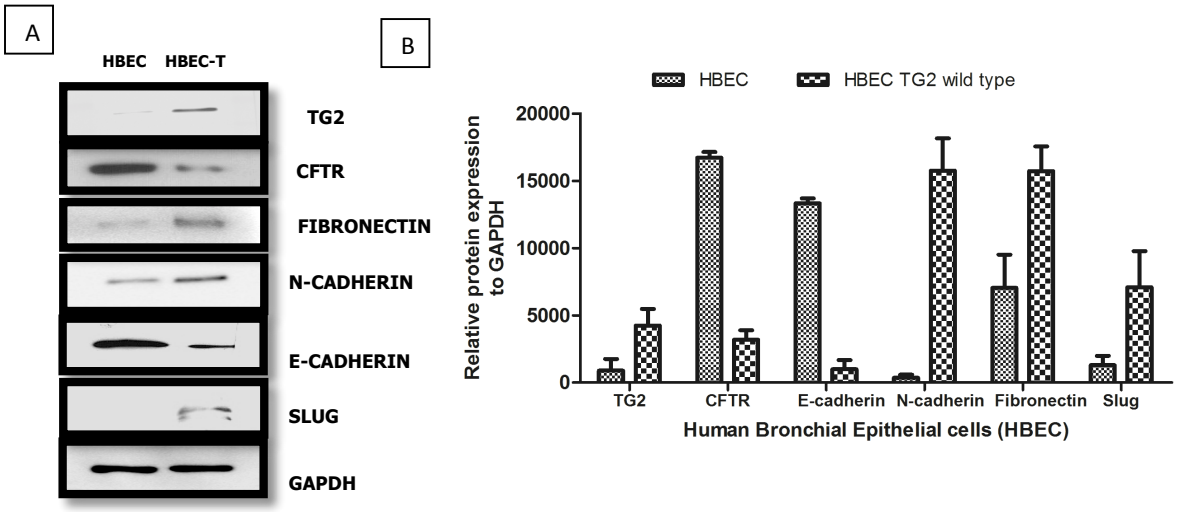

Figure 5.11A&B: Down regulation of CFTR and EMT markers corresponds to the elevation of TG2 after TG2 transduction. Western blots, **A**, of HBEC cells transduced with TG2-WT, HBEC-T, cultured in submerged medium. 50µg of protein was used for the Western blot assay. Monoclonal mouse anti-TG2, anti-CFTR, anti-*Slug*, anti-N&E-cadherin antibodies as well as polyclonal rabbit anti-fibronectin antibody (1:1000) were used to probe blots. GAPDH was used to normalise protein loading. Western blot represents 2 independent experiments with equal numbers of cells used at all times. **B.** Densitometry shows the mean values of 2 independent experiments normalised to GAPDH. Results indicate that an elevation of TG2 protein levels (HBEC-T) results in a decrease in CFTR and E-cadherin expression. However, fibronectin, N-cadherin and *Slug* expression was shown to be elevated.

These results show that an increase in TG2 expression down regulates CFTR and E-cadherin expression whilst increasing fibronectin, N-cadherin and *Slug* expression. This importantly points to the study by Snodgrass *et al*. (2013) which shows the

inhibition of CFTR protein expression by TGFβ1. In addition, regarding EMT, it was once more observed that HBEC-T cells have marginal expression of E-cadherin. This observation demonstrates that as TG2 levels increase and more matrix proteins are deposited, a consequent crosslinking and stabilisation of these proteins leads to matrix reorganisation with the loss of cell junctions as well as an increase in cell migration. Hence, cells assume the mesenchymal phenotype. It can be inferred here that since TGFβ1 levels increases in HBEC-T cells (results not shown) and CFTR is down regulated and Figure 5.11 shows that elevated TG2 down regulates CFTR, it can be suggested that TG2 via TGFβ1 regulates CFTR in a negative manner.

5.5 Discussion

The versatility of TG2 as an intracellular and extracellular protein together with its pro-fibrotic traits depicts the robust innate role it plays in various disease processes. Here, this study shows that the intricate developments preceding the initiation of fibrosis in CF can be construed to intrinsically involve a need for consistently elevated levels of TG2. This in turn drives the activation of other pro-fibrotic proteins, notably TGFβ1 while TG2 transient knockdown by siRNA or stable knockdown with shRNA reverses the EMT process. Consequently, these results postulate that the outcome of this knockdown might be related to a regain of cell-cell contact.

Considering the results observed in chapter 4 where elevated TG2 correlated with an increase in TGFβ1 level and the use of cell-permeable and impermeable TG2 inhibitors demonstrated a comparable effect of TG2 inhibition on fibronectin, N-cadherin, E-cadherin and *Slug* expression, the focus here was then centred on TG2 knockdown and its effects on EMT marker expression. Results showed that by transiently knocking down TG2, N-cadherin expression was inhibited (Figure 5.3). However, TG2 siRNA #1,5 and #7 showed marginal TG2 inhibition, both TG2 siRNA #1 and 6 demonstrated significant inhibition of N-cadherin expression. This differs with all siRNAs inhibiting TG2 activity (Figure. 5.4). Verma *et al*. (2008) showed that in pancreatic cancer cells, silencing TG2 with siRNA reduces metastatic cell invasion, which might have therapeutic implications. In continuance, TG2 shRNA was transduced into IB3 cells in order to produce stable knockdown cell lines with reproducibility of similar traits. The TG2 knockdown further confirmed TG2 involvement in EMT with the knockdown producing a markedly significant inhibition of fibronectin, N-cadherin and *Slug* protein expression compared to scrambled shRNA and untreated. The reduction of TGFβ1 levels showed again the involvement of TG2 in the activation of TGFβ1 in these cells. This confirms the link between TG2 and EMT where inhibition of its transamidating activity is comparable to the reversal of cell mesenchymal transition. Park *et al.,* (2013) described the relationship between TG2 and N-cadherin expression in EMT using A549 lung cancer cells. It was observed that silencing of TG2 using shRNA or elevation of TG2 via TG2-wild type plasmid down-regulated or increased TG2 expression respectively, thus suppressing or supporting EMT progression in this cell.

On establishing this involvement of TG2 in EMT, it became imperative to dissect out the mechanism by which TG2 carried out this function. Using different mutational variants of TG2 virally transduced into the control CF “add-back” cell, C38, TG2 function was investigated. The results show that in the presence of TG-WT plasmid, TG2 protein expression was significantly increased compared to untreated control. This increase corresponded with the increase in fibronectin, N-cadherin and *Slug* expression as well as an increase in transamidating activity (Figure 5.8). This justifies previous results in chapter three and four where elevated TG2 protein expression in IB3 cells was shown to correlate with increased TG2 activity. On further evaluating other TG2 variants, it was observed that W241A, which is devoid of transamidating activity, showed no changes to the phenotype. However, R580A, the GTP binding mutant with transamidating activity drove epithelial cells into EMT with an increase in fibronectin, N-cadherin and *Slug* as well as an increase in TG2 protein expression and activity (Figure 5.8 & 5.9). Against the observations by Kumar *et al.,* (2010), these results suggest that GTP binding might not be involved in TG2 dependent increase in EMT marker expression in IB3 cells. This together shows that in the presence of TG2 transamidation deficient mutant, W241A, the abrogation of TG2 activity mimics the inhibition observed with TG2 inhibitors. Hence, it can be suggested here that the transamidation activity of TG2 might be important in the pathological functioning of the enzyme in CF cells.

Using HBEC primary epithelial cells transduced with TG WT plasmid, results show a morphological change in transduced cells with the loss of the cobblestone-like structure, assuming a fibroblast-like morphology similar to an elevation of TGFβ1. Furthermore, this change in morphology was accompanied with an elevation of TG2, fibronectin, N-cadherin and *Slug* protein expression. On staining HBEC for fibronectin, it was observed that an increase in fibronectin deposition occurred around the cell indicating an up regulation of expression, which can be linked to elevated TG2 expression. On investigating the effect of active TG2 elevation in HBEC-T cells on E-cadherin and CFTR protein expression, the level were shown to be reduced probably due to enhanced levels of TGFβ1 hence driving the progression of EMT. Although Snodgrass *et al.* (2013) indicated that TGFβ1 negatively regulated CFTR, the results here suggest that the effect seen with TGFβ1 might be due to its activation by TG2. These results are preliminary findings and further studies might delineate the proposed mechanism.

5.6 Conclusion:

This study has for the first time defined the role and mechanism by which knockdown of active elevated TG2 levels in CF could abolish the progression of fibrosis and conversely showed that an elevation of TG2 drives the increase in fibronectin, N-cadherin and *Slug* whilst abolishing E-cadherin and CFTR expression. This leads to the conclusion that TG2 might be playing a major role in the progression of the EMT process in CF cells and its inhibition/knockdown might be a useful therapeutic tool in treating diseases where it has been implicated. However, further studies need to be carried out in *in vivo* or “near physiological conditions” to show whether these results can be translated to biological systems.

Chapter 6

A comparative study of TG2 and EMT marker expression in an *in vitro* pseudo-stratified model at ALI

6.1 Introduction:

Amongst the 6 classes of CFTR mutations, over 1900 mutations of the disease have been shown to exist which centres on the functionality of the channel (Bobadilla *et al*., 2002). The phenotypic variation between the mutants alters from high sodium in sweat, chronic pulmonary disease, pancreatic insufficiency and infertility amongst both sexes (all associated with classes I and II) to specific phenotypes associated with certain mutations i.e. pancreatic sufficiency (class IV and V) (Levy *et al*., 2010, de Gracia *et al*., 2005). However, the symptoms associated with these phenotypes are worsened in heterozygote patients carrying class I-II mutations in which the other allele is either a class IV or V mutation. Such patients have lower survival rates. The most common alteration which accounts for 70% of the worldwide mutational variants was described by Kerem *et al.* (1989) and is the loss of 3 base pairs on exon 10 of the gene coding for CFTR, resulting in the absence at position 508 of the amino acid, phenylalanine, thus inducing a processing defect. Although there exists a vast heterogeneity of mutations, studies have attempted to define the peculiarity of each mutant, which ultimately guides research approaches towards therapeutic outcomes.

Recent studies have been evaluating lead chemical compounds for “protein repair therapy”, aimed at repairing production, processing, regulation and conductance mutations and ultimately focuses on ensuring CFTR channel trafficking to the apical membrane and its functionality *in situ* (MacDonald *et al.*, 2007). From the early successes of the aminoglycoside, tobramycin and the recombinant human deoxyribonuclease, Dornase alfa, a premature termination codon (PTC) modulator and an enzyme that cleaves extracellular DNA reducing sputum viscosity respectively, researchers have explored other lead compounds, which are now targeted at maturation/processional and regulation defects (Konstan and Ratjen, 2012, Chuchalin *et al*., 2009, Altamura *et al*., 2013, Lai *et al*., 2004). Hence, Ivacaftor (VX-770), a CFTR channel “potentiator” has demonstrated therapeutic success as it has been shown to be capable of increasing the gating activity of CFTR in patients with G551D mutation (Ramsey *et al*., 2011b, Accurso *et al*., 2010, Van Goor *et al*., 2009). Other channel modifiers include ataluren (PTC124), an orally bioavailable compound used in the treatment of Duchenne muscular dystrophy (DMD) and CF where its capable of inducing ribosomes to read through nonsense stop mutations (Kerem *et al*., 2008) and lumecaftor (VX-880), another bioavailable CFTR “corrector” aimed at selectively correcting the ΔF508 mutation (Kerem *et al.*, 2008, Van Goor *et al*., 2011, Clancy *et al*., 2012). In the UK, Ivacaftor is currently available as an orally bioavailable tablet for

people with G551D mutation of 6 years and older. Lumecaftor is currently on clinical trials in combination with Ivacaftor for people homozygous or heterozygous for the ΔF508 mutation (Rowe and Verkman, 2013, Boyle *et al*., 2014). These compounds and other CFTR therapeutic agents in the pipeline demonstrate the advancement made in CF therapy and the impact on the quality of life (QOL) and life expectancy (Ashlock and Olson, 2011). Therefore, the forward approach would be to target CFTR mutational correction by using combination therapy, which synergistically or additively can enhance CFTR trafficking and conductance.

The use of TG2 inhibitors as therapeutic targets have increased the possibility of better prognosis in various diseases e.g. chronic kidney disease (Johnson *et al.*, 2007) and neurodegenerative diseases (Ruan and Johnson, 2007). Recently, TG2 has been implicated in the hyper-inflammatory responses typical to CF. Maiuri *et al.* (2008) described how in CF cells defective CFTR up-regulates intracellular TG2 activity that down regulates expression of the anti-inflammatory peroxisome proliferated activated receptor gamma (PPAR-γ). This was related to increased TG2-SUMOylation, which reduces ubiquitination and prevents TG2 degradation. Sustained intracellular TG2 activity may therefore provide the link between increased inflammation and defective CFTR.

Elevated TG2 levels were further shown to lead to defective beclin-1 mediated autophagy, a cell regulated process in which lysozymes degrade unwanted or dysfunctional cellular components. This was shown to be counteracted using TG2 inhibitors as proteostasis regulators. This was illustrated to restore ΔF508 mutation stability prior to treating with CFTR potentiators, which maintain protein homeostasis whilst synergistically regulating CFTR channel maturation and trafficking to the apical surface ie VX-770, VX-532 (Luciani *et al*., 2010a, Luciani *et al.*, 2012).

The recurring conundrum in respiratory cell biology revolves around the development of robust representative tissue or cell systems that depicts inherent physiological conditions with flexibility of replication and maintenance of intricate respiratory traits. Studies continue to be sought to occlude this lacuna, which bridges the transfer of observable outcomes from research in *in-vitro* systems to outcomes in normal human physiological conditions.

In respiratory medicine, the normal statutory lung milieu maintains cellular and matrix integrity and maintains tissue repair following insult caused by airborne particles and other injurious agents. Consequently, it is imperative to discern the mechanism through which this reparative process tips over into remodelling and fibrosis and develop

methods to abrogate faults in repair which ultimately leads to disease progression (Berube *et al.*, 2010). The use of animal models, *in vitro* and *ex vivo* systems illustrates the need to undertake research within models that are easy to use, reproduce and maintain certain basic characteristics (Balharry *et al.*, 2008, Coffman and Hessel, 2005). To this end, animal models have been widely used as their size negates the laborious use of large population for drug toxicology studies, low acquisition cost and provides direct evidence of transferable traits observed in *in-vitro* cell systems (Berube *et al.*, 2010). However, the lack of not mimicking human respiratory systems wholly in certain conditions opposes their use.

Traditional 2-D cell culturing remains the resolute method used in culturing airway epithelial cells. This allows for culturing cells under submerged conditions in petri dishes or flasks with the ease of manipulation and allowing the cells to proliferate in single monolayers whilst changing medium (Yankaskas *et al.,* 1985). Its also helps carrying out rapid, reproducible and rather simple experiments with the use of immortalised transformed or primary epithelial cells. However, with airway epithelial cells, a distortion of native cellular milieu by their removal from their native environment induces complex changes in the cells (Griffith and Swartz, 2006). Although, these 2D systems are robust, these changes have to be compensated for by developing models recreating the original native environment. Noteworthy of mentioning is the loss of tight junctions and polarity in 2-D systems. The importance of these tight junctions is depicted by their ability to control movement of ions and solute across the cell-matrix bed. Carterson *et al.* (2005) described whilst culturing A549 human lung epithelial cells on both cell culture flasks and Rotating Wall Vessel (RWV) bioreactors that cell polarity and tight junction was lower in 2-D submerged cultures than 3-D cultures and this impacts on the response of the cells to *Pseudomonas aeruginosa,* where infected submerged cells detached from their culture beds more easily than 3-D cultures.

The elaborate airway epithelial traits shown by cells cultured at Air-Liquid Interface (ALI) recapitulate the salient phenotypic characteristics in comparison to submerged cultures. The ALI structure presents airway epithelial cells in culture inserts with micronized pore membranes coated (e.g. with collagen IV), upon which cells are cultured. The inserts are placed in companion plates with basal medium from which the cells feed. Grainger *et al.,* (2006) showed in a comparative study using Calu-3 cells cultured in liquid covered culture (LCC) and at ALI that aside from the elevated trans-epithelial-electrical resistance (TEER) measured in ALI compared to LLC, the expression level of zona occludens 1 (ZO-1), a tight junction protein, was raised in ALI thus indicating that cells cultured at ALI assume a morphological status representative of airway epithelium. This thus brings to the fore the studies by Gruenert *et al*. (1995)

that described the culturing of airway epithelial cells at ALI to generate increased cilia, serous cell differentiation and mucus production under appropriate conditions as mentioned by Robinson and Wu. (1993), which includes appropriate medium, substrate (e.g. collagen IV) and exposure to air. This supports the growth of cells in a pseudo-stratified structure with exchange of cellular waste and nutrients across membrane.

In the preceding chapters using IB3 as the CF cell and the corrected "add-back " cell, C38 and human primary bronchial epithelial cell, HBEC, studies were carried out exclusively in submerged medium. The phenotypes in these cells were characterised under different conditions and treatments. This chapter attempts to undertake crucial experiments in an effort to recapture the phenotypes under ALI conditions. This would be confirmatory supporting our earlier results and prognosis. In addition, using cell-permeable and cell impermeable TG2 inhibitors as well as CFTR correctors and potentiators, an attempt is made to combine these compounds together in other to determine the effect of TG2 inhibition and CFTR correction on CFTR Cl^- channel rescue and via ion conductivity, thus directly examining the link between TG2 activity and CFTR functionality.

6.2 Aims:

This chapter is aimed at repeating the definitive experiments carried out in submerged medium, using the same cells but here cultured at ALI. Also, the study is aimed at showing the effect of combinational therapy involving TG2 inhibition on CFTR trafficking and conductivity. Here, IB3, C38, IB3-shRNA, HBEC and HBEC-T cells would be cultured in Transwells® at ALI for at least 28 days. During this period:

- TEER readings will be taken aimed at determining cell-cell tightness and barrier integrity.
- The effect of TG2 protein knockdown and TG2 up regulation on TG2 activity, TGFβ1 activity and TEER maintenance will be determined.
- Using immunofluorescent staining, the expression and localisation of EMT markers relative to TG2 protein in TG2 knockdown cells will be determined.
- Following pre-treatment of IB3 cells with TG2 inhibitors and CFTR correctors/inhibitors, determine CFTR maturation and trafficking using Western blot analysis of membrane fractions.
- Determine Cl^- conductance through mature CFTR channels using the Cl^- sensitive indicator, MQAE.

6.3 Methods:

6.3.1 Culturing of airway epithelial cells using the ALI model

3 x 10^4 of IB3, C38 or HBEC in 300µl of AEM were seeded on Transwell® insert membranes of 0.33cm^2 area and 0.4µm pore size, previously coated with 33 µl of 100µg/ml human placental Collagen IV in 3%(v/v) acetic acid. These inserts were placed in companion plates with 600µl of medium in basal compartment. The cells were cultured as described in chapter 2.2.1.4. TEER was measured in cells after culturing for 14 days, using a voltohmmeter as described in chapter 2.2.1.5.

6.3.2 Western blots of lysates of IB3, C38 and HBEC and their transduced variants

The cells cultured on inserts were gently rinsed twice with 1x PBS, pH 7.4, removed from companion plates and placed on dry tissue paper. Using a sterile scalpel, the membrane was cut out carefully and placed into pre-cooled eppendorf tubes with lysis buffer and lysed as described in chapter 2.2.2.2. The lysates were dissolved in sample buffer and loaded onto 6%(w/v), 8%(w/v) or 12%(w/v) polyacrylamide gels for SDS/PAGE as described in chapter 2.2.3. The percentage of acrylamide used was altered in order to get effective separation of the proteins different proteins to be detected ie fibronectin and N-cadherin [6%(w/v)], TG2 [8%(w/v)] and *Slug* [12%(w/v)]. Western blotting was carried out on the separated proteins as described in chapter 2.2.4. The membrane was stained with specific primary antibodies (1:1000) i.e. anti-TG2, anti-fibronectin, anti-N-cadherin, anti-*Slug*, anti-CFTR, anti-E-cadherin and anti-GAPDH (used as loading control).

6.3.3 Immunocytochemistry of cells cultured at ALI

After 28 days at ALI, the membranes were carefully cut out of the inserts and placed with cells uppermost in 12-well plates. Using, 200µl of 1x PBS, pH 7.4 cells were rinsed twice. Immunocytochemistry was carried out as described in chapter 2.2.16.1 using 150µl primary antibody (Ab) (1:100) in complete medium ie anti-TG2, anti-fibronectin, anti-N-cadherin or anti-CFTR followed by 200µl of either Fluorescein isothiocyanate,

FITC (green) or Tetramethylrhodamine, TRITC (red) conjugated secondary antibody (1:200).

6.3.4 TG2 activity of whole cell lysates of IB3, C38, HBEC and their transduced variants using the Biotin cadaverine incorporation assay

The TG2 activity assay was carried out on protein lysates of IB3, IB3-shRNA, C38, HBEC and HBEC-TG epithelial cells cultured in AEM. Initially, cells were cultured at ALI as described in chapter 2.2.1.4. The cells were carefully rinsed in 1x PBS, pH 7.4 twice. The membrane was cut out cells were lysed as described in chapter 2.2.2.2 and protein content quantified. The activity assay was carried out on 96-well plates pre-coated with fibronectin (5µg/ml) using 50µg of cell lysate protein per well as described in chapter 2.2.6.1.

6.3.4 Determination of plasma membrane proteins in IB3 cells using membrane fractionation

6.3.4.1: Submerged culture

5 x 10^5 of IB3 cells were sub cultured into 60mm petri dishes and allowed to attach for 4 h. Medium was discarded and replaced with treated medium containing VX-809 (Selleckchem®) (10µM), R283 (500µM), a combination of VX-809 and R283 or with DMSO (1:1000) as a control. The cells were cultured for 72 h with medium changed every 24 h. Cells were washed with ice cold 1x PBS, p.H 7.4 twice and membrane fractionation was carried out as described in chapter 2.2.17.1. Western blotting was carried out on membrane fractions as described in section 2.2.4.

6.3.4.2: ALI culture

3 x 10^4 of IB3 cells were sub-cultured into 0.33µm Transwell® insert membranes coated with collagen IV as described in chapter 2.2.1.4. The cells were allowed to attach for 6-8 h. The medium was removed from Transwell® inserts (i.e. apically) as well as in the companion plates (i.e. basally). 300µl of complete medium was inserted into the Transwell® inserts with 600µl added to the companion plates. Medium was supplemented with VX-809 (10µM), R283 (500µM), a combination of VX- 809 and R283 or with DMSO as vehicle control (1:1000). Basal medium was changed daily for

the first 4 days i.e. This is the time required to attain relevant physiological features typical of ALI cultures. The cells were cultured as described in chapter 2.2.1.4 supplementing medium with chemical compounds. Membrane fractionation was carried out on lysates as described in chapter 2.2.17.2. and Western blotting carried out on membrane fractions as described in chapter 2.2.4.

6.3.5 Chloride channel activity assay in IB3 cells in the presence of a chloride sensitive indicator, MQAE

1 x 10^5 IB3 cells were sub cultured into 100µl in 96-well plates and allowed to attach for 6 h. The medium was changed and replaced with medium supplemented with TG2 inhibitors with or without the CFTR corrector, VX-809 (10µM). The TG2 inhibitors used were R283 (500µM) and cystamine (250 µM). In order to load the cells with a chloride sensitive indicator, 10 mM MQAE in medium was added at 100µl/well according to the previously published method (West and Molloy, 1996) and cells were incubated at 37^{o}C for 16-18 h. The chloride conductance assay was then carried out as described in chapter 2.2.18.

6.4 Results:

6.4.1 EMT marker and TG2 expression in CF cells cultured at ALI mimics expression in submerged culture:

6.4.1.1: TG2, fibronectin and N-cadherin protein expression in IB3 and C38 cells is unchanged at ALI.

As earlier described, the ALI model attempts to mimic *in vivo* physiological conditions with cells assuming the pseudo-stratified ultrastructure seen in the lungs. Studies have confirmed that this model produces airway epithelial cells showing electrical resistance, increased ciliogenesis and mucus production consistent with the airways *in-vivo* and the features required for maintaining the integrity of the airways (Grainger *et al.*, 2006). Here, in concert with the results shown in chapter 3 and 4, an attempt is made to determine the expression of TG2 and EMT markers in IB3 and C38 cells cultured at ALI. The cells were cultured and Western blotting was performed as described in chapter 2.2.1.4 and 2.2.4 respectively. TEER was measured every other day to observe and estimate the appropriate epithelial resistance for cells to be harvested. Preliminary results have shown that from the 28th day (4 days in submerged and 24 days at ALI) cells attain TEER values of ≥300Ω cm^2, which was appropriate for the experiments (data not shown). Figure 6.1 shows Western blot analysis of TG2, fibronectin and N-cadherin expression by IB3 and C38 cells after 28 days at ALI. Here, TG2 and N-cadherin expression in IB3 cells were higher than C38 cells at ALI. Also, the expression of fibronectin was higher in IB3 cells compared with C38 cells. Previous studies have shown that the presence of collagen IV does not alter the protein expression of TG2 in these cells (results not shown). This was proven as TG2 levels were observed to be diminished in C38 cells compared to IB3 cells. This observation supports earlier results from submerged culture where expression patterns of TG2 and EMT markers were similar to that in ALI conditions (Figure 3.2 and 4.3).

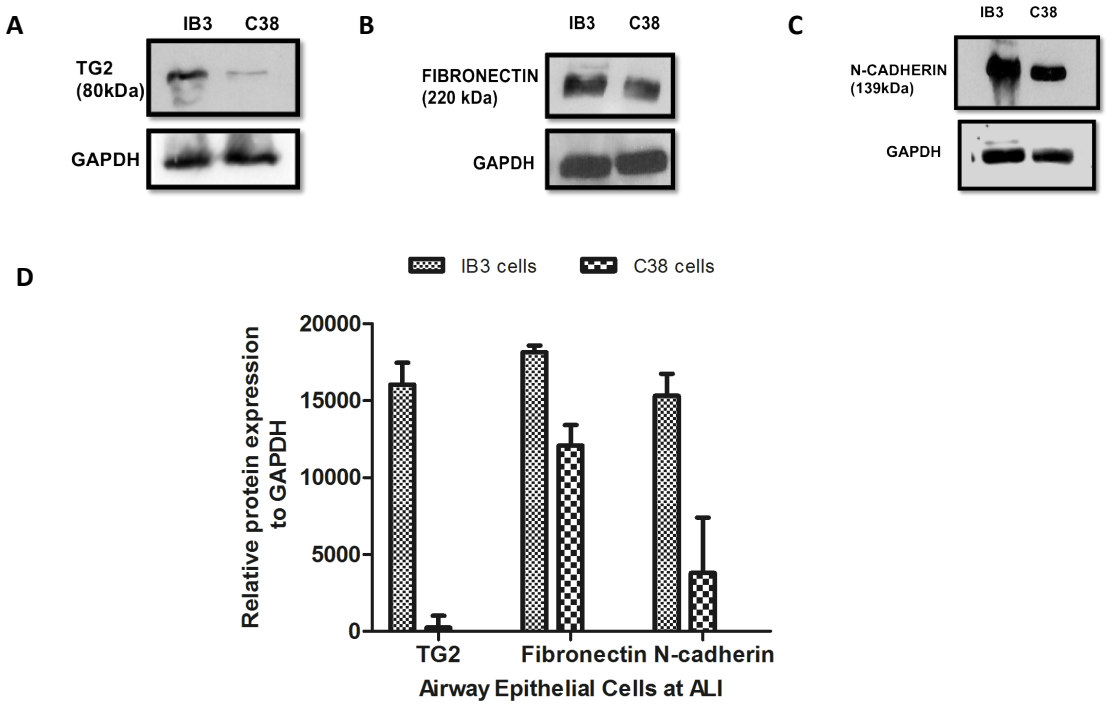

Figure 6.1A,B,C&D: Elevated TG2 and EMT marker expression in CF cells cultured at ALI corresponds with expression in submerged conditions. Western blots TG2, **A** fibronectin, **B** and N-cadherin, **C** expression in IB3 and C38 cells cultured at ALI. Cells were cultured for 28 days. 50µg of protein was used for the Western blot assay. Membranes were probed with monoclonal anti-TG2 and anti N-cadherin or polyclonal anti-fibronectin antibodies. GAPDH was used as the loading control to normalize protein expression. Densitometry, **D**, represents mean values of 2 independent experiments. Blot images represent a characteristic blot of 2 independent experiments with equal number of cells used at all times. Results show higher TG2 and N-cadherin expression in IB3 cells more than C38 cells. Fibronectin expression in IB3 cells was shown to be slightly higher than in C38 cells. The results observed above of TG2 and EMT markers expressed in IB3 and C38 cells show similarity with results observed in submerged cultures.

6.4.1.2: TG2 co-localises with N-cadherin and fibronectin in CF cells at ALI.

In previous chapters, the interaction between TG2 and EMT markers has been shown only in submerged culture. The results in Figure 6.1 suggest that protein expression of TG2 correlates to that of EMT markers in the ALI model in the same manner as was shown for submerged cultures. Here, emphasis has been made on determining the localisation of TG2 relative to that of the EMT markers when cultured at ALI. Figure 6.2 shows that TG2, N-cadherin and fibronectin expression in IB3 cells was higher than in C38 cells and that these were co-localised. In IB3 cells, fibronectin and N-cadherin

were expressed consistently around the cell membrane with distinct expression within the extracellular matrix. Very little fibrous fibronectin was found around the periphery of C38 cells. Together, the results show that with respect to cells cultured in submerged models, TG2 and EMT markers are expressed to similar levels in ALI culture for both cell types.

A

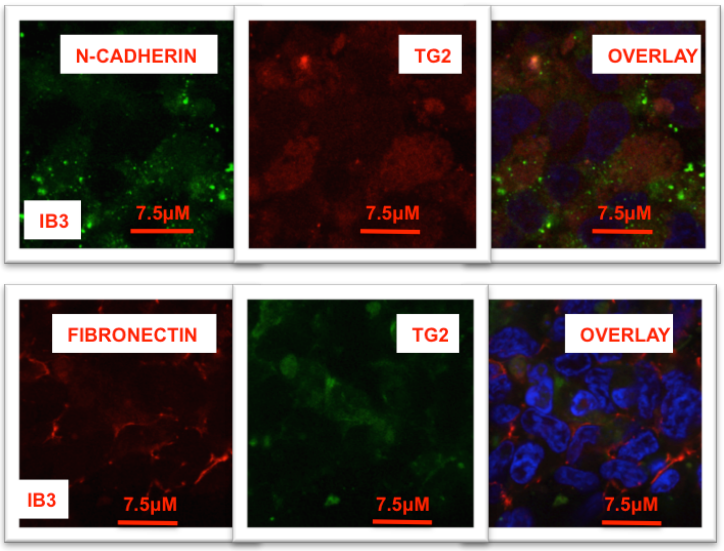

B

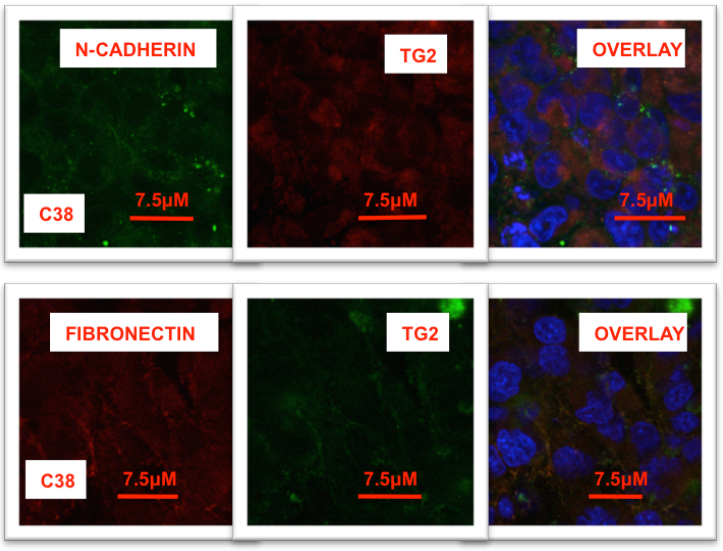

Figure 6.2A&B: TG2 co-localises with fibronectin and N-cadherin in IB3 and C38 cells at ALI. Immunofluorescent images showing the expression of TG2, fibronectin and N-cadherin in IB3, **A,** and C38, **B,** cells cultured at ALI. Polyclonal rabbit anti-TG2 and anti-fibronectin or monoclonal mouse anti-N-cadherin antibodies were used to stain cells with TRITC (red) or FITC (green), used as secondary conjugated antibody. Images are representative of 2 independent experiments carried out under comparable conditions. Mouse and Rabbit IgG were used as control (Figure 4.4). DAPI was used to stain nuclei. Images were visualised on the Leica® SP5 confocal microscope. Scale bar represents 7.5μm. Results show TG2 co-localising with fibronectin and N-cadherin in IB3 cells and C38 cells. However, the expression of TG2 and EMT markers were higher in IB3 cells than C38 cells.

6.4.2: TG2 inhibitors abrogate TG2 activity in CF cells cultured at ALI.

As previously observed from Figure 3.5, TG2 inhibitors play a major role in abrogating TG2 activity thus impeding the progression of EMT. Furthermore, it was observed that TG2 inhibitors inhibit TGFβ1 secretion and activity in IB3 cells cultured in submerged culture (Figure 3.6D) as well as blocking the effect of elevated TG2 in C38 cells treated with rTGFβ1, thus impeding an increase in EMT marker expression as shown in HBEC (Figure 4.9). Importantly, these results illustrate the link between TG2 and EMT with TGFβ1 playing a vital role in the process. Here, an attempt is made to use the cell-permeable and cell impermeable TG2 inhibitors, R283 and R281 respectively, to abolish TG2 activity in cells cultured at ALI. The cells were cultured in the presence of R283 and R281 (500μM each) basally for 28 days at ALI before lysis. The cell lysates were used in the TG2 activity assay to determine total cell TG2 activity measured by the incorporation of biotinylated cadaverine into fibronectin by TG2. The results show a 3-fold increase in total TG2 activity in untreated IB3 cells compared to C38 cells. It was demonstrated (Figure 6.3) that the presence of R283 and R281 completely abolished TG2 activity in both cell lines with a decrease in TG2 activity in R283 and R281 treated IB3 cells compared to negative control (with 10mM EDTA not shown). It was also observed that C38 cells showed little or no TG2 activity compared to IB3 cells, in agreement with data from submerged culture. This is in concert with the TG2 expression observed with the Western blots conducted and data from submerged culture (Figure 3.5) where R283 was shown to inhibit TG2 activity both in lysates and at the cell surface. It can be deduced here that culture at ALI maintains the characteristics of each cell type with IB3 cells retaining their high TG2 activity and C38 cells showing marginal TG2 activity, which suggests that normal airway epithelial cells have little or no TG2 expression or activity and the ALI model is a useful model depicting *in vivo* conditions. Also due to the non-differential inhibition of TG2 activity by TG2 cell-permeable and impermeable inhibitors, it can be hypothesised that cell surface TG2 might be playing a role in the mechanism that induces promotion of EMT in IB3 cells.

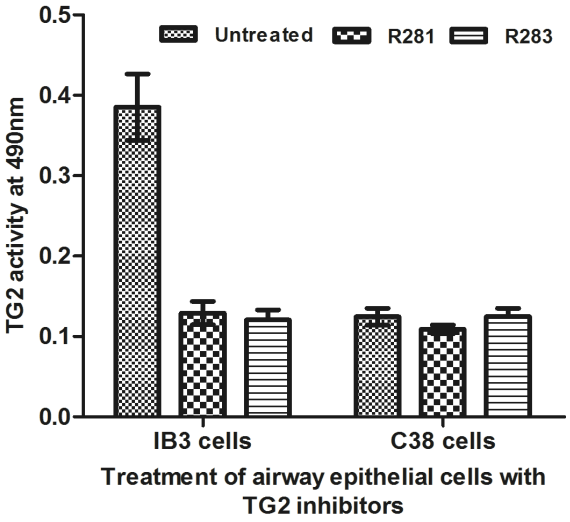

Figure 6.3: Cell permeable and impermeable TG2 inhibitors in IB3 cells at ALI inhibit TG2 activity. Biotin cadaverine TG2 activity assay was carried out on lysates of IB3 and C38 cells cultured at ALI under control conditions (no inhibitors) and in the presence of cell-permeable and cell impermeable TG2 inhibitors, R283 (500μM) and R281 (500μM) respectively. Results represent mean and standard deviation values of 2 independent experiments. Results show high TG2 basal activity in IB3 cells (untreated), which was inhibited by R283 and R281 equally. C38 cells showed marginal TG2 activity under control conditions (untreated) with little effect observed in the presence of either TG2 inhibitor.

6.4.3: Knockdown of TG2 restores airway integrity in a reparative manner.

6.4.3.1: TG2 shRNA transduction abolishes TG2 induced EMT progression in the IB3 cell line.

The abrogation of TG2 activity as observed in section 6.2 has demonstrated that culturing IB3 and C38 cells at ALI retains vital characteristics of the cells in terms of differential TG2 activity. Studies have shown that TG2 levels are elevated in wound healing where cellular migration/ invasion holds a reparative role in collagen deposition and re-epithelialisation and that active cell surface TG2 activity is involved (Telci and Griffin, 2006, Verderio *et al.*, 2004). Here, the ALI model is used to evaluate how TG2 knockdown could reverse EMT in IB3 cells. Using IB3 cells transduced with TG2 shRNA as described in chapter 2.2.19.5, cells were cultured at ALI to observe the effect of TG2 knockdown in IB3 cells on EMT marker expression. The results suggest a lowering of TG2 expression in the IB3 cells transduced with TG2-shRNA. The link

between high TG2 expression and EMT was further illustrated by the decrease in fibronectin, N-cadherin and *Slug* expression in TG2-shRNA IB3 cells compared to wild type IB3 cells (Figure 6.4). This shows a possible interaction between TG2 and fibronectin expression, which studies have shown to be both RGD and RGD independent (Verderio *et al.*, 2003, Telci *et al.*, 2008) and TG2 and N-cadherin, a cadherin cell adhesion protein which TG2 has been shown to up regulate in EMT and whose expression illustrates EMT progression in epithelial cells (Park *et al*., 2013, Kim *et al*., 2000).

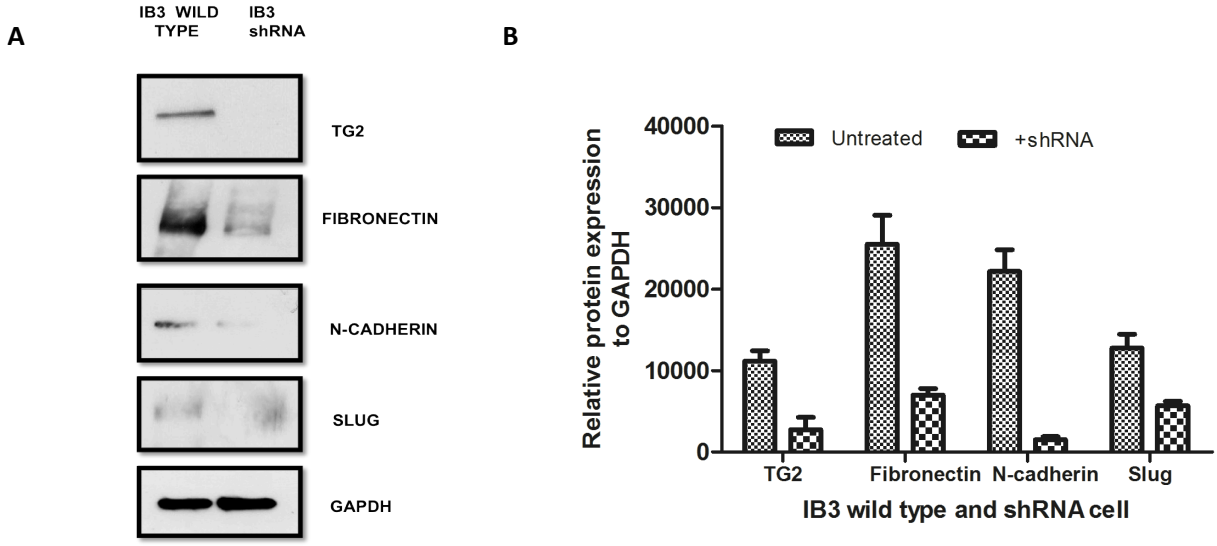

Figure 6.4 A&B: TG2 knockdown impedes fibronectin, N-cadherin and *Slug* expression in IB3 cells at ALI. Western blot analysis of fibronectin, N-cadherin and *Slug* expression in IB3 cells cultured at ALI and transduced with TG2 shRNA. IB3 cells were cultured at ALI for 28 days, within which cells were transduced. 50µg of protein was used for the Western blot assay. Monoclonal antibodies (anti-TG2, anti-N-cadherin and anti-*Slug*) and polyclonal anti-fibronectin antibody were used to probe blots. GAPDH was used to normalise protein loading. The blot image is characteristic of two independent repeats. Densitometry represents mean values of two independent experiments. Results show that as IB3 cells are transduced with TG2 shRNA, fibronectin, N-cadherin and *Slug* expression was inhibited.

6.4.4: Abrogation of TG2 activity restores tight junction cohesion

Previous experiments have shown that inhibition of TG2 activity reverses the progression of EMT as shown by reduced expression of EMT markers and also restores junction integrity with the up regulation of junction proteins i.e. adherin junction proteins like E-cadherin (Figure 5.9). Conversely, it was observed that an elevation of

TG2 expression and activity possibly reinstates the expression of EMT markers in airway epithelial cells (Figure 4.9 & 5.8). This suggests that TG2 might play a vital role in the regulation of EMT. Here, using the ALI model, abolishment of TG2 expression with TG2-shRNA is shown to inhibit TG2 activity. From the results in Figure 6.5, it was observed that in TG2 shRNA transduced cells, there was a reduction of TG2 activity in IB3 shRNA-transduced cells compared to wild type cells. This indicates referring back to Figure 6.3 that TG2 activity inhibited by TG2 inhibitors mimics the knockdown of TG2. This suggests that the effect observed might be solely related to the regulation of TG2 activity and hence implies that TG2 activity plays a vital role in promoting the expression of EMT markers.

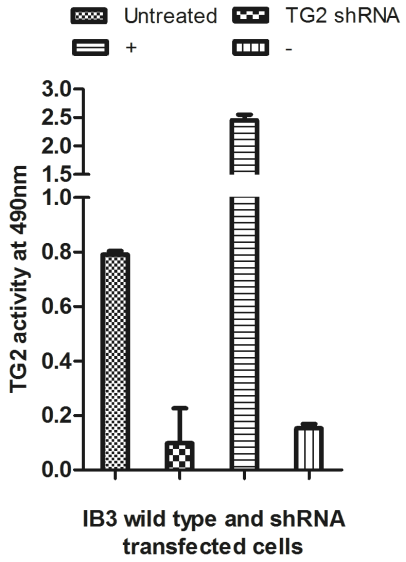

Figure 6.5: TG2 shRNA inhibits TG2 activity in IB3 cells cultured at ALI. TG2 activity in lysates of IB3 cells transduced with TG2 shRNA and cultured at ALI using the Biotin cadaverine assay. The cells were cultured at ALI for 28 days. 50μg of guinea pig liver TG2 (gplTG2) was used a positive control (+) with the substitution of calcium for 10 mM EDTA in the negative control (-). Results represent mean values of triplicates of two independent experiments. Results show that high TG2 activity in untreated IB3 cells is inhibited to marginal levels, compared to the negative control after transduction with TG2 shRNA.

Whilst demonstrating the importance of TG2 knockdown in abrogating EMT, it was hypothesised that the abolishment of TG2 activity, which ultimately impedes cell detachment and migration as well as matrix growth, should reestablish cell-cell adhesion thus restoring epithelial integrity. To demonstrate this, TEER of IB3 TG2 shRNA transduced cells cultured at ALI were measured.

Results show (Figure 6.6) a 2-fold increase in epithelial cell resistance in IB3 TG2 shRNA transduced cells compared to wild type cells, when cultured at ALI. The increase in electrical tightness, correlates with TG2 knockdown and inhibition of fibronectin, N-cadherin and *Slug* expression. However, C38 cells were observed to have similar TEER values to untreated IB3 cells. This might be due to the fact that C38 cells are "corrected" IB3 cells and so retain some phenotypes of IB3 cells. This illustrates that inhibiting TG2 can enhance electrical resistance in CF cells. Alongside, it can be postulated that abrogation of TG2-induced EMT, which is analogous to TG2 inhibition by TG2 inhibitors, restores epithelial cadherin and tight junction expression, thus restoring epithelial integrity.

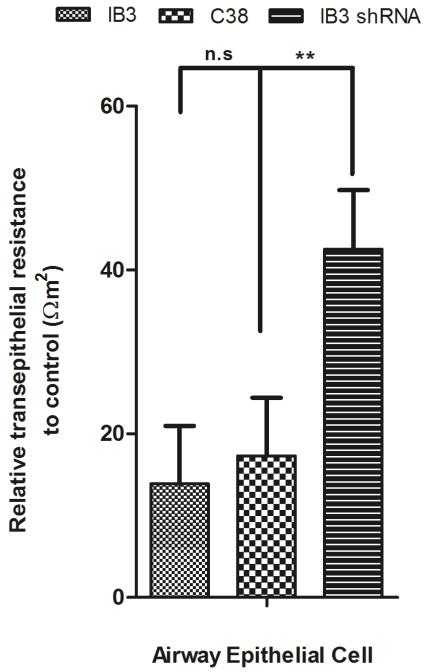

Figure 6.6: Epithelial "tightness" is restored in the presence of TG2 shRNA. TEER measurements of IB3, C38 and TG2 shRNA transduced IB3 cells cultured at ALI. The cells were cultured for 28 days at ALI. TEER measurements were carried out from 14 days at ALI. Resistance was measured on a voltohmmeter in ohms. Triplicate readings were carried out from each well. TEER values represent means and standard deviation from triplicates taken from 3 independent readings. Results show a significant increase in epithelial resistance in the presence of TG2 shRNA in IB3 transduced cells compared to untreated IB3 cells. C38 cells showed similar TEER values to untreated IB3 cells One-way Anova analysis with Bonferroni's Multiple comparison test: *$p<0.05$, **$p<0.01$, n.s. $p>0.05$.

The results presented here have shown that the TG2 expressional pattern in IB3 cells cultured at ALI correlates with that in submerged culture. These data also illustrate the link between TG2 knockdown, restoration of epithelial tightness and reversal of EMT

marker expression. To further support these findings, immunostaining to illustrate TG2 co-localisation with EMT markers at ALI was carried out with the aim of determining the effect of knockdown of TG2 *in situ* on expression of these proteins. Using IB3 cells transduced with TG2 shRNA, immunostaining was performed on cells cultured at ALI. Cells were cultured and immunocytochemistry was carried out as described in chapter 2.2.1.4 and 2.2.16.2 respectively. Results in Figure 6.7 depict TG2 and fibronectin localised outside the cells in both wildtype and TG2 shRNA transduced IB3 cells with DAPI staining the nucleus (blue). However, it was observed that expression was reduced in transduced cells compared to wild type with a reduction of the staining (TRITC-red) for both TG2 and fibronectin. This concurs with the Western blot results in Figure 6.4 where TG2 and fibronectin expression were reduced in transduced cells compared to wild type. Furthermore, this supports the hypothesis that TG2 regulates EMT progression in IB3 cells.

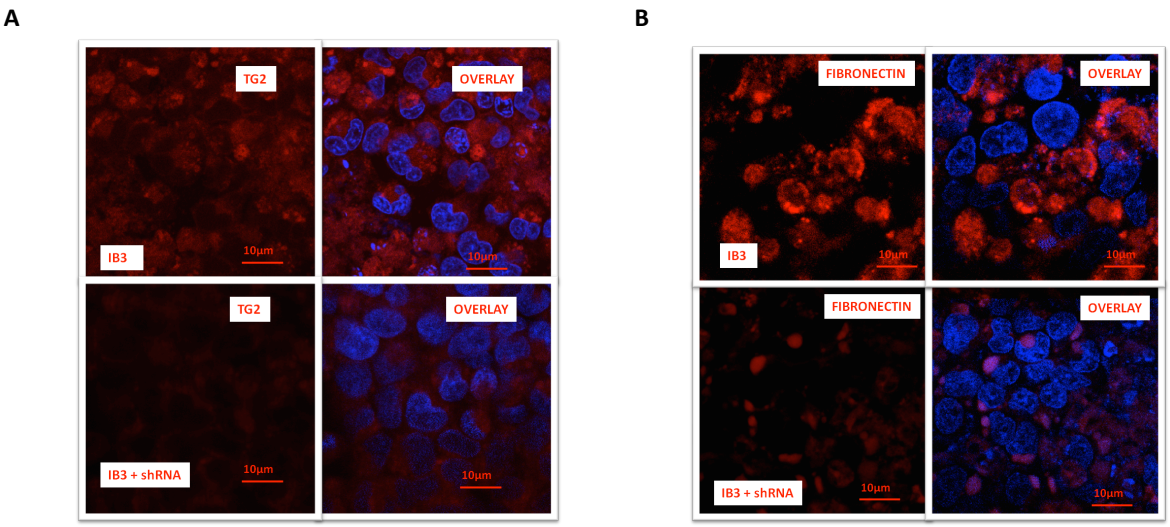

Figure 6.7A&B: TG2 shRNA reduces fibronectin expression by IB3 cells at ALI. Immunofluorescent confocal microscopy for TG2 (**A**) and fibronectin (**B**) in wild type IB3 cells (IB3) and in IB3 cells transduced with TG2 shRNA (IB3+ shRNA) cultured at ALI for 28 days. Polyclonal rabbit anti-TG2 and anti-fibronectin antibodies were used to stain cells. Images were taken using a Leica® SP5 confocal microscope. Mouse and Rabbit IgG were used as control (Figure 4.4). DAPI was used to stain nuclei. Images are representative of 2 independent experiments. Scale bar represents 10µm. Images show an inhibition of TG2 expression by TG2 shRNA indicating that blocking TG2 expression (with shRNA) reduces expression. Similarly, as TG2 expression was inhibited (in the presence of shRNA), fibronectin expression was reduced, **B.**

6.4.5: Up regulation of TG2 in HBEC cultured at ALI mimics the IB3 submerged phenotype.

Studies have suggested that whilst culturing primary bronchial epithelial cells at ALI, certain characteristic phenotypes of *in vivo* physiological airway can be recreated, which has aided research in understanding the potential mechanisms involved in airway pathologies (Stewart *et al.*, 2012). Albeit, because of the complexity of using this model and cost of primary cells, its use in this study has been limited to evaluating and confirming previous experiment carried out in submerged culture. Here TG2 wild type plasmid was transduced into human primary bronchial epithelial cells, HBEC, in order to observe whether an elevation of TG2 levels will induce or increase expression of EMT markers in the cell at ALI. HBEC (HBEC) and TG2 transduced cells (HBEC-T) were cultured at ALI for 28 days as previously described in chapter 2.2.1.4. Phase contrast images of the cells were captured using a Nikon camera mounted on a compound microscope. Figure 6.8 shows the cobblestone-like structures of HBEC cells with tight convoluted cell-cell adhesion compared to HBEC-T cells where cells have assumed a disoriented morphology and are seen to lose their adhesion and are rather migrating away from each other and assuming a morphology corresponding to an EMT phenotype. This relates with our observation in chapter four where HBEC were incubated with rTGFβ-1 protein and cells change their morphology with a decline in E-cadherin expression and an elevation of TG2, fibronectin and N-cadherin levels. Also this confirms the role of TG2 in the restoration of epithelial integrity in TG2 shRNA knockdown cells IB3 cells (Figure 6.4).

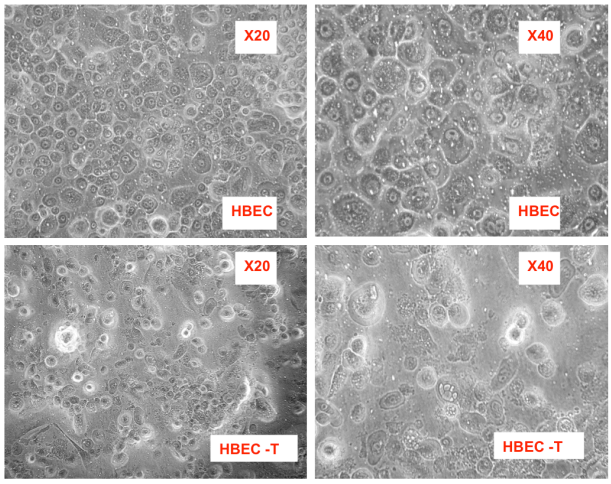

Figure 6.8: Up regulation of TG2 in HBEC alters epithelial morphology. Phase contrast images of untreated HBEC and TG2 transduced (HBEC-T) cells cultured at ALI. Cells were cultured for 28 days and images were taken *in situ* in Transwell® plates using a Nikon camera mounted on a microscope (magnification of x200 and x400 for left and right panels, respectively). Images are representative of 2 independent experiments. Images show a change in cell morphology from the characteristic epithelial cobblestone-like morphology in untreated HBEC to a disoriented fibroblast-like morphology seen in HBEC-T.

In furtherance to the observation of a change in cell morphology with TG2 wild type transduction, protein expression and immunostaining of the primary cells at ALI was carried out. The expression levels of TG2, fibronectin, N-cadherin and *Slug* were determined using Western blotting. The results again show that there is an increase in TG2 expression in HBEC-T cells compared to untreated HBEC and that this appears to associate with an increase in fibronectin and N-cadherin expression (Figure 6.9). The expression of *Slug* wasn't significantly different between untreated and transduced HBEC. TEER values were shown to slightly decrease in HBEC-T cells however, it was observed that values were higher than TEER in IB3 wild type cells cultured at ALI (Figure 6.6). These changes in EMT marker expression are in concert with the results in submerged culture but however show that although the cells might be going through EMT, the slight increase with *Slug* added to the decrease in TEER values in HBEC-T cells suggests that HBEC primary cells retain residual cell-cell adhesion compared to IB3 cells. This might be attributed to the inherent continuous feed back mechanism via TGFβ1 in IB3 cells, where TG2 remains elevated.

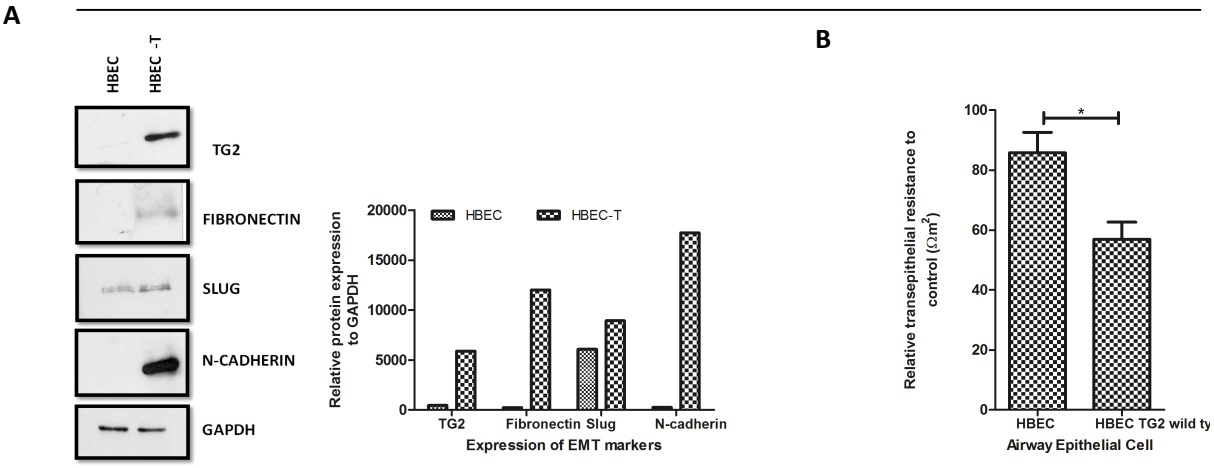

Figure 6.9A&B: Transduced TG2 protein expression in HBEC at ALI increases EMT marker expression and reduces TEER. Western blot, **A** analysis and TEER, **B** measurements for HBEC and HBEC-T cells cultured at ALI. The cells were cultured for 28 days during which TEER values were measured from the 14 days post ALI. 50µg of protein was used for the Western blot assay. Monoclonal (anti-TG2, anti-N-cadherin and anti-*Slug*) and polyclonal anti-fibronectin antibodies were used to probe blots. GAPDH was used to normalise protein loading. Densitometry represents protein expression normalised to GAPDH expression. TEER values represent the means of triplicate readings from 2 inserts at 3 different time points. Results show that an elevation of TG2 in HBEC-T cells induces an increase in fibronectin, N-cadherin and *Slug* expression. TEER values showed a reduction in resistance in untreated HBEC compared to HBEC-T cells.

Using immunostaining (Figure 6.10), it was apparent that elevated TG2 levels (green) found in HBEC-T cells were commensurate with raised fibronectin expression (red) (in agreement with observations from Western blots in Figure 6.9). Here, it was observed that deposits of fibronectin were distributed around the cells surface in concert with where TG2 was localised on the cell and across the cell matrix. Together, these suggest that elevation of TG2 expression in HBEC drives similar EMT marker expression to that observed in IB3 cells and supports the hypothesis that elevated TG2 levels increases the expression of fibronectin and N-cadherin and drives EMT in IB3 cells.

A

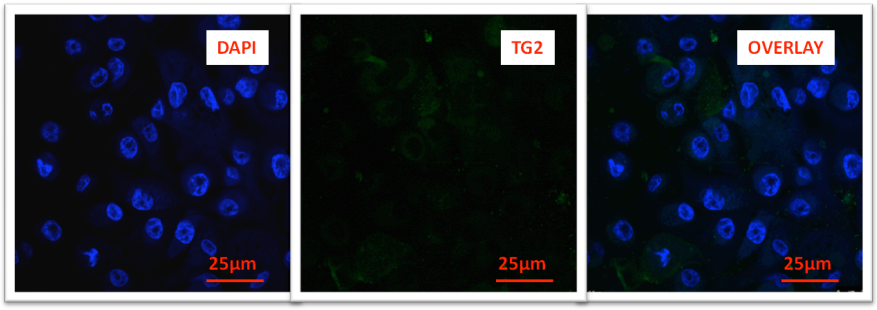

Figure 6.10A: TG2 induced expression increases TG2 fluorescence in HBEC-T cells. Immunofluorescent images showing TG2 expression in HBEC cells transduced with TG2-WT plasmid cultured at ALI. The cells were cultured for 28 days and stained with monoclonal mouse anti-TG2 antibody and secondary FITC anti-mouse antibody (green). Images were taken using the Leica® SP5 confocal microscope. DAPI was used to stain nuclei. Scale bar represents 25 µm. Images show an increase in fluorescence in HBEC-T cells as a consequence of increased TG2 expression.

B

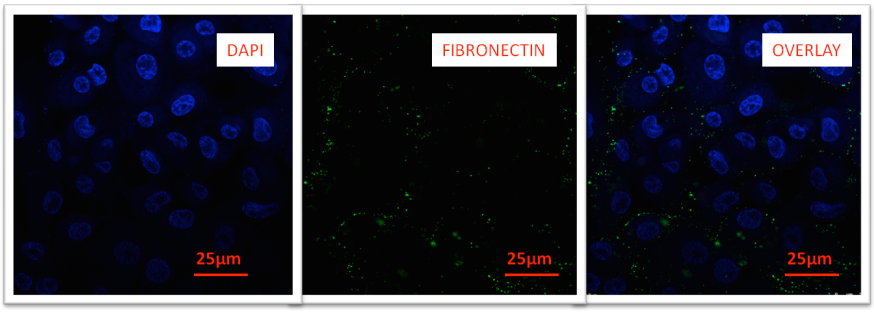

Figure 6.10B: TG2 induced expression increases fibronectin expression in HBEC-T cells. Immunofluorescent images of fibronectin expression in HBEC cells transduced with TG2-WT plasmid cultured at ALI. The cells were cultured for 28 days and stained with polyclonal anti-fibronectin antibody (rabbit) and secondary FITC anti-rabbit antibody (green). Images were taken using the Leica® SP5 confocal microscope. DAPI was used to stain nuclei. Scale bar represents 25 µm. Images show an elevation of fibronectin expression around the HBEC-T cells.

6.4.6: TG2 is a negative regulator of the CFTR chloride channel expression and activity.

6.4.6.1: Synergism between TG2 inhibition and CFTR correction elevates CFTR expression.

The recent milestone approval of Ivacaftor, VX-770, a CFTR potentiator for the treatment of heterozygote CF patients with the G551D mutation, signalled the opening of a range of novel classes of drugs used in the treatment of CF aimed at ameliorating CFTR protein mutations (Ramsey *et al.*, 2011a, Harrison *et al.*, 2013). The conventional therapy was aimed at alleviating patient symptoms but with the advent of these new compounds, treatment is centred on correcting the default in chloride conductance. This current study has primarily suggested the involvement of TG2 in the pathogenesis of the disease with insight into new therapeutical goals. Luciani *et al*. (2012) demonstrated using the CFTR potentiators, VX-325 or Corr-4a, that an increase in CFTR function in ΔF508-homozygous epithelial cells was not enough to sustain an increase in chloride conductance. Hence, the presence of a mature channel in the plasma membrane requires an increase in stability of the protein, which prevents premature proteosomal degradation so reducing the copies of the CFTR channel in the apical membrane. However, in the presence of the non–specific TG2 inhibitor or "proteostasis regulator", cystamine, the membrane status of the channel was maintained 12 h after washout of cystamine and cycloheximide treatment (Luciani *et al.*, 2012). Nonetheless, due to the ubiquitous nature of cystamine as a TG2 and caspase inhibitor, its function cannot be solely related to its inhibition of TGases (Lesort *et al*., 2003). With that background, this study is aimed at using the TG specific inhibitor, R283 in the presence of the CFTR corrector, VX-809 and determining the combined effect of these compounds in alleviating protein degradation, thus elevating the expression of mature CFTR in the apical surface of IB3 cells. Figure 6.11 shows Western blots of TG2 and CFTR protein expression (band C) in the presence of VX-809 (10μM) and R283 (500μM) in IB3 cells in submerged culture. Results show elevated TG2 expression in VX-809 treated groups compared to DMSO control. R283 inhibited TG2 expression slightly compared to untreated cells and in the presence of both R283 and VX-809, TG2 expression was significantly inhibited ($p<0.001$) compared to the DMSO control. Conversely, CFTR was marginally expressed at the membrane in untreated wild type cells, however in the presence of VX-809, expression was significantly elevated ($p<0.001$) compared to the DMSO control. Figure 6.11 shows that following treatment of IB3 cells with R283, membrane expression of CFTR increased significantly ($p<0.01$) above untreated groups however slightly below the VX-809 treated group compared with DMSO. CFTR expression in the presence of VX-

809/R283 was not significantly higher than VX-809 alone. The effects of R283 on CFTR expression suggest a novel role for TG2 in CF disease pathophysiology whereby TG2 activity is directly linked with CFTR maturation and indicates a potential future input of TG2 inhibitors as therapeutic compounds in patients with ΔF508 or W1282X mutation.

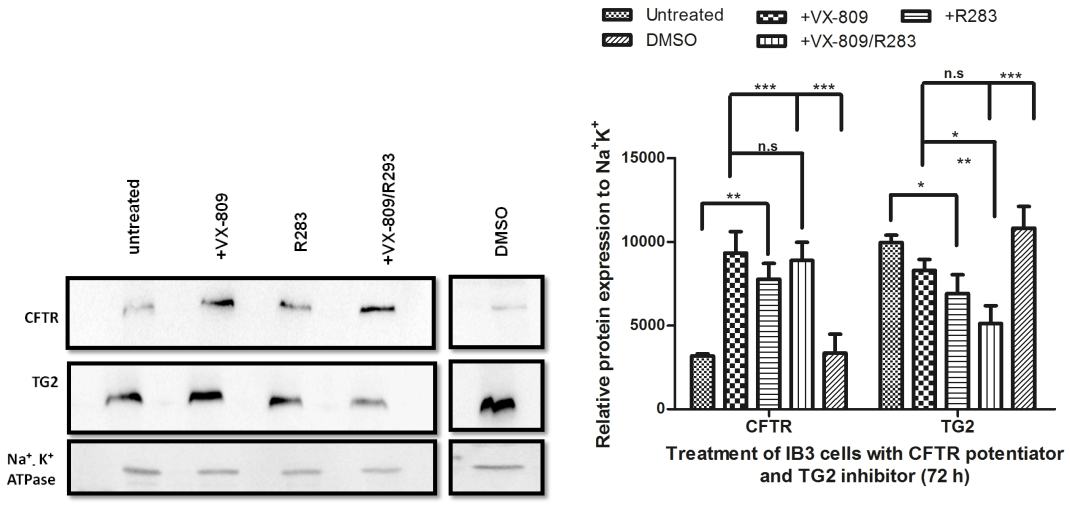

Figure 6.11: Partial correction of ΔF508 CFTR mutation by VX-809 and R283 augment CFTR protein copies on cell membrane. Left panel. Western blots showing TG2 and CFTR expression in IB3 cells under submerged culture treated with the TG2 inhibitor, R283 (500μM) or CFTR corrector, VX-809 (10μM). 250μg of protein was used for the Western blot assay. Monoclonal anti-TG2 and anti-CFTR antibodies were used to detect protein with Na^+-K^+-ATPase detection used as protein loading control. Blot image represents a characteristic blot of 3 independent experiments carried out with the same number of cells. **Right panel.** Densitometry represents mean and standard deviation of 3 independent experiments with protein expression normalised to Na^+-K^+-ATPase. Results show no change in TG2 expression in the presence of VX-809 compared to DMSO control however, the combination of VX-809 with R283 significantly inhibited TG2 expression. A reduction in TG2 expression was shown in the presence of R283 compared to untreated control. However, CFTR expression was shown to increase significantly in the presence of R283 compared to untreated control and markedly elevated in the presence of VX-809 and VX-809/R283 compared to DMSO control. Two-way Anova analysis with Bonferroni post-tests: *** $p<0.001$, ** $p<0.01$, * $p<0.05$, n.s. $p>0.05$.

6.4.6.2: Conformational correction induced by VX-809 salvages CFTR from early proteosomal degradation

Studies have shown that patients carrying the ΔF508 mutation, which is confined to the nuclear binding domain 1 (NBD-1) of the CFTR protein, acquire 15% of normal lung function when treated with the CFTR corrector, VX-809 (Van Goor *et al.*, 2011). Albeit,

the amelioration of lung function in the presence of VX-809 has been demonstrated to be due to the conformational modifications induced by the compound in the membrane-spanning domain 1 of the protein which enhances the interaction between NBD-1 and MSD-1 and 2 (Ren *et al.*, 2013). This brings to the fore the importance of the stability of the NBD-1 hence suggesting that compounds can synergistically improve CFTR expression by stabilising this domain interaction with MSD-1, which suppresses folding defects of ΔF508 mutation and forges the processing of mature CFTR which is trafficked to the plasma membrane. Here, IB3 cells were treated with VX-809 and R283 prior to immunocytochemical staining of the cells with antibodies to TG2 or CFTR to ascertain the effect of the compounds on CFTR expression and TG2 expression. Figure 6.12A shows that in untreated IB3 cells, expression of TG2 was high but expression of CFTR was marginal. In the presence of VX-809, high elevation of CFTR expression was observed with TG2 expression remaining unchanged. DAPI (blue) was used to stain nuclei. Expression of CFTR was shown as “glowing green dots” distributed around the cell (Figure 6.12B). Likewise, in the presence of R283 treatment, CFTR expression was highly expressed however slightly less than was expressed in VX-809 group but higher than untreated groups (Figure 6.12C). Figure 6.12D shows a combination of R283 and VX-809; here elevated expression of CFTR was marked with large widespread distribution across the cell whilst TG2 expression (red) was reduced. TG2 expression was shown to reduce in the presence of both R283 and VX-809/R283 (Figure 6.12 C and D). These results suggest that whilst the R283 inhibitor blocks TG2 expression, VX-809 corrects the conformational default of the ΔF508 mutation, thus allowing the channel to be processed properly, avoiding early degradation and presumably allowing glycosylated matured channel to be trafficked to the cell surface. Although, the functionality of the channels has not been tested, the prognosis is that this synergistic/additive effect can be construed as a merger of an abolished TG2 induced EMT and CFTR mutational correction.

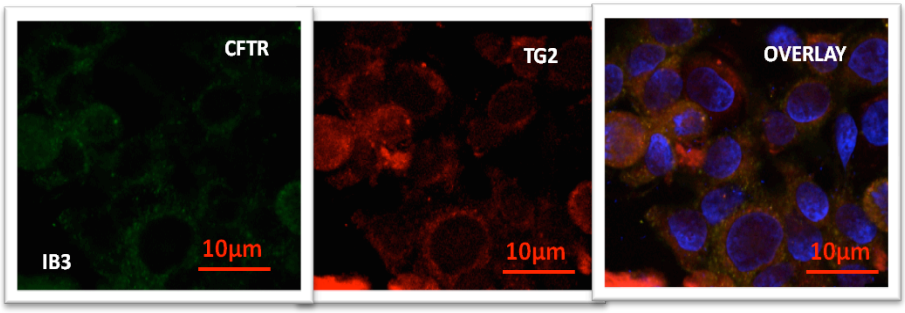

Figure 6.12A: Low CFTR expression in untreated IB3 cells in submerged culture. Immunofluorescent images of TG2 and CFTR expression in IB3 cells in submerged culture. Polyclonal rabbit anti-TG2 and monoclonal mouse anti-CFTR antibodies were used to stain cells. Images were taken under a Leica® SP5 confocal microscope. Mouse and Rabbit IgG were used as control (Figure 4.4). DAPI was used to stain nuclei. Images represent characteristic staining of 2 repeat experiments. Scale bar represents 10 µm. Images show marginal CFTR expression and high TG2 expression in IB3 cells.

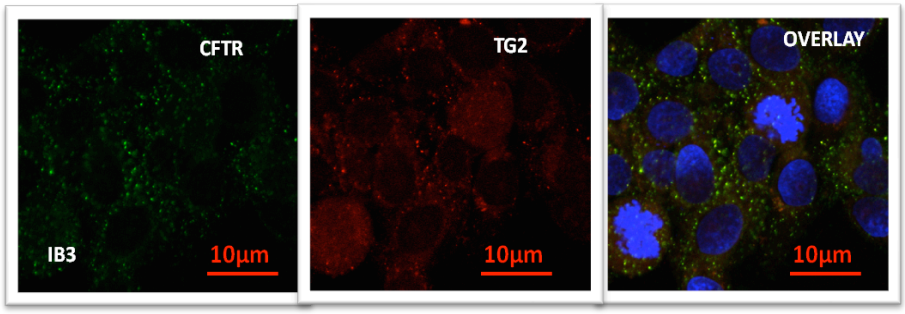

Figure 6.12B: VX-809 increases CFTR expression in IB3 cells. Immunofluorescent images showing TG2 and CFTR expression in IB3 cells in submerged culture. Cells were treated with the CFTR corrector, VX-809 (10µM) for 48 h prior to staining. Polyclonal rabbit anti-TG2 and monoclonal mouse anti-CFTR antibodies were used to stain cells. Images were taken under a Leica® SP5 confocal microscope. Mouse and Rabbit IgG were used as control (Figure 4.4). DAPI was used to stain nuclei. Images represent characteristic staining of 2 repeat experiments. Scale bar represents 10 µm. Images show an elevation of CFTR expression in IB3 cells in the presence of the CFTR corrector, VX-809 with no change in TG2 expression.

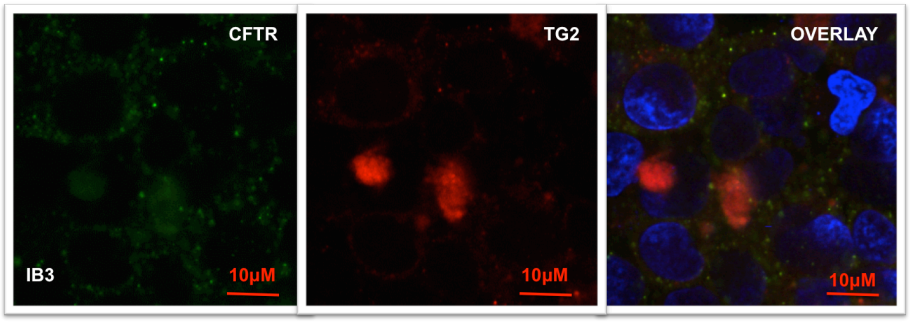

Figure 6.12C: R283 inhibits TG2 expression but up regulates CFTR expression in IB3 cells. Immunofluorescent images showing TG2 and CFTR expression, in the presence of cell permeable TG2 inhibitor, R283 (500μM). Polyclonal rabbit anti-TG2 and monoclonal mouse anti-CFTR antibodies were used to stain cells. Images were taken under a Leica® SP5 confocal microscope. Mouse and Rabbit IgG were used as control (Figure 4.4). DAPI was used to stain nuclei. Images represent characteristic staining of 2 repeat experiments. Scale bar represents 10 μm. Images show an inhibition of TG2 expression after incubating with R283 and that this corresponds with an increase in CFTR expression.

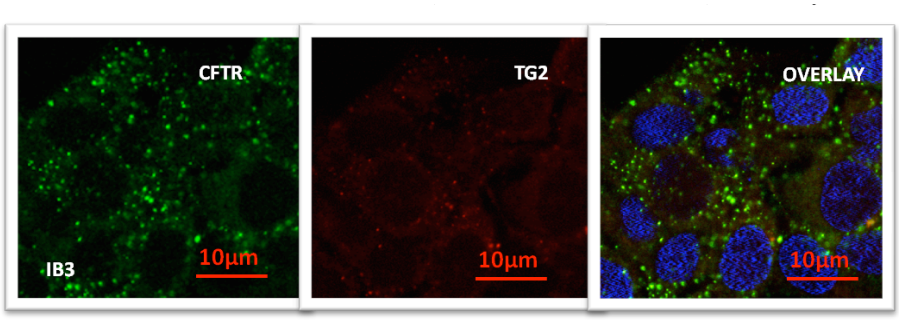

Figure 6.12D: VX-809 and R283 synergistically elevate CFTR levels in IB3 cells. Immunofluorescent images showing TG2 and CFTR in IB3 cells in submerged culture incubated with VX-809 (10μM) and R283 (500μM). Polyclonal rabbit anti-TG2 (red) and monoclonal mouse anti-CFTR (green) antibodies were used to stain cells. Images were taken under a Leica® SP5 confocal microscope. Mouse and Rabbit IgG were used as control (Figure 4.4). DAPI was used to stain nuclei. Images represent characteristic staining of 2 repeat experiments. Scale bar represents 10 μm. Images show marked elevation of CFTR expression in IB3 cells treated with VX-809 and R283 while TG2 expression is inhibited under these conditions.

6.4.6.3: Ivacaftor, VX-770, increases CFTR expression in IB3 cells.

In a recent study, Yu *et al*. (2012) showed that the CFTR potentiator, VX-770 could potentiate chloride conductivity in a variety of CFTR gating mutations ie G551D, G178R, G551S, S549N, S549R, G1244E, S1251N, S1255P and G1329D. In relation to this, the FDA recently approved that VX-770 can be used for these mutations mentioned above as well (De Boeck *et al*., 2014). However, VX-770 has also been demonstrated to improve chloride-gating activity in temperature corrected ΔF508 homozygous mutations or heterozygous mutations with at least one G551D allele (Van Goor *et al.*, 2009). The hypothesis suggests that VX-770 in combination with TG2 inhibitors might improve the trafficking of the channel to the plasma membrane as well as potentiate the conductance of chlorine. To support this hypothesis, IB3 cells in submerged culture were treated with VX-770 (10μM) alone and in combination with VX-809 (10μM) and R283 (500μM). Results from Figure 6.13 show that compared to cells treated with VX-770 alone, the combination of VX-770 with VX-809 elevated CFTR expression on the cells surface by 2-fold. On treating cells with VX-770 and R283, CFTR expression increased significantly ($p<0.05$) above the VX-770 alone treated groups but slightly less than that observed in the presence of VX-770/VX-809. These observations support previous results where R283 combination with the CFTR corrector, VX-809 improved CFTR expression by presumably stabilising the thermo unstable NBD-1 thus increasing the turnover of the protein on the plasma membrane.

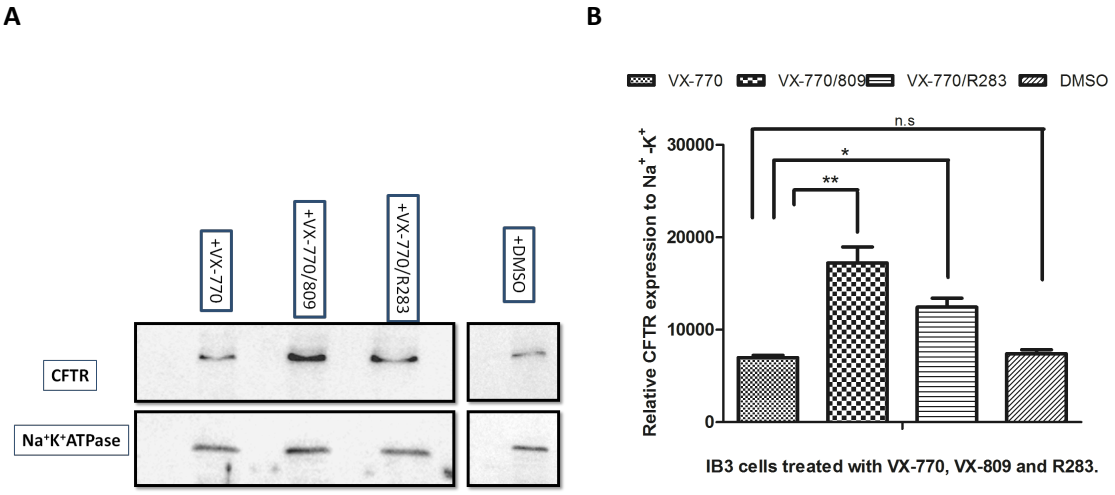

Figure 6.13A&B: Combinations of VX-770 with VX-809 or R283 ameliorates CFTR levels in IB3 cells. A. Western blots showing CFTR expression in IB3 cells cultured in submerged culture and treated with CFTR potentiator, VX-770 (10μM) and TG2 inhibitor, R283 (500μM). 250μg of protein was used for the Western blot assay. Monoclonal anti-mouse CFTR antibody was used with anti-Na^+-K^+-ATPase used as loading control. **B.** Densitometry represents means and standard deviation of 3 independent experiments normalised to Na^+-K^+-ATPase expressed. Blot image represents a characteristic blot of 3 independent experiments carried out with the same number of cells. Results show an increase in CFTR expression in the presence of either the combination of VX-770/VX-809 or VX-770/R283 with the former showing higher levels of CFTR expression. One way Anova with Bonferroni's multiple comparison test; **p<0.005, *p<0.05, n.s. p>0.05.

In concert with these findings above, IB3 cells treated with both VX-770 and R283 were evaluated to determine co-localisation of cell surface TG2 and CFTR and to observe the distribution of CFTR trafficked to the cell surface. Compared to results from VX-809, VX-770 improved CFTR expression (Figure 6.14A) with well distributed "glowing green dots" interspaced across the surface of cells, which was subsequently enhanced slightly in the presence of R283 (Figure 6.14B). TG2 expression was inhibited in the presence of R283 (Figure 6.14B). Together, this report concurs with previous studies suggesting that VX-770 can increase CFTR expression and inhibition of TG2 seemingly aids in stabilising mutated CFTR protein hence ameliorating channel trafficking.

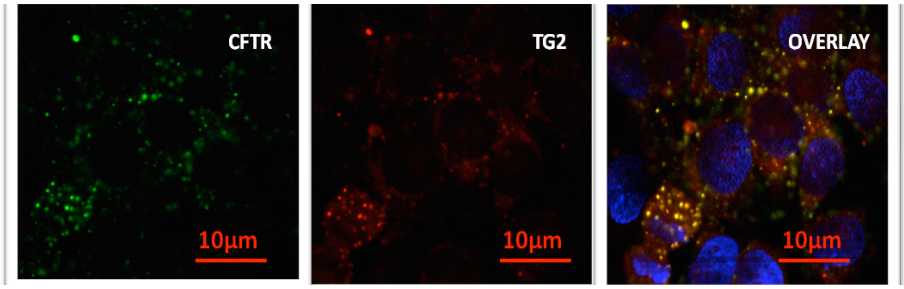

Figure 6.14A: VX-770 ameliorates CFTR expression in IB3 cells. Immunofluorescent staining for TG2 and CFTR in IB3 cells cultured in medium supplemented with VX-770 (10µM). Polyclonal rabbit anti-TG2 and monoclonal mouse anti-CFTR antibodies were used to stain cells. Images were taken under a Leica® SP5 confocal microscope. Mouse and Rabbit IgG were used as control (Figure 4.4). DAPI was used to stain nuclei. Images represent characteristic staining of 2 repeat experiments. Scale bar represents 10 µm. Results show an increase in CFTR expression in the presence of VX-770 in IB3 cells.

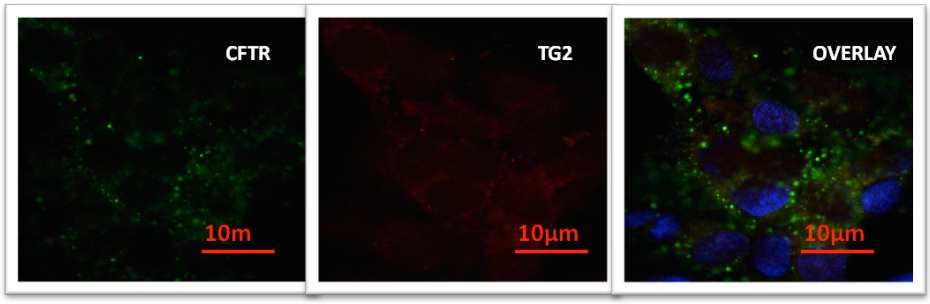

Figure 6.14B: CFTR expression is up regulated by a combination of VX-770 and R283. Immunofluorescent images showing IB3 cells in submerged culture stained with polyclonal rabbit anti-TG2 and monoclonal mouse anti-CFTR antibodies following treatment with VX-770 (10µM) and R283 (500µM). Images were taken under a Leica® SP5 confocal microscope. Mouse and Rabbit IgG were used as control (Figure 4.4). DAPI was used to stain nuclei. Images represent characteristic staining of 2 repeat experiments. Scale bar represents 10 µm. Images show a highly elevated CFTR expressed in IB3 cells in the presence of VX-770 and R283 with TG2 expression inhibited under these conditions.

6.4.6.4: Recapitulation of augmented CFTR expression with VX809 and R283 treatment in the ALI model

The robustness of the ALI model in depicting *in vivo* airway architecture was observed earlier when IB3, C38 and HBEC were cultured at ALI and TG2 and EMT marker expression determined (Figure 6.1 and 6.9). The results obtained illustrated similar

findings as observed in submerged medium. Therefore, using this model showed IB3 cells expressing high TG2 levels corresponding to elevated EMT markers and the effects of knockdown or up regulation of TG2 on EMT progression. Here, in order to confirm the recent findings of an elevation of CFTR expression in monolayer cell culture model where the correlation between CFTR and EMT marker expression has been established, IB3 cells were cultured at ALI for 28 days, treated with VX-809 and R283 and then TG2 and CFTR expression were determined. As observed in submerged culture, CFTR expression was shown to be elevated in the presence of VX-809 compared to control however, TG2 expression remains unaltered. On addition of R283, it is observed that CFTR expression is slightly elevated, beyond that seen in untreated cells and not as significantly elevated as observed in VX-809 treated cells (Figure 6.15A-C). CFTR expression was shown in IB3 cells to increase when cells were incubated with both VX-809 and R283. These results support the findings from submerged culture however, further investigation using 3-D images confirms from the cross-sectional image an increase in CFTR expression (green) shown to traffic from the basal cells to the cell surface in the presence of VX-809. DMSO controls need to be assessed to further confirm the results obtained. These images further show that in the presence of R283, CFTR levels were shown to increase with increased expression closer to the apical surface, however expression was less compared to VX-809 alone (Figure 6.14D). Together, these results culminate in illustrating that VX-809 treatment might be correcting processional CFTR defects (such as the ΔF508 mutation) in IB3 cells, which is further stabilised byTG2 inhibition with R283 hence allowing matured CFTR protein to be trafficked to the plasma membrane as suggested in the results presented.

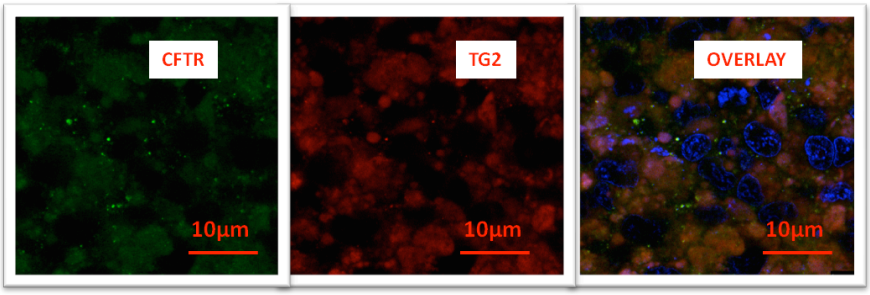

Figure 6.15A: Low CFTR expression in untreated IB3 cells cultured at ALI. Images showing TG2 and CFTR expression in untreated IB3 cells cultured at ALI. The cells were cultured for 28 days and stained with polyclonal rabbit anti-TG2 and monoclonal mouse anti-CFTR antibodies. Images were taken under a Leica® SP5 confocal microscope. Mouse and Rabbit IgG were used as control (Figure 4.4). DAPI was used to stain nuclei. Images represent characteristic staining of 2 repeat experiments. Scale bar represents 10 µm. Results show marginal CFTR and high TG2 expression in IB3 cells cultured at ALI.

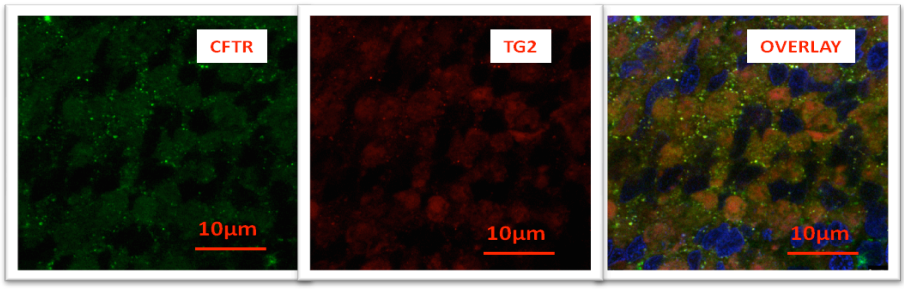

Figure 6.15B: Elevated CFTR expression in the presence of VX-809. Immunofluorescent images of TG2 and CFTR expression in IB3 cells cultured at ALI and treated with the CFTR corrector, VX-809 (10µM) and cultured at ALI. The cells were cultured for 28 days and polyclonal rabbit anti-TG2 and monoclonal mouse anti-CFTR antibodies were used to stain cells. Images were taken under a Leica® SP5 confocal microscope. Mouse and Rabbit IgG were used as control (Figure 4.4). DAPI was used to stain nuclei. Images represent characteristic staining of 2 repeat experiments. Scale bar represents 10 µm. Results show an elevation in CFTR expression in IB3 cells cultured in the presence of VX-809 with no change in TG2 expression.

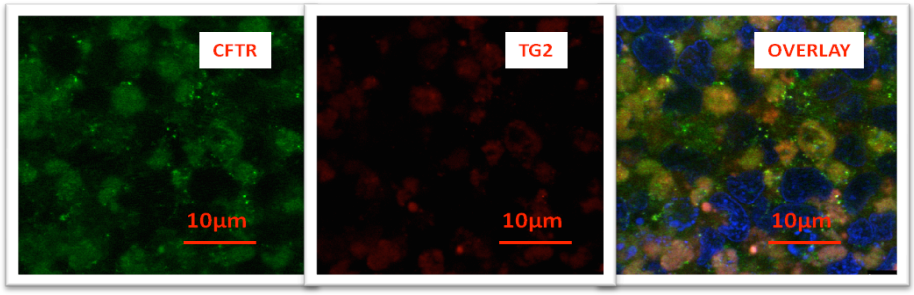

Figure 6.15C: TG2 inhibition up regulates CFTR expression in IB3 cells. Immunofluorescent images of TG2 and CFTR expression in IB3 cells cultured at ALI, in the presence of the cell-permeable TG2 inhibitor, R283 (500µM). The cells were cultured for 28 days and polyclonal rabbit anti-TG2 and monoclonal mouse anti-CFTR antibodies were used to stain cells. Images were taken under a Leica® SP5 confocal microscope. Mouse and Rabbit IgG were used as control (Figure 4.4). DAPI was used to stain nuclei. Images represent characteristic staining of 2 repeat experiments. Scale bar represents 10 µm. R283 inhibits TG2 expression and slightly increases CFTR expression in IB3 cells at ALI.

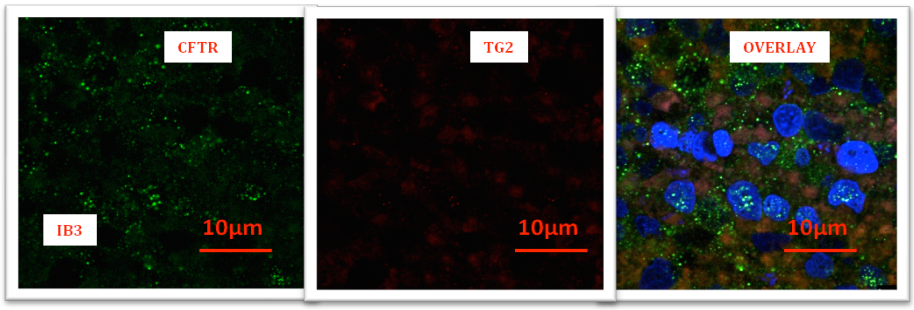

Figure 6.15D: VX-809 and R283 markedly increase CFTR expression in IB3 cells at ALI. Immunofluorescent staining of TG2 and CFTR protein expressed in IB3 cells cultured at ALI and treated with CFTR corrector, VX-809 (10µM) and TG2 inhibitor, R283 (500µM). The cells were cultured for 28 days and polyclonal rabbit anti-TG2 and monoclonal mouse anti-CFTR antibodies were used to stain cells. Images were taken under a Leica® SP5 confocal microscope. Mouse and Rabbit IgG were used as control (Figure 4.4). DAPI was used to stain nuclei. Images represent characteristic staining of 2 repeat experiments. Scale bar represents 10 µm. CFTR expression was markedly increased and TG2 expressed was reduced in IB3 cells cultured at ALI in the presence of VX-809 and R283.

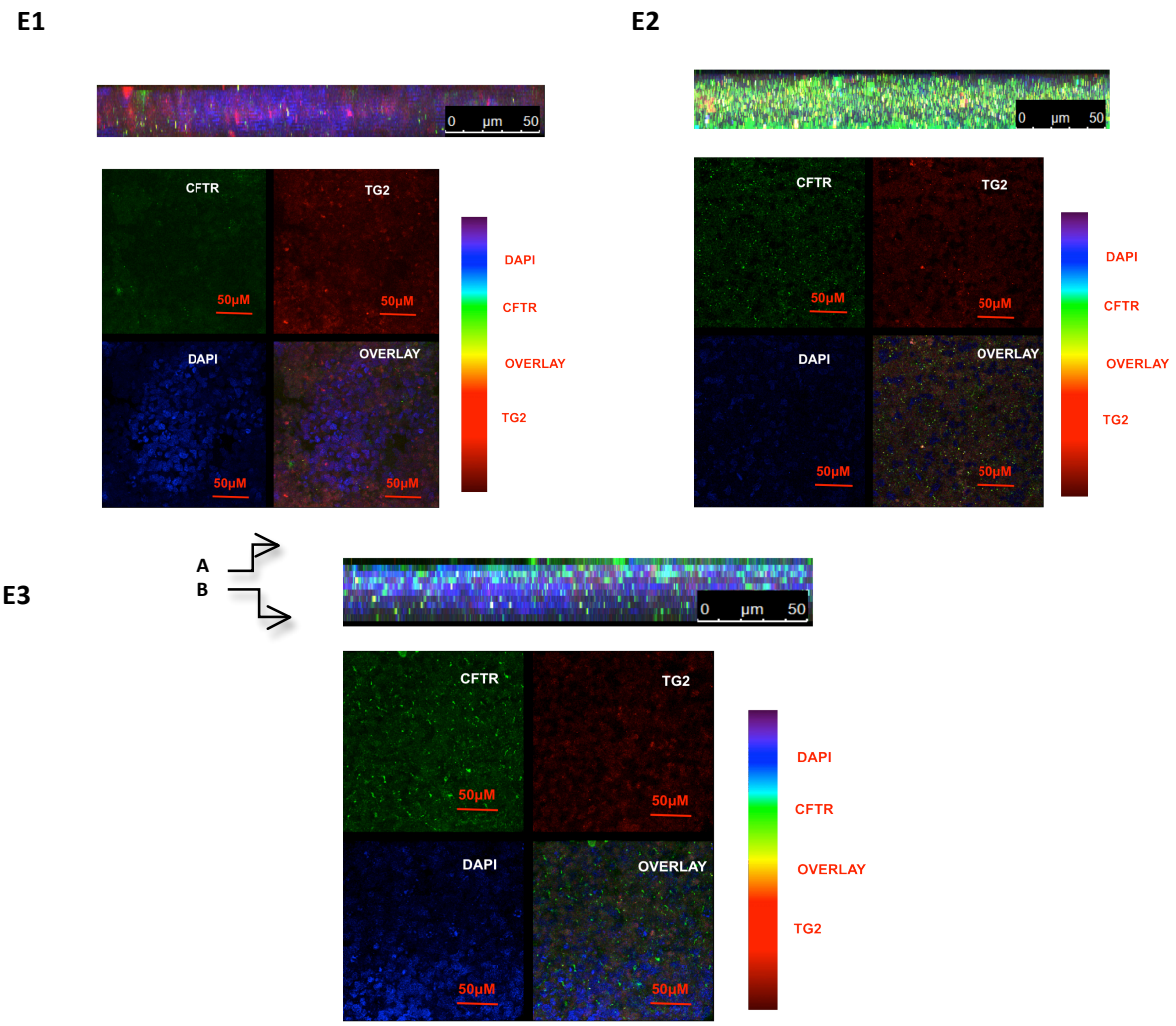

Figure 6.15E: VX-809 and R283 augment CFTR expression on the apical surface of IB3 cells at ALI. 3-D cross sections of TG2 (red) and CFTR (green) expression in untreated IB3 cells cultured at ALI, **E1**, IB3 cells cultured in medium supplemented with VX-809 (10µM), **E2**, and IB3 cells cultured in medium supplemented with R283 (500µM), **E3**. Cells were cultured for 28 days at ALI before staining with polyclonal rabbit anti-TG2 (red) or monoclonal mouse anti-CFTR (green) antibodies. Images were taken using the Leica® SP5 confocal microscope using 3-D projections where a cross section of the membrane with IB3 cells were visualised from the apical side, **A** to the basal, **B** using the z-stack acquisition panel. DAPI (blue) was used stain nuclei. Mouse and Rabbit IgG were used as control (Figure 4.4). Images represent characteristic staining of 2 repeat experiments. Images show z-stack from IB3 untreated and VX-809-treated cells having high TG2 expression whilst R283 treated cells have marginal TG2 levels. However, although CFTR expression is low in untreated IB3 cells, treatment with VX-809 or R283 produces an increase in apical CFTR expression with the former showing higher expression.

6.4.7: Chloride conductance rescued with CFTR corrector and TG2 inhibitors.

The underlying pathology of CF is centred on the low or absolute loss of chloride conductance within the airways. This maligning defect defines the disease prognosis and therapy has been palliative with treatment aimed at alleviating symptoms of the disease. However, with the milestone discovery of channel potentiators and recently correctors, the treatment regimen has been reformed with affirmative prognosis for patients. The results presented in this chapter have illustrated the vital role TG2 inhibition plays in ameliorating the disease as well as the combinatorial approach by TG2 inhibitors and CFTR correctors in forging an elevation in the CFTR turnover and trafficking to the plasma membrane. Here using both TG2 inhibitors, chloride conductance is been evaluated to provide an insight of the impact of elevated CFTR expression and trafficking on CFTR function. Results show (Figure 6.16) that when untreated IB3 cells were incubated in chloride free buffer, there was no increase in chloride conduction across CFTR channels. This suggests no change in the state of chloride dependent channels and consequently no efflux of MQAE bound intracellular chloride in the presence of chloride free buffer. Anderson and Welsh, (1991) described calcium dependent chloride secretion to be independent of the cAMP dependent chloride regulation, which is defective in CF. Their results showed that although cAMP regulates chloride secretion differently, they could ultimately produce an additive chloride secretion. Consequently, using chloride free containing buffer, IB3 cells were treated with dibutyryl cyclic adenosine monophosphate (db-cAMP) (1mM). The aim was to increase intracellular cAMP levels via increase in adenylate cyclase or mimic cAMP activity with db-cAMP. In addition, db-cAMP is a phosphodiesterase inhibitor (PDI), which inhibits the activity of phosphodiesterases involved in the breakdown of cAMP. The cells were excited at 350nm and emission was measured at 450nm. CFTR is cAMP dependent channel hence in the absence of cAMP, CFTR regulatory (R) domain is not phosphorylated and the channel is not open. As cAMP levels are elevated, the R-domain is phosphorylated, adenosine triphosphate (ATP) is hydrolysed in NDB, which in turn causes the MSD of the channel to open. In the presence of db-cAMP supplemented buffer (Figure 6.16), R283 was shown to significantly elevate CFTR conductance about 4-fold. However, CFTR conductance was highly elevated in the presence of the non-specific TG2 inhibitor cystamine, where conductance was stabilised at 270 mins. In line with these, in the presence of chloride free buffer (i.e. in the presence of a driving force for chloride movement), a significant elevation of chloride conductance in foskolin treated cells was observed (results not shown) which

was further elevated in the presence of db-cAMP. Interestingly, the elevated chloride movement observed illustrates targeted cAMP-mediated CFTR activation for both foskolin and db-cAMP groups, obviating chloride quenching with chloride free medium and in db-cAMP chloride free groups, enhanced chloride movement depicts added *in-situ* Phosphodiesterase inhibitor (PDI) function. Together, these results demonstrate a marginal increase in chloride conductance in IB3 cells attributed to the presence of residual functional CFTR copies found in the apical plasma membrane as shown in Figure 6.11.

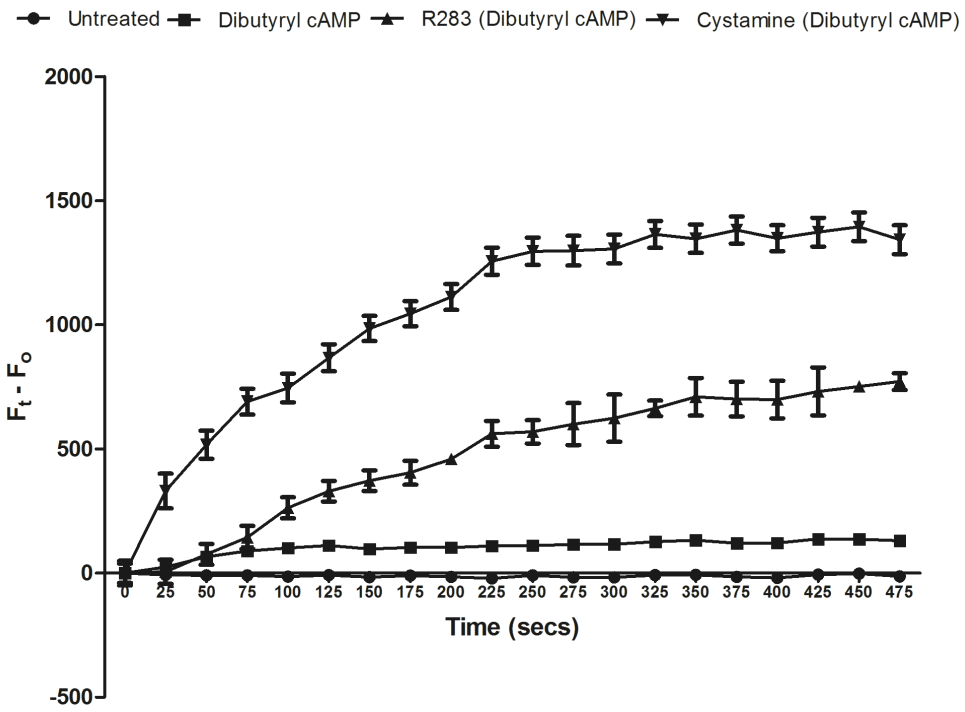

Figure 6.16: R283 and Cystamine augment chloride conductance in IB3 cells. Chloride conductance in IB3 cells in submerged culture incubated in chloride free buffer with Dibutyryl cAMP (db-cAMP) (1mM) in combination with the cell permeable TG2 inhibitors; R283 (500μM) or Cystamine (250 μM). The chloride indicator dye, MQAE (10 mM) was added to measure intracellular chloride levels. Results represent mean of 2 independent experiments each carried out in triplicates. Results show marginal chloride conductance in untreated IB3 cells (closed circles) with a slight increase in the presence of db-cAMP (closed squares). However, incubation with R283 or Cystamine markedly increased db-cAMP-dependent chloride conductance through the CFTR channel with the latter producing a higher effect.

As previously shown (Figure 6.11 and 6.15), the inhibition of TG2 activity in combination with conformational correction of MSD-1 of CFTR protein to sustain a stable NBD-1, in turn salvages ΔF508 mutation from proteosomal degradation, thus

enhancing functional CFTR protein trafficking to the plasma surface. Results from Western blotting and immunostaining have also shown that CFTR protein is well distributed on the plasma membrane after treating IB3 cells with VX-809, VX-770 and R283 and further increased after combination treatments (Figures 6.12, 6.13 and 6.14). The increase in chloride conductance observed in the presence of cystamine or R283 indicates that as channels open in the presence of db-cAMP, these cell-permeable TG2 inhibitors augment channel activity in IB3 cells. This suggests importantly that inhibition of cell surface TG2 in addition to a correction in ΔF508 CFTR protein increases both turn over and conductance of CFTR and chloride respectively. It can be inferred here that TG2 inhibition impedes EMT progression via TGFβ1, which in turn retards CFTR degradation induced by TGFβ1 consequently, reverting the CFTR mutational phenotype. This in concert with CFTR correctors, which stabilises NBD-1, ultimately leads to an enhanced CFTR maturation and trafficking to the plasma membrane. This augments chloride conductance.

6.5: Discussion:

The invasiveness of using human subjects in drug design has forged the design of culture models that mimic the *in vivo* environment. The burgeoning evidence from studies on the robustness of ALI models for modelling the respiratory tract and its use in determining salient functions of the respiratory system serves as a useful resource and remains a vital tool in obviating the cost and laborious constraints involved in using human samples. Over time, research into various CF mutations including the ΔF508 mutation and the recent discovery of the CFTR potentiator, VX-770, which is orally bioavailable and used in patients with G551D CFTR mutation and other gating mutations, unravelled an episode of research into other lead compounds capable of altering the phenotype of CFTR patients with other mutations (Kerem *et al.*, 1989, Van Goor *et al.*, 2006). However, the conundrum surrounds the non-availability of lead compounds to treat the most prevalent mutation, ΔF508, which accounts for about 70% of the world's population (Bobadilla *et al.*, 2002) .

This study has shown the vital role TG2 plays in CF disease pathophysiology. The nascent results obtained from the previous chapters leading up to this chapter have suggested the link between TG2 and EMT progression and have related this to elevated levels of the pro-fibrotic cytokine, TGFβ1 which studies have shown to inhibit CFTR biogenesis (Snodgrass *et al*., 2013) and suggested the remission of fibrosis in the disease due to TG2 inhibition/knockdown. In this chapter, using ALI models, results suggest some comparability to the results observed in submerged cultures where TG2 and EMT marker expression have been shown to be elevated in IB3 cells compared to C38 cells (Figure 6.1). They have also shown that knockdown of TG2 protein induces a restoration of cell-cell integrity with a 2-fold elevation of TEER values in TG2 shRNA transduced IB3 cells compared to untreated cells (Figure 6.4). On the contrary, it was observed using primary HBEC-T cells that an increase in TG2 expression, which mimicked CF phenotype, suggests a change in cell morphology and reduced TEER values as shown (Figure 6.8 and 6.9B). This demonstrates that elevation of TG2 supports the promotion of EMT, which progresses with an increase in cell migration. This also might be responsible for the loss of E-cadherin expression in HBEC-T cell transduced with TG2 wild type plasmid (Figure 5.11) in submerged culture. These results are in concert with similar studies using MCF-10A breast cancer cells, where EMT was shown to be promoted in TG2 transduced cells with an elevation of TG2, fibronectin, N-cadherin, Vimentin and β-catenin whilst E-cadherin expression was inhibited (Kumar *et al*., 2010). Also in a related study, increased TG2 expression in the presence of TGFβ1 in A549 lung cancer cells initiated an E-cadherin to N-cadherin

switch attributed to a down regulation of protein phosphatase 2A (PP2A) which activates C-Jun N-terminal Kinase (JNK) inducing EMT (Park *et al.*, 2013). The A549 wild type cells, $A549_{WT}$, migrated across Transwells® in the presence of TGFβ1 (100pg/ml) as well as A549 cells transduced with TG2 plasmid, $A549_{TG2}$. Migration was reduced in A549 cells transduced with TG2 shRNA, $A549_{shTG2}$ even when treated with TGFβ1 (100pg/ml). This infers that TG2 is involved in migration, which leads to an induction of EMT in epithelial cells. The results presented in this chapter represent for the first time where CF cells are cultured at ALI to determine the correlation between TG2 expression and ΔF508 mutation.

Luciani *et al.* (2012) showed using IB3 and CFBE41o- cells carrying heterozygous and homozygous ΔF508 mutations (ΔF508/W1282X and ΔF508/ΔF508 respectively) that pre-treatment with the TG2 inhibitor/proteostasis regulator, cystamine prior to the use of CFTR potentiators (VX-770, VX-532, Corr-4a) restored and sustained CFTR expression at the plasma membrane compared to the use of potentiators alone. Based on this approach, TG2 inhibitors were combined with the CFTR corrector, VX-809, since studies have also shown that VX-809 corrects the mutation defect in CF ΔF508 mutation similar to compounds like the transcriptional regulator, 4-phenyl-butyrate (4-PBA) (Rubenstein *et al.*, 1997, Van Goor *et al.*, 2011). This was carried out on the premise that ΔF508 mutation is a class II processing mutation where immature proteins are produced due to the deletion of phenylalanine at position 508. Hence, stabilising/correcting this defect with TG2 inhibitors/ CFTR corrector possibly by increased stabilisation of the MSD-1, increases interaction between the NBD-1 and intracellular loop 1 (ICL-1), involved in connecting the transmembrane segments of the MSD and thus priming ΔF508 for further correction by TG2 inhibitors. This may enhance CFTR read-through and production of matured protein from the endoplasmic reticulum (ER) thus obviating the proteosomal degradation or endosomal recycling (Okiyoneda *et al.*, 2010, Lukacs and Verkman, 2012, Ren *et al.*, 2013). Results show that both in submerged culture and at ALI, VX-809 significantly increases CFTR presence at the plasma membrane. However, in combination with R283, CFTR presence is significantly elevated for VX-809. Intriguingly, it was observed in the presence of VX-770, mature CFTR protein expression was further elevated in the presence of VX-809. R283 showed remarkable effects on CFTR alone further supporting its role as TG2 inhibitor involved in stabilizing the thermo unstable NBD-1 of the protein. CFTR membrane expression was high with VX-770/R283 combination but wasn't as high as with VX-809. It was further illustrated using immunocytochemistry that the observed elevation of CFTR matched with staining of the protein with CFTR and TG2 shown to co-localise around the cell. Interestingly, culturing IB3 cells at ALI

and applying the same treatment not only mimicked submerged culture results but also illustrated that the elevated CFTR observed at the plasma membrane was a synopsis of the distribution of CFTR from the apical membrane to the basal membrane. Figure 6.14D shows a high distribution of CFTR in VX-809 treated groups of cells cultured at ALI compared with untreated groups as well as a slightly elevated CFTR in R283 groups. It can be deduced here that an inhibition of TG2 supports an increase in CFTR maturation and trafficking and in combination with VX-809, additional CFTR proteins can be trafficked to the plasma membrane. No effect was observed of VX-809 on EMT reversal in IB3 cells (results not shown). This further supports the hypothesis that fibrosis in CF is an effect based on elevated TG2 levels and is an indirect rather than a direct consequence of the mutation.

Furthermore, increased CFTR-dependent chloride conductance was observed in the presence of both TG2 inhibitors and VX-809. Because of the non-selectivity of cystamine as a TG2 inhibitor, in-house synthesised cell-permeable and impermeable TG2 inhibitors were used. Chloride movement was observed in chloride free buffers as intracellular chloride bound to MQAE dye diffused out of the cell through chloride channels either via CFTR or CaCCs. The use of db-cAMP showed that the diffusion of chloride ions was due to the opening of cAMP activated channels. However, chloride conductance was shown to significantly increase with R283 but much more with cystamine, which again was attributed to its non-selectivity for TG2 and caspases. From these results, it can be hypothesised that targeting TG2/CFTR mutation with chemical compounds (TG2 inhibitors/CFTR correctors) can be used as combinatorial therapeutic agents in CF treatment.

The results presented in this chapter have suggested that CFTR maturation and trafficking in patients carrying the ΔF508 mutation can be alleviated by TG2 inhibitors and CFTR correctors. The potency of this synergism is suggested to be surrounded by the stabilisation of the NBD-1 and conformational correction of MSD-1 of the protein which ultimately leads to the production of mature and functional CFTR protein on the apical surface of CF airway epithelia.

6.6 Conclusion:

Together, this study suggests that TG2 inhibition in combination with CFTR mutational correction supports a sustained CFTR maturation and trafficking to the plasma surface, which maintains chloride conductance characteristics. Further experiments using DMSO control will help to delineate if the effect observed is due to the corrector/potentiator exclusively. Certain experiments need to be performed thrice in other to make statistically affirmative conclusions.

Chapter 7

Discussion

7.0 Discussion

The overarching challenge surrounding CF therapy has been the degenerative nature of the disease, which impacts on both the quality and number of years of life of the patient. Hence therapies have been targeted at increasing the life years of patients through rigorous palliative therapy centred on alleviating the untoward effects of the disease and more recently on corrective therapy targeted at the CFTR mutational defects. The current outlook for patients living with the disease has increased over the past decade with an increase in life expectancy from 31 years to 37 years in the US and a predicted increase of up to 50 years in the UK (O'Sullivan and Freedman, 2009, Dodge *et al.*, 2007). The common cause of mortality in CF is respiratory complications. In a cross-sectional study on the causes of death in CF patients in Canada, Mitchell *et al*. (2000) showed that more than 40% of patients presented with respiratory complication with most patients carrying *Pseudomonas aeruginosa, Staphylococcus aureus* or *Burkholderia cepacia* in their sputum and 75% of the total population dying due to this and other complications.

Albeit, successful therapeutic approaches have been used like dornase alfa, the recombinant human deoxyribonuclease and the inhaled aminoglycoside, Tobramycin, as chronic respiratory treatment together with other therapeutic strategies to combat disease symptoms like pulmonary exacerbations, the past decade heralded the advent of mutational specific therapies aimed at further improving CFTR protein read-through and restoring functionality to the channel at the apical surface. Though, these emerging therapies are at their nascent stages and are CFTR mutation class specific, their prognosis has been affirmative. Ataluren (PTC124), a bioavailable molecule that aids the read through of premature stop codons during mRNA translation has been used in class 1 mutation (Kerem *et al*., 2008, Kerem *et al*., 2014) where an increase in nasal chloride hyperpolarization was observed due to an increase in expression of apical full-length CFTR protein (Sermet-Gaudelus *et al*., 2010). Also, Ivacaftor, (VX-770), another bioavailable drug has been shown to improve CFTR conductance as a “potentiator” in patients carrying the G551D mutation and other CFTR mutations with gating defects (Van Goor *et al*., 2006, Yu *et al*., 2012). Recently, CFTR correctors were introduced which studies have shown to ultimately correct the processing of CFTR protein in patients with ΔF508 mutation and one of such correctors is VX-809, which has been shown to stabilise MSD-1 thus increasing NBD-1 interaction with intracellular loops (ICL) on MSD-1, leading to an improvement in folding and thermodynamic stability of the CFTR protein (Van Goor *et al*., 2011, Ren *et al.*, 2013). In all, although the recent therapies have improved disease prognosis, the fibrotic process and lung remodelling

involved as the disease progresses remains unresolved and lingers which ultimately debilitates and often leads to early mortality.

The ubiquitous nature of TG2 and disease modifying role of the pro-fibrotic cytokine, TGFβ1 have been linked to various diseases from cancer (Cao *et al.*, 2012), diabetic nephropathy (Huang *et al*., 2010), idiopathic pulmonary fibrosis (Olsen *et al*., 2011) and other diseases and TG2 has been suggested to drive the activation of TGFβ1 in these diseases. In CF, it has been shown that the recurring activation of TG2 via its possible SUMOylation has been linked to abnormal expression of TG2 in the disease and been suggested to drive fibrosis in the disease via the activation of the NFκB pathway as well as defective autophagy (Luciani *et al*., 2009a, Maiuri *et al*., 2008, Luciani *et al*., 2010b). However, the use of the TG2 inhibitor and competitive amine, cystamine, was shown to remarkably halt disease progression in CF mutant human cell via the abrogation of TG2 activity, restoration of beclin1, a tumour suppressor gene and the involvement of autophagy, ultimately restoring CFTR trafficking (Luciani *et al*., 2010b). Furthermore, pre-treating ΔF508 CFTR mutated cells with a proteostasis regulator like cystamine was suggested to aid in sustaining the stability of CFTR on the plasma membrane beyond drug withdrawal and has also been implied to aid CFTR potentiators, genistein or VX-770 in fresh isolated nasal brushings from homozygous ΔF508 CFTR patients (Villella *et al*., 2013, Luciani *et al*., 2012). Similarly, Snodgrass *et al.* (2013) demonstrated that TGFβ1 could functionally inhibit the biogenesis of CFTR both at mRNA and protein levels as well as induce an increase in N-cadherin expression in Human bronchial epithelial cells (HBEC) cultured for 24 h which was suggested not to match a reduction in E-cadherin levels corresponding to a mesenchymal phenotype. This report is refuted by Camara and Jarai (2010) where HBEC cells were cultured for 72 h and an increase in N-cadherin, α-SMA and vimentin and a corresponding decrease in E-cadherin expression was observed in the presence of TGFβ1. Also, TG2 has been demonstrated to be involved in the activation of TGFβ1 and likewise TGFβ1 involved in the regulation of TG2 (Nunes *et a*l., 1997, Kojima *et al*., 1993, Ritter and Davies, 1998). These relationships suggest that TG2 is involved in inducing a mesenchymal phenotype in cells via TGFβ1. Park *et al*. (2013) showed that in A549 lung cancer cells, TG2 induced EMT via TGFβ1 with an elevation of N-cadherin expression in the cells. These results suggest that TG2, via increasing TGFβ1 levels is involved in the fibrotic process in the lungs and in CF might be involved in the down regulation of the CFTR channel.

This study centred on understanding the role TG2 plays in the development of fibrosis in CF, evaluating the involvement of TG2 in the disease. It was shown that aberrant

TG2 expression activates TGFβ1 via an increase in TGFβ1 gene expression and cell medium levels observed in IB3 cells. This coincided with the study, which showed latent TGFβ1 released from latent TGFβ binding protein (LTBP-1) in bronchial epithelial cells was reported by Nunes *et al*. (1997) but using endothelial cells. Interestingly, in the current study, activation of TGFβ1 was equally blocked in the presence of TG2 cell impermeable (R292 and R294) and permeable inhibitors (R283 and Z-DON) (Figure 3.6D), irrespective of the site of action of the inhibitor. This suggests together with the high TG2 cell surface protein expressed in IB3 cells, that the observed effect of TG2 in CF cells might also be attributed to its presence on the cell surface where it is active as shown in Figure 3.5B where it has been shown to be involved in matrix and other crosslinking reactions (Verderio *et al.*, 1999, Verderio *et al*., 1998).

Abnormal regulation of TG2 correlates with the elevation of expression of some markers of EMT, a phenomenon where epithelial cells undergo morphological changes losing their cell-cell adhesion and polarity as well as cobblestone-like structure in order to assume a fibroblast-like morphology (Kumar *et al.*, 2010, Cao *et al*., 2012). The highlight of this process is the acquisition of a mesenchymal phenotype with an elevation in expression of EMT markers including fibronectin, N-cadherin and the transcriptional marker, *Slug*. This study has attributed the high expression of these markers to an up-regulation of the inflammatory cytokine, TGFβ1 in IB3 cells. This ultimately leads to an increase in cell migration, loss of cell-cell adhesion, polarity and morphological modification as shown in the study. Figures 4.1 to 4.4 show the increase in expression of EMT markers, at both gene and protein level in high TG2 expressing IB3 cells. This further suggests that an up regulation of TG2 levels drives EMT marker expression in IB3 cells. Similarly, a corresponding up regulation of TG2 and EMT marker expression in HBEC cells transfected with a TG2 overexpression plasmid, HBEC-T (Figure 5.11) and rTGFβ1 (Figure 4.9) was observed. Again, in the presence of the TG2 inhibitor, R283, the expression of the EMT marker was inhibited in HBEC and C38 cells where a change in cell morphology was impeded (Figure 4.8A-C and 4.9A&B). This suggests that an inhibition of TG2 in the CF cells supports a reversal of the mesenchymal phenotype and a possible introduction of a mesenchymal to epithelial transition.

In the lungs, TGFβ1 has been found to be the main regulator of EMT evidenced by fibrotic diseases such as in asthma and IPF (Olsen *et al*., 2011, Doerner and Zuraw, 2009, Sheppard, 2006a). In CF, studies have shown that polymorphism of TGFβ1 is associated with virulent pulmonary fibrosis, which remains the major cause of mortality in CF patients (Arkwright *et al*., 2000, Drumm *et al*., 2005). This work has shown

marginal TG2 and TGFβ1 levels in C38 cells, while elevated levels of TGFβ1 activated by TG2 in IB3 cells are likely to occur via the crosslinking of LTBP-1 to the ECM (Nunes *et al.*, 1997). Also, active TGFβ1 might in turn through the phosphorylation of its receptors, RI and RII promote a downward intracellular SMAD dependent signalling via SMAD 2 and 3 to an increase in TG2 expression (Figure 4.14). This coincides with the role TGFβ1 plays in up-regulating TG2 gene expression. Conversely, inhibition of TGFβ1 receptor binding in IB3 cells with a TGFβ neutralizing antibody reverses TG2 and EMT marker expression (Figure
4.10). This shows that inhibition of active TGFβ1 binding to its receptors abolishes the downstream transduction signalling, which impedes TG2 activation and hence blocks the EMT process.

The loss of the adhesion protein, E-cadherin and an increase in N-cadherin truncates cell anchorage and re-organization of the actin cytoskeleton (Wheelock and Johnson, 2003). This is the hallmark of the EMT process. TGFβ1 has been shown to play a key role in driving EMT in the lungs, kidney and pancreas (Rastaldi *et al.*, 2002, Willis and Borok, 2007) and this function involves nuclear restructuring via transcriptional repressors ie *Snail Slug* and *Twist* (Heldin *et al.*, 2012, Kawata *et al*., 2012). In the presence of 3ng/ml of rTGFβ1, it was observed that an increase in TG2 expression corresponded to a decrease in E-cadherin expression in HBEC (Figure 4.9). Similarly, in order to confirm that this effect is TG2 related, HBEC transduced with TG2 overexpressing plasmid, HBEC-T cells were evaluated for the expression of EMT markers (Figure 5.11). Again, it was observed that with an increase in TG2 expression, E-cadherin expression was inhibited. Interestingly, CFTR expression was shown to decrease in HBEC-T cells. This is in concert with the study by Snodgrass *et al*. (2013) where TGFβ1 was linked to an inhibition of CFTR biogenesis in HBEC cells. This was shown to be due to the activation of the TGFβ1 canonical pathway, which includes its activity on TG2 promoter site. In concert with this study, it can be suggested that TG2 activated TGFβ1 in IB3 cells drives EMT that results in the down regulation of CFTR expression levels and a consequent elevation in EMT markers.

This study has shown high levels of TG2 and EMT marker expression in IB3 cells compared to C38 cells (Figure 4.3), which coincided with an increase in the migration profile shown between the cells (Figure 4.6). Also, in the presence of R283, migration was impeded in both cell types. With TGFβ1 implicated in cell migration by its role in down regulating cell adhesion, cell surface TG2 was suspected to be involved in activating TGFβ1 from its latent forms in the extracellular matrix. Additionally, in the presence of TGFβ1, TG2 and EMT markers was shown to be elevated both at gene

and protein level. Again, the TG2 inhibitors, R283, 1-133 and 1-155 (the latter two are highly specific to TG2) were shown to inhibit the levels of these proteins. This is in agreement with results from Ritter and Davies (1998) where it was shown that TG2 gene expression is regulated by TGFβ1 via a TGFβ1 Response Element (TRE) on the promoter site of the TG2 gene and suggests further the extent of TG2 involvement in activation of this cytokine.

The development and stabilisation of the ECM is an important phenomenon in reparative wound repair however altered turnover of the ECM plays a major role in orchestrating a fibrotic cascade associated with various diseases. TGFβ1 has been implicated as an important ECM protein favouring increased ECM deposition and resistance to proteases (Bartram, 2004). In the lungs, TGFβ1 functions both as a pro- and anti-fibrotic cytokine where its role has been linked to EMT progression in various lung pathologies (Hackett *et al*., 2009, Doerner and Zuraw, 2009). Thus, activation of TGFβ1 by TG2 has been shown to correlate with enhancement of EMT (Kumar *et al*., 2010). Studies have importantly shown TG2 involved in crosslinking of matrix proteins via its transamidating activity hence promoting ECM stabilisation (Aeschlimann and Thomazy, 2000). Consequently with an increase in fibronectin deposition in C38 cells treated with TGFβ1, the untoward change in morphology observed was retarded in the presence of R283 (Figure 4.8A). It can therefore be hypothesised that a slowdown of the EMT process corresponds to an inhibition of TG2 activity. Knocking down TG2 with shRNA via Lentiviral transduction inhibited TG2 expression and activity in IB3 cells (Figure 5.5), which was followed by a significant reduction in fibronectin, N-cadherin, *Slug* expression and TGFβ1 activity. This was in concert with TG2 inhibition using TG2 inhibitors shown in Figure 4.5. This work reveals for the first time the direct link between TG2 activity and EMT expression in CF cells.

TG2 activity and conformational variants overtly showed TG2 alignment alters TG2 induced EMT in IB3 cells. The GTPase binding mutant, R580A showed that cell surface TG2 activity and not GTP binding might play a vital role in the progression of TG2-driven EMT with a significant increase in TG2 expression, matrix fibronectin deposition and other EMT markers (Figure 5.8). This was shown to be similar with cells transduced with the WT TG2 overexpressing plasmid with elevated TG2, fibronectin, N-cadherin and *Slug* expression. This further shows the involvement of TG2 transamidating activity as the transamidating mutant with a conserved GTPase binding activity, W241A showed significant knockdown of TG2 and reduced fibronectin, N-cadherin and *Slug* expression (Figure 5.8). This confirms that the transamidating activity is imperative for the TG2 related phenotype in IB3 cells and the GTPase

conformation does not play a role in TG2 related EMT progression in IB3 cells. Again, these results mimic the TGFβ1 related increase in TG2 as shown in control C38 cells and blockage of TG2 activity with TG2 inhibitors in IB3 cells.

In accordance with the study by Pruliere-Escabasse *et al*. (2005), where TGFβ1 was associated with a down regulation of CFTR mRNA and protein level in non-CF human nasal polyps, this study further observed that in the presence of TGFβ1, TG2, fibronectin and N-cadherin expression were elevated in C38 "CFTR corrected" bronchial epithelial cells. This shows the resilient dynamic processes existing between TG2 and TGFβ1 in regulating their expression concurrently. Nonetheless, this observable evidence was replicated at air liquid interface (ALI) where IB3, C38 and HBEC cells demonstrated similar epithelial characteristics to similar cells cultured in submerged culture. TG2 activity was suggested to increase in the presence of TG2 wild type transduced cells, HBEC-T and reversed in the presence of TG2 shRNA in IB3 cells (Figure 6.3 and 6.4). Importantly, the reduction of TG2 expression was matched with an increase in TEER and the up regulation of TG2 increased cell disorientation and reduced TEER values (Figure 6.6 and 6.9B). Conversely, an up regulation of TG2 expression in HBEC cells caused an increase in the expression of TG2 and EMT markers similar to the observations shown in submerged culture. This demonstrates the robustness of the ALI system in depicting *in vivo* conditions as well as linking TG2 expression with cell-cell interactions, migration and ultimately EMT.

The activation of TGFβ1 is associated with the up regulation of the integrin, $\alpha V\beta_6$ in the fibrotic lung (Sheppard, 2005, Sheppard, 2006b, Henderson and Sheppard, 2013). This association has been linked with the binding of αVβ6 and αVβ8 to the RGD motif of LAP on the LLC of TGFβ1 (Munger *et al*., 1999). This study shows a correlation between TG2 up regulation and elevation of αV expression in CF model, IB3 cell. Also co-immunoprecipation of αV and β6 with antibodies to TG2 showed an increase in TG2 "immunoprecipated" αV levels compared with β6. Similarly, αV levels were shown to be elevated in C38 cells in the presence of TGFβ1 (Figure 4.13 A2 and B2). Interestingly, R283 also inhibited the expression of αV "immunoprecipitated" β6 levels in IB3 cells indicating that the down regulation of TG2 directly influenced the expression of the αV protein. Since R283 has been shown earlier to inhibit TGFβ1 expression, it can be suggested, as illustrated in Figure 4.12, that TG2 might be interacting directly with αVβ6 integrin in CF in co-activating TGFβ1 from its latent form.

The advent of novel therapeutic strategies in CF therapy heralded the use of small chemical compounds used to increase CFTR channel read through and thus enhance

chloride conductance. The use of CFTR potentiators and correctors has been deemed as the recent breakthrough in CF therapy (Van Goor *et al*., 2011, Van Goor *et al*., 2009, Ramsey *et al*., 2011b). Using both R283 and VX-809, it was observed that CFTR expression significantly increased with a decrease in TG2 expression in IB3 cells (Figure 6.11). Although, VX-809 has no effect on EMT markers (not shown), the effect of R283 on EMT process, which could be suggested to be related to TG2 inhibition. Similarly it was observed that the copies of CFTR trafficked to the plasma membrane increased in the presence of VX-809 compared to R283, however, together, a high number of CFTR copies were observed on the plasma membrane both in submerged culture and at ALI (Figure 6.12D and 6.15D). As VX-809 has been described to function by stabilizing MSD-1 on the CFTR gene (Ren *et al*., 2013), a 3-D cross sectional analysis suggested that the CFTR channel was located at the apical channel in the presence of VX-809 and R283 compared to untreated cells (Figure 6.15E). This reaffirms the elevated CFTR protein levels observed and shows TG2 negatively regulating CFTR expression via TGFβ1 (Figure 5.11). Similarly, CFTR channel conductance was elevated in IB3 cells treated with R283 and Cystamine (Figure 6.16). The increase was attributed to an inhibition of TG2, which caused an increase in CFTR copies on the apical surface as well as an increase in conductance of the rescued CFTR channel. Luciani *et al*., (2012) observed in CFBE41o- cells transfected with ΔF508 CFTR that cystamine reduced the CFTR recycling and sustained the channel at the apical membrane compared to CFTR correctors, VX-325 or Corr-4a as well as significantly increasing the activity at the channel beyond the activity with CFTR corrector alone. This study supports the study carried out in chapter 6 suggesting that TG2 inhibitors prime ΔF508 CFTR and together with the CFTR corrector, VX-809 stabilize and increase NBD-1:ICL interactions. This in turn allows the read through of ΔF508 CFTR copies whilst precluding their proteosomal degradation, hence, increasing stable and mature CFTR copies trafficked to the plasma membrane.

Altogether, this study shows a link between TG2 expression and EMT in CF cells where TG2 activates TGFβ1, which plays a major role in orchestrating the downstream signalling involved in driving EMT. This phenomenon as illustrated in Figure 7.1 suggests a ΔF508 CFTR induced activation of TG2 due to the dysregulation of calcium levels in CF (Tabary *et al*., 2006, Ribeiro *et al*., 2005) inducing cell stress and a calcium-mediated activation of TG2. Once up regulated, TG2 is ultimately externalized by an unknown mechanism and remains active due to decreased GTPase inhibition and an increase in extracellular calcium stores, hence supporting the activation of TGFβ1 from their latent forms by TG2 mediated crosslinking of LLC to the matrix. Active TGFβ1 via its receptors, RI and RII signals the downstream transduction of

SMAD and non-SMAD pathways. Phosphorylation of SMADs 2 and 3 recruits recycling SMAD 4, where the heterocomplex formed is involved in activating TG2 on its promoter site via the TG2 response element (TRE). Increased TG2 activation supports the vicious cycle fuelling the continuous externalisation and activation of TGFβ1-TG2 in CF. Albeit, this is associated with a consequent loss of epithelial phenotype and acquisition of relatively high levels of EMT markers and transcriptional repressors which mechanistically drive the fibrosis in the disease. Concurrently, the ΔF508 mutation prevents the maturation and trafficking of matured CFTR from the endoplasmic reticulum to the plasma membrane due to premature denaturation. This study has demonstrated the "swiss-army knife" approach of TG2 in CF, where its inhibition blocks both intracellular and extracellular activation thus preventing the activation of TGFβ1 and its effects on the SMAD/non-SMAD pathways. Also, a synergy between TG2 inhibitors and CFTR correctors was shown to block a TG2 induced TGFβ1 mediated down regulation of CFTR, increase CFTR protein read through and maturation and its trafficking to the apical surface to function as a chloride conducting channel. Although other studies have attempted to relate EMT in alveoli cells to an aberration of TGFβ1, this study has provided the interrelationship between TG2 and TGFβ1 in a bronchial epithelial model of CF and for the first time shows fibrosis to be mediated via a TG2-TGFβ1-EMT driven pathway.

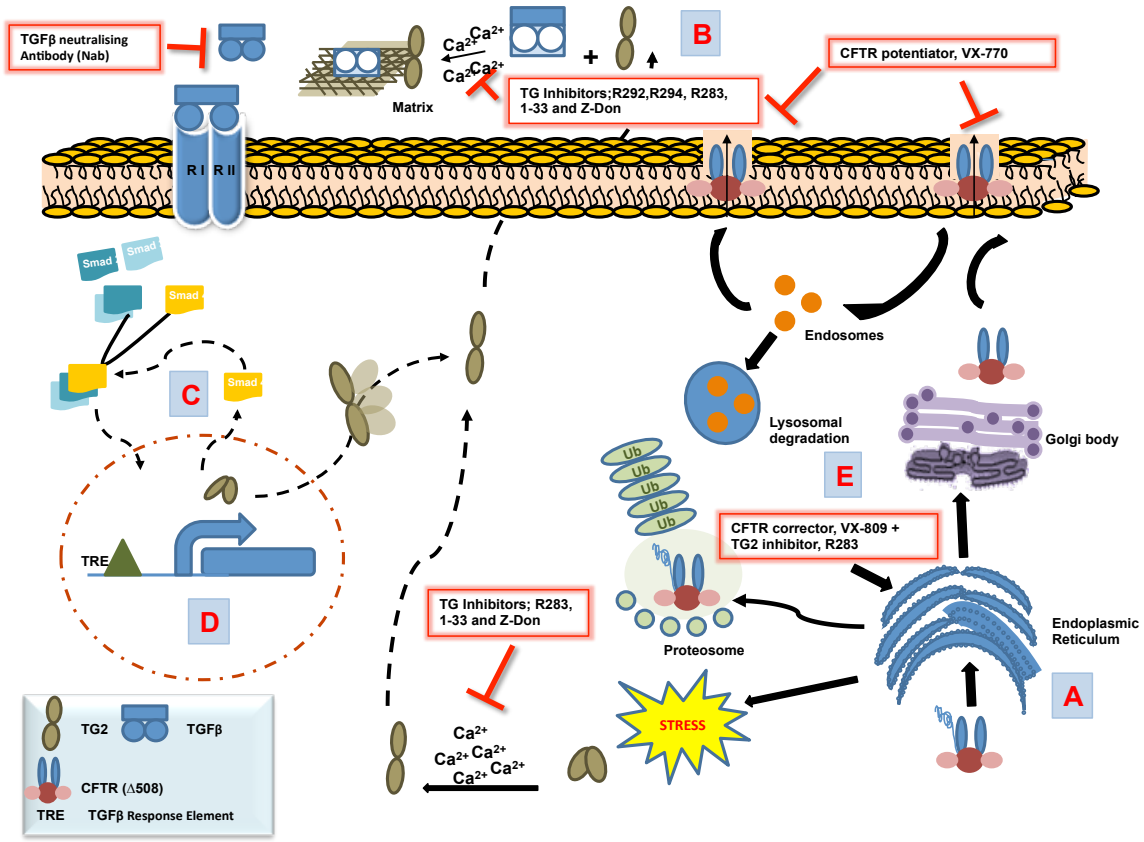

Figure 7.1: **Schematic representation of TG2 regulated EMT via TGFβ1 and the reparative effect of TG2 inhibitors/CFTR correctors in CF**. The ΔF508 mutation induces cell stress, **A** which distorts cellular milieu increasing intracellular TG2 levels. Externalisation of TG2 activates TGFβ1 from its latent forms, **B** thus orchestrating a down stream activation of SMAD pathway via SMADS 2,3 and 4, **C**. TG2 gene activation via its response element, TRE, further elevates TG2 synthesis, **D**. Similarly, ΔF508 mutation impedes trafficking of matured CFTR to the apical surface. The use of TG2 inhibitors/CFTR corrector stabilizes and supports the trafficking of matured CFTR copies to the apical surface deluding proteosomal degradation, **E**.

Chapter 8

Future work

8.1 Future Work

In other to continue the work carried out in this study, further investigation can be undertaken as follows:

- Determine the apical expression of CFTR in IB3, IB3-TG2 shRNA, C38 and HBEC cells using a robust membrane fractionation kit in both ALI and submerged medium as well as using Zona Occludens-1/E-cadherin as a membrane marker.

- Using primary human bronchial epithelial cells, HBEC with wild type and mutant CFTR transduced into these cells to determine the CFTR phenotype with regards to EMT markers expression in submerged and at ALI.

- Following culture of cells at ALI, histological analysis of CF mutant cell, IB3 cells and CFTR mutant transfected human bronchial epithelial cell ie HBEC-ΔF508CFTR and control HBEC treated with CFTR correctors ie VX-809, VX-532 or Corr-4A and the TG2 cell-permeable/impermeable inhibitors ie 1-133/1-155. Then determine apical surface TG2/CFTR expression as well as EMT expression in these cells.

- Determine the intracellular Ca^{2+} ion levels in IB3 cells and mutant CFTR cells transduced HBEC in order to predict active intracellular/extracellular TG2 activation in-situ in CF.

- Investigate the use of Human bronchial epithelial cells from CF patients for the effect of TG2 inhibitors/CFTR correctors on CFTR maturation and trafficking

- Demonstrate using chloride dye, CFTR conductance in IB3 cells, C38 cells HBEC and HBEC transduced with mutant CFTR in the presence of TG2 cell-permeable/impermeable inhibitors and CFTR correctors.

- Use cDNA of the 3 different domains of the CFTR channel to investigate the effect of TG2 inhibitors on the stability and interactions of the domains towards enhancing CFTR channel read-through.

- Undertake animal studies, where TG2 inhibitors can be used in CFTR wild type and deficient mice and in combination with CFTR correctors to observe their *in-vivo* effect on CFTR maturation.

References

Anonymous, 1993. Correlation between genotype and phenotype in patients with cystic fibrosis. The Cystic Fibrosis Genotype-Phenotype Consortium. *N Engl J Med,* 329**,** 1308-13.

Abe, M., Harpel, J. G., Metz, C. N., Nunes, I., Loskutoff, D. J. & Rifkin, D. B. 1994. An assay for transforming growth factor-beta using cells transfected with a plasminogen activator inhibitor-1 promoter-luciferase construct. *Anal Biochem,* 216**,** 276-84.

Accurso, F. J., Rowe, S. M., Clancy, J. P., Boyle, M. P., Dunitz, J. M., Durie, P. R., Sagel, S. D., Hornick, D. B., Konstan, M. W., Donaldson, S. H., Moss, R. B., Pilewski, J. M., Rubenstein, R. C., Uluer, A. Z., Aitken, M. L., Freedman, S. D., Rose, L. M., Mayer-Hamblett, N., Dong, Q., Zha, J., Stone, A. J., Olson, E. R., Ordonez, C. L., Campbell, P. W., Ashlock, M. A. & Ramsey, B. W. 2010. Effect of VX-770 in persons with cystic fibrosis and the G551D-CFTR mutation. *N Engl J Med,* 363**,** 1991-2003.

Achyuthan, K. E. & Greenberg, C. S. 1987. Identification of a guanosine triphosphate-binding site on guinea pig liver transglutaminase. Role of GTP and calcium ions in modulating activity. *J Biol Chem,* 262**,** 1901-6.

Aeschlimann, D., Kaupp, O. & Paulsson, M. 1995. Transglutaminase-catalyzed matrix crosslinking in differentiating cartilage: identification of osteonectin as a major glutaminyl substrate. *J Cell Biol,* 129**,** 881-92.

Aeschlimann, D. & Thomazy, V. 2000. Protein crosslinking in assembly and remodelling of extracellular matrices: the role of transglutaminases. *Connect Tissue Res,* 41**,** 1-27.

Aeschlimann, D., Wetterwald, A., Fleisch, H. & Paulsson, M. 1993. Expression of tissue transglutaminase in skeletal tissues correlates with events of terminal differentiation of chondrocytes. *J Cell Biol,* 120**,** 1461-70.

Akimov, S. S. & Belkin, A. M. 2001a. Cell surface tissue transglutaminase is involved in adhesion and migration of monocytic cells on fibronectin. *Blood,* 98**,** 1567-76.

Akimov, S. S. & Belkin, A. M. 2001b. Cell-surface transglutaminase promotes fibronectin assembly via interaction with the gelatin-binding domain of fibronectin: a role in TGFbeta-dependent matrix deposition. *J Cell Sci,* 114**,** 2989-3000.

Altamura, N., Castaldo, R., Finotti, A., Breveglieri, G., Salvatori, F., Zuccato, C., Gambari, R., Panin, G. C. & Borgatti, M. 2013. Tobramycin is a suppressor of premature termination codons. *J Cyst Fibros,* 12**,** 806-11.

Amaral, M. D., Pacheco, P., Beck, S., Farinha, C. M., Penque, D., Nogueira, P., Barreto, C., Lopes, B., Casals, T., Dapena, J., Gartner, S., Vasquez, C., Perez-Frias, J., Olveira, C., Cabanas, R., Estivill, X., Tzetis, M., Kanavakis, E., Doudounakis, S., Dork, T., Tummler, B., Girodon-Boulandet, E., Cazeneuve, C., Goossens, M., Blayau, M., Verlingue, C., Vieira, I., Ferec, C., Claustres, M., Des Georges, M., Clavel, C., Birembaut, P., Hubert, D., Bienvenu, T., Adoun, M., Chomel, J. C., De Boeck, K., Cuppens, H. & Lavinha, J. 2001. Cystic fibrosis patients with the 3272-26A>G splicing mutation have milder disease than F508del homozygotes: a large European study. *J Med Genet,* 38**,** 777-83.

Anderson, M. P. & Welsh, M. J. 1991. Calcium and cAMP activate different chloride channels in the apical membrane of normal and cystic fibrosis epithelia. *Proc Natl Acad Sci U S A,* 88**,** 6003-7.

Ann, D. K., Wu, M. M., Huang, T., Carlson, D. M. & Wu, R. 1988. Retinol-regulated gene expression in human tracheobronchial epithelial cells. Enhanced expression of elongation factor EF-1 alpha. *J Biol Chem,* 263**,** 3546-9.

Annes, J. P., Chen, Y., Munger, J. S. & Rifkin, D. B. 2004. Integrin alphaVbeta6-mediated activation of latent TGF-beta requires the latent TGF-beta binding protein-1. *J Cell Biol,* 165**,** 723-34.

Antonyak, M. A., Miller, A. M., Jansen, J. M., Boehm, J. E., Balkman, C. E., Wakshlag, J. J., Page, R. L. & Cerione, R. A. 2004. Augmentation of tissue transglutaminase expression and activation by epidermal growth factor inhibit doxorubicin-induced apoptosis in human breast cancer cells. *J Biol Chem,* 279**,** 41461-7.

Arentz-Hansen, H., Korner, R., Molberg, O., Quarsten, H., Vader, W., Kooy, Y. M., Lundin, K. E., Koning, F., Roepstorff, P., Sollid, L. M. & Mcadam, S. N. 2000. The intestinal T cell response to alpha-gliadin in adult celiac disease is focused on a single deamidated glutamine targeted by tissue transglutaminase. *J Exp Med,* 191**,** 603-12.

Arkwright, P. D., Laurie, S., Super, M., Pravica, V., Schwarz, M. J., Webb, A. K. & Hutchinson, I. V. 2000. TGF-beta(1) genotype and accelerated decline in lung function of patients with cystic fibrosis. *Thorax,* 55**,** 459-62.

Ashlock, M. A. & Olson, E. R. 2011. Therapeutics development for cystic fibrosis: a successful model for a multisystem genetic disease. *Annu Rev Med,* 62**,** 107-25.

Assemat, E., Bazellieres, E., Pallesi-Pocachard, E., Le Bivic, A. & Massey-Harroche, D. 2008. Polarity complex proteins. *Biochim Biophys Acta,* 1778**,** 614-30.

Badarau, E., Mongeot, A., Collighan, R., Rathbone, D. & Griffin, M. 2013. Imidazolium-based warheads strongly influence activity of water-soluble peptidic transglutaminase inhibitors. *Eur J Med Chem,* 66**,** 526-30.

Bailey, C. D. & Johnson, G. V. 2006. The protective effects of cystamine in the R6/2 Huntington's disease mouse involve mechanisms other than the inhibition of tissue transglutaminase. *Neurobiol Aging,* 27**,** 871-9.

Bakin, A. V., Tomlinson, A. K., Bhowmick, N. A., Moses, H. L. & Arteaga, C. L. 2000. Phosphatidylinositol 3-kinase function is required for transforming growth factor beta-mediated epithelial to mesenchymal transition and cell migration. *J Biol Chem,* 275**,** 36803-10.

Balharry, D., Sexton, K. & Berube, K. A. 2008. An in vitro approach to assess the toxicity of inhaled tobacco smoke components: nicotine, cadmium, formaldehyde and urethane. *Toxicology,* 244**,** 66-76.

Balklava, Z., Verderio, E., Collighan, R., Gross, S., Adams, J. & Griffin, M. 2002. Analysis of tissue transglutaminase function in the migration of Swiss 3T3 fibroblasts: the active-state conformation of the enzyme does not affect cell motility but is important for its secretion. *J Biol Chem,* 277**,** 16567-75.

Barrallo-Gimeno, A. & Nieto, M. A. 2005. The Snail genes as inducers of cell movement and survival: implications in development and cancer. *Development,* 132**,** 3151-61.

Bartram, U. 2004. The Role of Transforming Growth Factor in Lung Development and Disease. *Chest,* 125**,** 754-765.

Belkin, A. M. 2011. Extracellular TG2: emerging functions and regulation. *FEBS J,* 278**,** 4704-16.

Beninati, S. & Piacentini, M. 2004. The transglutaminase family: an overview: minireview article. *Amino Acids,* 26**,** 367-72.

Bergamini, C. M. 1988. GTP modulates calcium binding and cation-induced conformational changes in erythrocyte transglutaminase. *FEBS Lett,* 239**,** 255-8.

Bergamini, C. M. & Signorini, M. 1993. Studies on tissue transglutaminases: interaction of erythrocyte type-2 transglutaminase with GTP. *Biochem J,* 291 (Pt 1)**,** 37-9.

Berkowitz, R. D., Hammarskjold, M. L., Helga-Maria, C., Rekosh, D. & Goff, S. P. 1995. 5' regions of HIV-1 RNAs are not sufficient for encapsidation: implications for the HIV-1 packaging signal. *Virology,* 212**,** 718-23.

Berube, K., Aufderheide, M., Breheny, D., Clothier, R., Combes, R., Duffin, R., Forbes, B., Gaca, M., Gray, A., Hall, I., Kelly, M., Lethem, M., Liebsch, M., Merolla, L., Morin, J. P., Seagrave, J., Swartz, M. A., Tetley, T. D. & Umachandran, M.

2009. In vitro models of inhalation toxicity and disease. The report of a FRAME workshop. *Altern Lab Anim,* 37**,** 89-141.

Berube, K., Prytherch, Z., Job, C. & Hughes, T. 2010. Human primary bronchial lung cell constructs: the new respiratory models. *Toxicology,* 278**,** 311-8.

Bobadilla, J. L., Macek, M., Fine, J. P. & Farrell, P. M. 2002. Cystic fibrosis: A worldwide analysis ofCFTR mutations?correlation with incidence data and application to screening. *Human Mutation,* 19**,** 575-606.

Bombieri, C., Claustres, M., De Boeck, K., Derichs, N., Dodge, J., Girodon, E., Sermet, I., Schwarz, M., Tzetis, M., Wilschanski, M., Bareil, C., Bilton, D., Castellani, C., Cuppens, H., Cutting, G. R., Drevinek, P., Farrell, P., Elborn, J. S., Jarvi, K., Kerem, B., Kerem, E., Knowles, M., Macek, M., Jr., Munck, A., Radojkovic, D., Seia, M., Sheppard, D. N., Southern, K. W., Stuhrmann, M., Tullis, E., Zielenski, J., Pignatti, P. F. & Ferec, C. 2011. Recommendations for the classification of diseases as CFTR-related disorders. *J Cyst Fibros,* 10 Suppl 2**,** S86-102.

Bompadre, S. G., Sohma, Y., Li, M. & Hwang, T. C. 2007. G551D and G1349D, two CF-associated mutations in the signature sequences of CFTR, exhibit distinct gating defects. *J Gen Physiol,* 129**,** 285-98.

Bonfield, T. L., Konstan, M. W. & Berger, M. 1999. Altered respiratory epithelial cell cytokine production in cystic fibrosis. *J Allergy Clin Immunol,* 104**,** 72-8.

Boyer, A. S., Erickson, C. P. & Runyan, R. B. 1999. Epithelial-mesenchymal transformation in the embryonic heart is mediated through distinct pertussis toxin-sensitive and TGFbeta signal transduction mechanisms. *Dev Dyn,* 214**,** 81-91.

Boyle, M. P., Bell, S. C., Konstan, M. W., Mccolley, S. A., Rowe, S. M., Rietschel, E., Huang, X., Waltz, D., Patel, N. R. & Rodman, D. 2014. A CFTR corrector (lumacaftor) and a CFTR potentiator (ivacaftor) for treatment of patients with cystic fibrosis who have a phe508del CFTR mutation: a phase 2 randomised controlled trial. *Lancet Respir Med,* 2**,** 527-38.

Bremer, L. A., Blackman, S. M., Vanscoy, L. L., Mcdougal, K. E., Bowers, A., Naughton, K. M., Cutler, D. J. & Cutting, G. R. 2008. Interaction between a novel TGFB1 haplotype and CFTR genotype is associated with improved lung function in cystic fibrosis. *Hum Mol Genet,* 17**,** 2228-37.

Breuss, J. M., Gallo, J., Delisser, H. M., Klimanskaya, I. V., Folkesson, H. G., Pittet, J. F., Nishimura, S. L., Aldape, K., Landers, D. V., Carpenter, W. & Et Al. 1995. Expression of the beta 6 integrin subunit in development, neoplasia and tissue repair suggests a role in epithelial remodeling. *J Cell Sci,* 108 (Pt 6)**,** 2241-51.

Breuss, J. M., Gillett, N., Lu, L., Sheppard, D. & Pytela, R. 1993. Restricted distribution of integrin beta 6 mRNA in primate epithelial tissues. *J Histochem Cytochem,* 41**,** 1521-7.

Busk, M., Pytela, R. & Sheppard, D. 1992. Characterization of the integrin alpha v beta 6 as a fibronectin-binding protein. *J Biol Chem,* 267**,** 5790-6.

Camara, J. & Jarai, G. 2010. Epithelial-mesenchymal transition in primary human bronchial epithelial cells is Smad-dependent and enhanced by fibronectin and TNF-alpha. *Fibrogenesis Tissue Repair,* 3**,** 2.

Candi, E., Oddi, S., Terrinoni, A., Paradisi, A., Ranalli, M., Finazzi-Agro, A. & Melino, G. 2001. Transglutaminase 5 cross-links loricrin, involucrin, and small proline-rich proteins in vitro. *J Biol Chem,* 276**,** 35014-23.

Cano, A., Perez-Moreno, M. A., Rodrigo, I., Locascio, A., Blanco, M. J., Del Barrio, M. G., Portillo, F. & Nieto, M. A. 2000. The transcription factor snail controls epithelial-mesenchymal transitions by repressing E-cadherin expression. *Nat Cell Biol,* 2**,** 76-83.

Cao, L., Shao, M., Schilder, J., Guise, T., Mohammad, K. S. & Matei, D. 2012. Tissue transglutaminase links TGF-beta, epithelial to mesenchymal transition and a stem cell phenotype in ovarian cancer. *Oncogene,* 31**,** 2521-34.

Carterson, A. J., Honer Zu Bentrup, K., Ott, C. M., Clarke, M. S., Pierson, D. L., Vanderburg, C. R., Buchanan, K. L., Nickerson, C. A. & Schurr, M. J. 2005. A549 lung epithelial cells grown as three-dimensional aggregates: alternative tissue culture model for Pseudomonas aeruginosa pathogenesis. *Infect Immun,* 73**,** 1129-40.

Casadio, R., Polverini, E., Mariani, P., Spinozzi, F., Carsughi, F., Fontana, A., Polverino De Laureto, P., Matteucci, G. & Bergamini, C. M. 1999. The structural basis for the regulation of tissue transglutaminase by calcium ions. *Eur J Biochem,* 262**,** 672-9.

Castellani, C., Bonizzato, A., Pradal, U., Filicori, M., Foresta, C., La Sala, G. B. & Mastella, G. 1999. Evidence of mild respiratory disease in men with congenital absence of the vas deferens. *Respir Med,* 93**,** 869-75.

Chacko, B. M., Qin, B. Y., Tiwari, A., Shi, G., Lam, S., Hayward, L. J., De Caestecker, M. & Lin, K. 2004. Structural basis of heteromeric smad protein assembly in TGF-beta signaling. *Mol Cell,* 15**,** 813-23.

Chmiel, J. F. & Davis, P. B. 2003. State of the art: why do the lungs of patients with cystic fibrosis become infected and why can't they clear the infection? *Respir Res,* 4**,** 8.

Cho, H. J., Baek, K. E., Saika, S., Jeong, M. J. & Yoo, J. 2007. Snail is required for transforming growth factor-beta-induced epithelial-mesenchymal transition by

activating PI3 kinase/Akt signal pathway. *Biochem Biophys Res Commun,* 353**,** 337-43.

Cho, S. Y., Jeon, J. H., Kim, C. W., Shin, D. M., Jang, G. Y., Jeong, E. M., Lee, S. E., Song, K. Y. & Kim, I. G. 2010. Monoclonal antibodies to human transglutaminase 4. *Hybridoma (Larchmt),* 29**,** 263-7.

Choo-Kang, L. R. & Zeitlin, P. L. 2001. Induction of HSP70 promotes DeltaF508 CFTR trafficking. *Am J Physiol Lung Cell Mol Physiol,* 281**,** L58-68.

Chopra, D. P., Klinger, M. M. & Sullivan, J. K. 1989. Effects of vitamin A on growth and differentiation of human tracheobronchial epithelial cell cultures in serum-free medium. *J Cell Sci,* 93 (Pt 1)**,** 133-42.

Chuchalin, A., Amelina, E. & Bianco, F. 2009. Tobramycin for inhalation in cystic fibrosis: Beyond respiratory improvements. *Pulm Pharmacol Ther,* 22**,** 526-32.

Clancy, J. P., Rowe, S. M., Accurso, F. J., Aitken, M. L., Amin, R. S., Ashlock, M. A., Ballmann, M., Boyle, M. P., Bronsveld, I., Campbell, P. W., De Boeck, K., Donaldson, S. H., Dorkin, H. L., Dunitz, J. M., Durie, P. R., Jain, M., Leonard, A., Mccoy, K. S., Moss, R. B., Pilewski, J. M., Rosenbluth, D. B., Rubenstein, R. C., Schechter, M. S., Botfield, M., Ordonez, C. L., Spencer-Green, G. T., Vernillet, L., Wisseh, S., Yen, K. & Konstan, M. W. 2012. Results of a phase IIa study of VX-809, an investigational CFTR corrector compound, in subjects with cystic fibrosis homozygous for the F508del-CFTR mutation. *Thorax,* 67**,** 12-8.

Coffman, R. L. & Hessel, E. M. 2005. Nonhuman primate models of asthma. *J Exp Med,* 201**,** 1875-9.

Colin, A. A., Sawyer, S. M., Mickle, J. E., Oates, R. D., Milunsky, A. & Amos, J. A. 1996. Pulmonary function and clinical observations in men with congenital bilateral absence of the vas deferens. *Chest,* 110**,** 440-5.

Collighan, R. J. & Griffin, M. 2009. Transglutaminase 2 crosslinking of matrix proteins: biological significance and medical applications. *Amino Acids,* 36**,** 659-70.

Comer, D. M., Ennis, M., Mcdowell, C., Beattie, D., Rendall, J., Hall, V. & Elborn, J. S. 2009. Clinical phenotype of cystic fibrosis patients with the G551D mutation. *QJM,* 102**,** 793-8.

Comijn, J., Berx, G., Vermassen, P., Verschueren, K., Van Grunsven, L., Bruyneel, E., Mareel, M., Huylebroeck, D. & Van Roy, F. 2001. The two-handed E box binding zinc finger protein SIP1 downregulates E-cadherin and induces invasion. *Mol Cell,* 7**,** 1267-78.

Cutting, G. R., Kasch, L. M., Rosenstein, B. J., Zielenski, J., Tsui, L. C., Antonarakis, S. E. & Kazazian, H. H., Jr. 1990. A cluster of cystic fibrosis mutations in the first nucleotide-binding fold of the cystic fibrosis conductance regulator protein. *Nature,* 346**,** 366-9.

Dalemans, W., Barbry, P., Champigny, G., Jallat, S., Dott, K., Dreyer, D., Crystal, R. G., Pavirani, A., Lecocq, J. P. & Lazdunski, M. 1991. Altered chloride ion channel kinetics associated with the delta F508 cystic fibrosis mutation. *Nature,* 354**,** 526-8.

Davis, P. & Di Sant'agnese, P. 1984. Diagnosis and treatment of cystic fibrosis. An update. *Chest,* 85**,** 802-809.

De Boeck, K., Munck, A., Walker, S., Faro, A., Hiatt, P., Gilmartin, G. & Higgins, M. 2014. Efficacy and safety of ivacaftor in patients with cystic fibrosis and a non-G551D gating mutation. *J Cyst Fibros*.

De Gracia, J., Mata, F., Alvarez, A., Casals, T., Gatner, S., Vendrell, M., De La Rosa, D., Guarner, L. & Hermosilla, E. 2005. Genotype-phenotype correlation for pulmonary function in cystic fibrosis. *Thorax,* 60**,** 558-63.

De Jong, P. M., Van Sterkenburg, M. A., Hesseling, S. C., Kempenaar, J. A., Mulder, A. A., Mommaas, A. M., Dijkman, J. H. & Ponec, M. 1994. Ciliogenesis in human bronchial epithelial cells cultured at the air-liquid interface. *Am J Respir Cell Mol Biol,* 10**,** 271-7.

Derynck, R. & Zhang, Y. E. 2003. Smad-dependent and Smad-independent pathways in TGF-beta family signalling. *Nature,* 425**,** 577-84.

Dimango, E., Ratner, A. J., Bryan, R., Tabibi, S. & Prince, A. 1998. Activation of NF-kappaB by adherent Pseudomonas aeruginosa in normal and cystic fibrosis respiratory epithelial cells. *J Clin Invest,* 101**,** 2598-605.

Dodge, J. A., Lewis, P. A., Stanton, M. & Wilsher, J. 2007. Cystic fibrosis mortality and survival in the UK: 1947-2003. *Eur Respir J,* 29**,** 522-6.

Doerner, A. M. & Zuraw, B. L. 2009. TGF-beta1 induced epithelial to mesenchymal transition (EMT) in human bronchial epithelial cells is enhanced by IL-1beta but not abrogated by corticosteroids. *Respir Res,* 10**,** 100.

Drumm, M. L., Konstan, M. W., Schluchter, M. D., Handler, A., Pace, R., Zou, F., Zariwala, M., Fargo, D., Xu, A., Dunn, J. M., Darrah, R. J., Dorfman, R., Sandford, A. J., Corey, M., Zielenski, J., Durie, P., Goddard, K., Yankaskas, J. R., Wright, F. A. & Knowles, M. R. 2005. Genetic modifiers of lung disease in cystic fibrosis. *N Engl J Med,* 353**,** 1443-53.

Dubbink, H. J., De Waal, L., Van Haperen, R., Verkaik, N. S., Trapman, J. & Romijn, J. C. 1998. The human prostate-specific transglutaminase gene (TGM4): genomic organization, tissue-specific expression, and promoter characterization. *Genomics,* 51**,** 434-44.

Dubbink, H. J., Verkaik, N. S., Faber, P. W., Trapman, J., Schroder, F. H. & Romijn, J. C. 1996. Tissue specific and androgen-regulated expression of human prostate-specific transglutaminase. *Biochem J,* 315 (Pt 3)**,** 901-8.

Dull, T., Zufferey, R., Kelly, M., Mandel, R. J., Nguyen, M., Trono, D. & Naldini, L. 1998. A third-generation lentivirus vector with a conditional packaging system. *J Virol,* 72**,** 8463-71.

Eckert, R. L. 1989. Structure, function, and differentiation of the keratinocyte. *Physiol Rev,* 69**,** 1316-46.

Edwards, D. R., Murphy, G., Reynolds, J. J., Whitham, S. E., Docherty, A. J., Angel, P. & Heath, J. K. 1987. Transforming growth factor beta modulates the expression of collagenase and metalloproteinase inhibitor. *EMBO J,* 6**,** 1899-904.

Eickmeier, O., Boom, L., Schreiner, F., Lentze, M. J., D, N. G., Schubert, R., Zielen, S. & Schmitt-Grohe, S. 2013. Transforming growth factor beta1 genotypes in relation to TGFbeta1, interleukin-8, and tumor necrosis factor alpha in induced sputum and blood in cystic fibrosis. *Mediators Inflamm,* 2013**,** 913135.

Feingold, J. & Guilloud-Bataille, M. 1999. Genetic comparisons of patients with cystic fibrosis with or without meconium ileus. Clinical Centers of the French CF Registry. *Ann Genet,* 42**,** 147-50.

Ferec, C. & Cutting, G. R. 2012. Assessing the Disease-Liability of Mutations in CFTR. *Cold Spring Harb Perspect Med,* 2**,** a009480.

Fesus, L., Thomazy, V., Autuori, F., Ceru, M. P., Tarcsa, E. & Piacentini, M. 1989. Apoptotic hepatocytes become insoluble in detergents and chaotropic agents as a result of transglutaminase action. *FEBS Lett,* 245**,** 150-4.

Folk, J. E. & Finlayson, J. S. 1977. The epsilon-(gamma-glutamyl)lysine crosslink and the catalytic role of transglutaminases. *Adv Protein Chem,* 31**,** 1-133.

Fontana, L., Chen, Y., Prijatelj, P., Sakai, T., Fassler, R., Sakai, L. Y. & Rifkin, D. B. 2005. Fibronectin is required for integrin alphavbeta6-mediated activation of latent TGF-beta complexes containing LTBP-1. *FASEB J,* 19**,** 1798-808.

Frank, J., Roux, J., Kawakatsu, H., Su, G., Dagenais, A., Berthiaume, Y., Howard, M., Canessa, C. M., Fang, X., Sheppard, D., Matthay, M. A. & Pittet, J. F. 2003. Transforming growth factor-beta1 decreases expression of the epithelial sodium channel alphaENaC and alveolar epithelial vectorial sodium and fluid transport via an ERK1/2-dependent mechanism. *J Biol Chem,* 278**,** 43939-50.

Frischmeyer, P. A. & Dietz, H. C. 1999. Nonsense-mediated mRNA decay in health and disease. *Hum Mol Genet,* 8**,** 1893-900.

Fulmer, S. B., Schwiebert, E. M., Morales, M. M., Guggino, W. B. & Cutting, G. R. 1995. Two cystic fibrosis transmembrane conductance regulator mutations have different effects on both pulmonary phenotype and regulation of outwardly rectified chloride currents. *Proc Natl Acad Sci U S A,* 92**,** 6832-6.

Gaudry, C. A., Verderio, E., Aeschlimann, D., Cox, A., Smith, C. & Griffin, M. 1999a. Cell surface localisation of tissue transglutaminase is dependent on a

fibronectin-binding site in its N-terminal beta-sandwich domain. *J Biol Chem,* 274**,** 30707-14.

Gaudry, C. A., Verderio, E., Jones, R. A., Smith, C. & Griffin, M. 1999b. Tissue transglutaminase is an important player at the surface of human endothelial cells: evidence for its externalisation and its colocalisation with the beta(1) integrin. *Exp Cell Res,* 252**,** 104-13.

George, M. D., Vollberg, T. M., Floyd, E. E., Stein, J. P. & Jetten, A. M. 1990. Regulation of transglutaminase type II by transforming growth factor-beta 1 in normal and transformed human epidermal keratinocytes. *J Biol Chem,* 265**,** 11098-104.

Graff, J. M., Bansal, A. & Melton, D. A. 1996. Xenopus Mad proteins transduce distinct subsets of signals for the TGF beta superfamily. *Cell,* 85**,** 479-87.

Grainger, C. I., Greenwell, L. L., Lockley, D. J., Martin, G. P. & Forbes, B. 2006. Culture of Calu-3 Cells at the Air Interface Provides a Representative Model of the Airway Epithelial Barrier. *Pharmaceutical Research,* 23**,** 1482-1490.

Grande, J. P. 1997. Role of transforming growth factor-beta in tissue injury and repair. *Proc Soc Exp Biol Med,* 214**,** 27-40.

Grande, M., Franzen, A., Karlsson, J. O., Ericson, L. E., Heldin, N. E. & Nilsson, M. 2002. Transforming growth factor-beta and epidermal growth factor synergistically stimulate epithelial to mesenchymal transition (EMT) through a MEK-dependent mechanism in primary cultured pig thyrocytes. *J Cell Sci,* 115**,** 4227-36.

Greenberg, C. S., Birckbichler, P. J. & Rice, R. H. 1991. Transglutaminases: multifunctional crosslinking enzymes that stabilize tissues. *FASEB J,* 5**,** 3071-7.

Griffin, M., Casadio, R. & Bergamini, C. M. 2002. Transglutaminases: nature's biological glues. *Biochem J,* 368**,** 377-96.

Griffin, M., Mongeot, A., Collighan, R., Saint, R. E., Jones, R. A., Coutts, I. G. & Rathbone, D. L. 2008. Synthesis of potent water-soluble tissue transglutaminase inhibitors. *Bioorg Med Chem Lett,* 18**,** 5559-62.

Griffin, M., Smith, L. L. & Wynne, J. 1979. Changes in transglutaminase activity in an experimental model of pulmonary fibrosis induced by paraquat. *Br J Exp Pathol,* 60**,** 653-61.

Griffith, L. G. & Swartz, M. A. 2006. Capturing complex 3D tissue physiology in vitro. *Nat Rev Mol Cell Biol,* 7**,** 211-24.

Grosso, H. & Mouradian, M. M. 2012. Transglutaminase 2: biology, relevance to neurodegenerative diseases and therapeutic implications. *Pharmacol Ther,* 133**,** 392-410.

Grove, D. E., Rosser, M. F. N., Ren, H. Y., Naren, A. P. & Cyr, D. M. 2009. Mechanisms for Rescue of Correctable Folding Defects in CFTR F508. *Molecular Biology of the Cell,* 20**,** 4059-4069.

Gruenert, D. C., Finkbeiner, W. E. & Widdicombe, J. H. 1995. Culture and transformation of human airway epithelial cells. *Am J Physiol,* 268**,** L347-60.

Gundemir, S., Colak, G., Tucholski, J. & Johnson, G. V. 2012. Transglutaminase 2: a molecular Swiss army knife. *Biochim Biophys Acta,* 1823**,** 406-19.

Gundemir, S. & Johnson, G. V. 2009. Intracellular localisation and conformational state of transglutaminase 2: implications for cell death. *PLoS One,* 4**,** e6123.

Haardt, M., Benharouga, M., Lechardeur, D., Kartner, N. & Lukacs, G. L. 1999. C-terminal truncations destabilize the cystic fibrosis transmembrane conductance regulator without impairing its biogenesis. A novel class of mutation. *J Biol Chem,* 274**,** 21873-7.

Hackett, T. L., Warner, S. M., Stefanowicz, D., Shaheen, F., Pechkovsky, D. V., Murray, L. A., Argentieri, R., Kicic, A., Stick, S. M., Bai, T. R. & Knight, D. A. 2009. Induction of epithelial-mesenchymal transition in primary airway epithelial cells from patients with asthma by transforming growth factor-beta1. *Am J Respir Crit Care Med,* 180**,** 122-33.

Hamosh, A., Rosenstein, B. J. & Cutting, G. R. 1992. CFTR nonsense mutations G542X and W1282X associated with severe reduction of CFTR mRNA in nasal epithelial cells. *Hum Mol Genet,* 1**,** 542-4.

Harrison, C. A., Layton, C. M., Hau, Z., Bullock, A. J., Johnson, T. S. & Macneil, S. 2007. Transglutaminase inhibitors induce hyperproliferation and parakeratosis in tissue-engineered skin. *Br J Dermatol,* 156**,** 247-57.

Harrison, M. J., Murphy, D. M. & Plant, B. J. 2013. Ivacaftor in a G551D homozygote with cystic fibrosis. *N Engl J Med,* 369**,** 1280-2.

Hasegawa, G., Suwa, M., Ichikawa, Y., Ohtsuka, T., Kumagai, S., Kikuchi, M., Sato, Y. & Saito, Y. 2003. A novel function of tissue-type transglutaminase: protein disulphide isomerase. *Biochem J,* 373**,** 793-803.

Hata, A., Lagna, G., Massague, J. & Hemmati-Brivanlou, A. 1998. Smad6 inhibits BMP/Smad1 signaling by specifically competing with the Smad4 tumor suppressor. *Genes Dev,* 12**,** 186-97.

Hay, E. D. 1995. An overview of epithelio-mesenchymal transformation. *Acta Anat (Basel),* 154**,** 8-20.

Heath, D. J., Christian, P. & Griffin, M. 2002. Involvement of tissue transglutaminase in the stabilisation of biomaterial/tissue interfaces important in medical devices. *Biomaterials,* 23**,** 1519-26.

Hegedus, T., Aleksandrov, A., Mengos, A., Cui, L., Jensen, T. J. & Riordan, J. R. 2009. Role of individual R domain phosphorylation sites in CFTR regulation by protein kinase A. *Biochim Biophys Acta,* 1788**,** 1341-9.

Heldin, C. H., Miyazono, K. & Ten Dijke, P. 1997. TGF-beta signalling from cell membrane to nucleus through SMAD proteins. *Nature,* 390**,** 465-71.

Heldin, C. H., Vanlandewijck, M. & Moustakas, A. 2012. Regulation of EMT by TGFbeta in cancer. *FEBS Lett,* 586**,** 1959-70.

Henderson, N. C. & Sheppard, D. 2013. Integrin-mediated regulation of TGFbeta in fibrosis. *Biochim Biophys Acta,* 1832**,** 891-6.

Hiiragi, T., Sasaki, H., Nagafuchi, A., Sabe, H., Shen, S. C., Matsuki, M., Yamanishi, K. & Tsukita, S. 1999. Transglutaminase type 1 and its crosslinking activity are concentrated at adherens junctions in simple epithelial cells. *J Biol Chem,* 274**,** 34148-54.

Hilliard, T. N., Regamey, N., Shute, J. K., Nicholson, A. G., Alton, E. W., Bush, A. & Davies, J. C. 2007. Airway remodelling in children with cystic fibrosis. *Thorax,* 62**,** 1074-80.

Hoodless, P. A., Haerry, T., Abdollah, S., Stapleton, M., O'connor, M. B., Attisano, L. & Wrana, J. L. 1996. MADR1, a MAD-related protein that functions in BMP2 signaling pathways. *Cell,* 85**,** 489-500.

Hoot, K. E., Lighthall, J., Han, G., Lu, S. L., Li, A., Ju, W., Kulesz-Martin, M., Bottinger, E. & Wang, X. J. 2008. Keratinocyte-specific Smad2 ablation results in increased epithelial-mesenchymal transition during skin cancer formation and progression. *J Clin Invest,* 118**,** 2722-32.

Huang, L., Haylor, J. L., Fisher, M., Hau, Z., El Nahas, A. M., Griffin, M. & Johnson, T. S. 2010. Do changes in transglutaminase activity alter latent transforming growth factor beta activation in experimental diabetic nephropathy? *Nephrol Dial Transplant,* 25**,** 3897-910.

Ichinose, A. & Davie, E. W. 1988. Characterization of the gene for the a subunit of human factor XIII (plasma transglutaminase), a blood coagulation factor. *Proc Natl Acad Sci U S A,* 85**,** 5829-33.

Iismaa, S. E. 2003. Evolutionary specialization of a tryptophan indole group for transition-state stabilisation by eukaryotic transglutaminases. *Proceedings of the National Academy of Sciences,* 100**,** 12636-12641.

Iismaa, S. E., Mearns, B. M., Lorand, L. & Graham, R. M. 2009. Transglutaminases and disease: lessons from genetically engineered mouse models and inherited disorders. *Physiol Rev,* 89**,** 991-1023.

Ikenouchi, J., Matsuda, M., Furuse, M. & Tsukita, S. 2003. Regulation of tight junctions during the epithelium-mesenchyme transition: direct repression of the gene expression of claudins/occludin by Snail. *J Cell Sci,* 116**,** 1959-67.

Jacquot, J., Tabary, O., Le Rouzic, P. & Clement, A. 2008. Airway epithelial cell inflammatory signalling in cystic fibrosis. *The International Journal of Biochemistry & Cell Biology,* 40**,** 1703-1715.

Jilling, T. & Kirk, K. L. 1997. The biogenesis, traffic, and function of the cystic fibrosis transmembrane conductance regulator. *Int Rev Cytol,* 172**,** 193-241.

Johnson, G. V., Cox, T. M., Lockhart, J. P., Zinnerman, M. D., Miller, M. L. & Powers, R. E. 1997a. Transglutaminase activity is increased in Alzheimer's disease brain. *Brain Res,* 751**,** 323-9.

Johnson, L. G., Dickman, K. G., Moore, K. L., Mandel, L. J. & Boucher, R. C. 1993. Enhanced Na+ transport in an air-liquid interface culture system. *Am J Physiol,* 264**,** L560-5.

Johnson, T. S., Fisher, M., Haylor, J. L., Hau, Z., Skill, N. J., Jones, R., Saint, R., Coutts, I., Vickers, M. E., El Nahas, A. M. & Griffin, M. 2007. Transglutaminase Inhibition Reduces Fibrosis and Preserves Function in Experimental Chronic Kidney Disease. *Journal of the American Society of Nephrology,* 18**,** 3078-3088.

Johnson, T. S., Griffin, M., Thomas, G. L., Skill, J., Cox, A., Yang, B., Nicholas, B., Birckbichler, P. J., Muchaneta-Kubara, C. & Meguid El Nahas, A. 1997b. The role of transglutaminase in the rat subtotal nephrectomy model of renal fibrosis. *J Clin Invest,* 99**,** 2950-60.

Johnson, T. S., Knight, C. R., El-Alaoui, S., Mian, S., Rees, R. C., Gentile, V., Davies, P. J. & Griffin, M. 1994. Transfection of tissue transglutaminase into a highly malignant hamster fibrosarcoma leads to a reduced incidence of primary tumour growth. *Oncogene,* 9**,** 2935-42.

Johnson, T. S., Skill, N. J., El Nahas, A. M., Oldroyd, S. D., Thomas, G. L., Douthwaite, J. A., Haylor, J. L. & Griffin, M. 1999. Transglutaminase transcription and antigen translocation in experimental renal scarring. *J Am Soc Nephrol,* 10**,** 2146-57.

Jones, R. A., Kotsakis, P., Johnson, T. S., Chau, D. Y., Ali, S., Melino, G. & Griffin, M. 2006. Matrix changes induced by transglutaminase 2 lead to inhibition of angiogenesis and tumor growth. *Cell Death Differ,* 13**,** 1442-53.

Jones, R. A., Nicholas, B., Mian, S., Davies, P. J. & Griffin, M. 1997. Reduced expression of tissue transglutaminase in a human endothelial cell line leads to changes in cell spreading, cell adhesion and reduced polymerisation of fibronectin. *J Cell Sci,* 110 (Pt 19)**,** 2461-72.

Junn, E., Ronchetti, R. D., Quezado, M. M., Kim, S. Y. & Mouradian, M. M. 2003. Tissue transglutaminase-induced aggregation of alpha-synuclein: Implications for Lewy body formation in Parkinson's disease and dementia with Lewy bodies. *Proc Natl Acad Sci U S A,* 100**,** 2047-52.

Kalin, N., Claass, A., Sommer, M., Puchelle, E. & Tummler, B. 1999. DeltaF508 CFTR protein expression in tissues from patients with cystic fibrosis. *J Clin Invest,* 103**,** 1379-89.

Kalluri, R. & Neilson, E. G. 2003. Epithelial-mesenchymal transition and its implications for fibrosis. *J Clin Invest,* 112**,** 1776-84.

Kaminski, N., Allard, J. D., Pittet, J. F., Zuo, F., Griffiths, M. J., Morris, D., Huang, X., Sheppard, D. & Heller, R. A. 2000. Global analysis of gene expression in pulmonary fibrosis reveals distinct programs regulating lung inflammation and fibrosis. *Proc Natl Acad Sci U S A,* 97**,** 1778-83.

Karpuj, M. V., Becher, M. W., Springer, J. E., Chabas, D., Youssef, S., Pedotti, R., Mitchell, D. & Steinman, L. 2002. Prolonged survival and decreased abnormal movements in transgenic model of Huntington disease, with administration of the transglutaminase inhibitor cystamine. *Nat Med,* 8**,** 143-9.

Kasai, H., Allen, J. T., Mason, R. M., Kamimura, T. & Zhang, Z. 2005. TGF-beta1 induces human alveolar epithelial to mesenchymal cell transition (EMT). *Respir Res,* 6**,** 56.

Katoh, D., Nagaharu, K., Shimojo, N., Hanamura, N., Yamashita, M., Kozuka, Y., Imanaka-Yoshida, K. & Yoshida, T. 2013. Binding of alphavbeta1 and alphavbeta6 integrins to tenascin-C induces epithelial-mesenchymal transition-like change of breast cancer cells. *Oncogenesis,* 2**,** e65.

Katona, E., Nagy, B., Kappelmayer, J., Baktai, G., Kovacs, L., Marialigeti, T., Dezso, B. & Muszbek, L. 2005. Factor XIII in bronchoalveolar lavage fluid from children with chronic bronchoalveolar inflammation. *J Thromb Haemost,* 3**,** 1407-13.

Kawata, M., Koinuma, D., Ogami, T., Umezawa, K., Iwata, C., Watabe, T. & Miyazono, K. 2012. TGF-beta-induced epithelial-mesenchymal transition of A549 lung adenocarcinoma cells is enhanced by pro-inflammatory cytokines derived from RAW 264.7 macrophage cells. *J Biochem,* 151**,** 205-16.

Kelley, J., Fabisiak, J. P., Hawes, K. & Absher, M. 1991. Cytokine signaling in lung: transforming growth factor-beta secretion by lung fibroblasts. *Am J Physiol,* 260**,** L123-8.

Kerem, B., Rommens, J. M., Buchanan, J. A., Markiewicz, D., Cox, T. K., Chakravarti, A., Buchwald, M. & Tsui, L. C. 1989. Identification of the cystic fibrosis gene: genetic analysis. *Science,* 245**,** 1073-80.

Kerem, E., Hirawat, S., Armoni, S., Yaakov, Y., Shoseyov, D., Cohen, M., Nissim-Rafinia, M., Blau, H., Rivlin, J., Aviram, M., Elfring, G. L., Northcutt, V. J., Miller, L. L., Kerem, B. & Wilschanski, M. 2008. Effectiveness of PTC124 treatment of cystic fibrosis caused by nonsense mutations: a prospective phase II trial. *Lancet,* 372**,** 719-27.

Kerem, E., Konstan, M. W., De Boeck, K., Accurso, F. J., Sermet-Gaudelus, I., Wilschanski, M., Elborn, J. S., Melotti, P., Bronsveld, I., Fajac, I., Malfroot, A., Rosenbluth, D. B., Walker, P. A., Mccolley, S. A., Knoop, C., Quattrucci, S., Rietschel, E., Zeitlin, P. L., Barth, J., Elfring, G. L., Welch, E. M., Branstrom, A., Spiegel, R. J., Peltz, S. W., Ajayi, T. & Rowe, S. M. 2014. Ataluren for the treatment of nonsense-mutation cystic fibrosis: a randomised, double-blind, placebo-controlled phase 3 trial. *Lancet Respir Med*.

Kim, D. S., Park, S. S., Nam, B. H., Kim, I. H. & Kim, S. Y. 2006. Reversal of Drug Resistance in Breast Cancer Cells by Transglutaminase 2 Inhibition and Nuclear Factor- B Inactivation. *Cancer Research,* 66**,** 10936-10943.

Kim, H. 2001. Crystallization and Preliminary X-Ray Analysis of Human Transglutaminase 3 from Zymogen to Active Form. *Journal of Structural Biology,* 135**,** 73-77.

Kim, J. B., Islam, S., Kim, Y. J., Prudoff, R. S., Sass, K. M., Wheelock, M. J. & Johnson, K. R. 2000. N-Cadherin extracellular repeat 4 mediates epithelial to mesenchymal transition and increased motility. *J Cell Biol,* 151**,** 1193-206.

Kim, S. Y., Grant, P., Lee, J. H., Pant, H. C. & Steinert, P. M. 1999. Differential expression of multiple transglutaminases in human brain. Increased expression and crosslinking by transglutaminases 1 and 2 in Alzheimer's disease. *J Biol Chem,* 274**,** 30715-21.

Kojima, S., Nara, K. & Rifkin, D. B. 1993. Requirement for transglutaminase in the activation of latent transforming growth factor-beta in bovine endothelial cells. *J Cell Biol,* 121**,** 439-48.

Komaromi, I., Bagoly, Z. & Muszbek, L. 2011. Factor XIII: novel structural and functional aspects. *J Thromb Haemost,* 9**,** 9-20.

Konstan, M. W., Hilliard, K. A., Norvell, T. M. & Berger, M. 1994. Bronchoalveolar lavage findings in cystic fibrosis patients with stable, clinically mild lung disease suggest ongoing infection and inflammation. *Am J Respir Crit Care Med,* 150**,** 448-54.

Konstan, M. W. & Ratjen, F. 2012. Effect of dornase alfa on inflammation and lung function: potential role in the early treatment of cystic fibrosis. *J Cyst Fibros,* 11**,** 78-83.

Kretzschmar, M. & Massague, J. 1998. SMADs: mediators and regulators of TGF-beta signaling. *Curr Opin Genet Dev,* 8**,** 103-11.

Kumar, A., Xu, J., Brady, S., Gao, H., Yu, D., Reuben, J. & Mehta, K. 2010. Tissue transglutaminase promotes drug resistance and invasion by inducing mesenchymal transition in mammary epithelial cells. *PLoS ONE,* 5**,** e13390.

Kumar, A., Xu, J., Sung, B., Kumar, S., Yu, D., Aggarwal, B. B. & Mehta, K. 2012. Evidence that GTP-binding domain but not catalytic domain of transglutaminase 2 is essential for epithelial-to-mesenchymal transition in mammary epithelial cells. *Breast Cancer Res,* 14**,** R4.

Kuncio, G. S., Tsyganskaya, M., Zhu, J., Liu, S. L., Nagy, L., Thomazy, V., Davies, P. J. & Zern, M. A. 1998. TNF-alpha modulates expression of the tissue transglutaminase gene in liver cells. *Am J Physiol,* 274**,** G240-5.

Kwong, K., Niang, S., Literat, A., Zhu, N., Ramanathan, R., Jones, C. & Minoo, P. 2006. Expression of transforming growth factor beta (TGF-b1) by human preterm lung inflammatory cells☆. *Life Sciences,* 79**,** 2349-2356.

Laemmli, U. K. 1970. Cleavage of structural proteins during the assembly of the head of bacteriophage T4. *Nature,* 227**,** 680-5.

Lai, C. H., Chun, H. H., Nahas, S. A., Mitui, M., Gamo, K. M., Du, L. & Gatti, R. A. 2004. Correction of ATM gene function by aminoglycoside-induced read-through of premature termination codons. *Proc Natl Acad Sci U S A,* 101**,** 15676-81.

Lai, T. S., Slaughter, T. F., Koropchak, C. M., Haroon, Z. A. & Greenberg, C. S. 1996. C-terminal deletion of human tissue transglutaminase enhances magnesium-dependent GTP/ATPase activity. *J Biol Chem,* 271**,** 31191-5.

Lauzier, A., Charbonneau, M., Paquette, M., Harper, K. & Dubois, C. M. 2012. Transglutaminase 2 crosslinking activity is linked to invadopodia formation and cartilage breakdown in arthritis. *Arthritis Res Ther,* 14**,** R159.

Leask, A. & Abraham, D. J. 2004. TGF-beta signaling and the fibrotic response. *FASEB J,* 18**,** 816-27.

Lee, J. H., Jang, S. I., Yang, J. M., Markova, N. G. & Steinert, P. M. 1996. The proximal promoter of the human transglutaminase 3 gene. Stratified squamous epithelial-specific expression in cultured cells is mediated by binding of Sp1 and ets transcription factors to a proximal promoter element. *J Biol Chem,* 271**,** 4561-8.

Lee, J. M., Dedhar, S., Kalluri, R. & Thompson, E. W. 2006. The epithelial-mesenchymal transition: new insights in signaling, development, and disease. *J Cell Biol,* 172**,** 973-81.

Lee, K. N., Arnold, S. A., Birckbichler, P. J., Patterson, M. K., Jr., Fraij, B. M., Takeuchi, Y. & Carter, H. A. 1993. Site-directed mutagenesis of human tissue transglutaminase: Cys-277 is essential for transglutaminase activity but not for GTPase activity. *Biochim Biophys Acta,* 1202**,** 1-6.

Lesort, M., Lee, M., Tucholski, J. & Johnson, G. V. 2003. Cystamine inhibits caspase activity. Implications for the treatment of polyglutamine disorders. *J Biol Chem,* 278**,** 3825-30.

Levy, H., Cannon, C. L., Asher, D., Garcia, C., Cleveland, R. H., Pier, G. B., Knowles, M. R. & Colin, A. A. 2010. Lack of correlation between pulmonary disease and cystic fibrosis transmembrane conductance regulator dysfunction in cystic fibrosis: a case report. *J Med Case Rep,* 4**,** 117.

Lewis, P., Hensel, M. & Emerman, M. 1992. Human immunodeficiency virus infection of cells arrested in the cell cycle. *EMBO J,* 11**,** 3053-8.

Lilja, H. & Laurell, C. B. 1985. The predominant protein in human seminal coagulate. *Scand J Clin Lab Invest,* 45**,** 635-41.

Liu, S., Cerione, R. A. & Clardy, J. 2002. Structural basis for the guanine nucleotide-binding activity of tissue transglutaminase and its regulation of transamidation activity. *Proc Natl Acad Sci U S A,* 99**,** 2743-7.

Lowry, O. H., Rosebrough, N. J., Farr, A. L. & Randall, R. J. 1951. Protein measurement with the Folin phenol reagent. *J Biol Chem,* 193**,** 265-75.

Luciani, A., Villella, V. R., Esposito, S., Brunetti-Pierri, N., Medina, D., Settembre, C., Gavina, M., Pulze, L., Giardino, I., Pettoello-Mantovani, M., D'apolito, M., Guido, S., Masliah, E., Spencer, B., Quaratino, S., Raia, V., Ballabio, A. & Maiuri, L. 2010a. Defective CFTR induces aggresome formation and lung inflammation in cystic fibrosis through ROS-mediated autophagy inhibition. *Nat Cell Biol,* 12**,** 863-75.

Luciani, A., Villella, V. R., Esposito, S., Brunetti-Pierri, N., Medina, D., Settembre, C., Gavina, M., Pulze, L., Giardino, I., Pettoello-Mantovani, M., D'apolito, M., Guido, S., Masliah, E., Spencer, B., Quaratino, S., Raia, V., Ballabio, A. & Maiuri, L. 2010b. Defective CFTR induces aggresome formation and lung inflammation in cystic fibrosis through ROS-mediated autophagy inhibition. *Nature Cell Biology,* 12**,** 863-875.

Luciani, A., Villella, V. R., Esposito, S., Gavina, M., Russo, I., Silano, M., Guido, S., Pettoello-Mantovani, M., Carnuccio, R., Scholte, B., De Matteis, A., Maiuri, M. C., Raia, V., Luini, A., Kroemer, G. & Maiuri, L. 2012. Targeting autophagy as a novel strategy for facilitating the therapeutic action of potentiators on DeltaF508 cystic fibrosis transmembrane conductance regulator. *Autophagy,* 8.

Luciani, A., Villella, V. R., Vasaturo, A., Giardino, I., Raia, V., Pettoello-Mantovani, M., D'apolito, M., Guido, S., Leal, T., Quaratino, S. & Maiuri, L. 2009a. SUMOylation of Tissue Transglutaminase as Link between Oxidative Stress and Inflammation. *The Journal of Immunology,* 183**,** 2775-2784.

Luciani, A., Villella, V. R., Vasaturo, A., Giardino, I., Raia, V., Pettoello-Mantovani, M., D'apolito, M., Guido, S., Leal, T., Quaratino, S. & Maiuri, L. 2009b. SUMOylation of tissue transglutaminase as link between oxidative stress and inflammation. *J Immunol,* 183**,** 2775-84.

Lukacs, G. L., Chang, X. B., Bear, C., Kartner, N., Mohamed, A., Riordan, J. R. & Grinstein, S. 1993. The delta F508 mutation decreases the stability of cystic fibrosis transmembrane conductance regulator in the plasma membrane. Determination of functional half-lives on transfected cells. *J Biol Chem,* 268**,** 21592-8.

Lukacs, G. L., Mohamed, A., Kartner, N., Chang, X. B., Riordan, J. R. & Grinstein, S. 1994. Conformational maturation of CFTR but not its mutant counterpart (delta F508) occurs in the endoplasmic reticulum and requires ATP. *EMBO J,* 13**,** 6076-86.

Lukacs, G. L. & Verkman, A. S. 2012. CFTR: folding, misfolding and correcting the DeltaF508 conformational defect. *Trends Mol Med,* 18**,** 81-91.

Luo, J., Pato, M. D., Riordan, J. R. & Hanrahan, J. W. 1998. Differential regulation of single CFTR channels by PP2C, PP2A, and other phosphatases. *Am J Physiol,* 274**,** C1397-410.

Macdonald, K. D., Mckenzie, K. R. & Zeitlin, P. L. 2007. Cystic fibrosis transmembrane regulator protein mutations: 'class' opportunity for novel drug innovation. *Paediatr Drugs,* 9**,** 1-10.

Maiuri, L., Ciacci, C., Ricciardelli, I., Vacca, L., Raia, V., Rispo, A., Griffin, M., Issekutz, T., Quaratino, S. & Londei, M. 2005. Unexpected role of surface transglutaminase type II in celiac disease. *Gastroenterology,* 129**,** 1400-13.

Maiuri, L., Luciani, A., Giardino, I., Raia, V., Villella, V. R., D'apolito, M., Pettoello-Mantovani, M., Guido, S., Ciacci, C., Cimmino, M., Cexus, O. N., Londei, M. & Quaratino, S. 2008. Tissue transglutaminase activation modulates inflammation in cystic fibrosis via PPARgamma down-regulation. *J Immunol,* 180**,** 7697-705.

Mak, V., Zielenski, J., Tsui, L. C., Durie, P., Zini, A., Martin, S., Longley, T. B. & Jarvi, K. A. 2000. Cystic fibrosis gene mutations and infertile men with primary testicular failure. *Hum Reprod,* 15**,** 436-9.

Mamuya, F. A. & Duncan, M. K. 2012. aV integrins and TGF-beta-induced EMT: a circle of regulation. *J Cell Mol Med,* 16**,** 445-55.

Marchetti, A., Colletti, M., Cozzolino, A. M., Steindler, C., Lunadei, M., Mancone, C. & Tripodi, M. 2008. ERK5/MAPK is activated by TGFbeta in hepatocytes and required for the GSK-3beta-mediated Snail protein stabilisation. *Cell Signal,* 20**,** 2113-8.

Martinet, N. 2003. In Vivo Transglutaminase Type 1 Expression in Normal Lung, Preinvasive Bronchial Lesions, and Lung Cancer. *American Journal of Respiratory Cell and Molecular Biology,* 28**,** 428-435.

Martinez, J., Chalupowicz, D. G., Roush, R. K., Sheth, A. & Barsigian, C. 1994. Transglutaminase-mediated processing of fibronectin by endothelial cell monolayers. *Biochemistry,* 33**,** 2538-45.

Massague, J. 1996. TGFbeta signaling: receptors, transducers, and Mad proteins. *Cell,* 85**,** 947-50.

Massague, J., Seoane, J. & Wotton, D. 2005. Smad transcription factors. *Genes Dev,* 19**,** 2783-810.

Massaous, J. & Hata, A. 1997. TGF-beta signalling through the Smad pathway. *Trends Cell Biol,* 7**,** 187-92.

Melino, G., Farrace, M. G., Ceru, M. P. & Piacentini, M. 1988. Correlation between transglutaminase activity and polyamine levels in human neuroblastoma cells. Effect of retinoic acid and alpha-difluoromethylornithine. *Exp Cell Res,* 179**,** 429-45.

Mian, S., El Alaoui, S., Lawry, J., Gentile, V., Davies, P. J. & Griffin, M. 1995. The importance of the GTP-binding protein tissue transglutaminase in the regulation of cell cycle progression. *FEBS Lett,* 370**,** 27-31.

Miettinen, P. J., Ebner, R., Lopez, A. R. & Derynck, R. 1994. TGF-beta induced transdifferentiation of mammary epithelial cells to mesenchymal cells: involvement of type I receptors. *J Cell Biol,* 127**,** 2021-36.

Mirza, A., Liu, S. L., Frizell, E., Zhu, J., Maddukuri, S., Martinez, J., Davies, P., Schwarting, R., Norton, P. & Zern, M. A. 1997. A role for tissue transglutaminase in hepatic injury and fibrogenesis, and its regulation by NF-kappaB. *Am J Physiol,* 272**,** G281-8.

Mitchell, I., Nakielna, E., Tullis, E. & Adair, C. 2000. Cystic fibrosis. End-stage care in Canada. *Chest,* 118**,** 80-4.

Miyoshi, H., Blomer, U., Takahashi, M., Gage, F. H. & Verma, I. M. 1998. Development of a self-inactivating lentivirus vector. *J Virol,* 72**,** 8150-7.

Monsonego, A., Friedmann, I., Shani, Y., Eisenstein, M. & Schwartz, M. 1998. GTP-dependent conformational changes associated with the functional switch between Galpha and crosslinking activities in brain-derived tissue transglutaminase. *J Mol Biol,* 282**,** 713-20.

Moreno-Bueno, G., Cubillo, E., Sarrio, D., Peinado, H., Rodriguez-Pinilla, S. M., Villa, S., Bolos, V., Jorda, M., Fabra, A., Portillo, F., Palacios, J. & Cano, A. 2006. Genetic profiling of epithelial cells expressing E-cadherin repressors reveals a distinct role for Snail, Slug, and E47 factors in epithelial-mesenchymal transition. *Cancer Res,* 66**,** 9543-56.

Mu, D., Cambier, S., Fjellbirkeland, L., Baron, J. L., Munger, J. S., Kawakatsu, H., Sheppard, D., Broaddus, V. C. & Nishimura, S. L. 2002. The integrin alpha(v)beta8 mediates epithelial homeostasis through MT1-MMP-dependent activation of TGF-beta1. *J Cell Biol,* 157**,** 493-507.

Munger, J. S., Harpel, J. G., Giancotti, F. G. & Rifkin, D. B. 1998. Interactions between growth factors and integrins: latent forms of transforming growth factor-beta are ligands for the integrin alphavbeta1. *Mol Biol Cell,* 9**,** 2627-38.

Munger, J. S., Harpel, J. G., Gleizes, P. E., Mazzieri, R., Nunes, I. & Rifkin, D. B. 1997. Latent transforming growth factor-beta: structural features and mechanisms of activation. *Kidney Int,* 51**,** 1376-82.

Munger, J. S., Huang, X., Kawakatsu, H., Griffiths, M. J., Dalton, S. L., Wu, J., Pittet, J. F., Kaminski, N., Garat, C., Matthay, M. A., Rifkin, D. B. & Sheppard, D. 1999. The integrin alpha v beta 6 binds and activates latent TGF beta 1: a mechanism for regulating pulmonary inflammation and fibrosis. *Cell,* 96**,** 319-28.

Murthy, S. N., Iismaa, S., Begg, G., Freymann, D. M., Graham, R. M. & Lorand, L. 2002. Conserved tryptophan in the core domain of transglutaminase is essential for catalytic activity. *Proc Natl Acad Sci U S A,* 99**,** 2738-42.

Nadalutti, C., Viiri, K. M., Kaukinen, K., Maki, M. & Lindfors, K. 2011. Extracellular transglutaminase 2 has a role in cell adhesion, whereas intracellular transglutaminase 2 is involved in regulation of endothelial cell proliferation and apoptosis. *Cell Prolif,* 44**,** 49-58.

Naldini, L., Blomer, U., Gallay, P., Ory, D., Mulligan, R., Gage, F. H., Verma, I. M. & Trono, D. 1996. In vivo gene delivery and stable transduction of nondividing cells by a lentiviral vector. *Science,* 272**,** 263-7.

Nicholas, B., Smethurst, P., Verderio, E., Jones, R. & Griffin, M. 2003. Crosslinking of cellular proteins by tissue transglutaminase during necrotic cell death: a mechanism for maintaining tissue integrity. *Biochem J,* 371**,** 413-22.

Niger, C., Beazley, K. E. & Nurminskaya, M. 2013. Induction of chondrogenic differentiation in mesenchymal stem cells by TGF-beta cross-linked to collagen-PLLA [poly(L-lactic acid)] scaffold by transglutaminase 2. *Biotechnol Lett,* 35**,** 2193-9.

Nunes, I., Gleizes, P. E., Metz, C. N. & Rifkin, D. B. 1997. Latent transforming growth factor-beta binding protein domains involved in activation and

transglutaminase-dependent crosslinking of latent transforming growth factor-beta. *J Cell Biol,* 136**,** 1151-63.

O'sullivan, B. P. & Freedman, S. D. 2009. Cystic fibrosis. *Lancet,* 373**,** 1891-904.

Okiyoneda, T., Barriere, H., Bagdany, M., Rabeh, W. M., Du, K., Hohfeld, J., Young, J. C. & Lukacs, G. L. 2010. Peripheral protein quality control removes unfolded CFTR from the plasma membrane. *Science,* 329**,** 805-10.

Olsen, K. C., Epa, A. P., Kulkarni, A. A., Kottmann, R. M., Mccarthy, C. E., Johnson, G. V., Thatcher, T. H., Phipps, R. P. & Sime, P. J. 2013. Inhibition of Transglutaminase 2, a Novel Target for Pulmonary Fibrosis, by two Small Electrophilic Molecules. *Am J Respir Cell Mol Biol*.

Olsen, K. C., Sapinoro, R. E., Kottmann, R. M., Kulkarni, A. A., Iismaa, S. E., Johnson, G. V., Thatcher, T. H., Phipps, R. P. & Sime, P. J. 2011. Transglutaminase 2 and its role in pulmonary fibrosis. *Am J Respir Crit Care Med,* 184**,** 699-707.

Osika, E., Cavaillon, J. M., Chadelat, K., Boule, M., Fitting, C., Tournier, G. & Clement, A. 1999. Distinct sputum cytokine profiles in cystic fibrosis and other chronic inflammatory airway disease. *Eur Respir J,* 14**,** 339-46.

Ozdamar, B., Bose, R., Barrios-Rodiles, M., Wang, H. R., Zhang, Y. & Wrana, J. L. 2005. Regulation of the polarity protein Par6 by TGFbeta receptors controls epithelial cell plasticity. *Science,* 307**,** 1603-9.

Park, M. K., You, H. J., Lee, H. J., Kang, J. H., Oh, S. H., Kim, S. Y. & Lee, C. H. 2013. Transglutaminase-2 induces N-cadherin expression in TGF-beta1-induced epithelial mesenchymal transition via c-Jun-N-terminal kinase activation by protein phosphatase 2A down-regulation. *Eur J Cancer,* 49**,** 1692-705.

Pasyk, S., Li, C., Ramjeesingh, M. & Bear, C. E. 2009. Direct interaction of a small-molecule modulator with G551D-CFTR, a cystic fibrosis-causing mutation associated with severe disease. *Biochem J,* 418**,** 185-90.

Pellegrin, S. & Mellor, H. 2007. Actin stress fibres. *J Cell Sci,* 120**,** 3491-9.

Piacentini, M., Autuori, F., Dini, L., Farrace, M. G., Ghibelli, L., Piredda, L. & Fesus, L. 1991. "Tissue" transglutaminase is specifically expressed in neonatal rat liver cells undergoing apoptosis upon epidermal growth factor-stimulation. *Cell Tissue Res,* 263**,** 227-35.

Piacentini, M., Fesus, L., Sartori, C. & Ceru, M. P. 1988. Retinoic acid-induced modulation of rat liver transglutaminase and total polyamines in vivo. *Biochem J,* 253**,** 33-8.

Piek, E., Moustakas, A., Kurisaki, A., Heldin, C. H. & Ten Dijke, P. 1999. TGF-(beta) type I receptor/ALK-5 and Smad proteins mediate epithelial to mesenchymal transdifferentiation in NMuMG breast epithelial cells. *J Cell Sci,* 112 (Pt 24)**,** 4557-68.

Pinkas, D. M., Strop, P., Brunger, A. T. & Khosla, C. 2007. Transglutaminase 2 undergoes a large conformational change upon activation. *PLoS Biol,* 5**,** e327.

Pittet, J. F., Griffiths, M. J., Geiser, T., Kaminski, N., Dalton, S. L., Huang, X., Brown, L. A., Gotwals, P. J., Koteliansky, V. E., Matthay, M. A. & Sheppard, D. 2001. TGF-beta is a critical mediator of acute lung injury. *J Clin Invest,* 107**,** 1537-44.

Plenz, A., Fritz, P., Konig, G., Laschner, W. & Saal, J. G. 1996. Immunohistochemical detection of factor XIIIa and factor XIIIs in synovial membranes of patients with rheumatoid arthritis or osteoarthritis. *Rheumatol Int,* 16**,** 29-36.

Porta, R., Esposito, C., De Santis, A., Fusco, A., Iannone, M. & Metafora, S. 1986. Sperm maturation in human semen: role of transglutaminase-mediated reactions. *Biol Reprod,* 35**,** 965-70.

Postigo, A. A., Depp, J. L., Taylor, J. J. & Kroll, K. L. 2003. Regulation of Smad signaling through a differential recruitment of coactivators and corepressors by ZEB proteins. *EMBO J,* 22**,** 2453-62.

Proesmans, M., Vermeulen, F. & De Boeck, K. 2008. What's new in cystic fibrosis? From treating symptoms to correction of the basic defect. *Eur J Pediatr,* 167**,** 839-49.

Pruliere-Escabasse, V., Fanen, P., Dazy, A. C., Lechapt-Zalcman, E., Rideau, D., Edelman, A., Escudier, E. & Coste, A. 2005. TGF-beta 1 downregulates CFTR expression and function in nasal polyps of non-CF patients. *Am J Physiol Lung Cell Mol Physiol,* 288**,** L77-83.

Ramalho, A. S., Beck, S., Meyer, M., Penque, D., Cutting, G. R. & Amaral, M. D. 2002. Five percent of normal cystic fibrosis transmembrane conductance regulator mRNA ameliorates the severity of pulmonary disease in cystic fibrosis. *Am J Respir Cell Mol Biol,* 27**,** 619-27.

Ramsey, B. W., Davies, J., Mcelvaney, N. G., Tullis, E., Bell, S. C., Drevinek, P., Griese, M., Mckone, E. F., Wainwright, C. E., Konstan, M. W., Moss, R., Ratjen, F., Sermet-Gaudelus, I., Rowe, S. M., Dong, Q., Rodriguez, S., Yen, K., Ordonez, C. & Elborn, J. S. 2011a. A CFTR potentiator in patients with cystic fibrosis and the G551D mutation. *N Engl J Med,* 365**,** 1663-72.

Ramsey, B. W., Davies, J., Mcelvaney, N. G., Tullis, E., Bell, S. C., Drevinek, P., Griese, M., Mckone, E. F., Wainwright, C. E., Konstan, M. W., Moss, R., Ratjen, F., Sermet-Gaudelus, I., Rowe, S. M., Dong, Q., Rodriguez, S., Yen, K., Ordonez, C., Elborn, J. S. & Group, V. X. S. 2011b. A CFTR potentiator in patients with cystic fibrosis and the G551D mutation. *N Engl J Med,* 365**,** 1663-72.

Rastaldi, M. P., Ferrario, F., Giardino, L., Dell'antonio, G., Grillo, C., Grillo, P., Strutz, F., Muller, G. A., Colasanti, G. & D'amico, G. 2002. Epithelial-mesenchymal

transition of tubular epithelial cells in human renal biopsies. *Kidney Int,* 62**,** 137-46.

Ratjen, F. & Doring, G. 2003. Cystic fibrosis. *Lancet,* 361**,** 681-9.

Reddy, M. M., Light, M. J. & Quinton, P. M. 1999. Activation of the epithelial Na+ channel (ENaC) requires CFTR Cl- channel function. *Nature,* 402**,** 301-4.

Ren, H. Y., Grove, D. E., De La Rosa, O., Houck, S. A., Sopha, P., Van Goor, F., Hoffman, B. J. & Cyr, D. M. 2013. VX-809 corrects folding defects in cystic fibrosis transmembrane conductance regulator protein through action on membrane-spanning domain 1. *Mol Biol Cell,* 24**,** 3016-24.

Ribeiro, C. M., Paradiso, A. M., Carew, M. A., Shears, S. B. & Boucher, R. C. 2005. Cystic fibrosis airway epithelial Ca2+ i signaling: the mechanism for the larger agonist-mediated Ca2+ i signals in human cystic fibrosis airway epithelia. *J Biol Chem,* 280**,** 10202-9.

Richards, R. J., Masek, L. C. & Brown, R. F. 1991. Biochemical and cellular mechanisms of pulmonary fibrosis. *Toxicol Pathol,* 19**,** 526-39.

Riordan, J. R., Rommens, J. M., Kerem, B., Alon, N., Rozmahel, R., Grzelczak, Z., Zielenski, J., Lok, S., Plavsic, N., Chou, J. L. & Et Al. 1989. Identification of the cystic fibrosis gene: cloning and characterization of complementary DNA. *Science,* 245**,** 1066-73.

Ritter, S. J. & Davies, P. J. 1998. Identification of a transforming growth factor-beta1/bone morphogenetic protein 4 (TGF-beta1/BMP4) response element within the mouse tissue transglutaminase gene promoter. *J Biol Chem,* 273**,** 12798-806.

Robinson, C. B. & Wu, R. 1993. Mucin synthesis and secretion by cultured tracheal cells: effects of collagen gel substratum thickness. *In Vitro Cell Dev Biol Anim,* 29A**,** 469-77.

Rosser, M. F., Grove, D. E., Chen, L. & Cyr, D. M. 2008. Assembly and misassembly of cystic fibrosis transmembrane conductance regulator: folding defects caused by deletion of F508 occur before and after the calnexin-dependent association of membrane spanning domain (MSD) 1 and MSD2. *Mol Biol Cell,* 19**,** 4570-9.

Rowe, S. M. & Verkman, A. S. 2013. Cystic fibrosis transmembrane regulator correctors and potentiators. *Cold Spring Harb Perspect Med,* 3.

Ruan, Q. & Johnson, G. V. 2007. Transglutaminase 2 in neurodegenerative disorders. *Front Biosci,* 12**,** 891-904.

Ruan, Q., Tucholski, J., Gundemir, S. & Johnson Voll, G. V. 2008. The Differential Effects of R580A Mutation on Transamidation and GTP Binding Activity of Rat and Human Type 2 Transglutaminase. *Int J Clin Exp Med,* 1**,** 248-59.

Rubenstein, R. C., Egan, M. E. & Zeitlin, P. L. 1997. In vitro pharmacologic restoration of CFTR-mediated chloride transport with sodium 4-phenylbutyrate in cystic fibrosis epithelial cells containing delta F508-CFTR. *J Clin Invest,* 100**,** 2457-65.

Sato, M., Muragaki, Y., Saika, S., Roberts, A. B. & Ooshima, A. 2003. Targeted disruption of TGF-beta1/Smad3 signaling protects against renal tubulointerstitial fibrosis induced by unilateral ureteral obstruction. *J Clin Invest,* 112**,** 1486-94.

Schorpp, M., Jager, R., Schellander, K., Schenkel, J., Wagner, E. F., Weiher, H. & Angel, P. 1996. The human ubiquitin C promoter directs high ubiquitous expression of transgenes in mice. *Nucleic Acids Res,* 24**,** 1787-8.

Schwiebert, E. M., Benos, D. J., Egan, M. E., Stutts, M. J. & Guggino, W. B. 1999. CFTR is a conductance regulator as well as a chloride channel. *Physiol Rev,* 79**,** S145-66.

Seissler, J., Schott, M., Boms, S., Wohlrab, U., Ostendorf, B., Morgenthaler, N. G. & Scherbaum, W. A. 1999. Autoantibodies to human tissue transgutaminase identify silent coeliac disease in Type I diabetes. *Diabetologia,* 42**,** 1440-1.

Seitz, J., Keppler, C., Rausch, U. & Aumuller, G. 1990. Immunohistochemistry of secretory transglutaminase from rodent prostate. *Histochemistry,* 93**,** 525-30.

Sermet-Gaudelus, I., Boeck, K. D., Casimir, G. J., Vermeulen, F., Leal, T., Mogenet, A., Roussel, D., Fritsch, J., Hanssens, L., Hirawat, S., Miller, N. L., Constantine, S., Reha, A., Ajayi, T., Elfring, G. L. & Miller, L. L. 2010. Ataluren (PTC124) induces cystic fibrosis transmembrane conductance regulator protein expression and activity in children with nonsense mutation cystic fibrosis. *Am J Respir Crit Care Med,* 182**,** 1262-72.

Shah, M., Revis, D., Herrick, S., Baillie, R., Thorgeirson, S., Ferguson, M. & Roberts, A. 1999. Role of elevated plasma transforming growth factor-beta1 levels in wound healing. *Am J Pathol,* 154**,** 1115-24.

Sharma, M., Pampinella, F., Nemes, C., Benharouga, M., So, J., Du, K., Bache, K. G., Papsin, B., Zerangue, N., Stenmark, H. & Lukacs, G. L. 2004. Misfolding diverts CFTR from recycling to degradation: quality control at early endosomes. *J Cell Biol,* 164**,** 923-33.

Sheppard, D. 2005. Integrin-mediated activation of latent transforming growth factor beta. *Cancer Metastasis Rev,* 24**,** 395-402.

Sheppard, D. 2006a. Transforming Growth Factor : A Central Modulator of Pulmonary and Airway Inflammation and Fibrosis. *Proceedings of the American Thoracic Society,* 3**,** 413-417.

Sheppard, D. 2006b. Transforming growth factor beta: a central modulator of pulmonary and airway inflammation and fibrosis. *Proc Am Thorac Soc,* 3**,** 413-7.

Shoshani, T., Augarten, A., Gazit, E., Bashan, N., Yahav, Y., Rivlin, Y., Tal, A., Seret, H., Yaar, L., Kerem, E. & Et Al. 1992. Association of a nonsense mutation (W1282X), the most common mutation in the Ashkenazi Jewish cystic fibrosis patients in Israel, with presentation of severe disease. *Am J Hum Genet,* 50**,** 222-8.

Shweke, N., Boulos, N., Jouanneau, C., Vandermeersch, S., Melino, G., Dussaule, J.-C., Chatziantoniou, C., Ronco, P. & Boffa, J.-J. 2008. Tissue Transglutaminase Contributes to Interstitial Renal Fibrosis by Favoring Accumulation of Fibrillar Collagen through TGF-β Activation and Cell Infiltration. *The American Journal of Pathology,* 173**,** 631-642.

Siegel, M. & Khosla, C. 2007. Transglutaminase 2 inhibitors and their therapeutic role in disease states. *Pharmacology & Therapeutics,* 115**,** 232-245.

Siegel, M., Strnad, P., Watts, R. E., Choi, K., Jabri, B., Omary, M. B. & Khosla, C. 2008. Extracellular transglutaminase 2 is catalytically inactive, but is transiently activated upon tissue injury. *PLoS One,* 3**,** e1861.

Skill, N. J., Johnson, T. S., Coutts, I. G., Saint, R. E., Fisher, M., Huang, L., El Nahas, A. M., Collighan, R. J. & Griffin, M. 2004. Inhibition of transglutaminase activity reduces extracellular matrix accumulation induced by high glucose levels in proximal tubular epithelial cells. *J Biol Chem,* 279**,** 47754-62.

Small, K., Feng, J. F., Lorenz, J., Donnelly, E. T., Yu, A., Im, M. J., Dorn, G. W., 2nd & Liggett, S. B. 1999. Cardiac specific overexpression of transglutaminase II (G(h)) results in a unique hypertrophy phenotype independent of phospholipase C activation. *J Biol Chem,* 274**,** 21291-6.

Smethurst, P. A. & Griffin, M. 1996. Measurement of tissue transglutaminase activity in a permeabilized cell system: its regulation by Ca2+ and nucleotides. *Biochem J,* 313 (Pt 3)**,** 803-8.

Snodgrass, S. M., Cihil, K. M., Cornuet, P. K., Myerburg, M. M. & Swiatecka-Urban, A. 2013. Tgf-beta1 inhibits Cftr biogenesis and prevents functional rescue of DeltaF508-Cftr in primary differentiated human bronchial epithelial cells. *PLoS ONE,* 8**,** e63167.

Sparbel, K. J. & Tluczek, A. 2011. Patient and family issues regarding genetic testing for cystic fibrosis: a review of prenatal carrier testing and newborn screening. *Annu Rev Nurs Res,* 29**,** 303-29.

Stewart, C. E., Torr, E. E., Mohd Jamili, N. H., Bosquillon, C. & Sayers, I. 2012. Evaluation of differentiated human bronchial epithelial cell culture systems for asthma research. *J Allergy (Cairo),* 2012**,** 943982.

Sturniolo, M. T., Chandraratna, R. A. & Eckert, R. L. 2005. A novel transglutaminase activator forms a complex with type 1 transglutaminase. *Oncogene,* 24**,** 2963-72.

Sun, F., Mi, Z., Condliffe, S. B., Bertrand, C. A., Gong, X., Lu, X., Zhang, R., Latoche, J. D., Pilewski, J. M., Robbins, P. D. & Frizzell, R. A. 2008. Chaperone displacement from mutant cystic fibrosis transmembrane conductance regulator restores its function in human airway epithelia. *FASEB J,* 22**,** 3255-63.

Tabary, O., Boncoeur, E., De Martin, R., Pepperkok, R., Clément, A., Schultz, C. & Jacquot, J. 2006. Calcium-dependent regulation of NF-κB activation in cystic fibrosis airway epithelial cells. *Cellular Signalling,* 18**,** 652-660.

Tanfani, F., Bertoli, E., Signorini, M. & Bergamini, C. M. 1993. Structural investigation of transglutaminase by Fourier transform infrared spectroscopy. *Eur J Biochem,* 218**,** 499-505.

Telci, D., Collighan, R. J., Basaga, H. & Griffin, M. 2009. Increased TG2 expression can result in induction of transforming growth factor beta1, causing increased synthesis and deposition of matrix proteins, which can be regulated by nitric oxide. *J Biol Chem,* 284**,** 29547-58.

Telci, D. & Griffin, M. 2006. Tissue transglutaminase (TG2)--a wound response enzyme. *Front Biosci,* 11**,** 867-82.

Telci, D., Wang, Z., Li, X., Verderio, E. A., Humphries, M. J., Baccarini, M., Basaga, H. & Griffin, M. 2008. Fibronectin-tissue transglutaminase matrix rescues RGD-impaired cell adhesion through syndecan-4 and beta1 integrin co-signaling. *J Biol Chem,* 283**,** 20937-47.

Thibaut, S., Cavusoglu, N., De Becker, E., Zerbib, F., Bednarczyk, A., Schaeffer, C., Van Dorsselaer, A. & Bernard, B. A. 2008. Transglutaminase-3 Enzyme: A Putative Actor in Human Hair Shaft Scaffolding? *Journal of Investigative Dermatology,* 129**,** 449-459.

Thiery, J. P. 2002. Epithelial-mesenchymal transitions in tumour progression. *Nat Rev Cancer,* 2**,** 442-54.

Thomas, P. J., Shenbagamurthi, P., Ysern, X. & Pedersen, P. L. 1991. Cystic fibrosis transmembrane conductance regulator: nucleotide binding to a synthetic peptide. *Science,* 251**,** 555-7.

Tovar-Vidales, T., Clark, A. F. & Wordinger, R. J. 2011. Transforming growth factor-beta2 utilizes the canonical Smad-signaling pathway to regulate tissue transglutaminase expression in human trabecular meshwork cells. *Exp Eye Res,* 93**,** 442-51.

Towbin, H., Staehelin, T. & Gordon, J. 1979. Electrophoretic transfer of proteins from polyacrylamide gels to nitrocellulose sheets: procedure and some applications. *Proc Natl Acad Sci U S A,* 76**,** 4350-4.

Travis, S. M., Berger, H. A. & Welsh, M. J. 1997. Protein phosphatase 2C dephosphorylates and inactivates cystic fibrosis transmembrane conductance regulator. *Proc Natl Acad Sci U S A,* 94**,** 11055-60.

Trezise, A. E. & Buchwald, M. 1991. In vivo cell-specific expression of the cystic fibrosis transmembrane conductance regulator. *Nature,* 353**,** 434-7.

Tsukita, S., Furuse, M. & Itoh, M. 2001. Multifunctional strands in tight junctions. *Nat Rev Mol Cell Biol,* 2**,** 285-93.

Upchurch, H. F., Conway, E., Patterson, M. K., Jr. & Maxwell, M. D. 1991. Localisation of cellular transglutaminase on the extracellular matrix after wounding: characteristics of the matrix bound enzyme. *J Cell Physiol,* 149**,** 375-82.

Uttamsingh, S., Bao, X., Nguyen, K. T., Bhanot, M., Gong, J., Chan, J. L., Liu, F., Chu, T. T. & Wang, L. H. 2008. Synergistic effect between EGF and TGF-beta1 in inducing oncogenic properties of intestinal epithelial cells. *Oncogene,* 27**,** 2626-34.

Van Goor, F., Hadida, S., Grootenhuis, P. D., Burton, B., Cao, D., Neuberger, T., Turnbull, A., Singh, A., Joubran, J., Hazlewood, A., Zhou, J., Mccartney, J., Arumugam, V., Decker, C., Yang, J., Young, C., Olson, E. R., Wine, J. J., Frizzell, R. A., Ashlock, M. & Negulescu, P. 2009. Rescue of CF airway epithelial cell function in vitro by a CFTR potentiator, VX-770. *Proc Natl Acad Sci U S A,* 106**,** 18825-30.

Van Goor, F., Hadida, S., Grootenhuis, P. D., Burton, B., Stack, J. H., Straley, K. S., Decker, C. J., Miller, M., Mccartney, J., Olson, E. R., Wine, J. J., Frizzell, R. A., Ashlock, M. & Negulescu, P. A. 2011. Correction of the F508del-CFTR protein processing defect in vitro by the investigational drug VX-809. *Proc Natl Acad Sci U S A,* 108**,** 18843-8.

Van Goor, F., Straley, K. S., Cao, D., Gonzalez, J., Hadida, S., Hazlewood, A., Joubran, J., Knapp, T., Makings, L. R., Miller, M., Neuberger, T., Olson, E., Panchenko, V., Rader, J., Singh, A., Stack, J. H., Tung, R., Grootenhuis, P. D. & Negulescu, P. 2006. Rescue of DeltaF508-CFTR trafficking and gating in human cystic fibrosis airway primary cultures by small molecules. *Am J Physiol Lung Cell Mol Physiol,* 290**,** L1117-30.

Vankeerberghen, A., Cuppens, H. & Cassiman, J. J. 2002. The cystic fibrosis transmembrane conductance regulator: an intriguing protein with pleiotropic functions. *J Cyst Fibros,* 1**,** 13-29.

Varga, K., Jurkuvenaite, A., Wakefield, J., Hong, J. S., Guimbellot, J. S., Venglarik, C. J., Niraj, A., Mazur, M., Sorscher, E. J., Collawn, J. F. & Bebok, Z. 2004. Efficient intracellular processing of the endogenous cystic fibrosis transmembrane conductance regulator in epithelial cell lines. *J Biol Chem,* 279**,** 22578-84.

Venkatakrishnan, A., Stecenko, A. A., King, G., Blackwell, T. R., Brigham, K. L., Christman, J. W. & Blackwell, T. S. 2000. Exaggerated activation of nuclear factor-kappaB and altered IkappaB-beta processing in cystic fibrosis bronchial epithelial cells. *Am J Respir Cell Mol Biol,* 23**,** 396-403.

Verderio, E., Gaudry, C., Gross, S., Smith, C., Downes, S. & Griffin, M. 1999. Regulation of cell surface tissue transglutaminase: effects on matrix storage of latent transforming growth factor-beta binding protein-1. *J Histochem Cytochem,* 47**,** 1417-32.

Verderio, E., Nicholas, B., Gross, S. & Griffin, M. 1998. Regulated expression of tissue transglutaminase in Swiss 3T3 fibroblasts: effects on the processing of fibronectin, cell attachment, and cell death. *Exp Cell Res,* 239**,** 119-38.

Verderio, E. A., Johnson, T. & Griffin, M. 2004. Tissue transglutaminase in normal and abnormal wound healing: review article. *Amino Acids,* 26**,** 387-404.

Verderio, E. A., Telci, D., Okoye, A., Melino, G. & Griffin, M. 2003. A novel RGD-independent cel adhesion pathway mediated by fibronectin-bound tissue transglutaminase rescues cells from anoikis. *J Biol Chem,* 278**,** 42604-14.

Vergani, P., Basso, C., Mense, M., Nairn, A. C. & Gadsby, D. C. 2005. Control of the CFTR channel's gates. *Biochem Soc Trans,* 33**,** 1003-7.

Verma, A., Guha, S., Diagaradjane, P., Kunnumakkara, A. B., Sanguino, A. M., Lopez-Berestein, G., Sood, A. K., Aggarwal, B. B., Krishnan, S., Gelovani, J. G. & Mehta, K. 2008. Therapeutic significance of elevated tissue transglutaminase expression in pancreatic cancer. *Clin Cancer Res,* 14**,** 2476-83.

Vij, N., Mazur, S. & Zeitlin, P. L. 2009. CFTR is a negative regulator of NFkappaB mediated innate immune response. *PLoS ONE,* 4**,** e4664.

Villalta, D., Bizzaro, N., Tonutti, E. & Tozzoli, R. 2002. IgG anti-transglutaminase autoantibodies in systemic lupus erythematosus and Sjogren syndrome. *Clin Chem,* 48**,** 1133.

Villella, V. R., Esposito, S., Maiuri, M. C., Raia, V., Kroemer, G. & Maiuri, L. 2013. Towards a rational combination therapy of cystic fibrosis: How cystamine restores the stability of mutant CFTR. *Autophagy,* 9**,** 1431-4.

Vollberg, T. M., George, M. D., Nervi, C. & Jetten, A. M. 1992. Regulation of type I and type II transglutaminase in normal human bronchial epithelial and lung carcinoma cells. *Am J Respir Cell Mol Biol,* 7**,** 10-8.

Wakshlag, J. J., Antonyak, M. A., Boehm, J. E., Boehm, K. & Cerione, R. A. 2006. Effects of tissue transglutaminase on beta -amyloid1-42-induced apoptosis. *Protein J,* 25**,** 83-94.

Wang, Z., Collighan, R. J., Gross, S. R., Danen, E. H., Orend, G., Telci, D. & Griffin, M. 2010. RGD-independent cell adhesion via a tissue transglutaminase-fibronectin matrix promotes fibronectin fibril deposition and requires syndecan-4/2 and {alpha}5{beta}1 integrin co-signaling. *J Biol Chem,* 285**,** 40212-29.

Wang, Z., Collighan, R. J., Pytel, K., Rathbone, D. L., Li, X. & Griffin, M. 2012. Characterization of heparin-binding site of tissue transglutaminase: its importance in cell surface targeting, matrix deposition, and cell signaling. *J Biol Chem,* 287**,** 13063-83.

Wang, Z., Perez, M., Caja, S., Melino, G., Johnson, T. S., Lindfors, K. & Griffin, M. 2013. A novel extracellular role for tissue transglutaminase in matrix-bound VEGF-mediated angiogenesis. *Cell Death Dis,* 4**,** e808.

Wang, Z., Wade, P., Mandell, K. J., Akyildiz, A., Parkos, C. A., Mrsny, R. J. & Nusrat, A. 2007. Raf 1 represses expression of the tight junction protein occludin via activation of the zinc-finger transcription factor slug. *Oncogene,* 26**,** 1222-30.

Ward, C. L., Omura, S. & Kopito, R. R. 1995. Degradation of CFTR by the ubiquitin-proteasome pathway. *Cell,* 83**,** 121-7.

Weber, A. J., Soong, G., Bryan, R., Saba, S. & Prince, A. 2001. Activation of NF-kappaB in airway epithelial cells is dependent on CFTR trafficking and Cl- channel function. *Am J Physiol Lung Cell Mol Physiol,* 281**,** L71-8.

Welsh, M. J. & Smith, A. E. 1993. Molecular mechanisms of CFTR chloride channel dysfunction in cystic fibrosis. *Cell,* 73**,** 1251-4.

West, M. R. & Molloy, C. R. 1996. A microplate assay measuring chloride ion channel activity. *Anal Biochem,* 241**,** 51-8.

Wheelock, M. J. & Johnson, K. R. 2003. Cadherin-mediated cellular signaling. *Curr Opin Cell Biol,* 15**,** 509-14.

Willis, B. C. & Borok, Z. 2007. TGF-beta-induced EMT: mechanisms and implications for fibrotic lung disease. *Am J Physiol Lung Cell Mol Physiol,* 293**,** L525-34.

Wilschanski, M., Miller, L. L., Shoseyov, D., Blau, H., Rivlin, J., Aviram, M., Cohen, M., Armoni, S., Yaakov, Y., Pugatsch, T., Cohen-Cymberknoh, M., Miller, N. L., Reha, A., Northcutt, V. J., Hirawat, S., Donnelly, K., Elfring, G. L., Ajayi, T. & Kerem, E. 2011. Chronic ataluren (PTC124) treatment of nonsense mutation cystic fibrosis. *Eur Respir J,* 38**,** 59-69.

Wilschanski, M., Yahav, Y., Yaacov, Y., Blau, H., Bentur, L., Rivlin, J., Aviram, M., Bdolah-Abram, T., Bebok, Z., Shushi, L., Kerem, B. & Kerem, E. 2003.

Gentamicin-induced correction of CFTR function in patients with cystic fibrosis and CFTR stop mutations. *N Engl J Med,* 349**,** 1433-41.

Winter, M. C. & Welsh, M. J. 1997. Stimulation of CFTR activity by its phosphorylated R domain. *Nature,* 389**,** 294-6.

Wu, R., Martin, W. R., Robinson, C. B., St George, J. A., Plopper, C. G., Kurland, G., Last, J. A., Cross, C. E., Mcdonald, R. J. & Boucher, R. 1990. Expression of mucin synthesis and secretion in human tracheobronchial epithelial cells grown in culture. *Am J Respir Cell Mol Biol,* 3**,** 467-78.

Wu, R., Yankaskas, J., Cheng, E., Knowles, M. R. & Boucher, R. 1985. Growth and differentiation of human nasal epithelial cells in culture. Serum-free, hormone-supplemented medium and proteoglycan synthesis. *Am Rev Respir Dis,* 132**,** 311-20.

Xu, J., Lamouille, S. & Derynck, R. 2009. TGF-beta-induced epithelial to mesenchymal transition. *Cell Res,* 19**,** 156-72.

Yamaya, M., Finkbeiner, W. E., Chun, S. Y. & Widdicombe, J. H. 1992. Differentiated structure and function of cultures from human tracheal epithelium. *Am J Physiol,* 262**,** L713-24.

Yanagisawa, K., Osada, H., Masuda, A., Kondo, M., Saito, T., Yatabe, Y., Takagi, K. & Takahashi, T. 1998. Induction of apoptosis by Smad3 and down-regulation of Smad3 expression in response to TGF-beta in human normal lung epithelial cells. *Oncogene,* 17**,** 1743-7.

Yang, J., Mani, S. A., Donaher, J. L., Ramaswamy, S., Itzykson, R. A., Come, C., Savagner, P., Gitelman, I., Richardson, A. & Weinberg, R. A. 2004. Twist, a master regulator of morphogenesis, plays an essential role in tumor metastasis. *Cell,* 117**,** 927-39.

Yankaskas, J. R., Cotton, C. U., Knowles, M. R., Gatzy, J. T. & Boucher, R. C. 1985. Culture of human nasal epithelial cells on collagen matrix supports. A comparison of bioelectric properties of normal and cystic fibrosis epithelia. *Am Rev Respir Dis,* 132**,** 1281-7.

Yi, J. Y., Shin, I. & Arteaga, C. L. 2005. Type I transforming growth factor beta receptor binds to and activates phosphatidylinositol 3-kinase. *J Biol Chem,* 280**,** 10870-6.

Yu, H., Burton, B., Huang, C. J., Worley, J., Cao, D., Johnson, J. P., Jr., Urrutia, A., Joubran, J., Seepersaud, S., Sussky, K., Hoffman, B. J. & Van Goor, F. 2012. Ivacaftor potentiation of multiple CFTR channels with gating mutations. *J Cyst Fibros,* 11**,** 237-45.

Zavadil, J. & Bottinger, E. P. 2005. TGF-beta and epithelial-to-mesenchymal transitions. *Oncogene,* 24**,** 5764-74.

Zennou, V., Petit, C., Guetard, D., Nerhbass, U., Montagnier, L. & Charneau, P. 2000. HIV-1 genome nuclear import is mediated by a central DNA flap. *Cell,* 101**,** 173-85.

Zhang, M., Zhang, Z., Pan, H. Y., Wang, D. X., Deng, Z. T. & Ye, X. L. 2009. TGF-beta1 induces human bronchial epithelial cell-to-mesenchymal transition in vitro. *Lung,* 187**,** 187-94.

Zhang, Y., Feng, X., We, R. & Derynck, R. 1996. Receptor-associated Mad homologues synergize as effectors of the TGF-beta response. *Nature,* 383**,** 168-72.

Zielenski, J. 2000. Genotype and phenotype in cystic fibrosis. *Respiration,* 67**,** 117-33.

Zufferey, R., Donello, J. E., Trono, D. & Hope, T. J. 1999. Woodchuck hepatitis virus posttranscriptional regulatory element enhances expression of transgenes delivered by retroviral vectors. *J Virol,* 73**,** 2886-92.

Zufferey, R., Dull, T., Mandel, R. J., Bukovsky, A., Quiroz, D., Naldini, L. & Trono, D. 1998. Self-inactivating lentivirus vector for safe and efficient in vivo gene delivery. *J Virol,* 72**,** 9873-80.